CR-120927

HIGH POWER MICROWAVE COMPONENTS FOR SPACE COMMUNICATIONS SATELLITES

By M. Jankowski
A. Geia

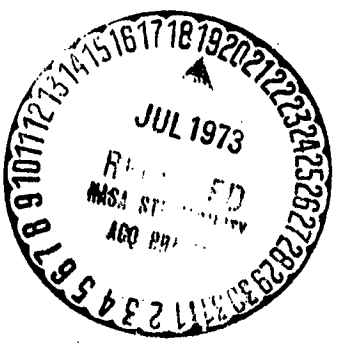

General Electric Co.
Space Division
Philadelphia, Pa.

Prepared for:

National Aeronautics and Space Administration
NASA Lewis Research Center
Contract NAS3-13727

CR-120927

HIGH POWER MICROWAVE COMPONENTS FOR SPACE COMMUNICATIONS SATELLITES

By H. Jankowski
A. Geia

General Electric Co.
Space Division
Philadelphia, Pa.

Prepared for:

NATIONAL AERONAUTICS AND SPACE ADMINISTRATION
NASA Lewis Research Center
Contract NAS3-13727

1. Report No. CR-120927	2. Gov't Accession No.	3. Recipient's Catalog No.
4. Title HIGH POWER MICROWAVE COMPONENTS FOR SPACE COMMUNICATIONS SATELLITES		5. Report Date February 1972
		6. Performing Organiz. Code
7. Authors H. JANKOWSKI and A. GEIA		8. Perf. Organiz. Rpt. No.
9. Performing Organization Name and Address GENERAL ELECTRIC COMPANY SPACE DIVISION PHILADELPHIA, PA. 19101		10. Work Unit No.
		11. Contract No. NAS3-13727
12. Sponsoring Agency Name and Address NATIONAL AERONAUTICS AND SPACE ADMINISTRATION LEWIS RESEARCH CENTER CLEVELAND, OHIO		13. Type of Report CONTRACTOR REPORT
		14. Sponsoring Agency Code
15. Supplementary Notes PROJECT MANAGER: PERRY W. KUHNS NASA/LEWIS RESEARCH CENTER, CLEVELAND, OHIO		

16. Abstract

This program was to analyze, develop, and test high power microwave components for communications satellites systems. Included were waveguide and flange configurations with venting, a harmonic filter, forward and reverse power monitors, electrical fault sensors, and a diplexer for two channel simultaneous transmission. The assembly of 8.36 GHz components was bench tested, and then operated for 60 hours at 3.5 kW CW in a high vacuum. The diplexer was omitted from this test pending a modification of its end irises. An rf leakage test showed only that care is required at flange junctions; all other components were rf tight. Designs were extrapolated for 12 GHz and 2.64 GHz high power satellite systems.

17. Key Words		18. Distribution Statemt.
WAVEGUIDE COMPONENTS HIGH POWER TRANSMISSION TRANSMITTERS, MICROWAVE	COMMUNICATIONS SATELLITES	UNCLASSIFIED

19. Security Classification	20. Classification - Page	21. No. Pages	22. Price
UNCLASSIFIED	UNCLASSIFIED	175	

FOREWORD

The technical accomplishments of this program were largely by personnel at the General Electric Space Division. In addition, the harmonic filter (Section 5.2) and Diplexer (Section 5.4) were developed by C. C. Allen and J. Maurer of General Electric's Corporate Research and Development, assisted by R. L. Williams of the Heavy Military Electronic Equipment Department.

TABLE OF CONTENTS

LIST OF ILLUSTRATIONS

LIST OF ILLUSTRATIONS (Cont'd)

LIST OF TABLES

SUMMARY

This program was to analyze, design, and evaluate waveguide components at 12 GHz and 2.64 GHz for operation with a CW power level greater than 1 kW, in support of a spaceborne high power microwave transmitter in geostationary orbit. The objective was to include experimental verification of a reliable long life capability in space, low loss and distortion for a high power signal, minimum weight and size, and direct applicability to a spaceborne high power transmitter.

The design study included evaluations and concepts for harmonic filters, power monitors for both forward and reverse power, a diplexer for two-channel simultaneous transmission, thermal control, electrical breakdown sensors, a high voltage DC waveguide blocking flange, and the supporting areas of waveguide, flanges, and rf seals. The assembly was to be of open construction to operate as a high vacuum waveguide in space. The fabrication involved designs of optimum components for each item, except that the high voltage DC blocking flange was excluded. The components were assembled and tested in a high vacuum at high rf power. Tests were at 8.36 GHz, the available test facility frequency, and extrapolation functions were derived to predict operation at the two design frequencies of 12 and 2.64 GHz. Final testing was for rf leakage.

Conventional silver plated aluminum waveguide with miniature flanges and soft aluminum gasket seals were found to be suitable for all cases except the diplexer. The high voltage DC blocking flange was deleted because it can be circumvented by simpler means, it would be a relatively weak element of the system, and other problems present such as harmonic leakage greatly complicate the entire approach. A unique leaky wall harmonic filter was developed, combining two filter techniques for optimum performance. The forward power monitor was a relatively straightforward cross-guide coupler development; the reverse power monitor had more severe requirements, including a reverse power measuring accuracy of 20% with a VSWR of only 1.05. This was accomplished with a multi-aperture directional coupler combined with very careful adjustment of the termination to optimize directivity. The diplexer was fabricated of invar because of the extreme stability required in its cavities. The diplexer was slightly overdesigned with respect to bandwidth, but a resonance effect restricted its power capability; this would be corrected in subsequent models.

A special breakdown test section permitted a high power evaluation of electrical fault sensors in a vacuum environment. The results of the tests indicated that three sensors should be used to observe the presence of either multipactor breakdown or arcing; these were the reverse power monitor (VSWR indicator), optical diodes to note visual arcing, and biased probes at points where multipacting may occur to detect electron and ion flow. All three sensors were incorporated into the waveguide assembly.

Bench tests indicated a somewhat greater insertion loss than expected at certain frequencies when the diplexer was used; without it, loss was less than the specification. In a vacuum environment, the diplexer overheated, and the resonance in the end irises was discovered. These irises were restricted to

dielectric loading in the design that evolved; a different approach eliminating the dielectric to avoid the overheating has been suggested.

The waveguide assembly was tested at 3.5 kW (CW) 61 hours with no indication of difficulties. Power was increased briefly to about 8 kW with only a small accompanying increase in outgassing. A magnetic field was applied with no detectable effects. The final test was for rf leakage. One of the flanges had some leakage, indicating that the facing of the flanges prior to assembly is critical, and should be performed very carefully. The other flanges, when carefully tightened, had no detectable leakage at the -122 dB level; the components were rf tight.

The general conclusions were that the components as developed were appropriate for a long life satellite system incorporating a high power transmitter. Scaling of effects to 12 and 2.64 GHz showed they should both be acceptable frequencies for adapting the 8.36 GHz components as developed. Specific recommendations for the two design frequencies include design changes for the diplexer to permit high power operation, smaller harmonic filters and power monitors for the 2.64 GHz case where size may be critical, and other techniques which could improve individual components. Mechanical testing and extended thermal testing to simulate eclipse conditions are also recommmended for subsequent programs.

SECTION I. INTRODUCTION

1.1 BACKGROUND

This program is one of a number of feasibility studies being implemented to evaluate high power radio frequency transmission problems and techniques from satellite to earth. Specifically covered are the waveguide components for a high power microwave transmitter. Typical applications are communications satellites for voice and data communications. The results have a direct applicability to future power microwave space transmitter systems.

The application of satellites for communication relays has been well demonstrated by the INTELSAT series as well as by other similar satellites. However, these required large and expensive ground stations as a consequence of the low power transmitters used, up to a few watts. In addition the 4 GHz and 6 GHz bands used are becoming crowded which makes the higher frequencies around 12 GHz more attractive, particularly for domestic and special services. The 2.6 GHz region has been identified as having potential for effective satellite systems, particularly where costs and heavy rainfall are critical factors (ref.1), but again this is a crowded area of the spectrum.

Canada is presently developing a 200 watt 12 GHz experimental satellite, called the Communication Technology Satellite, which will provide basic experience for developing this frequency region for higher power systems. Transmitter tubes for supporting operation in this region also are being investigated on several NASA Lewis Research Center contracts.

1.2 SCOPE OF EFFORT

This program was to analyze, design, and evaluate space-oriented waveguide components applicable to frequencies from 2.6 to 12 GHz at a power level above one kilowatt, in support of spaceborne high power microwave transmitters in geostationary orbits. The general relationship of the rf subsystem to the overall satellite system is shown in Figure 1.1.

The program was directed at the development of waveguide components required in a high power satellite transmitter to insure continuous operation over a 5 year life. The components specifically included in the program were:

Waveguide, Flanges, Gaskets, and Venting
Harmonic Filter
Power Monitors for Reflected and Transmitted Power
Diplexer - Two Channel
Mounting Plate for Thermal Control
Fault Sensors
Impedance Matching
High Voltage DC Isolation Flange (Analysis Phase - not fabricated)
Special Breakdown Test Section (for calibration only)

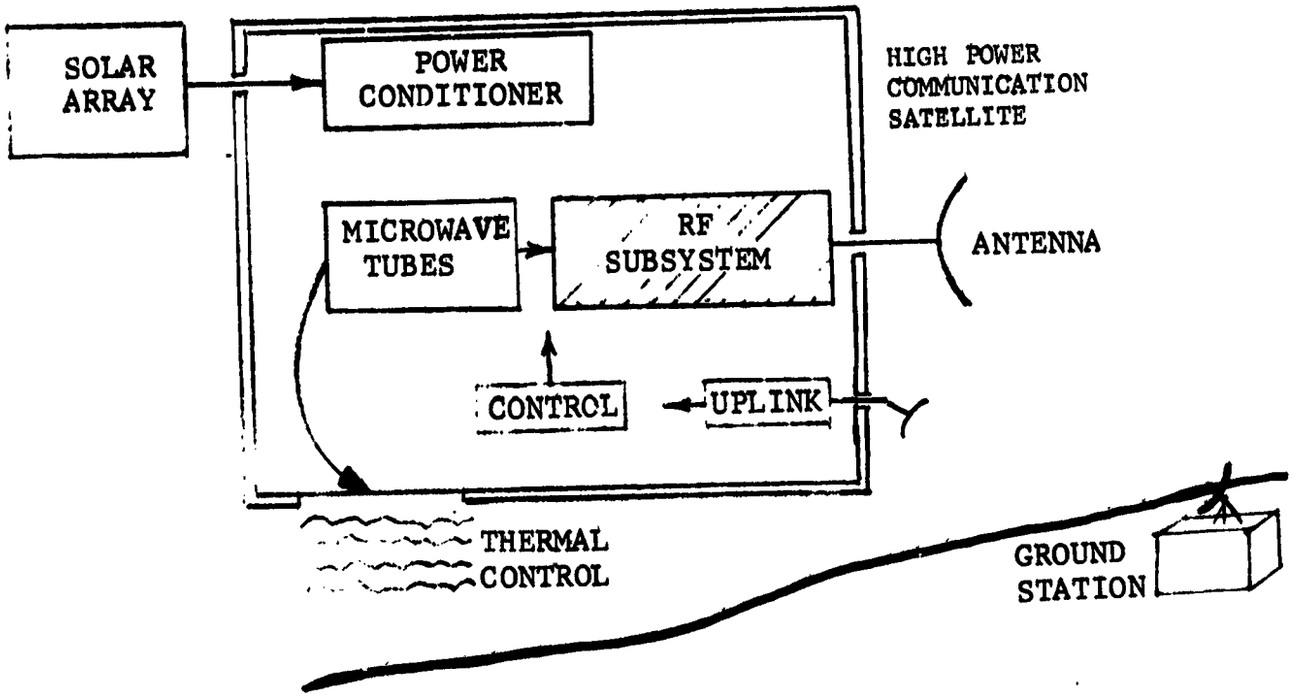

FIGURE 1.1 Relation of Program to High Power Satellite Transmitter System

Each of these items was analyzed and evaluated in terms of overall system requirements. The fabricated components were assembled and tests performed to satisfy the basic requirements for high power operation in the high vacuum environment of space.

1.3 SYSTEM IMPLICATIONS

The primary purpose of the program was to develop and test appropriate waveguide components. Also important are the interfaces between the waveguide components and the other parts of the satellite system where an interrelation exists. Emphasis was placed on low weight and size, low loss, and high reliability which are fundamental factors for any high power communication satellite system. The electrical relations interfaces fundamental in achieving good performance include the output power amplifier tube, antenna, and the protective control circuitry. The thermal effects of the waveguide components are also of importance where a high power transmitter's losses may create an overall thermal problem of a substantial magnitude.

1.4 APPLICABILITY TO OTHER SYSTEMS

The waveguide component designs can be extrapolated to other frequencies by direct wavelength scaling in most cases. Performance at other frequencies is predictable through the use of scaling functions derived in this program. Specific designs were developed for 2.64 and 12 GHz, the two required design frequencies, and at 8.36 GHz which was the test frequency, used because of the high power availability. The components are applicable in general to any high power satellite transmitter operating in the microwave frequeney spectrum and using waveguide transmission.

1.5 PURPOSE AND GENERAL REQUIREMENTS

This program was established to determine the feasibility, design, and performance of vital waveguide components for future high power communication type satellites. An initial experimental satellite is presently being developed by Canada; it will include transmission at the 200 watt CW level at 12 GHz. The objective power levels for some of the 12 GHz tubes now under development by NASA are in the one to two kW range; the reference equivalent testing power used in this program was 1.5 kW at 12 GHz. The component designs developed were to be directly applicable to communications satellites of this or higher powers. Performance predictions can be made for waveguide subsystems at frequencies above 12 GHz if desired.

Results permit straightforward design and fabrication of components for a selected frequency. In limited instances, normal manufacturing tolerances, materials variations, and extreme theoretical complexity may necessitate some design iterations, as exact designs are not possible. Means for handling these to minimize additional engineering are defined in this report.

1.6 APPROACH AND PROCEDURES

The program was directed at the development of waveguide components for 12 and 2.64 GHz, possible frequencies for future high power communication satellites. Initial emphasis was placed on the 12 GHz band, but no high power test source was available to evaluate waveguide components at that frequency. The experimental assembly, therefore, was developed at 8.36 GHz where the combination of a 5 kW source and a large vacuum chamber was available for environmental tests. Analytical scaling for component designs at the two design frequencies is a part of this program.

The approaches for individual components are directly related to requirements, with a consideration for materials suitable for space systems. An analysis was performed for predicted operation of each component, each was fabricated, and the assembly was tested in a preliminary bench test at accomplish impedance matching. The assembly was then run at high power in a high vacuum for 60 hours. Finally, it was checked for possible rf leakage interference. The components were developed to meet the specifications as listed in the next Section.

SECTION II. SPECIFICATIONS AND CONSTRAINTS

2.1 SPECIFICATIONS

The requirements for the subsystem and its components are as follows:

2.1.1 General

- Operate in a simulated space environment; subsystem to be capable of five year life in geostartionary orbit while operating continuously at rated power.

- Space Environment:

  Utilize open construction (as opposed to pressurized sealed enclosure)
  Materials must have negligible outgassing; multipactor breakdown may require low secondary emission waveguide walls.
  One week dormancy in orbit before high power applied.

- Launch Environment:

  Shock - 30g for 8 msec.
  Acceleration - 7g for all axes
  RMS Vibration - 1g from 10 to 60 Hz, 2g from 70 to 2000 Hz
  Temperature - 323°K (50°C) ambient in satellite.

- Signals (frequency, bandwidth, power)

  12 and 2.64 GHz design frequencies; experimental components at selected intermediate frequency (used 8.36 GHz)
  Bandwidth (no diplexer) = 0.5 GHz at 12 GHz
  = 0.25 GHz at 2.64 GHz
  Power = 1.5 kW maximum cw
  Harmonics from power amplifier more than 20dB below fundamental

- Magnetic Field Environment

  Simulate leakage from magnetic field of TWT per Figure 2.1:

  B_o = 5 KG for 12 GHz
  B_o = 1 KG for 2.64 GHz

  Maximum required is equivalent to field at one waveguide width from TWT

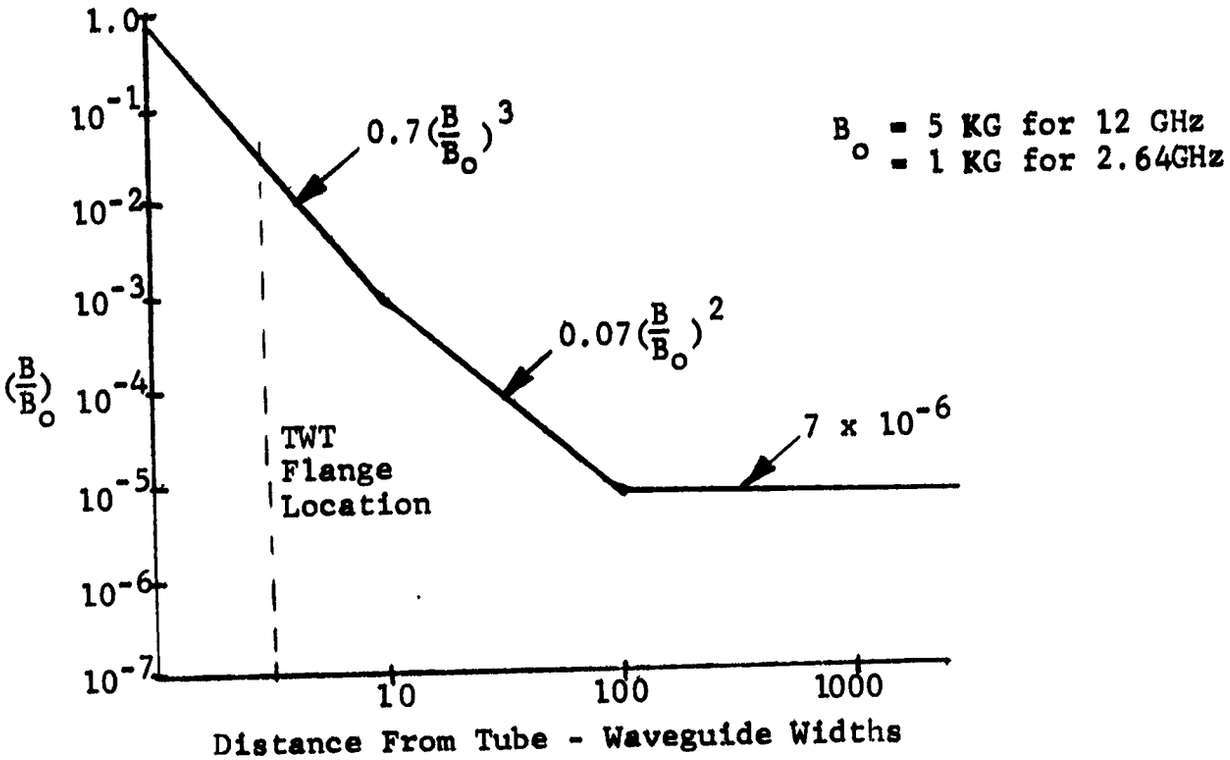

FIGURE 2.1 Test Magnetic Field Distribution

- Temperature in Orbit

  Ambient in satellite nominally between 313°K (40°C) and 323°K (50°C)
  In eclipse, may drop to 193°K (-80°C) for one hour.

2.1.2 Subsystem Operating Requirements

- Impedances, Input and Output

  Match to WR75 for 12 GHz; to WR340 for 2.64 GHz
  VSWR of source (tube) = 1.2 max.
  VSWR of antenna line = 1.1 max.

- VSWR

  Less than 1.05 at center frequency (matched load)
  Less than 1.15 over band (per 2.1.1 above)
  Second Harmonic: less than 1.5

- o Weight
  Objective: $\leq$15.9 kg (35 pounds) at 12 GHz
  $\leq$20.6 kg (45 pounds) at 2.64 GHz

- o Size
  Objective: $\leq$8194 cm^3 (500 in^3) at 12 GHz
  $\leq$13,000 cm^3 (800 in^3) at 2.64 GHz

- o Insertion Loss

  Objective: $\leq$0.5 dB at carrier; $\leq$0.3 dB (7%) variation over bandwidth (less diplexer)
  With diplexer, $\leq$1.5 dB at carrier (12 GHz)

- o RF Leakage

  Less than -80 dBw at design power level (1.5 kW)

- o Venting

  As required; TBD.

2.1.3 Component Requirements

- Waveguides and Flanges

  As required to meet above subsystem specifications

- High Voltage DC Isolation Flange

  Insulation for 10 kV while conducting 1.5 kW rf power
  Meet leakage specifications of Section 2.1.2 above
  (Note: this component not fabricated; see Sections 3.3.8 and 5.8)

- Harmonic Filter

  Attenuation shall exceed: 30 dB at $2f_c$
  20 dB at $3f_c$
  10 dB at 4 and $5f_c$

  VSWR at $2f_c$ less than 1.5
  (Measurement required at $2f_c$ only)

- Power Monitors

  Forward Accuracy = 0.5 dB (11%)
  Reflected Accuracy = 1.5 dB with directivity of about -51 dB at carrier and -41.8 dB across band

- Diplexer

  Power capability = 1.5 kW in either input port
  or = 0.75 kW in each port simultaneously
  Bandpass characteristic and isolation per Figure 2.2

2.1.4 Scaling of Specifications to 8.36 GHz

All specifications were listed for 12 and 2.64 GHz; breadboarding and tests were performed at 8.36 GHz. For compatibility and interpretation of data, scaling functions were used to determine an equivalent specification at the test frequency to achieve the same performance as expected from a 12 GHz component. Scaling is discussed in Sections 3.2.3 and 5.9. These were used to derive some equivalent specifications as follows:

Bandwidth = 0.35 GHz min at 8.36 GHz
Power = 1.6 kW min. (applies to long duration tests; other powers for breakdown tests only)
Weight: between 15.9 Kg (35 lbs) and 20.6 Kg (45 lbs)
Size: increases by about 50% in each dimension, or up to 27,850 cm^3 ($1700\ in^3$)
Diplexer Bandpass: Scale from 12 GHz case = 105 MHz
Diplexer Insertion Loss: 0.66 ± 0.16 dB
System Insertion Loss Without Diplexer: 0.4 ± 0.25 dB
(Note the original specification was the same for both frequencies considered, so this imposed requirement is the more severe of the two cases)
Magnetic Field Environment: B_o = 5 KG in Figure 2.1

Other specifications were the same for both frequencies, and the same values are used for the 8.36 GHz test frequency.

2.2 TEST REQUIREMENTS AND CONSTRAINTS

Tests were to be performed at a convenient frequency between 5.5 and 12 GHz. Power levels of more than 3 kW were desirable at the test frequency to show a significant margin of capability. (For these tests, the facility was a 5 kW klystron at 8.36 GHz; standard WR112 waveguide was used, and scaling factors developed to extrapolate performance to other frequencies with other waveguide cross sections). The three major tests on the waveguide assembly were:

Bench Tests - Matching and insertion loss tests, vacuum not required.
Vacuum Tests - Breakdown, outgassing, and high-power loss tests; - followed by a 60 hour run at rated or higher power (scaled as appropriate). This test was to determine loss factors, effectiveness of materials selection and venting techniques, effect of a magnetic field on vacuum operation, breakdown tendencies, and all electrical performance data that may be influenced by the environment.
Anechoic Chamber Tests - determine the rf leakage level of the fundamental and second harmonic.

Test plans were required prior to developing the final rf components.

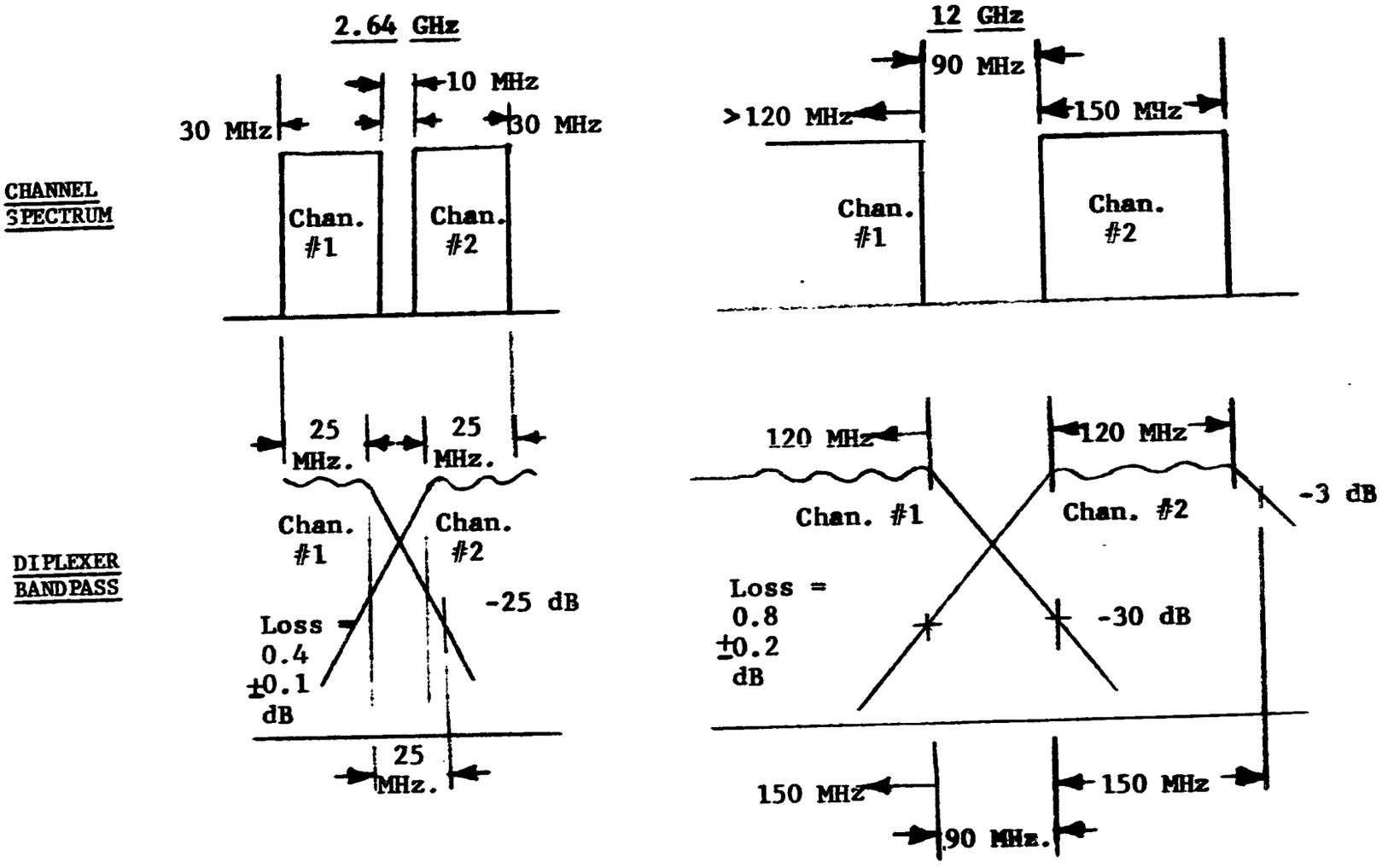

FIGURE 2.2 Bandpass and Isolation Requirements of Diplexer

2.3 FINAL DESIGN

A design with drawings and fabrication data is required for each component at each of the two selected frequencies: 12 and 2.64 GHz. These were to be direct frequency translations, but include suitable variations where a direct 1:1 correspondence does not occur. Also, materials dimensions and standard parts do not necessarily scale directly, and were to be included appropriately in the final designs.

SECTION III. RESULTS

3.1 SUMMARY OF RESULTS

The waveguide subsystem developed, fabricated, and tested in the program gave excellent performance, meeting or exceeding specifications; a minor exception was the diplexer which developed a power-limiting stray resonance which can be removed easily but there was insufficient time on the current program to effect a fix. Component and assembly tests were satisfactorily performed on the bench, in the vacuum chamber, and in the rf leakage tests. The designs were scaled for fabrication at 12 and 2.64 GHz. Special design instructions are included for the few instances where a direct scaling might not provide correct operation, either due to normal manufacturing tolerances or some form of non-linearity or dimensioning. The deviations are discussed in Section IV on Recommendations and in the technical details of Sections V and VI.

The major requirements and results of the program are listed in Table 3.1. The specific factors and component performances involved are discussed below. The results indicate the approaches used were satisfactory, and the designs which evolved are directly applicable to space systems. The components included in the program are adequate for a complete space transmitter; possibly an rf switch may have some utility and could be included in future programs.

Detailed components data is included in Section V. The effect of these results in determining an optimum waveguide assembly are included there as well as in Section VI on the assembly and testing.

3.2 WAVEGUIDE ASSEMBLY

3.2.1 Description of Waveguide Assembly

The waveguide assembly developed includes the several components listed in the program scope in Section 1.2. The final assembly is in Figure 3.1, and a layout sketch is in Figure 3.2. The complete assembly was developed using venting to achieve an "open" configuration to insure that there can be no pressure buildup should any of the materials in the assembly be a source of any outgassing. Materials which outgas in a vacuum were carefully avoided, and all parts were cleaned thoroughly before final assembly and placing in the vacuum chamber. For this program, baking was accomplished by rf heating in the preliminary tests; deliberate baking would be advised before launch in an operational equipment. With these precautions, no arcing forms of breakdown were expected in final testing, and none were observed.

Analyses performed during the study indicated no expected source of multipacting, which would only occur in a high vacuum within a certain range of rf power for a given electrode configuration, operating voltage, and frequency. No special

TABLE 3.1. Waveguide Subsystem Performance

Component/Frequency	Objective	Achievement
Subsystem Heat Run	60 hours	61 hours
Insertion Loss (loss diplexer)	< 0.5 dB	0.3 dB
Variation	< ±0.3 dB	±0.2 dB
VSWR (loss diplexer) - center	1.05	1.02* (est.)
- over band	1.15	1.05*
Magnetic Field Effect	no breakdown in presence of field	verified no breakdown
Bandwidth - 12 GHz	500 MHz (scales to 350 MHz)	---
- 8.36 GHz	250 MHz	500 MHz
- 2.6 GHz		---
Power - 12 GHz	1.5 kW max to 2.75 kW (scales differently for different parameters)	---
- scaled to 8.36 GHz		3 kW for 60 hours, to 8 kW for breakdown evaluation
Temperature	in 323°K (50°C) ambient	in 323°K (50°C) ambient
Harmonics - $2f_o$	30 dB attentuation	60 dB TE_{10} 38 dB TE_{01}
Harmonic VSWR	1.5 at $2f_o$	1.12 worst case
Weight - 12 GHz	15.9 kg (35 lbs.)	Est. 1.63 kg (3.6 lbs.)
- 8.36 GHz	---	4.65 kg (10.25 lbs.)
- 2.64 GHz	20.4 kg (45 lbs.)	Est. 58 kg (128 lbs.)
Volume (with mounting plate) - 12.0 GHz	8200 cm^3 (500 in^3)	Est. 2210 cm^3 (135 $in.^3$)
- 8.36 GHz	---	6650 cm^3 (406 in^3) (no external connections)
RF Leakage - fundamental	< -80 dBW	~ -90 dBW

* Measuring Equipment Accuracy = 1.02 at band edges
Tuned to 1.00 at f_o

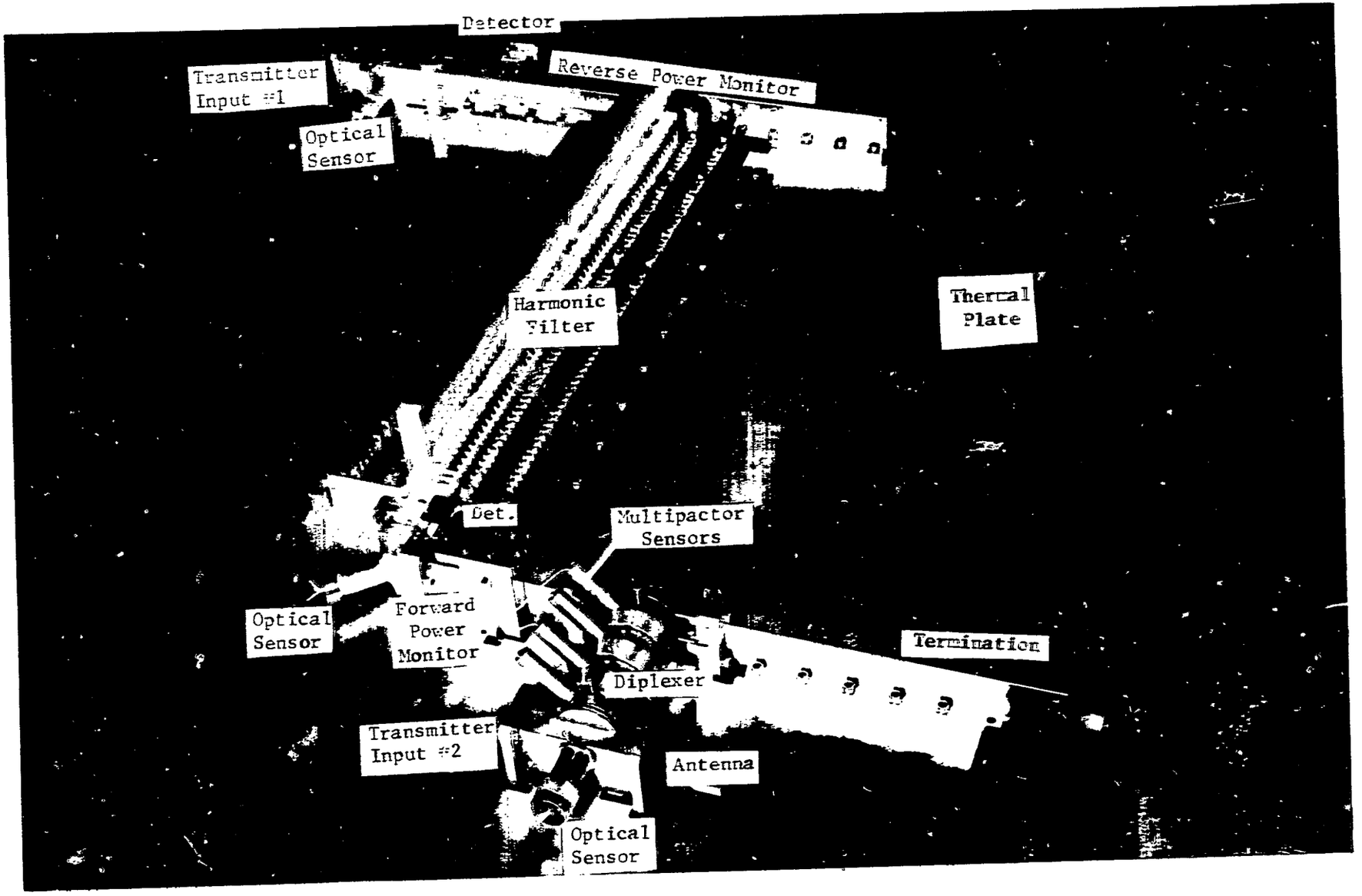

FIGURE 3.1. WAVEGUIDE ASSEMBLY

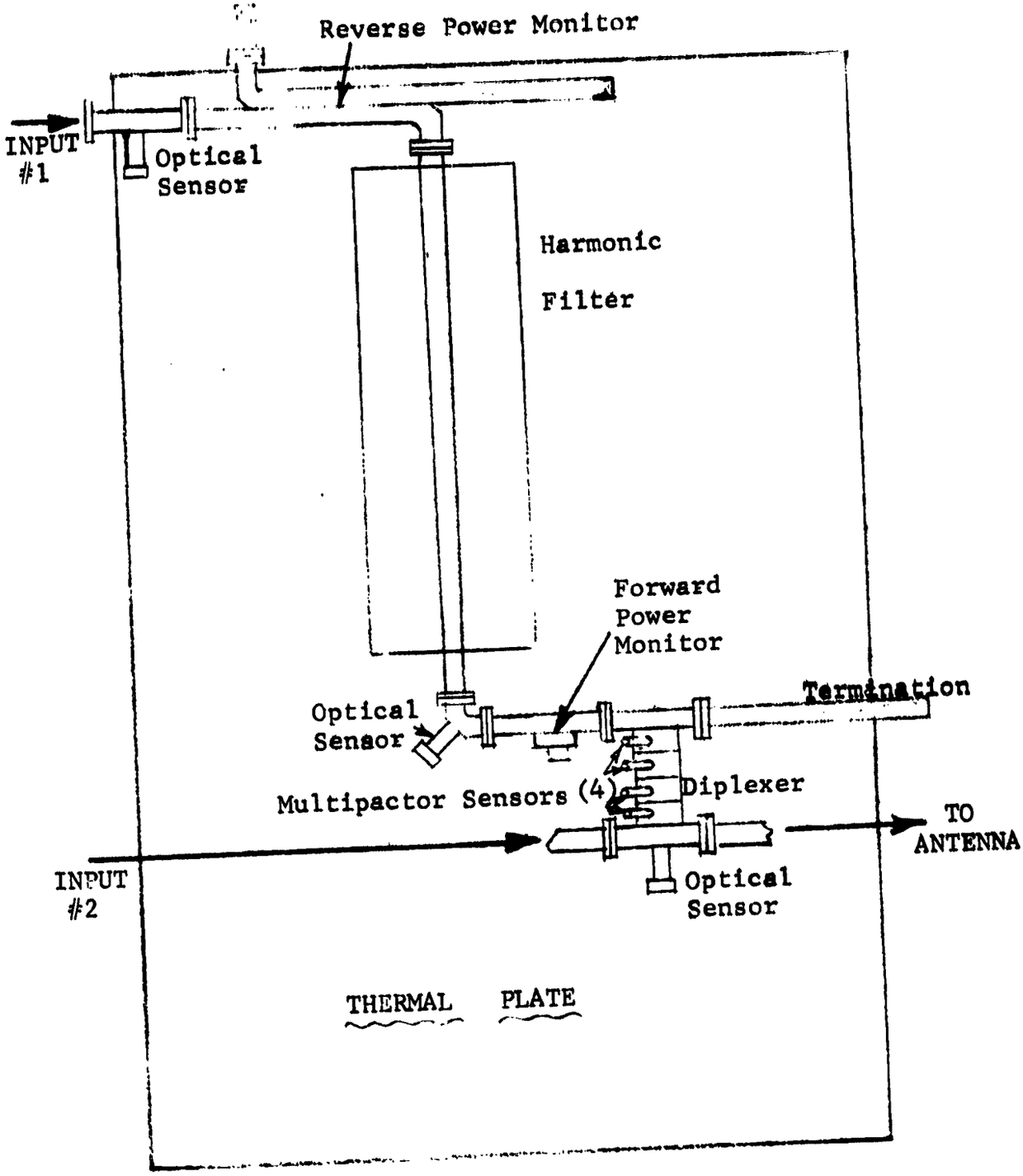

FIGURE 3.2. WAVEGUIDE COMPONENTS ASSEMBLY LAYOUT

materials or techniques were thus used or considered necessary to prevent multipactor breakdown. Sensors for this type of breakdown were included in the diplexer which was the only component having a high voltage field which might have caused a breakdown. Appendix I further discusses breakdown prevention techniques, should some component in the future include a questionable region.

The components in Figures 3.1 and 3.2 showed separate power monitors for forward and reverse power measurements; the latter provides a measure of system VSWR. This approach was desirable because of substantially differing requirements for forward and reverse power accuracy, and because reverse power should be measured near the transmitter tube output while forward power is best measured close to the antenna. Modifications of this arrangement may be desirable for any specific individual transmitter system. The assembly shown is considered optimum for a demonstration of waveguide component techniques and performance capabilities. The components are mounted on a 0.635 cm (1/4 inch) thick jig plate which is somewhat heavier than would be required for space; a thinner mounting plate would result in slightly higher component temperatures for a given average radiation temperature, but the effect is not significant.

These and the other components will be described in more detail later in this Section of the report. The harmonic filter may be omitted if a diplexer is used since the initial tests indicate the latter is an excellent harmonic filter, at least for the 2nd harmonics in the basic modes, TE_{10} and TE_{01}. Optical diode arc sensors are shown at three points which are sufficient to see all parts of the subsystem and to warn of any arcing. The input and output terminals were arranged merely for the convenience of testing in this program, and a different orientation may be required in a final system.

3.2.2 Performance of Waveguide Assembly

The performance of the waveguide assembly was assessed in three major tests: bench testing to match the assembly for a low VSWR, a 60 hour run in a vacuum chamber at high power, and a leakage test to insure an rf tight structure.

3.2.2-1 Bench Testing

Bench testing was to determine VSWR, insertion loss, and power monitor calibration. The initial testing was performed without the diplexer, and only a small matching iris was found to be required at the elbow below the harmonic filter to achieve an excellent match. All other components had been individually corrected for a matched load, and the resulting VSWR was below the measuring equipment accuracy and well under that required by the specifications. The VSWR and loss over the band are shown in Figure 3.3. After this tuning, the diplexer was added and the resulting VSWR and loss were those shown in Figure 3.4. The increase in insertion loss is greater than that predicted from the component measurement. The cause of the difference was not determined; the two measurements were made with different equipment at different locations. High power tests later confirmed a high loss but this was due to a substantial extent to the stray resonance which would be designed out of subsequent models. (Note that the diplexer met basic VSWR and loss requirements over the region in the center of the bandpass in either case, but should be better than specifications ultimately.)

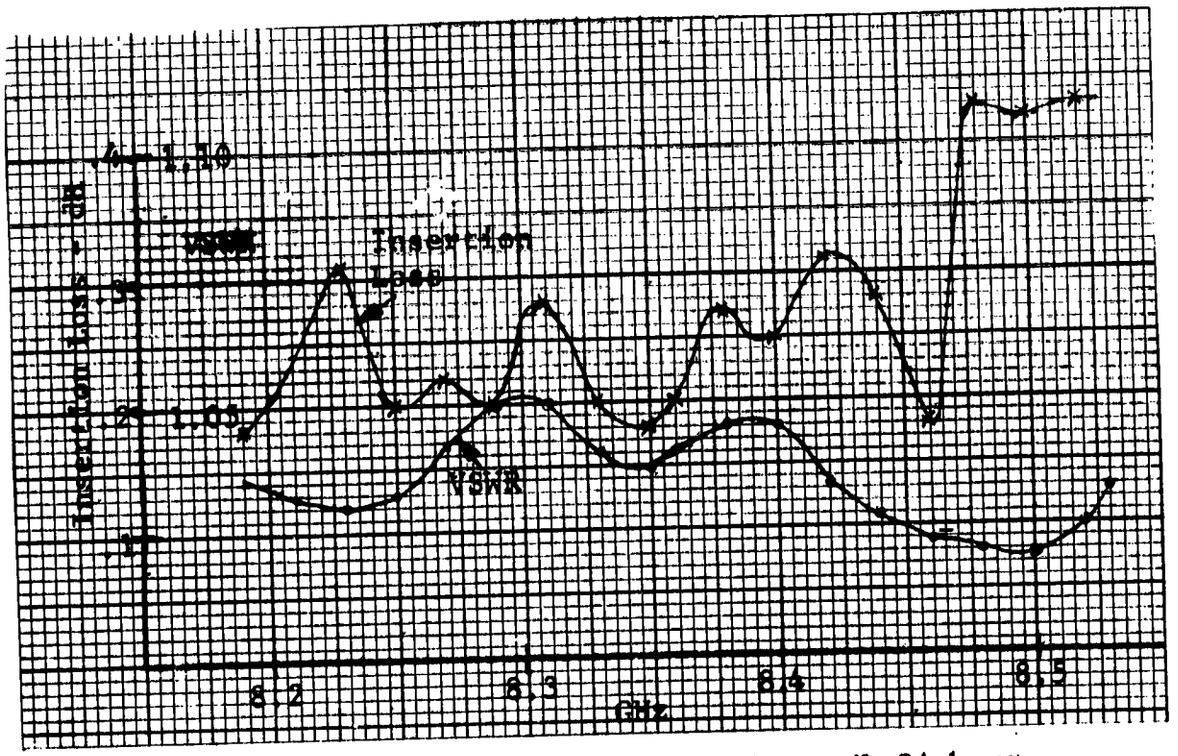

Figure 3.3. VSWR and Insertion Loss - No Diplexer

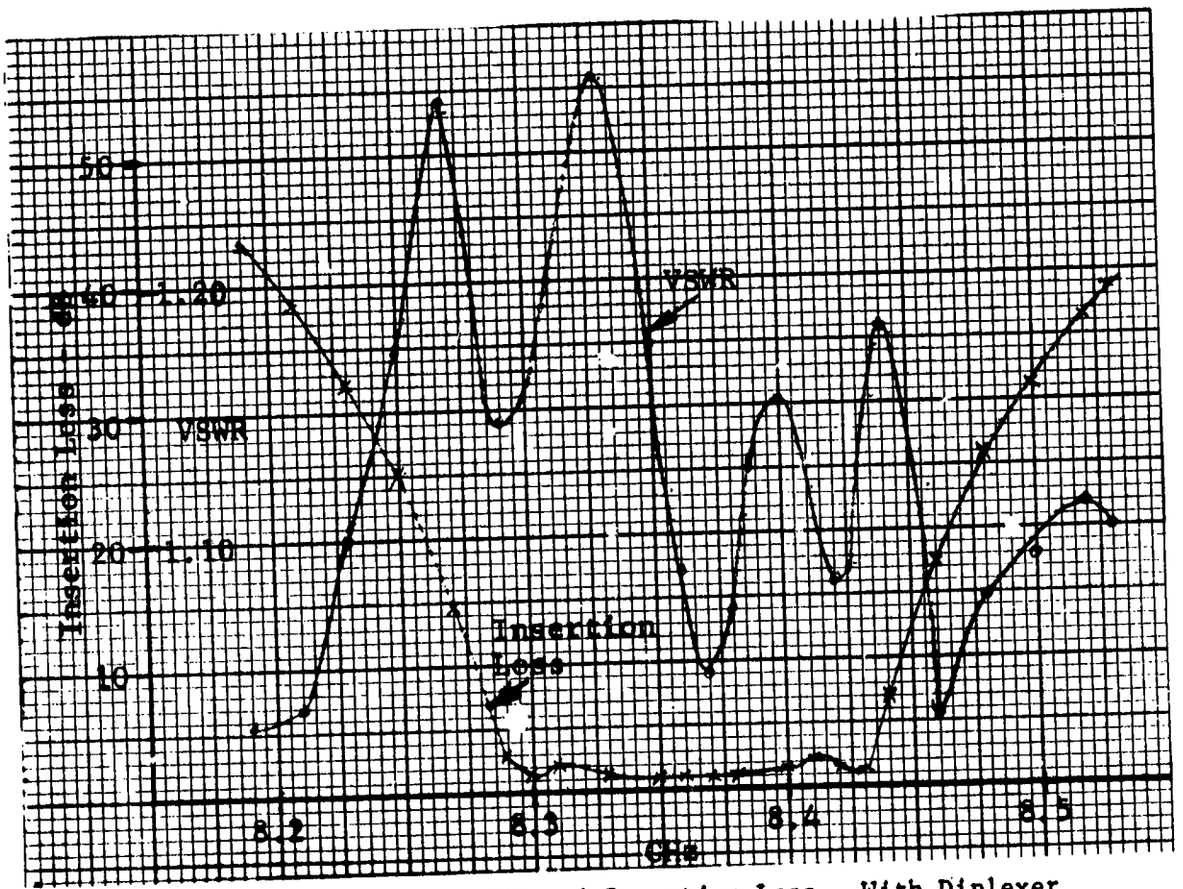

Figure 3.4. VSWR and Insertion Loss - With Diplexer

Having completed the basic tests, the entire system was then placed in the vacuum chamber for high power tests.

3.2.2-2 Vacuum Chamber Testing

Water cooling was added to the baseplate to simulate the effects of radiating heat to space (see Section 5.5.1). Otherwise, the thermal loss of the plate would be insufficient to maintain a reasonable temperature if only radiating to the room-temperature chamber.

The initial test with the diplexer in place showed that the ends of the diplexer tended to heat much more than expected although operation in air might be acceptable with sufficient cooling. In the vacuum, the boron-nitride inserts in the end irises of the diplexer (see Section 3.3.5 for description and purpose) became red hot at about 300 watts CW, and the diplexer had to be removed. A stray coaxial resonance mode appears to be responsible for the localized heating. The rest of the system was operated about 8 hours over a three day interval in the vacuum, and then the 60 hour test was run at a power level of 3.5 kW CW, twice the minimum required power level. After the 60 hours were complete, the power was elevated to about 8 kW with no difficulties except a small increase in outgassing. Thus the major operational requirement was accomplished but without the diplexer in the circuit.

The vacuum levels were read with two gauges, one in the waveguide output port at the exit from the chamber, and the other in the chamber wall. The readings indicated a slight leak probably existed at the waveguide window; pressures measured were:

	Newton/m^2	(Torr)
Main tank pressure	0.67×10^{-4}	(0.5×10^{-6})
Waveguide open into tank	1.73×10^{-4}	(1.3×10^{-6})
Waveguide assembly attached, - no power	6.67×10^{-4}	(5×10^{-6})
Waveguide at end of 60 hour run at 3.5 kW	12.0×10^{-4}	(9×10^{-6})

There is a little outgassing present, observable particularly if the power is increased. The cooling also is increased to maintain a nearly constant temperature, so the outgassing is localized and affected by the power level. It is believed to be largely due to the harmonic filter which was not baked prior to installation. These pressures, however, are three orders of magnitude below the critical arcover pressure, so the overall results indicate a large breakdown safety margin. The components therefore are suitable for a space application in their developed form.

The equipment was not baked prior to the vacuum test, so a significant amount of outgassing occurred for the first couple of hours, in part from the metal surfaces. This suggests that initial operation in space include a gradual increase of transmitter power, perhaps in 4 or 5 steps at an hour each, letting the transmitter provide the bake-out function for the surface absorption. In the initial tests, outgassing was generally held below 6.7×10^{-2} N/m^2 (5×10^{-4} Torr) by a combination of power adjustment and water cooling as necessary.

Temperatures were greatest on the mounting plate away from the water cooling. Typical temperatures maintained during the test after steady state was reached were:

Plate	369°K	(96°C)	(near harmonic filter away from cooling pipe)
First Elbow	350°K	(77°C)	
Second Elbow	346°K	(73°C)	
Harmonic Filter, Top	348°K	(75°C)	
Harmonic Filter, Near Water	349°K	(76°C)	
Power Monitor Terminations - reverse:	327°K	(54°C)	(near water)
forward:	339°K	(66°C)	
Surrounding Ambient	298°K	(25°C)	

The water cooling averaged about 175 watts and radiation cooling was estimated to be 45 watts. This calculation indicates a loss of 0.28 dB with an output power of 3500 watts.

A 12 GHz system with 1.5 kW input might have 105 watts loss with a temperature of 60°C, which should present no problems in space if proper design techniques are used. With the diplexer in place, the 8.36 GHz test system would have removed the extra heat by additional water cooling, while the 12 GHz assembly would experience a temperature rise to about 373°K (100°C) with an expected diplexer loss of 0.4 dB. Thermal design aspects are considered further in Sections 3.3.7 and 5.5.

A magnetic field, simulating a TWT focus field, was added at the completion of the test; it had no detectable effect on waveguide operation.

3.2.2-3 RF Leakage Testing

Following the high power test, the waveguide assembly was checked for rf leakage in an rf anechoic chamber, with the diplexer in place. For this test, a 16 watt transmitter was used as a source, and the receiver and horn provided a sensitivity to -126 dBW, the noise level observed. The second harmonic measurement had about the same sensitivity, but a source of 0.05 watts and a larger horn were used. In all cases, no detectable signal was discerned after carefully tightening all flanges (with the exception of one faulty flange facing indicated below.)

The requirements and measuring sensitivity of the leakage from the waveguide assembly were:

Fundamental Frequency	Required -111.75 dB Achieved up to -122 dB
Harmonics (assumed 20 dB below f_o)	Required -91.75 dB Achieved up to -95 dB

The measurement results assumed a point source if there were radiation from any component of the system, and the horn was placed directly at the component which is well inside the far field near-limit. The far field starts at a distance of about 30.5 cm (12 inches) for both the fundamental and harmonic with the specific horns used; measurements were made down to about 1/10 this distance to give 10 dB more sensitivity than in the far field measurement.

The major difficulty in achieving low leakage was in the flanges. In each case, the eight bolts per flange were tightened heavily; ideally they should supply about 1800 Kg (4000 pounds) clamping pressure (for 8.36 GHz) which is within limits for the eight stainless steel 6-32 bolts. However, the flange between the first optical diode section and the reverse power monitor input would not tighten sufficiently, indicating an inadequate facing on one of the two flanges. Normally, these pieces would be disassembled and refaced. For the purposes of this program, a covering was placed over the flange seam so the other components could be checked for rf leakage without this interference. The unused waveguide terminals (two power monitor detectors and second input guide of diplexer) were shorted for this test, but would add no problems other than the normal caution in insuring that accessory waveguide or coaxial line be well shielded against leakage.

3.2.3 Scaling Results to Other Frequencies

The waveguide components were developed for testing at 8.36 GHz, but final designs are provided for the same components at 12 and 2.64 GHz, with performance predictable such that further experimental development is not required. The quantities considered in equating performance of the components at different frequencies are listed in Table 3.2, which shows the power for the 8.36 GHz test frequency to provide the same performance as would be encountered at the other frequencies. The functions consider the differences in waveguide cross section dimensions (WR340 at 2.6 GHz and WR75 at 12 GHz have sides with ratio of 2:1 while WR112 used for testing at 8.36 GHz has sides with ratio of 2.258:1, the factor used is $\Upsilon = 0.886$) as well as the differences in wall thickness as it influences heat conduction (1.28 for the 12 GHz case and 0.80 for 2.64 GHz). The frequency ratio, f, in the Table is freq/8.36 (1.435 for 12 GHz and 0.316 for 2.64 GHz).

The two columns at the right indicate the worst case power required at 8.36 GHz to simulate a given power effect at either of the other two frequencies and the power in kilowatts at 8.36 GHz to simulate performance equivalent to 1.5 kW at the worst case. The term showing the greatest discrepancy is the thermal radiation term, but little dependency is placed on direct thermal radiation from any of the components so this term is greater than would ever be experienced. The harmonic filter is partly cooled by self-radiation, so the equivalent power for it lies somewhere between the conduction power and radiation power, possibly about half way between or at about 2.7 kW. This power would also be required for ionization tests and is considered an upper limit as a firm requirement.

Practically, the conduction loss is about the most significant for high power continuous tests. Thus testing could have been performed at 2.04 kW to simulate the 1.5 kW at 12 GHz. Electrical breakdowns due to ionization were checked with power levels to about 8 kW but no effects were observed. The I^2R loss relates to the insertion loss overall heating effect and is not as significant a test criterion as is conduction of the thermal loss. The 3.5 kW used for the test thus covered all circumstances that are considered pertinent for continuous operation testing. Conduction losses, of course, are always related to CW operation.

3.3 COMPONENT DESIGN, FABRICATION, AND TESTING

This Section summarizes the results of the analysis and design phase for each component, the fabrication used, and the component test results. Details on the evolution of the results are in Section V. The components are discussed in the following order:

1. Waveguide, Flanges, Gaskets, and Vents
2. Harmonic Filter
3. Power Monitor, Forward
4. Power Monitor, Reverse
5. Diplexer
6. Fault Sensors
7. Thermal Mounting Plate
8. High-Voltage Isolation Flange

3.3.1 Waveguide, Flanges, Gaskets, and Venting

3.3.1-1 Waveguide

This task provided the groundwork for the fabrication of all the waveguide components. The general recommendation for all components is to use silver plated aluminum waveguide with standard dimensions, except for the diplexer which must be of Invar. Copper guide could also be used effectively without a plating. In either case, a gold or rhodium flash should be applied to retard corrosion effects. Typical theoretical losses at 12 GHz (WR75) are:

- plain aluminum, ideally smooth		.233 dB/m	(.071 dB/ft)
- silver plated, 0.762 microns (30 μin.)	rough	.170 dB/m	(.052 dB/ft)
- silver plated, 0.254 microns (10 μin.)	rough	.141 dB/m	(.043 dB/ft)

The latter reduces the waveguide loss over the rougher finish by about 17%, which may be significant if the waveguide absorbs 0.5 dB (10%) or more of the rf transmitter power.

An experimental evaluation of electropolishing of aluminum waveguide showed the improvement in performance to be negligible, indicating that the waveguide roughness from the manufacturing process was a "coarse" sort of roughness which did not greatly contribute to resistivity. It appears then that waveguide can be purchased with the necessary smoothness. However, a waveguide lot when purchased should be checked to determine the roughness and whether electropolishing would improve the performance significantly. A 6061-F aluminum alloy was used for the experimental components which would be heat treated to T6 temper for flight components. An 1100 alloy should be used where electron beam welding is employed.

The diplexer uses Invar with a heavy silver plate. The elements of the device would be electropolished prior to assembly because of the limitations imposed by the configuration.

TABLE 3.2 Frequency Scaling Factors

Parameter	Power Scaling Function	$P_{8.36}$ Worst Case	$P_{8.36}$ kW for Tests
Ionization Breakdown	γf^2	1.824 P_{12}	2.74 kW
Multipactor Breakdown	γ^3	0.7 P_{either}	1.05
Paschen's Minimum Gas Arc Breakdown	$\frac{1}{\gamma}$	1.129 P_{either}	1.70
- Pressure Minimum	$\frac{1}{\gamma f}$	n.a.	n.a.
I^2R Loss per Unit Length	$\gamma f^{3/2}$	1.53 P_{12}	2.29
- per Guide Wavelength	$\gamma f^{1/2}$	1.06 P_{12}	1.59
Thermal Loss - Conduction	$\gamma\gamma f^{1/2}$	1.36 P_{12}	2.04
- Radiation	$\gamma f^{5/2}$	2.18 P_{12}	3.27

γ = 0.886
f = 1.435 for 12 GHz
f = 0.316 for 2.64 GHz
γ = 1.28 for 12 GHz
γ = 0.80 for 2.6 GHz

Oversize low-loss waveguide is generally not recommended except possibly for long runs, either straight or with very few bends. Oversize waveguide would provide only a small saving in power, at the expense of an extensive development program and sensitive operating characteristics of the components. The complexity would lead to an impractical approach in most cases.

3.3.1-2 Flanges

Standard CMR112 small flanges were selected. These are physically small, but have eight bolts for a mechanically solid and low rf leakage joint between waveguide components. Dimensions are in Figure 3.5; material was 6061 aluminum alloy, with Invar flanges used on the diplexer.

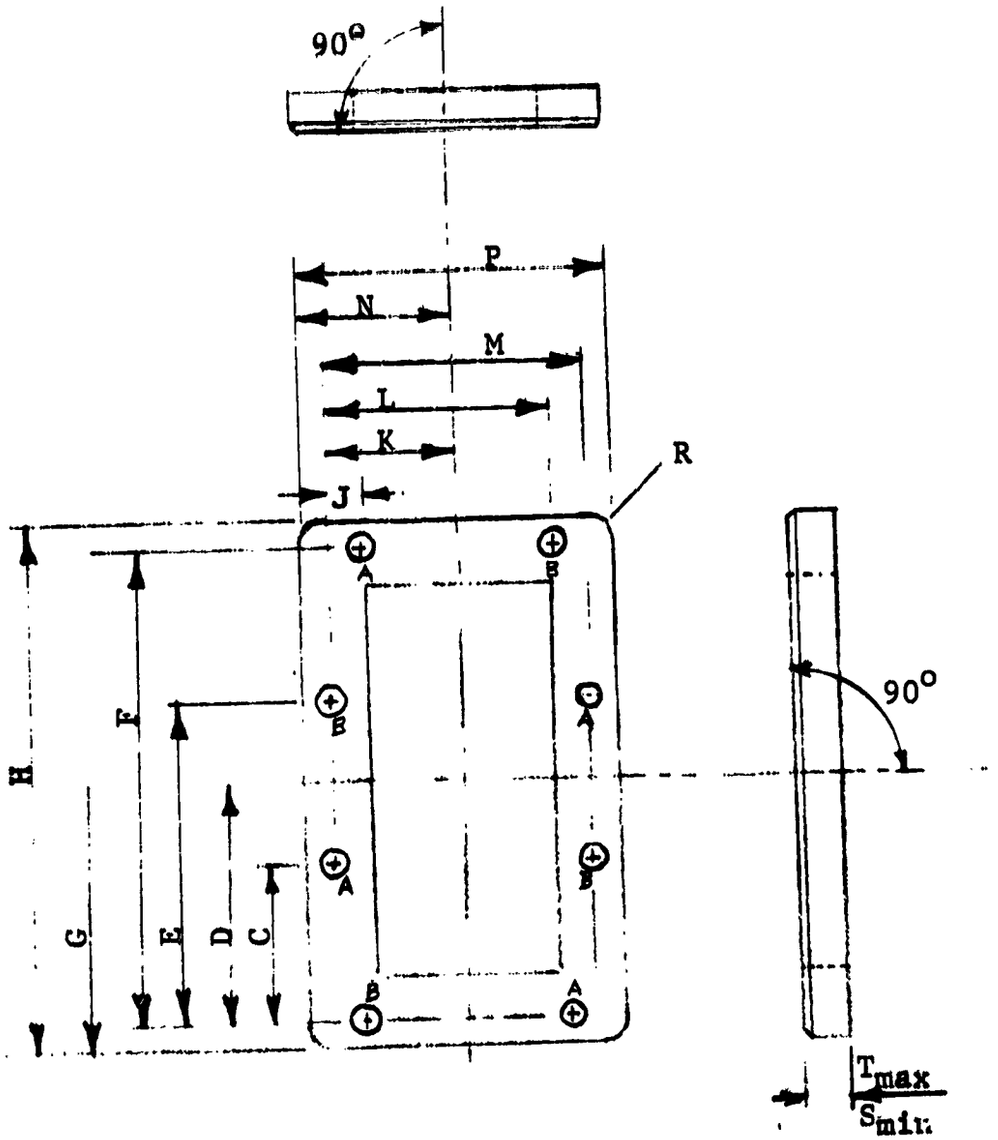

Dimensions - Centimeters (Inches)

A.	Tap 6-32	
B.	0.373	(0.147)
C.	1.405	(0.553)
D.	2.108	(0.830)
E.	2.812	(1.107)
F.	4.210	(1.660)
G.	2.560	(1.007)
H.	5.120	(2-1/64)
J.	0.602	(0.237)
K.	1.314	(0.517)
L.	2.023	(0.797)
M.	2.625	(1.034)
N.	1.763	(0.694)
P.	3.493	(1-3/8)
R.	0.318	(1/8)
S.	0.508	(0.200)
T.	0.635	(0.250)

Note: See drawings for tolerances and details

FIGURE 3.5. CMR-112 FLANGE DIMENSIONS

3.3.1-3 Gasket

Gasket seals are of soft aluminum with a photo-etched cross-hatch pattern between the clamping bolts and the waveguide inside periphery. The cross-hatch lines are raised about .05 mm (.002 in.) on each side of the gasket such that when clamped, the aluminum will depress to give a very tight rf seal. Figure 3.6 is a photograph of the gasket. This design is based on similar types which keep rf leakage at about -130 dB when properly clamped. A resilient type with silver loading can give comparable results but the silicone used could result in some outgassing. For use as gaskets, this would be negligible, but the resilient type isn't necessary since the soft aluminum type is adequate.

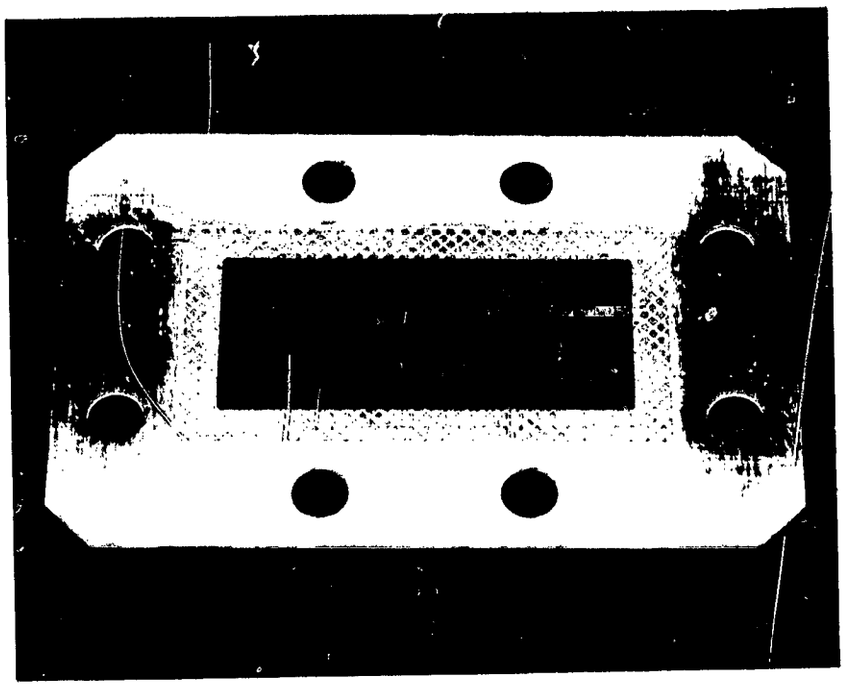

FIGURE 3.6. RFI Gasket

3.3.1-4 Venting

Three approaches were used for vents to remove outgassing from the waveguide components' interiors. Components containing SiC terminations generally used an inverted channel along the guide surface, with small holes into the channel from the waveguide and the outside, suitably staggered. The channel dimension is small enough to be beyond the fifth harmonic cutoff; holes are spaced such that the channel length between holes is at least five times the hole diameter. This keeps the rf leakage per hole down to -150 dB or less. The channel type vent shown in Figure 3.7a, was used on the two power monitors and the diplexer termination.

In other components, vertical tunnels were used, retaining the length to diameter ratio of five. Figure 3.7b shows the basic approach. This type was used for the harmonic filter where each of the 390 side guides required a vent. Each of the six sets of side guides is topped with a 0.794 cm (5/16 inch) aluminum bar, brazed in place to prevent rf leakage along the seams. Each side guide then has a 0.159 cm (1/16 inch) hole drilled through the bar for venting.

The third approach was used on waveguide sections which did not appear to require extensive venting, such as the optical sensor guides. Here the flange depth was used to advantage as in Figure 3.7c, and a hole about 0.159 cm (1/16 inch) was drilled through the flange and guide which have a total depth of more than 1.142 cm (7/16 inches). The 0.159 cm (1/16 inch) hole through the flange is more than adequate for most of the components that have no significant outgassing sources.

No difficulty from outgassing was experienced, and the approaches were judged to be adequate for waveguide subsystems of the type developed. Initial outgassing which would be expected in any system was rapidly removed by heating the assembly at low rf power levels, and then raising the level to the operating point. Pressure in the vacuum environment was constant at less than twice ambient for the final two-thirds of the 60 hour continuous run at over 3 kW CW.

3.3.2 Harmonic Filter

The harmonic filter was quite successful, providing performance beyond requirements. The basic design is a combination of two types of leaky wall harmonic filters. The two end sections are the conventional slotted type of Figure 3.8a, tapering the slots at the ends to obtain a good VSWR; the center section is of open-end waveguide as in Figure 3.8b. The latter is particularly effective for the higher harmonics (Reference 2) while the end sections give good harmonic absorption of the lower, more intense, harmonics with less loss than the open-end section. The filter was fabricated of 6061 aluminum alloy, using slot and tab construction with dip brazing. Terminations were type SP silicon carbide, fabricated in groups of 11 spikes to reduce mounting problems and manufacturing costs for the 390 required in the unit. The completed filter is shown in Figure 3.9.

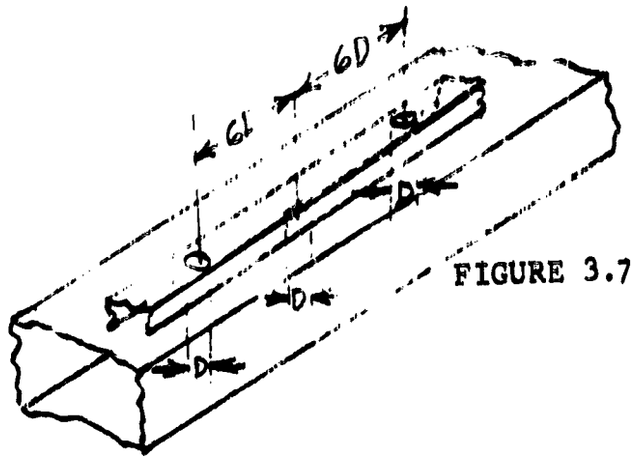

FIGURE 3.7a. Channel Type Vent

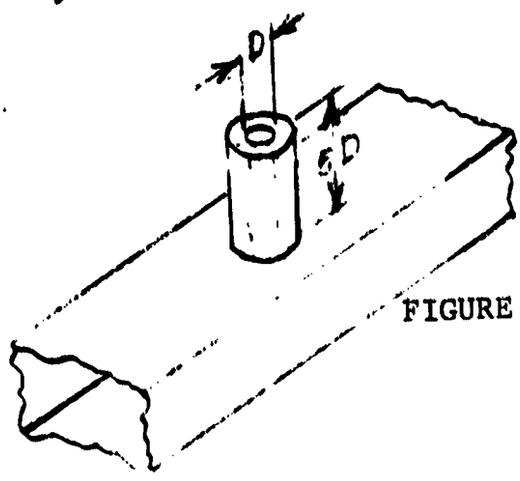

FIGURE 3.7b. Vertical Tunnel Type Vent

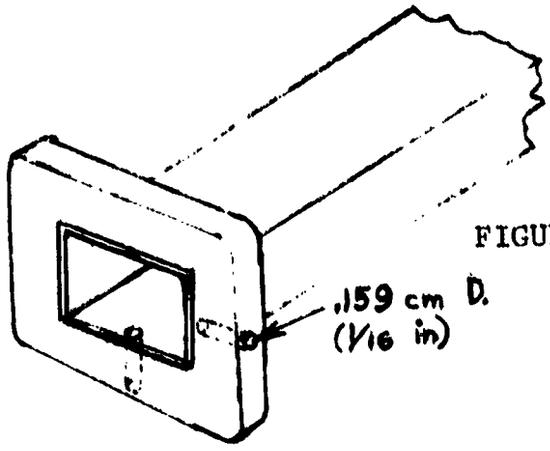

FIGURE 3.7c. Flange Type Vent

FIGURE 3.7. VENTING TECHNIQUES

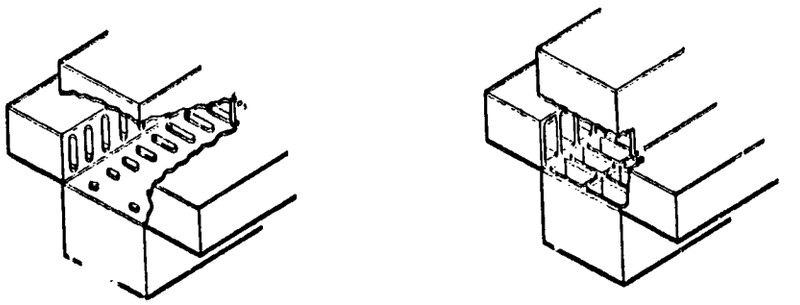

a) Leaky Wall End Sections

b) Open Guide Center Section

Figure 3.8. Approach to Harmonic Filter

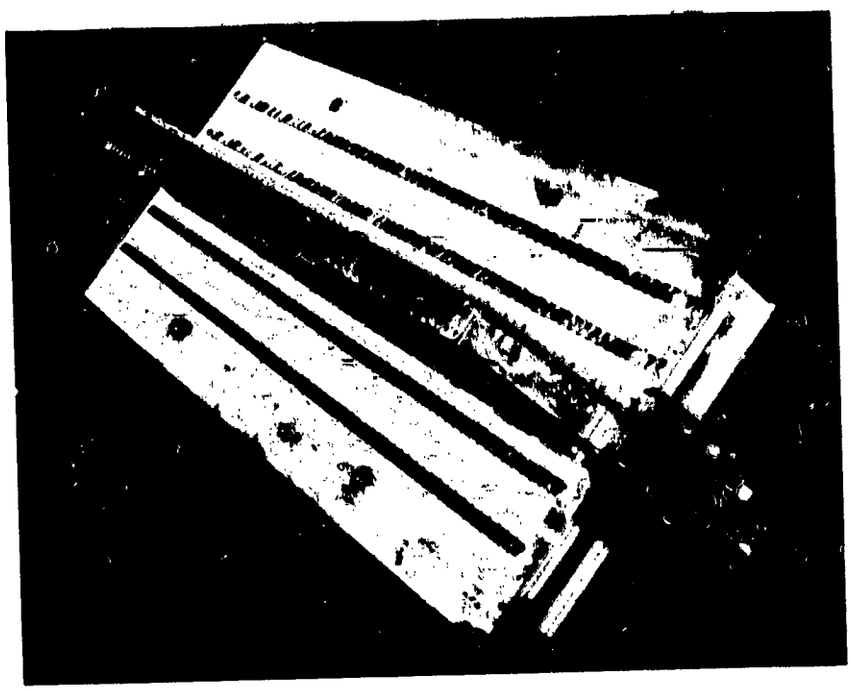

Figure 3.9. Harmonic Filter

The filter required additional matching effort to reduce it's VSWR at the test frequency of 8.36 GHz. Reflections were largely from the junctions of the end and center sections, so a small slot redesign effort is suggested to reduce this mismatch. Boron nitride dielectric irises were added for the program tests. Final results were:

Insertion Loss at f_c: 0.2 dB
Insertion Loss, Maximum in Band: 0.28 dB (at high end)
VSWR at f_c: < 1.02
VSWR over Band: $1.03 \pm .02$
2nd Harmonic Attenuation: $>$ 60 dB for TE_{10} mode
$\sim$ 39 dB minimum for TE_{01} mode

2nd Harmonic VSWR: 1.12 for TE_{10}
1.05 for TE_{01}

Estimates from low-frequency slot coupling measurements indicated the other harmonics are attenuated well within requirements, and should be about:

3rd harmonic - 23 dB
4th harmonic - 16 dB
5th harmonic - 12 dB

There were no facilities or requirements to perform these measurements. Each harmonic can take on a number of different modes, and each mode has a different attenuation. A more effective approach would be to use the actual TWT for the system, measuring the harmonics radiated by the tube alone, and by the waveguide system with the harmonic filter in place.

The particular configuration developed is ideal for 12 GHz, combining good harmonic attenuation with moderate insertion loss. This design would be very large at 2.6 GHz, so a different type might be preferred which may have a little more loss but much less weight; the loss could still be within specifications. Physically smaller harmonic filters are briefly described in Section 5.2.8.

3.3.3 Power Monitor, Reverse

The reverse power monitor is a multi-hole type, using a six hole-pair array centered on the waveguide broadwalls (Reference 3). The reverse power monitor is located as close to the transmitter tube as possible to provide a fault signal for breakdown anywhere within the waveguide system. The unit has a -21.25 dB coupling and a directivity which varied from 48 to 61 dB over the band. The impedance matching was accomplished by a slight narrowing of the waveguide at the points of reflection, resulting in a VSWR of less than 1.02 which was the measuring equipment accuracy. A photograph of the unit is in Figure 3.10.

This component was fabricated of 6061 aluminum and dip brazed. The termination is a spear of silicon carbide which was bolted to an end piece which was in turn brazed to the waveguide.

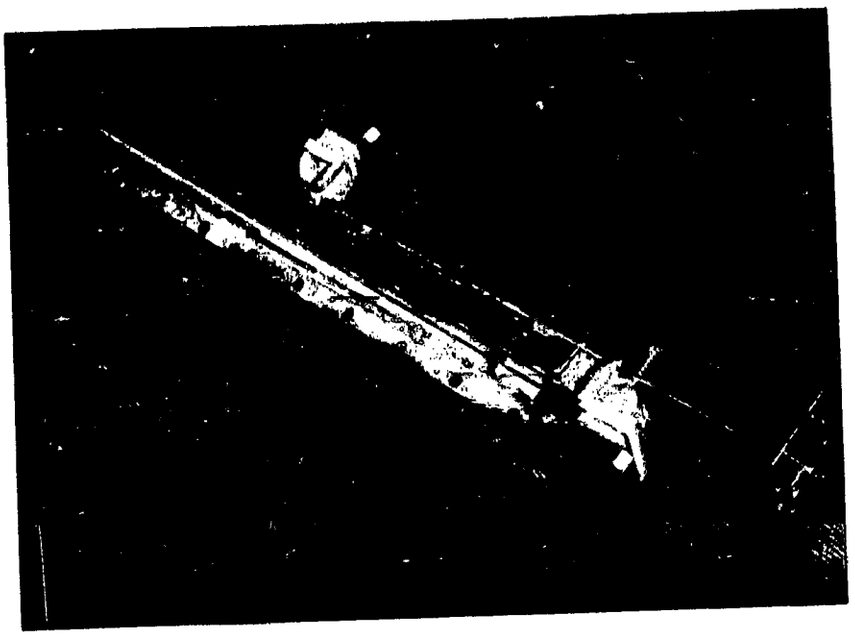

Figure 3.10. Reverse Power Monitor

This type of coupler is necessary to achieve the very high directivity specified for the reflected power accuracy. At 2.6 GHz, however, the component becomes quite large, about 0.610 meters (two feet) long. For purposes of measuring the VSWR near the transmitter tube output flange, a simpler device could be used, and the threshold of the protective circuitry using the signal be adjusted accordingly. A further evaluation of the necessity for the very high reflected power accuracy is suggested before the high-directivity type is fabricated for low frequency operation; a loop coupler would probably suffice for most systems, as is discussed in Section 5.3.3.

3.3.4 Power Monitor, Forward

The output power of the transmitter is measured after the harmonic filter to obtain a reading as near the output terminal as possible. The monitor uses a Moreno cross-guide directional coupler (Reference 3) with a coupling of -54.4 dB across the band. This unit was impedance matched by making small depressions on the waveguide sides, resulting in a VSWR of less than 1.02, the limit in measuring accuracy. The coupler's directivity was 29.6 dB which is not critical for this component.

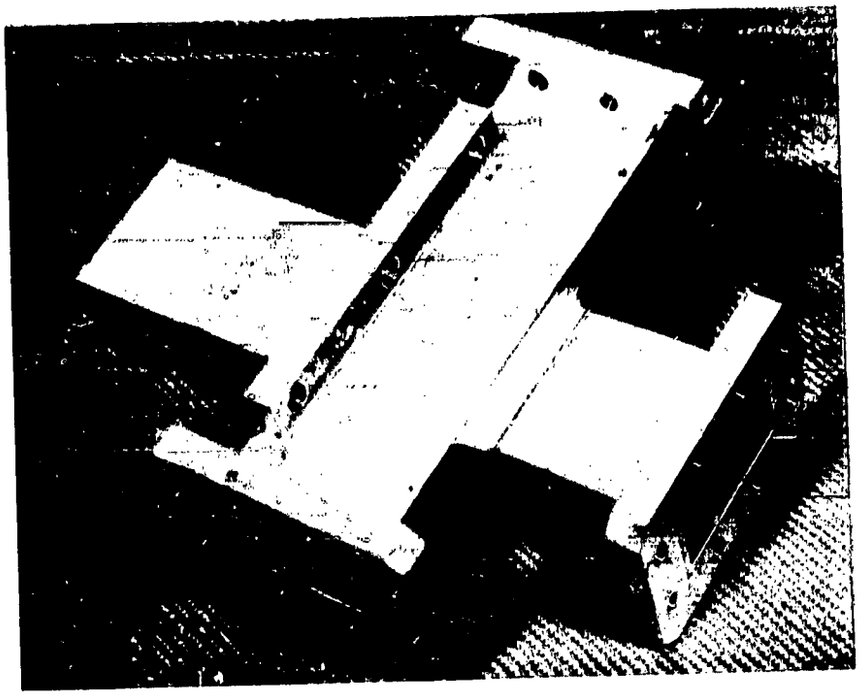

Figure 3.11. Forward Power Monitor

The cross-guide coupler was fabricated of 6061 aluminum using electron beam welding. Future units, if electron beam welded, should be fabricated from an 1100 aluminum alloy which is more suited to this type of fabrication. Alternately, dip brazing can be used. The termination is silicon carbide.

This type of coupler is recommended for 12 GHz operation and could be used at 2.6 GHz. However, a loop coupler would be adequate for the latter, and would have some weight advantage. This is considered further in Section 5.3.3.

3.3.5 Diplexer

The purpose of the diplexer is to provide an isolation between two transmitters with frequency separation but using a common antenna; these two may or may not operate simultaneously. The device is essentially a filter which passes power within it's bandpass limits, but it also has a directional characteristic so the power transmitted into the 2-port output waveguide will travel in only one direction. The sketch of Figure 3.12 shows the signal passing through the unit when in the passband (output from upper port) and being ignored by the filter when outside the passband (output from lower port). Alternately, a second transmitter out of the passband can be connected to the upper input port so that both the in-band and out-of-band signals emerge from the upper output port.

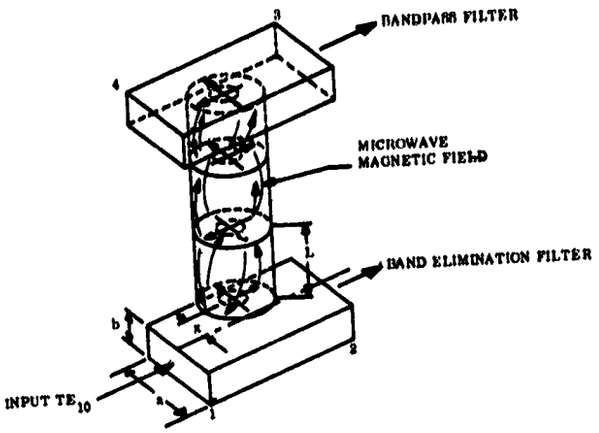

Figure 3.12. Directional Filter Operation

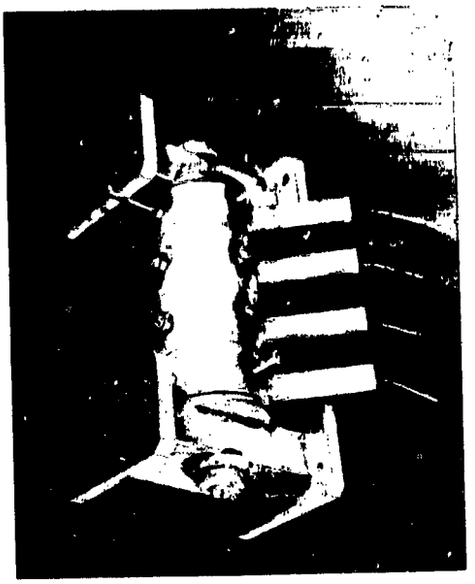

Figure 3.13. Diplexer

The directional filter is a four cavity configuration. Operation is accomplished when the input signal couples almost completely to the cylindrical cavity filter, changing from the TE_{10} mode of the rectangular waveguide to a TE111 mode in the cavities. The latter mode accounts for the relatively low loss of the unit as compared with a rectangular cavity filter. Coupling between rectangular and circular sections is accomplished at both ends by locating the coupling iris at the point where the H_x and H_z magnitudes are the same, thus inducing a circularly polarized field in the circular cavities with a linear polarization in the rectangular guide. Unfortunately, after extensive analysis and experimental work, it was discovered that the end circular irises for a four cavity filter cannot be large enough physically to provide sufficient coupling without extending beyond the waveguide wall; this was not the case of the three cavity filter which is quite well developed. Thus extending the state of the art of directional filters led to the problem of how to increase coupling between the rectangular guide and the cylindrical cavities. Three solutions were considered: adding dielectric to the iris, reducing the height of the waveguide to about 1/10 its normal height at the iris, and changing from a circular to a slotted iris. The best approach appears to be a combination of the latter two, using a three-slot coupling arrangement with undersized slots, and reducing the height of the waveguide but not as drastically as noted above.

The time schedule and resources did not permit such redesign effort so the simpler dielectric filling approach was implemented. A major problem with this approach is affixing the dielectric, boron nitride in this case, to the iris for heat conduction. An analysis indicated this should not be necessary up to about 2 kW at 8.36 GHz, but a stray resonance was found in the final unit, and high power operation was not possible. This resonance has been identified as a radial line resonance mode which could be avoided if the iris were redesigned without the dielectric loading. A visual inspection of operation at 300 watts input in a vacuum showed a bright red glow in the diplexer, evidently due to heating in the boron nitride.

The bandpass characteristic is shown in Figure 3.14. The center region is well within requirements, although a higher insertion loss was measured when the device was included in the overall waveguide assembly. The 0.3 to 0.4 dB loss is expected as normal; the measurement in the system was about 0.4 dB greater, which is about the specification limit. The heating effect of the iris indicates the

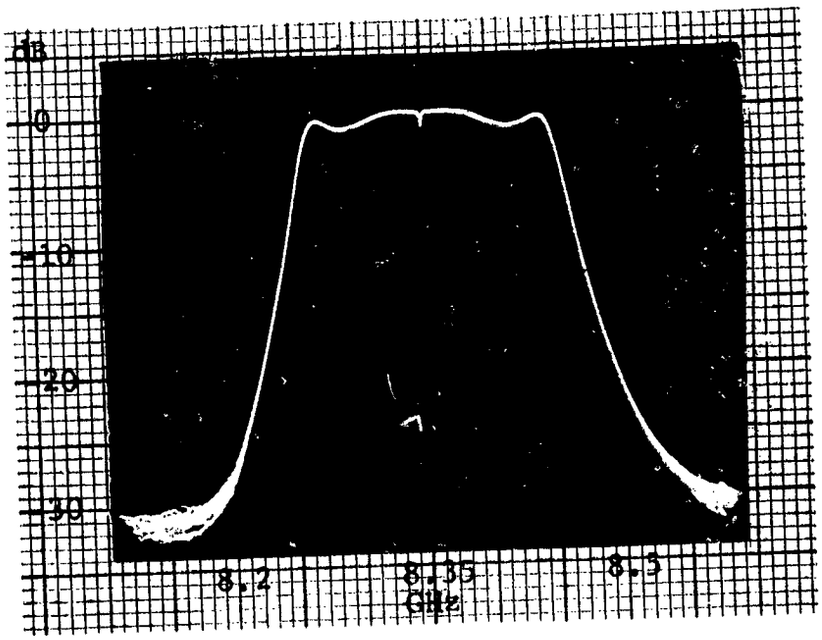

Figure 3.14. Bandpass of Diplexer

loss would tend to be greater than that first measured. The bandpass in Figure 3.14 is greater than required, but the dips in the outer regions of the Tchebycheff response are also larger than desired, indicating the filter needs additional trimming for the operational model.

The skirts of the filter show the 30 dB dropoff requirement to be accomplished in 70 MHz at the low end and in about 100 MHz at the high end; the objective was 90 MHz. The operation is considered acceptable. The slope dropoffs at the bandpass limit should improve somewhat with the dielectric removed from the two irises. The bandpass for the second transmitter channel, which would lie in the reject region of this filter, is considered in more detail in Section 5.4.5-1. In general, it has a negligible loss, .01 dB or better, and shows a much steeper bandedge slope than for the bandpass region.

The filter was fabricated completely of invar with a heavy silver plating; invar is a very poor conductor in itself. The parts were machined, and assembled by oven brazing. The four probes for detecting multipactor breakdown, visible in Figure 3.13, were brazed in place later; these are designed to have low rf leakage, using rf absorber inserts.

The mount for the diplexer presented the most difficult thermal problem in that the relatively small unit generated much concentrated heat. For the test system, a large aluminum block was used as the bed for the cylindrical cavities. Heavy aluminum straps were added to hold the diplexer tightly against the block and to provide a thermal path for heat generated near the top of the diplexer. In addition, a resilient gasket of high thermal conductivity material was placed between the cylinder and block to take up the differences in thermal expansions between the aluminum block (and straps) and the invar diplexer. Although this arrangement worked moderately well, the diplexer mounting design should be revised to eliminate bolted junctions as far as possible, and to braze rather than bolt the mounting block to the thermal mounting plate. The arrangement used dropped the diplexer temperature from 388°K (115°C) to 318°K (45°C) in two minutes in air, and to ambient at 295°K (22°C) in less than two additional minutes, indicating a moderately good thermal path. Specific recommendations for mounting subsequent models are included in Sections 4.3.5 and 5.4.7.

3.3.6 Electrical Breakdown Sensors

Two types of breakdown sensors were added in addition to the VSWR which is sensed by the reverse power monitor. Optical sensors use light diodes, like the EG&G SGD-100A photodiode, with a quartz rod light guide affixed to extend to the waveguide interior wall such that any light-emitting breakdowns in the waveguide would be detected. For the system developed, three diodes observe all but the final output waveguide which would be covered by a fourth unit. Configurations for a detector in a straight waveguide run and in an elbow for looking down two waveguides at right-angles are shown in Figure 3.15. Also shown is the arrangement of components within the barrel: a boron nitride seat holds the diode and quartz rod in position, an rf absorber (Lundy) is placed above the diode for low rf leakage, and a compression piece of silicon is added at the top to hold all parts firmly in position. The waveguide interior includes a shoulder to insure a solid seating for the quartz rod.

For multipactor breakdown detection, biased probes were added, flush with the waveguide wall and biased 15 volts. The diplexer was judged to have conditions closest of any of the components to those that would lead to multipactor breakdown, although none was expected and none observed. Four coaxial bypass capacitor probes were used, adding a Lundy absorber to minimize the rf leakage through the probe support tube.

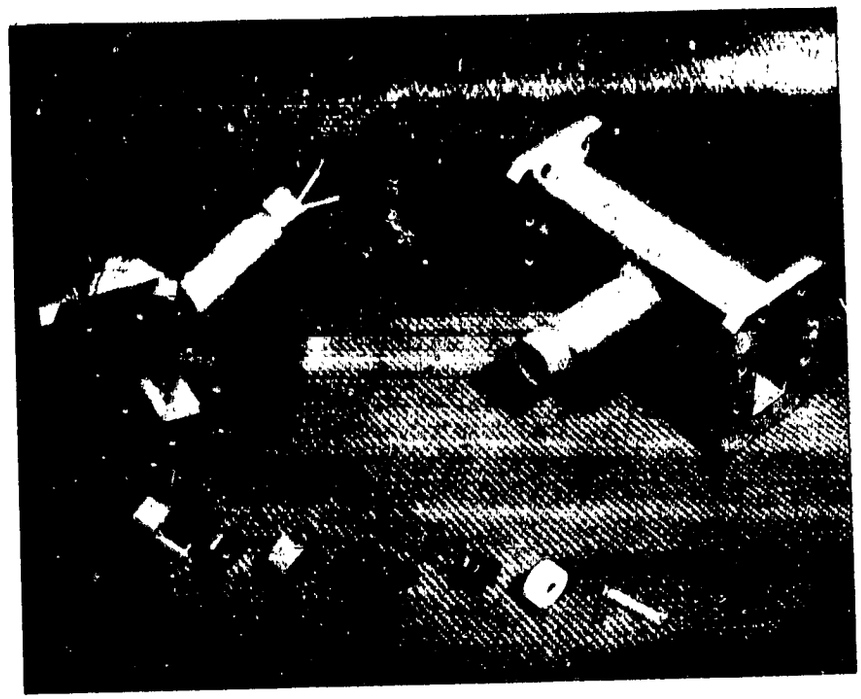

Figure 3.15. Optical Dioce Light Sensors

Both of these sensor types were tested first in the special breakdown test section described in Sections 3.4 and 5.7. Both types gave satisfactory performance, and the only engineering problem was to design the holders to have very low rf leakage. The RFI material used was adequate for the fundamental and 2nd harmonic; a longer piece, perhaps two inches, is suggested for the high harmonic isolation. The locations of the three photodiodes and the diplexer biased probes are shown in the layout of Figures 3.1 and 3.2.

3.3.7 Thermal Mounting Plate

The entire waveguide assembly was mounted on a 0.635 cm (1/4 in) thick jig plate with external dimensions of 0.610 x 0.914 meters (24 x 36 inches). The jig plate assured a flat surface for mounting the components with a good thermal interface. The temperature of the plate reached about 369°K (96°C) in the center remote from the water cooling, and about 348°K (75°C) where measured elsewhere. This is representative of the operating temperatures expected in a space application. The mounting plate used is included in Figures 3.1 and 3.2. Temperatures in the 60 hour continuous heat run could be controlled easily by the cooling water flow rate, which was about 0.95×10^{-2} m^3 (2.5 gallons) per hour.

For a 12 GHz space system a 0.318 cm (1/8 inch) thick plate should suffice. The aluminum surface should have an oxide finish applied since this has a higher emission coefficient than does bright metal. In practice, the thermal plate must be large enough to radiate all the absorbed power without exceeding the component temperature limits.

3.3.8 DC Blocking Flange

The intent of this task was to devise a waveguide flange which could tolerate 10,000 volts dc but which would have no degrading effects on the waveguide operation. The purpose of such a flange would be to permit the TWT to have a large dc voltage on the output cavity and waveguide, which would facilitate a voltage-jump TWT should one be used.

After some study, the problems became clearer, and the decision was made that this is not a practical component for the current approach because the flange must be an rf filter to keep rf leakage to a tolerable level, and also the filter must be essentially a harmonic filter since there is a stringent specification on harmonic leakage. A preferred approach, if one were to be used, is rearrange biasing to put such a flange at the TWT input where the signal is perhaps 40 dB lower, and the rf leakage is correspondingly less critical. Another problem lies in the tube, which normally would use the flange only with a voltage-jump TWT; some sort of leakage reduction technique also must be incorporated into the TWT jump section to make the whole approach effective. A substantial radiation may otherwise appear from that point on the tube.

The type of flange filter that appeared most applicable for a first development was a two-stub band-stop filter with a lossy dielectric at the periphery of the flange. The latter would also have to be a good insulator for the 10,000 volts across the flange. A possible arrangement for the flange is shown in Figure 3.16,

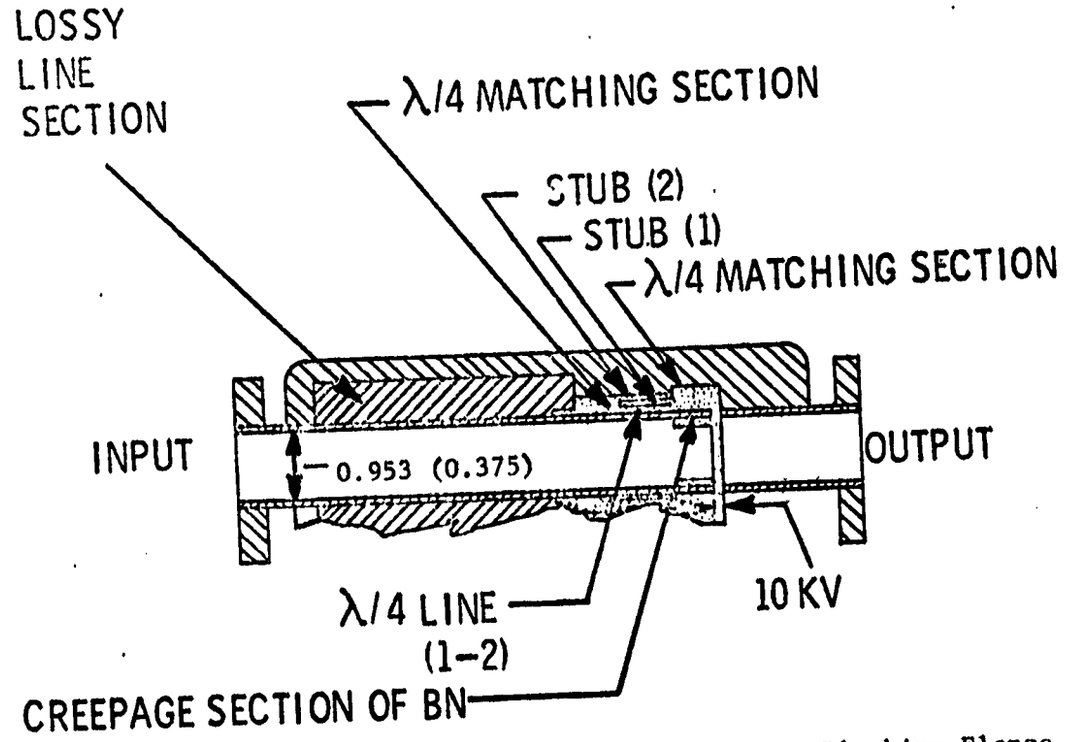

Figure 3.16. Configuration for DC High Voltage Blocking Flange

which would be fabricated largely by a series of boron-nitride depositions with suitable metal deposition to form the filter surfaces. This flange would operate satisfactorily, however, only if it were located after the harmonic filter, which would then have to be insulated to operate with 10,000 volts dc. Otherwise, the harmonic leakage of the isolation flange of Figure 3.16 could be quite large and would probably exceed leakage specifications.

3.4 SPECIAL BREAKDOWN SECTION TESTS

A low height waveguide section was fabricated to provide a means for creating electrical breakdowns under controlled conditions. For these tests, a height of .018 cm (.007 inches) was used in a half-wave long section, with two-step quarter-wave impedance matching sections at each end to match to the standard waveguide height. Three types of sensors were used to detect electrical faults; an optical diode to detect glow, biased probes (Faraday Cups) for electron flows between the two plates, and a VSWR meter. The photograph of Figure 3.17 shows the breakdown section with the top broadwall removed to make the .018 cm (.007 inch) region and the impedance matching steps visible. The optical diode used for the tests was in a separate waveguide section, as in Figure 3.15. A water cooling pipe was incorporated for possible future cw tests; it was not required for the low duty cycle pulses used here. The breakdown section tests used pulsed rf power to provide a control over the breakdown process and avoid the CW avalanch effects which would cloud the data and negate anlayses of the effects.

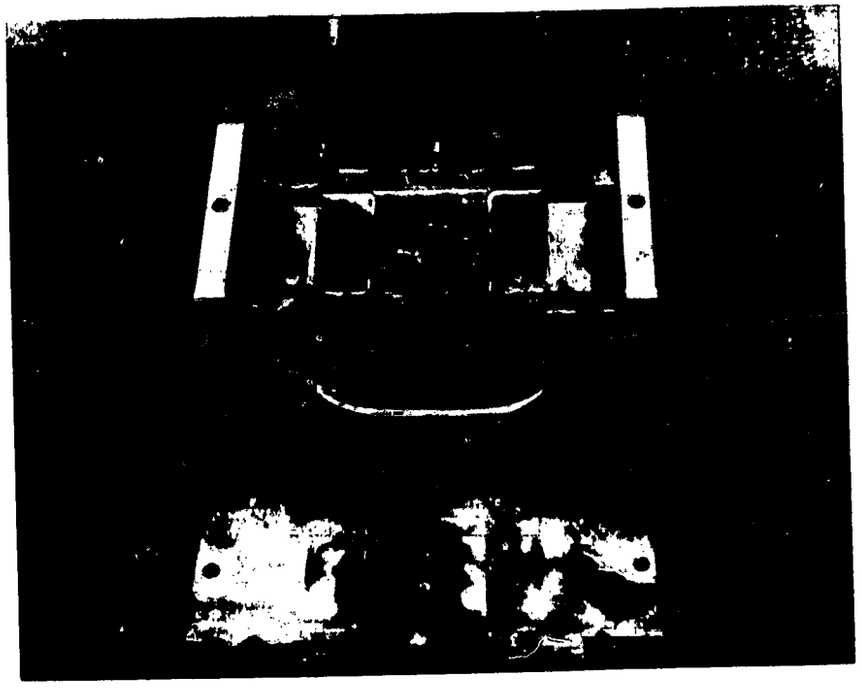

Figure 3.17. Special Electrical Breakdown Section

Tests were conducted for both multipactor breakdown and arcing, the latter requiring a substantial atmosphere. The data provided a means to compare operation with earlier results (Reference 4) as well as determining the performance of the three sensing techniques employed.

3.4.1 Multipactor Breakdown

The initial tests were to calibrate the multipactor breakdown phenomenon. Here free electrons and subsequent secondary electrons leaving the broadwalls of the waveguide oscillate between the walls in synchronism with the applied rf field. On the average, for most metals, each electron crossing between the broadwalls will dislodge more than one secondary electron from the opposite wall, which can sustain the breakdown. Nine biased probes of .127 cm (.050 inch) diameter performed as Faraday Cup type devices to detect the multipactor electrons on the waveguide broadwall.

An initial estimate indicated breakdown should occur at about 52 volts for f·d = 150 MHz-cm (reference 4), or near 630 watts. The data showed some dependency on the actual gap used so the 800 to 900 watt breakdown level observed is considered to be a verification of previous measured data. A "cleaning" process was first performed, using a low duty cycle pulsed rf signal to provide a "cleaning" function of releasing surface contamination which hindered consistency of breakdown operation.

The results showed the probes to be excellent detectors of multipactor breakdown as long as they are in the breakdown region. The current and rf power recordings of a typical test are shown in Figure 3.18. Here the peak power is about 1 kW in the multipactor region, and the current measured was about one microampere per probe through a 10,000 ohm resistor with 15 volts bias. When the peak power was reduced to 830 watts, the multipacting disappeared. These tests were made with a 3% duty cycle.

The effect of the multipacting is also evident from the cover plate of the test section, in Figure 3.17. There were no multipactor electrons in the small spaces surrounding the insulated probes. Elsewhere, the marks are quite evident. (The plate also shows arcing marks which will be discussed next.)

The optical diode was less sensitive than the probes, but gave a strong indication in a CW breakdown where the effect avalanches. The reverse power monitor had a large output also in the more drastic CW breakdown test but was somewhat erratic under the pulse conditions. The pressure in the waveguide was also measured, and indicated when a fault existed. However, it varied with power level and was not consistent enough to use as a threshold-type breakdown indicator.

3.4.2 Arc Breakdown

In a weak atmosphere, between 1.33 and 9300 N/m^2 (.01 to 70 Torr) for the equipment tested, a gas arc can occur. Tests were begin at a high pressure working toward a lower one, and then with a low pressure working upward. Tests were performed with a 3 kW pulse at a 3% duty cycle. The arcing tended to occur away from the flat surfaces of the .018 cm (.007 inch) high section, and the multipactor sensors did not register. At low pressures, around 13 to 133 N/m^2 (10^{-1} to 10^{-2}

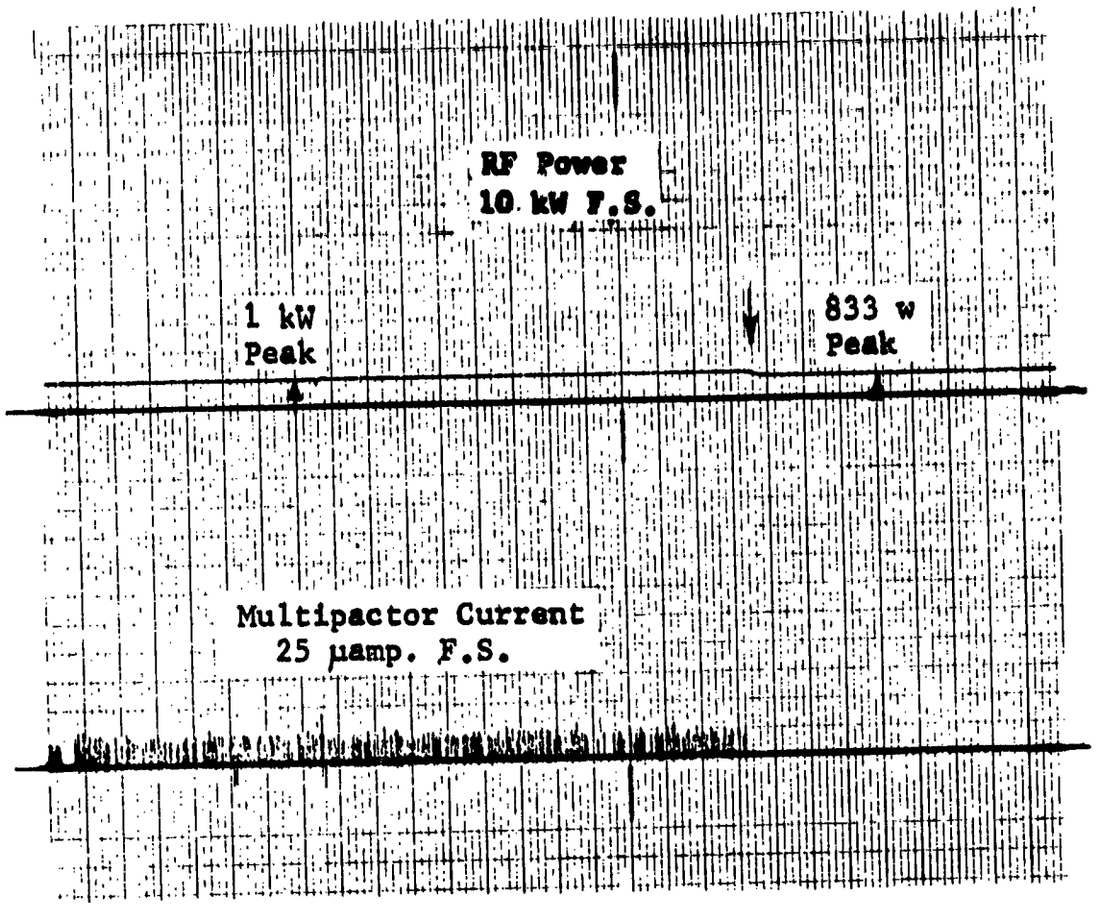

Figure 3.18. Power Level and Multipactor Current in Special Test Section

Torr), multipacting and arcing appeared to occur together, and the two types of breakdown could not be distinguished. At the higher pressures in the 53 to 106 N/m^2 (40 to 80 Torr) region, only the light diode and the VSWR sensors indicated outputs; both gave good signals. An inspection of the breakdown test section after the tests indicated strong breakdowns near the edges of the step sections; arcing frequently begins at such sharp edges. The effect can be seen in Figure 3.17.

The general conclusion is that arcing is not likely in the waveguide assembly if the vacuum is maintained below 1.33 N/m^2 (10^{-2} Torr). Where arcing is likely, the optical diode and VSWR (reverse power monitor) sensors provide good fault signals for protection of the system. Probe type sensors should not be depended upon for arc detection.

3.4.3 Magnetic Field Effects

Magnetic fields can affect the initiation and characteristics of electrical breakdowns in certain situations. A check on the breakdown section and associated waveguide indicated no tendency to break down or change characteristics. A field of over 100 Gauss was used at the breakdown section.

3.4.4 Conclusion

All three sensor types should be included in a waveguide subsystem. Their applicability is as follows:

probe, biased	- output to 30 microamps each, but location important
optical diode	- output varies widely, but indications are considered reliable for GW operation, particularly for arcing
reverse power (VSWR)	- weak indication for weak breakdowns; operates well with strong multipacting and arcing

3.5 SYSTEM IMPLICATIONS

A consideration was given to the impact of the various features of the waveguide assembly in a satellite system. In most of the interfaces, conventional engineering techniques and precautions are sufficient to insure no erupting problem areas, but care must be exereised to recognize aspects critical to a space environment.

3.5.1 Size and Weight

Size and weight are of primary concern in all satellite systems. The waveguide assembly, as such, is probably not as significant as the surface area required for cooling the components, particularly at higher frequencies. At lower frequencies, the volume and linear dimensions of the waveguide assembly become large, and efforts to reduce component size might be considered. For instance, the harmonic filter as developed would be nearly 1.5 meters (5 feet) long at 2.6 GHz (including flanges) and a smaller but more lossy type could be more desirable. For instance, a 0.25 dB loss leaky wall filter at 12 GHz would have very low loss at 2.6 GHz. A smaller one with dimensions of 0.3 to 0.6 meters (one to two feet) might have about the same 0.25 dB loss, generally considered acceptable.

In many cases, overall size is dictated by thermal considerations. A critical item is the photo-diode used for detecting the presence of arcing or multipacting; it should be held under 423°K (150°C), which places an overall temperature limit on the entire assembly which may contain three or more of these sensors. The 0.610m x 0.914m (2' x 3') plate used in this program was conservative with no diplexer, and acceptable with a diplexer.

3.5.2 Amplifier Stage

The waveguide assembly will have either a klystron or TWT as the rf power source. The waveguide input VSWR should be small for a low reflected power level at the tube's output port. Many beam type amplifier tubes cannot tolerate a significant reverse power level without becoming unstable or distorting the output signal badly. Without the diplexer, a very low VSWR is attainable; the diplexer tends to increase the VSWR, but with a good design the waveguide subsystem should still be adequate. With the diplexer as developed in this program, the VSWR had peaks as high as 1.3, but these could probably be reduced with some careful impedance matching to the 1.15 requirement. For greater reduction of reflected signal, a circulator might be used although the trade-offs for using this device will require careful consideration at higher frequencies.

3.5.3 Antenna Transmission Line

The transmission line VSWR specification is 1.1 or less, while the waveguide assembly was tuned for a matched load. The antenna mismatch can be tolerated, but final system matching should be performed with the antenna and feed line in-place at the waveguide assembly output port. Alternately, the antenna line can be tuned in advance to present a matched load.

3.5.4 Power and Breakdown Monitors

The electrical outputs of the several sensors in the waveguide assembly must be integrated into the overall transmitter system. In particular, the power monitors are used both for the telemetry subsystem (forward and reverse power monitoring) and for the fault sensing subsystem. Since the VSWR is a measure of reflected powers, an out-of-tolerance reading would indicate a fault exists. In addition, the optical diode and multipactor probe sensor outputs must be integrated into the protective logic circuitry within the system. A buffer circuit is used to convert any fault indication signals into a pulse which is used as an off trigger. The method for reinstating operation is subject to evaluation, comparing telemetry control from the ground with an on-board time-delay circuit.

3.5.5 Harmonic and Leakage Power

Neither of these are considered to be a problem in an overall satellite system using a well developed waveguide subsystem. The harmonic filter removes the harmonics very effectively while the rf leakage of the fundamental from the waveguide components is substantially lower in magnitude than the back-lobe and side-lobe power of the antenna, and possibly the leakage from the tube itself. No problems are anticipated in these areas.

3.5.6 Mechanical

The systems implications of the mechanical nature of the waveguide assembly were considered briefly in Section 3.5.1. An additional factor to be considered explicitly is the launch environment which places certain stresses on the waveguide components. The waveguide subsystem is generally considered to be mechanically adequate to meet the shock, acceleration, and vibration specifications of Section 2.3.1.

A tight and solid contact between each component and the thermal mounting plate is required of all components to insure adequate heat transfer. Thus there should be no mechanical difficulties from lack of rigidity. Exceptions are the terminations and loads, which are cantilever in configuration and the SiC used is a relatively fragile material. No mechanical tests were performed within the scope of this contract, but shake tests to destruction should be performed at some future time to determine the safety margin expected in these devices. Manufacturing techniques or configuration designs may have to be adjusted to insure sufficient strength.

3.5.7 Thermal

System specifications require operation in a 323°K (50°C) ambient environment which presents no problems except that any lossy components, of which only the diplexer is of concern, must have a sufficient radiating surface to avoid overheating of the optical diodes used as fault sensors. Testing was not performed at the low temperature specification of 193°K (-80°C), and this temperature may cause some thermal stress problems if transmitted to the TWT or klystron output window. Within the waveguide assembly, the two areas of concern are the optical diodes with temperature limitations, and the diplexer which is of invar and has a much different coefficient of expansion than does the aluminum of the mounting plate and other components. To minimize stresses, some form of automatic louver control on the thermal plate may be considered to keep the temperature from dropping as low as 193°K (-80°C).

3.5.8 System Operating Requirements

After system definition, the components required in the waveguide assembly should be reviewed, and those to be employed reconsidered if different from those of this program. Questions that will arise include the use of the diplexer versus two antennas for the two transmitters, and the use of a single antenna with switched transmitters to be operated independently. The system requirements for a specific application will determine the applicability of the subsystem developed herein and also the necessity for considering any other possible candidate components. Section IV on recommendations will expand in this area.

3.6 DRAWINGS

Drawings are provided separately to detail the construction of each component. For the purpose of this program, the components developed at 8.36 GHz are scaled directly to 12 GHz and 2.6 GHz. Where the resulting component is unwieldly or undesirable for some reason, the recommended changes in approach are included in the next Section on Recommendations.

SECTION IV. RECOMMENDATIONS

4.1 APPLICATION OF RESULTS

1) Designs are generally applicable; they may be scaled mechanically according to wavelength for operation in other bands.

2) Operational scaling effects are predictable per functions of Section 3.2.3.

3) Physically smaller components may be desirable at 2.6 GHz; suggestions are made in Section 4.3 for smaller harmonic filter and power monitors. These are less effective but may be sufficient to meet operating requirements.

4.2 SUBSYSTEM RECOMMENDATIONS

1) Single channel and two channel representative configurations are shown in Figures 4.1 and 4.2. No diplexer is required for a single channel system, but it requires a waveguide switch. The second circuit is applicable for both simultaneous or sequential two channel operation. An alternative is to use two independent transmitters with separate antennas.

2) The diplexer performs well as a harmonic filter and is shown instead of an added leaky wall type in the upper part of Figure 4.2. The loss is somewhat higher but is acceptable where the diplexer is required anyway. It could also serve as a harmonic filter at lower frequencies where the large size of the leaky wall type is undesirable.

3) Channel spacing in a two channel system should be at least 90 MHz at 12 GHz with the diplexer specified.

4) A permanent water cooling pipe should be included for ground testing.

5) Vented open construction provides breakdown-free performance in a space environment; nothing should be pressurized.

6) A waveguide switch should be developed for potential single-channel systems or for switching common-channel TWT's.

7) The RFI specification is more stringent than usually is necessary for a satellite system. Other rf leakage sources could be substantially worse, including antenna backlobes and TWT leakage from a voltage-jump junction and possibly from the depressed collector.

8) The transmitter stage should have stepped power level capability or a variable duty cycle pulse capability to accommodate residual outgassing triggered by the waveguide heating. Four or five variation steps to maximum power are adequate.

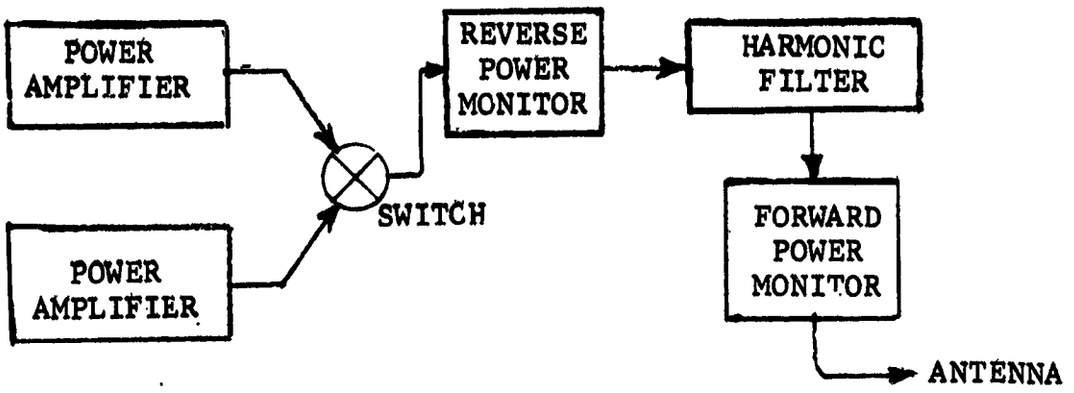

FIGURE 4.1. SINGLE CHANNEL TRANSMITTER SYSTEM

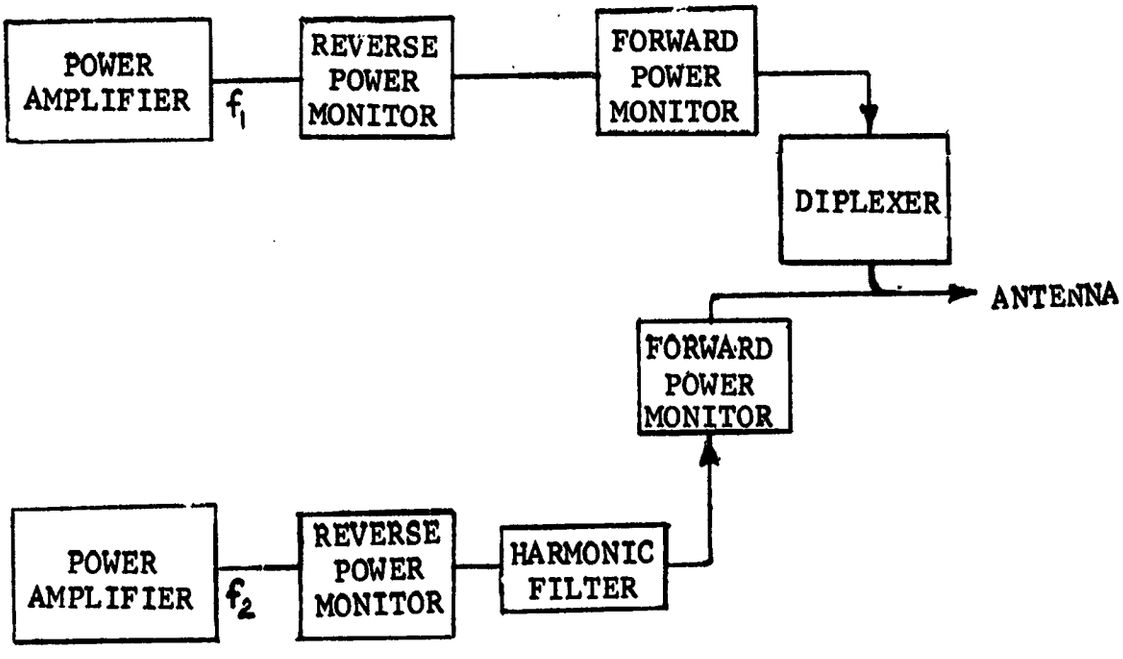

FIGURE 4.2. TWO CHANNEL TRANSMITTER SYSTEM

9) The entire equipment should be baked out before final tests in a vacuum. Heaters are also desirable to hasten outgassing in space before transmitter turn-on, particularly if low power initial operation cannot be implemented for bakeout.

10) Matching for a low VSWR can be facilitated if the antenna transmission line is well matched by itself.

4.3 COMPONENT RECOMMENDATIONS

1) In general, the components as developed form suitable models for developing space type hardware. The recommendations which follow include variations which can lead to improvements in either operation or mechanical configurations. Otherwise, the components should be used as developed.

4.3.1 Waveguide, Flanges, Gaskets, and Seals

1) The generally recommended waveguide is 6061-T6 aluminum with a silver or copper plating; alternately, an all-copper waveguide could be used. In either case, a rhodium or gold flashing is required to retard atmospheric surface contamination. Inside surface roughness should be specified as 0.254 microns (10 μin) or less to avoid an electropolishing step. Small CMR aluminum flanges are used, and these should be of 6061-T6 for a high strength. After complete assembly, each flange should be faced and lapped to obtain a flat surface. Bolts should be large enough to permit a high pressure on the seal (see Section 5.1.3). Gaskets are photo-etched soft aluminum and are good for one use only. All components must be vented, with more venting on components which are more likely to have some outgassing; vents should be small tunnels with length/diameter of at least 5/1.

2) Dip brazing is generally preferred, using tab and slot fabrication for an accurate assembly. Electron beam welding may be used with an 1100 aluminum alloy or with dissimilar metals; some warping resulted with the soft 6061-F aluminum. Heliarc welding is applicable for add-ons such as the RFI seal around the harmonic filter and the multipactor sensor tubes for the diplexer.

3) Invar waveguide and flanges, with silver plating for conduction, are required for the diplexer to avoid thermal stresses at the junctions of cavities and waveguide.

4.3.2 Harmonic Filter

1) A brass model should be fabricated for impedance matching at the two points where the leaky-wall sections join the open-waveguide section. Irises or changes in slot taper can then be established for a good match before final model fabrication. This approach is preferred over adding an iris after assembly.

2) Lengths of the slotted and open-guide sections may be altered to suit impedance matching and changes in harmonic attenuation requirements. The filter is somewhat overdesigned, and could be shortened while still meeting specifications.

3) A zig-zag type of harmonic filter (see Section 5.2.8) has a small size for 2.64 GHz operation; it would generally be preferred at that frequency but becomes inefficient at higher frequencies. The diplexer developed on this program also proved to be an excellent harmonic filter although performance was evaluated at just the 2nd harmonic in this program.

4) Tab and slot construction with dip brazing should be used. A die is recommended for precision cutting of the cross plates since the computer-controlled nibbler had small but significant variations.

4.3.3 Power Monitor, Reverse

1) Specification on directivity is generally more stringent than usually required, but can be achieved with the design as developed; measurement of small reflected signal should not have to be precise.

2) For lower frequencies near 2.6 GHz, a loop type coupler is much smaller and will provide reasonable operation but not up to specifications. The trade-off in size and weight versus accuracy should be assessed before a final design for low frequencies.

3) Use limiter with detector to prevent burnout in the event of a large reverse signal resulting from an electrical breakdown in the waveguide.

4) Dip brazing is recommended for fabrication.

4.3.4 Power Monitor, Forward

1) For lower frequencies near 2.6 GHz, a loop type coupler is smaller and lighter, and will provide sufficient accuracy for most operation. The trade-off in size and weight versus accuracy should be assessed before final design for low frequencies.

2) Dip brazing is recommended for fabrication.

4.3.5 Diplexer

1) Design

The computer design (Section 5.4.1) is suitable for a 3 or 4 cavity directional filter diplexer. The two problem areas in the diplexer are the input and output irises, and the thermal control. Invar must be used because of the dimensional control required of the cavities to achieve sufficient frequency stability.

2) Input/Output Irises

The analytical design of these two irises (identical for this application) showed they would have to extend outside the waveguide. The effective electrical aperture, therefore, must appear larger than the physical aperture. This can be achieved by:

- using slots which can be lengthened for tighter coupling
- using a low height (and low impedance) waveguide
- using a combination of these two techniques

The latter is recommended. The diplexer should be fabricated in brass first, and the slot irises trimmed for proper coupling. The available analysis is not precise for the large apertures used, and some trimming is required for any final design.

3) Iris Heating

A brief analysis showed the irises could become very hot by virtue of the poor thermal conductivity of invar in the substantial distance between the iris inside edges and the surface of the cylindrical cavities. Better thermal conductivity can be achieved by using a sandwich material for the irises; a heavier invar plate of .152 cm (.060 inches) thickness would provide a good mechanical stability, and a cladding of .013 cm (.005 inches) of copper on each side would provide a thermal path with less than 1/7 of the thermal resistivity of the invar alone. The iris plate should be tapered to perhaps .025 cm (.010 inches) thickness at the iris because best operation is obtained with very thin iris coupling between cavities. This should be verified in a brass model.

4) A copper-on-invar laminate can also be considered for the barrels of the cylindrical filters of the diplexer. This would provide a better thermal distribution and avoid hot spots.

5) Thermal Mounting

The thermal mounting used is sufficient for 8.36 GHz but is not considered optimum. Techniques for using a corrugated aluminum or copper interface to replace the compressible silicon are included in Section 5.4.6; this is to insure the component can tolerate the temperature ranges from 193°K (-80°C) to maximum operating temperature, have a good thermal path throughout, and avoid excessive mechanical stresses in the mounting.

6) The invar rectangular guide should be longer, 10 cm (4 inches) or more, to ease the problem of tightening the flange bolts; one bolt on each flange could not be used with the 7.5cm (3 inch) long rectangular sections.

4.3.6 Breakdown Sensors

1) All three types of sensors: optical, biased probe, and reverse power, should be incorporated into the waveguide assembly. The photodiode to detect visual breakdowns in the diplexer should be better thermally insulated to prevent overheating. It should also be made somewhat less sensitive than the other photodiodes since there will be considerable iris heating, particularly if the copper-laminant is not employed.

2) The quartz rod light guide should be thinner to insure 5th harmonic cutoff in the light diode assemblies preceeding the harmonic filter. The 0.254cm (0.1 inch) diameter rod with $\epsilon \approx 4$ should be reduced to .117cm (.046 inches) diameter for 12 GHz operation; operation will still be adequate.

3) The RFI material for the optical diodes and multipactor sensor probes may be longer, 5 to 7.5cm (2 to 3 inches). It has 14.2 dB attenuation per cm (36 dB/in), about 1/3 of the attenuation for a non-vacuum-oriented material. The greater length than 2.5cm (1 inch) would reduce possible harmonic leakage from components preceeding the harmonic filter.

4.3.7 Other Components

1) The mounting plate should be aluminum or other highly conductive metal, with an oxide surface treatment to increase radiation. Aluminum oxide is considered to be a good radiator if the thickness is greater than 7 microns (275 μin) (anodizing would be used).

2) A dc blocking flange is not recommended for the system specifications of this program. It is too complex for the harmonic attenuation required. An input waveguide blocking flange would be preferred for a TWT if one is required.

3) The lower (second) elbow should have an iris brazed into place; this can be oversize and then trimmed to minimize the reflection.

4.4 TESTING PROGRAM

1) Future models should be tested in a vacuum environment for tolerance to a 193°K (-80°C) temperature for a 60 to 90 minute period, followed by almost immediate transmitter operation in a 323°K (50°C) ambient. Simulated radiation cooling might involve some minor problems in procedures; achieving the 193°K (-80°C) would require a liquid nitrogen wall adjacent to the radiation surface of the waveguide assembly mounting plate. (Cold testing was not required in the program.)

2) Mechanical tests of shock, acceleration and vibration should be performed initially on susceptible components, particularly the SiC terminations which should tolerate the relatively conservative requirements but which have not been checked. No other components are sensitive, and would only fail in the event of some fault in fabrication.

SECTION V. DETAILED TECHNICAL RESULTS, COMPONENTS

This section details component developments. The purpose is to show the paths followed in the developments, and provide the data used for the final designs. Where the developments pointed to approaches for possible further improvements, such approaches are described.

5.1 WAVEGUIDES, FLANGES, GASKETS, AND VENTING

5.1.1 Waveguides

Selection: The waveguide assembly designed, fabricated, and tested in this program operates at a frequency of 8.36 GHz, and was designed to simulate a system as would be developed for 12 GHz, with results extended to 2.6GHz. Figure 5.1 shows the three bands considered and how they relate on a percentage basis. All operation would be near the center of the recommended frequency range so any differences among the three in terms of band location are not significant.

The 8.36 GHz was selected because of the in-place 5 kW testing facility associated with a vacuum chamber. Different phenomena, particularly electrical breakdown and thermal effects, will vary with frequency and waveguide dimensions so scaling factors are necessary to predict accurately the effects of these phenomena at the two final design frequencies of 12 and 2.64 GHz; these are discussed in Sections 3.2.3 and 5.9.

Standard waveguide sizes are used in all cases:

			Centimeters	(Inches)
12. GHz	WR75	i.d. =	0.952 x 1.905	(0.375 x 0.750)
8.36 GHz	WR112	i.d. =	1.263 x 2.850	(0.497 x 1.122)
2.64 GHz	WR340	i.d. =	4.318 x 8.636	(1.700 x 3.400)

Compensation for the different height/width ratios is included in the scaling functions of Section 5.9.

The basic waveguide used was of 6061-F aluminum alloy, to EIA Standards RS-261A except that an interior surface finish of 0.254 microns (10 microinches) RMS and an interior tolerance of $\pm$ .0254mm ($\pm$ 0.001 inch) were specified. In a flight system, 6061-T6 would be used for its better mechanical properties as a result of heat treating and aging. The availability of beryllium copper waveguide in 0.4 mm (1/64 inch) thick walls also was checked for possible use where aluminum may encounter difficulties. Both types are available in 6 to 8 weeks ARO. Weight reduction by milling the waveguide external walls is not necessary at 12 GHz where the guide weighs 0.298 kg/m (0.2 lbs./ft.), but may be desirable at 2.64 GHz where components are much larger.

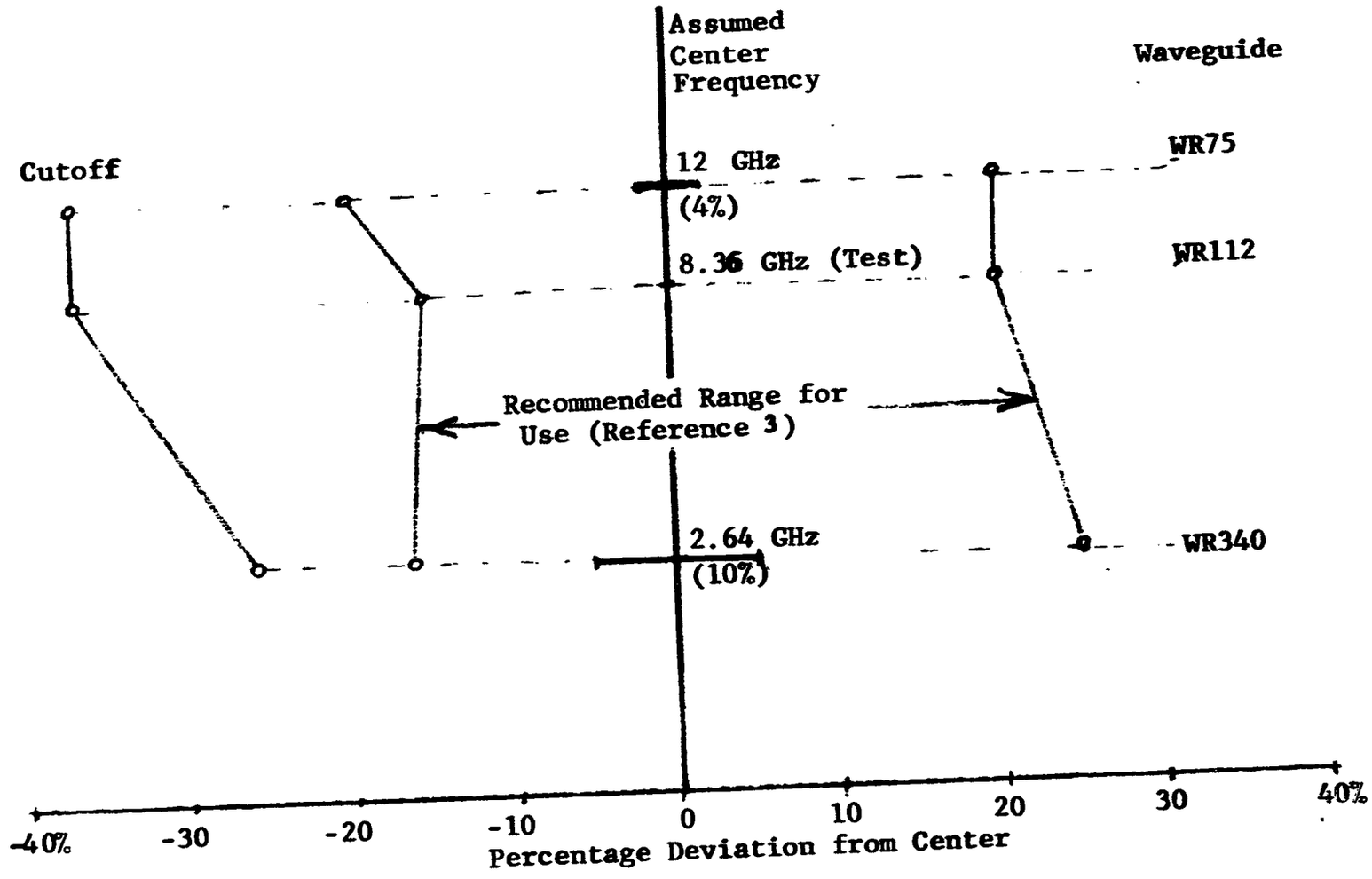

Figure 5.1. Comparisons of Three Frequency Bands Considered – TE_{10}

Several materials were considered to identify preferred ones for space waveguide subsystems. Beryllium showed the best characteristics, but is very difficult to work and was rejected. Aluminum is an excellent choice when all factors are considered, and a silver or copper plating reduces the losses considerably. Copper is also a good choice and would not require plating. Table 5.1 lists characteristics of various materials. Invar with a silver plate is required for the cavities of the diplexer which require extreme mechanical stability to avoid serious detuning as temperature varies. The rectangular waveguide connected to the diplexer cavities should also be of invar, silverplated, to avoid severe thermal stresses. A rhodium or gold flash is applied over the silver or copper to retard corrosion in the atmosphere.

Plating: Silver or copper plating can be applied by electroplating of an electroless method; the latter is particularly useful in intricate configurations. Electropolishing prior to plating will result in a smoother and less lossy interior, but it was not significant in this program because the waveguide was obtained with a 0.254 micron (10 μin) surface roughness, considered to be a reasonable value. Plating thickness should be at least three skin depths. The one-δ skin depths for aluminum and silver at the three frequencies of interest are:

f	δ_{Al}, cm	(μin)	δ_{Ag}, cm	(μin)
12 GHz	7.4×10^{-5}	(29.1)	5.7×10^{-5}	(22.4)
2.64 GHz	16×10^{-5}	(63.0)	12.4×10^{-5}	(48.9)
8.36 GHz	9×10^{-5}	(35.4)	7.0×10^{-5}	(27.6)

Thus three skin depths in silver is 1.71 to 3.72 microns (67 to 145 μin). A roughness of 0.254 microns (10 μin) increases the loss in silver by approximately 6% at S-band and about twice that at X-band over the theoretical perfect case. These losses are considered acceptable compromises when comparing loss against finishing costs for extreme smoothness. Attenuations for the three guides with silverplatings and a 0.254 micron (10 μin) roughness are listed in Table 5.2.

Assembly Methods: Fabrication techniques to be used are those available for precision work with moderately difficult metals, particularly aluminum and invar. The general methods to be used are as follows:

Aluminum: Dip braze or vacuum braze, follow with heat treatment. Electron beam welding also can be used but usually is not required.

Invar: Furnace braze

Difficult Situations involving dissimilar metals and/or critical dimensional control: Electron beam welding.

Silver Plate: Electroless process - gives uniform coverage up to a depth of 5×10^{-4} cm (2×10^{-4} in) for intricate assemblies; use at least three skin-depths to minimize diffusion effects between Al and Ag and to minimize resistive loss.

TABLE 5.1
WAVEGUIDE MATERIALS

MATERIAL	RELATIVE SURFACE RESISTIVITY	WEIGHT Kg/cm^3	WEIGHT $(\#/in^3)$	RELATIVE STIFFNESS/WT.	RELATIVE THERM.COND.	FABRICATION COMPLEXITY
SILVER, FINE	1.00	.0105	(.379)	0.10	1.00	LOW
CA 110 COPPER	1.04	.0089	(.322)	0.52	0.87	LOW
6061 - T6 ALUMINUM	1.64	.0027	(.098)	1.00	0.37	MODERATE
CA 172 BERYLLIUM COPPER	2.02	.0083	(.298)	0.63	0.26	MODERATE
301 OR 304 STAINLESS	6.71	.0080	(.290)	0.95	0.039	MODERATE
INVAR	7.18	.0081	(.293)	0.70	0.025	MODERATE
BERYLLIUM	1.67	.0018	(.066)	6.7	0.41	VERY HIGH
MAGNESIUM A 63A	2.84	.0018	(.066)	0.66	0.18	MODERATE

- 6061-T ALUMINUM CHOSEN AS BASIC WAVEGUIDE MATERIAL
- INVAR TO BE USED FOR DIPLEXER
- MATERIALS TO BE SILVER PLATED, MAY BE RH OR AU FLASHED

TABLE 5.2
WAVEGUIDE RF LOSS

FREQUENCY	WAVEGUIDE	LOSS - IDEAL SILVER PLATE		LOSS - SILVER WITH .254 MICRON (10 μIN) ROUGHNESS		LOSS - ALUMINUM WITH .254 MICRON (10 μIN) ROUGHNESS	
		dB/m	(dB/ft)	db/m	(dB/ft)	dB/m	(dB/ft)
12. GHz	WR 75	.125	(.038)	.144	(.044)	.269	(.082)
8.36 GHz	WR 112	.076	(.023)	.082	(.025)	.131	(.040)
2.64 GHz	WR 340	.0013	(.004)	.0013	(.004)	.002	(.006)

IDEAL SILVER
OVERSIZE WAVEGUIDE 12 GHz

	cm x cm	(in x in)	
NORMAL	0.952 x 1.904	(.375 x .750)	.125 dB/m (.038 dB/ft)
MEDIUM	1.422 x 2.844	(.560 x 1.12)	.066 dB/m (.020 dB/ft)
LARGE	4.80 x 9.60	(1.89 x 3.78)	.0013 dB/m (.004 dB/ft)

Electroplating must be used for plating greater than 5×10^{-4}cm (2×10^{-4} in)

Silver Plate Protection: can use a silver-conversion rather than Au or Rh flashing

Thus the techniques available will provide for all the fabrication required for optimum space oriented waveguide components.

Electropolishing: Electropolishing was considered as a means to reduce rf losses due to roughness of waveguide interior walls (ref. 3, page 27). Electropolishing is the reverse of electroplating; it removes material from the object, more from the peaks than from the valleys, which results in less rough surface. Reducing roughness from .762 microns (30 μin) to .381 microns (15 μin) will remove about .0254 mm (.001 inch) of surface material, which is usually negligible. This amount of electropolishing should reduce losses as follows, assuming .762 microns (30 μin) initial roughness:

12 GHz	- 23.5%
8.36 GHz	- 20.7%
2.64 GHz	- 12.5%

A loss test was performed on a .305 meter (12 inch) electropolished section of waveguide but no significant improvement was observed. The conclusion was that the .254 micron (10 μin) specification placed on the waveguide vendor was met and further polishing will have little or no improvement.

Oversize Waveguide: Oversize waveguide has been considered as a means for reducing losses; typical values for two such guides are at the bottom of Table 5.2. Oversize guide would be relatively lower in effectiveness for the harmonic filter since there are many more higher order modes possible than in standard guide. The approach also may be undesirable for accurate power monitoring using directional couplers. The diplexer design may be impossibly complicated in the coupling irises. Thus the recommendations for use of oversize waveguide is limited to the run from the rf assembly output to the feed horn and would be considered only for long runs. The WR-75 waveguide has a loss of about 3.2% per meter (1% per foot), and a run of some distance would have to be involved before the oversize guide is considered advisable.

From Figure 5.2, a 12 GHz oversize rectangle waveguide, retaining the TE_{10} mode, could take on the following dimensions for a 1.64% (.0706 dB) loss per meter (0.5% or .022 dB per foot):

	cm x cm	(in x in)	
height x width =	1.42 x 2.84	(0.56 x 1.12)	(1:2)
=	2.03 x 2.03	(0.80 x 0.80)	(1:1)
=	3.56 x 1.78	(1.40 x 0.70)	(2:1)

These assumed $R_s/\eta = 7.96 \times 10^{-5}$ for silverplated aluminum. In each case, mode control becomes a problem since additional modes can be supported for the fundamental frequency as well as harmonics. Even bends, which are about the simplest component, must be designed with great care to avoid power conversion into

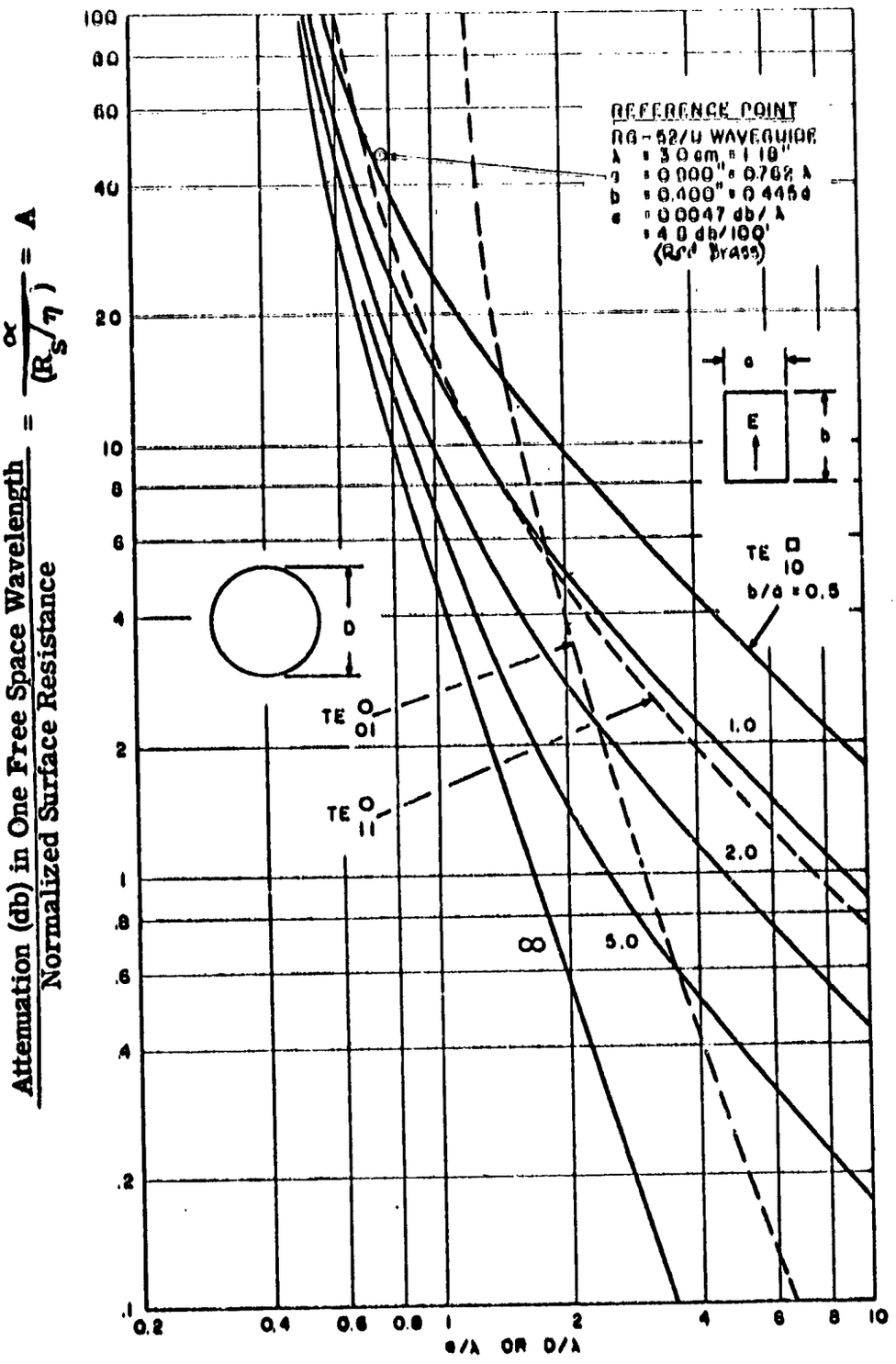

Figure 5.2. Normalized Waveguide Attenuation

unwanted modes. Transition tapers from standard size waveguide to oversize cause the generation of spurious modes, which can be minimized by using relatively long tapers. This further emphasizes the recommendation that oversize waveguide should be used only for long runs where the loss reductions would be significant and long transition tapers are tolerable.

5.1.2 Disconnect Flanges

Standard CMR type flanges were utilized for disconnect purposes between components and at the input and output terminals. (In the flight configuration, only one flanges should be bolted and all others welded after operation is satisfactory.) The CMR flange, a miniature EIA rectangular type, was shown in Figure 3.5; it is small and light, and can achieve a very tight junction when used with a sealing gasket. The eight bolts with rather close spacing can provide a high compression force between flange faces.

Other types of flanges considered were the larger CPR version of the EIA rectangular flange, a choke/cover and cover/cover type, and a quick disconnect type; these types with their relative advantages and disadvantages are in Figure 5.3.

5.1.3 Gaskets

Gaskets may be of two types: soft aluminum with a raised cross-hatch contact area, or resilient material, a silicone, with embedded silver spheres. The first type, which was shown in Figure 3.6, was used in this program. The gasket was of 6061 aluminum, .02 cm (.010 inches) thick with a cross-hatch area raised .005 cm (.002 inches) on each side. The cross-hatch pattern consisted of .0127 cm (.005 inch) width raised lines spaced .089 cm (.035 inches.) The shape of the gasket is that of the flange. This gasket requires a considerable clamping pressure to insure the flange will crush the .005 cm (.002 inch) cross-hatch region sufficiently to make a solid contact to eliminate all rf leakage. Typical pressures required to achieve a -130 dB leakage are:

12 GHz	1,043 kg	(2,300 lbs.)
8.36 GHz	1,814 kg	(4,000 lbs.)
2.64 GHz	10,000 kg	(22,000 lbs.)

These are no problem with appropriate sized stainless steel bolts. Gasket fabrication used conventional photo-etch methods. Insertion losses per gasket were computed to be:

12 GHz	0.002 dB
8.36 GHz	0.0012 dB
2.64 GHz	0.0002 dB

Resilient gaskets that may be considered are cut from Chomerics 1224 material or equivalent. This is a low outgassing silicone with a copper screen sandwiched

EIA RECTANGULAR

- ADVANTAGES
  - CMR LIGHTEST WEIGHT
  - LOW RF LEAKAGE
  - READILY AVAILABLE
- DISADVANTAGES
  - REQUIRES RF SEAL GASKET
  - TIME TO DISCONNECT
- RECOMMEND USE OF CMR MINIATURE VERSION

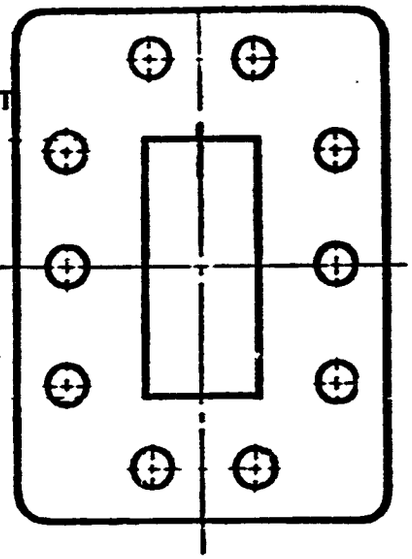

MARMAN CLAMP

AXIAL CLAMPING FORCE "F"

KNURLED

WAVEGUIDE FLANGE

SEAL

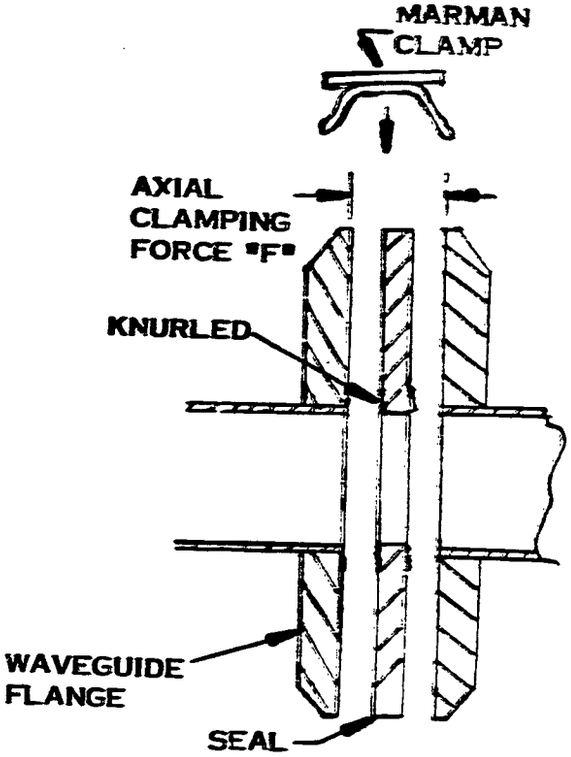

CHOKE/COVER & COVER/COVER

- ADVANTAGES
  - POPULAR USE
- DISADVANTAGES
  - LOSSY
  - RF LEAKAGE
  - HEAVY
  - VSWR
- NOT RECOMMENDED

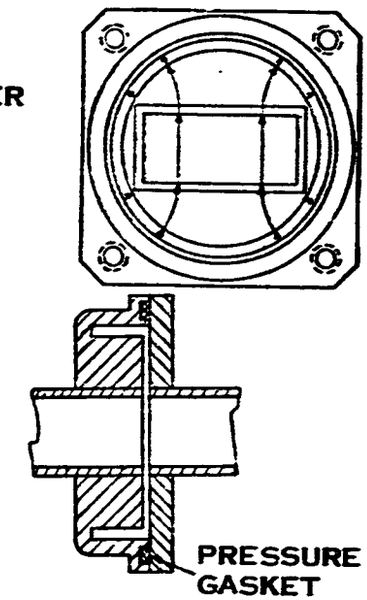

PRESSURE GASKET

QUICK DISCONNECT

- ADVANTAGES
  - LOW RF LEAKAGE
  - QUICK DISCONNECT
- DISADVANTAGES
  - HEAVY
  - REQUIRES DEVELOPMENT
- RECOMMENDED ONLY IF QUICK DISCONNECT IMPORTANT

Figure 5.3. Alternate Flange Types

for stability, and loaded with silver spheres for conductivity. The material is generally acceptable (Appendix II) since outgassing is low after a suitable bakeout and very little outgassing surface is exposed to the waveguide interior. It has a computed VSWR of 1.005 which is satisfactory, and clamping pressure is much less than for the metallic gasket:

12 GHz	36 kg	(80 lbs.)
8.36 GHz	75 kg	(165 lbs.)
2.64 GHz	750 kg	(1650 lbs.)

These gaskets may be reused, but should be cleaned and baked for use in vacuum tests. Losses will be three times that of the aluminum gasket because of its greater thickness and tendency to deform, but .006 dB per flange at 12 GHz is still quite nominal.

5.1.4 Venting

The purpose of venting is to insure that no significant amount of gas or sublimation particles can accumulate at a point within a waveguide component to cause disruptive rf arcs. The entire waveguide system is vented to give an "open" effect; a pressurized waveguide approach would result in a total system failure if a small leak ever developed. The vented system is obviously more reliable when the thermal stresses between 193°K (-80°C) and 373°K (+100°C) are considered, and the generally fragile nature of the waveguide windows and electrical connections are recognized. The task has the restriction, however, that the rf leakage from the vents must be low enough to keep the total rf leakage from all sources below the specification of -80 dBW at either 12 or 2.64 GHz. For practical considerations, the total leakage from the vents is nominally set at -130 dB, or the equivalent of -98 dBW.

Vent Size to Remove Outgassing: The initial objective of venting is to insure adequate open area for gas particles to egress. The effect of venting on gas particles can be expressed in different ways: a rate of flow of number of particles, volume change rate, or pressure change rate. The first approach is expressed by (ref. 5, page 90):

$$\frac{dN}{dt} = \frac{1}{4} v_a . A(n_2 - n_1)$$

where $\frac{dN}{dt}$ is the rate of molecule outflow, v_a is the molecular velocity (from Boyle's Law), A is the orifice area, and n_2 and n_1 are the number densities of gas particles on the high and low pressure sides of the orifice. At the coldest temperature that might exist, 193°K (-80°C) in an eclipse, the particle velocity is of the order 20,000 cm/sec (7870 in/sec) for a molecule like Al_2O_3 and 50,000 cm/sec (19,700 in/sec) for a water molecule. At a temperature of 323°K (50°C), v_a increases by 30%, so the v_a's are large in all cases. An indication of the rate of molecule outflow as a function of orifice diameter is indicated in Figure 5.4. These curves assume n_1 is negligible, or the lower pressure is much less than the high. These curves show clearly that even in the safe operating region of .0133 N/m^2 (10^{-4} Torr), an opening of .127 cm (.05 inches) diameter will pass 10^{14} molecules per second or 2.5% of the molecules in 10^3 cc (1 liter). With ten vents per 10^3 cc (1 liter), the exhaust certainly would be complete in a matter of minutes.

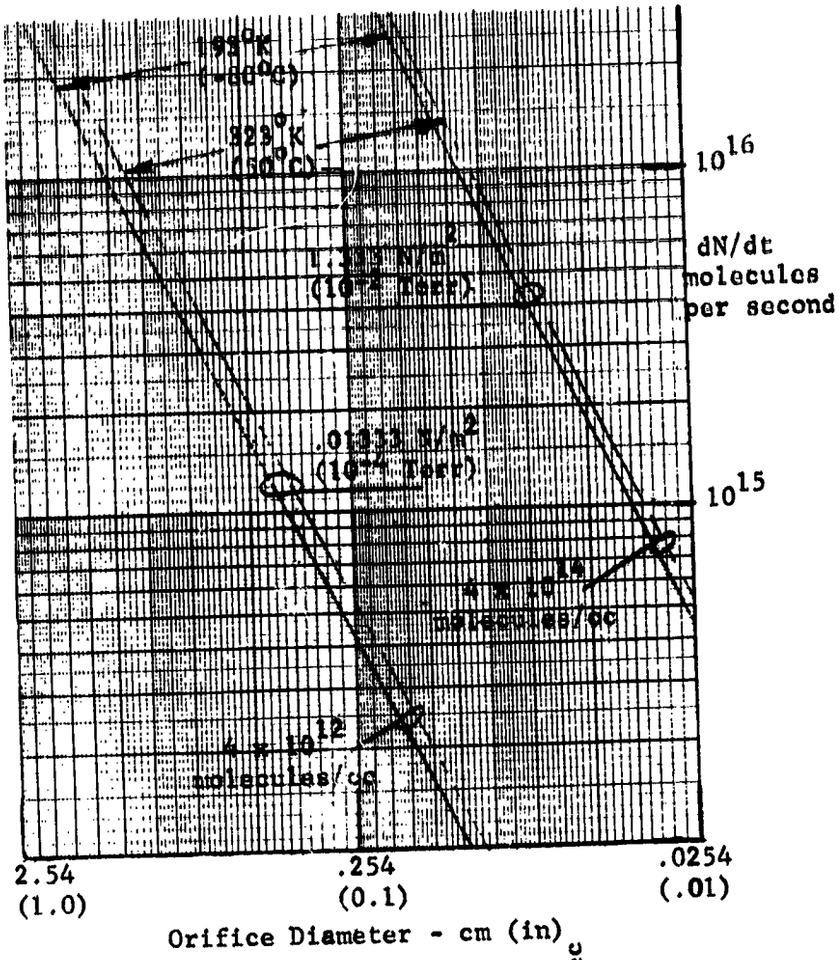

Figure 5.4

Molecular Flow Rate
Through Orifice Versus
Orifice Diameter
(for water)

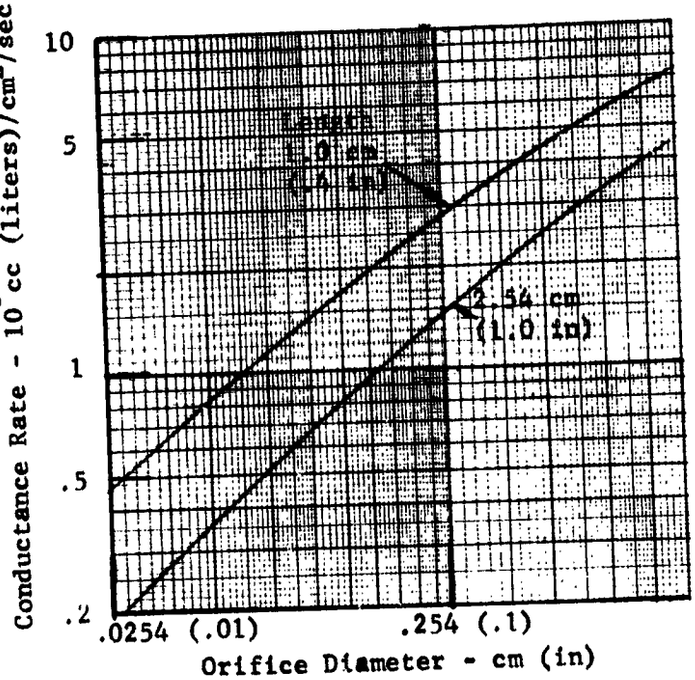

Figure 5.5

Vent Conductance Rate
Versus Orifice Diameter

The outgassing can also be expressed in cubic centimeters or liters per second per square centimeter, which is a convenient comparison parameter since 1200 cc (12 liters)/sec/cm^2 is about the maximum that can be achieved with molecular flow (mean free path large compared to dimensions of component being considered). Figure 5.5 indicates the outflow rate that would be achieved (Reference 5, page 92). From this data, it would appear that a vent size of .127 cms (.05 inches) and a length of 1.016 cm (0.4 inches) would result in a maximum conductance rate of 20 cc/sec which, again, would provide a complete outgassing function in a matter of minutes for most components which generate little contamination. A check on pressure reduction rate indicated a .127 cm (.05 inch) diameter orifice would reduce pressure by a decade in 33 seconds, again showing orifice size is not a problem.

Outgassing from metal surfaces is usually negligible after a short time in a vacuum, particularly if heat is applied such as from rf losses in a waveguide. Outgassing may be significant from oily uncleaned components, organic materials, and porous materials such as the SiC terminations used in the system. The first item can be avoided by a complete and careful cleaning process for every component and part of the system as assembly progresses. In this program, this procedure was implemented.

Organic materials are generally avoided. Some interconnecting waveguide, not a part of the subsystem, used gaskets of Chomerics 1224 material during vacuum testing. If this contributed to the residual gas in the waveguide system, the effect was negligible. However, the components for the space-oriented transmitter can avoid organic materials.

The porous termination material is not avoidable. But its effect can be minimized by baking before installing, and further heating in space for several hours before full transmitter power is applied.

Outgassing of rf absorbers is also not well defined. The GE Tube Department bakes SiC at 873°K (600°C) for 8 hours. Outgassing varies as a function of the exponential of temperature, although the expression for the variation is not simple (ref. 6, page 38). As an order of magnitude, an assumption that the simple gas law applies permits equating P/T° for the two conditions, and at 323°K (50°C), a termination size piece should outgas adequately in about a day. It would thus appear that an ambient of 323°K (50°C) and a week to permit completion of the outgassing process should suffice for SiC material. In the test program of Section 6.3.3, outgassing had stabilized at about a pressure of 6.7×10^{-4} N/m^2 (0.5×10^{-5} Torr), and was continuing at the test termination.

RF Leakage from Vents: The outgassing removal did not place any severe restriction on the orifices, but rf leakage must also be considered. For the requirement that the 5th harmonic must be attenuated, no radiation should be permitted from the vents at that harmonic. Thus the vent diameter will be smaller than the cutoff limit for cylindrical waveguide:

f	5f	D (cutoff)
12. GHz	60.0 GHz	0.292 cm (0.115 inches)
8.35 GHz	41.75 GHz	0.419 cm (0.165 ")
2.6 GHz	13.0 GHz	1.344 cm (0.529 ")

Attenuation is given by:

$$\alpha = \frac{2\pi}{\lambda c} \sqrt{1 - \left(\frac{f}{f_c}\right)^2} \quad \text{nepers/length,}$$

which applies for all cases. Practically, where α should be fairly large, f/f_c could be set at about 0.8 which would then provide an attenuation at the fifth harmonic of 19 dB per diameter of length, but would approach the limit of 31.9 dB per diameter of length for lower harmonic frequencies where frequency is much less than cutoff. Thus the maximum vent diameters should be:

12.0 GHz	0.234 cm (0.092 inches)
8.35 GHz	0.335 cm (0.132 ")
2.6 GHz	1.074 cm (0.423 ")

The length of the tunnel for each of the orifices determines the attenuation, and the total number of tubes must be considered in determining overall attenuation. To meet rf leakage requirements, vent leakage has been restricted to less than -130 dB. The number of vents used in the waveguide subsystem was about 40 plus 400 in the harmonic filter. To keep the leakage low, each of the 40 vents had a length/diameter ratio of 5, giving -160 dB leakage per vent and -143.5 dB for the total. The harmonic filter had vents with length/diameter ratios of 7, and the 400 vents should leak no more than -197 dB. In experimental tests, no rf leakage was discernible.

Vents were generally placed where outgassing was possible. All SiC terminations were vented at about one inch intervals. Other components such as straight waveguide sections were vented only at the flanges. The diameters used, actually .160 cm (.063 inches) in most cases, was adequate as can be deduced from Figures 5.4 and 5.5.

Vent Configurations

The three techniques shown in Figure 3.7 can be used in whatever form best fits a given component configuration. The type should be identified before fabrication so any materials to be added, such as the inverted channel of Figure 3.7a, can be included as an integral part of the assembly. Note that the outgassing rate for the inverted channel configuration is about half that for a straight tunnel, but this factor is not of significance.

5.2 HARMONIC FILTER

5.2.1 Performance Requirement

The specifications for the harmonic filter, as noted in Section 2.1.3, were to insure a minimum of harmonic interference from the transmitter. In addition, the filter should have a minimum detrimental effect on the transmitter performance. Pertinent specifications, all of which were bettered, are:

Attenuation: f_o = < 0.3dB

$2f_o$ = > 30dB

*$3f_o$ = >20dB

*4 and $5f_o$ =>10dB

* (These were not measured herein)

VSWR: f_o = < 1.05 at center

f_n = < 1.5

RF Leakage: f_o = less than -111.75dB
f_n = less than -91.75dB

The implication of these characteristics is that the transmitter tube may generate at least 5 significant harmonics that may be as great as -20dB, and the filter should be capable of accommodating such performance.

This is not a likely situation for the type of tube to be used at 12 GHz, which will be either a klystron or a coupled-cavity TWT and usually will have lower power at the higher harmonics. Typical values are (Reference 9):

	$2f_o$	$3f_o$	$4f_o$	$5f_o$
Klystron	-30dB	-40dB	-40dB*	-40dB*
TWT (Cavity Type)	-30dB	-40dB	-	-

(*Estimated Maximum)

Thus the attenuations noted should reduce the harmonics well beyond 50dB below the carrier. Only a helix type TWT is likely to have high power harmonics and thus would require a filter with greater attenuation.

The requirement for measuring the harmonic effectiveness of the filter was limited to include only the TE_{01} and TE_{10} modes of the second harmonic. The second harmonic can appear in five different modes with significant energy from a TWT or klystron likely in the TE_{11} and TM_{11} modes in addition to the TE_{10} and TE_{01}. The third harmonic can appear in eleven different modes, although the four mentioned will tend to predominate. By noting the relative coupling of the various harmonic modes to the harmonic attenuator cavities, the effectiveness at the unusual modes can be deduced qualitatively. This qualitative approach was considered sufficient for the higher and odd modes harmonics in present program.

5.2.2 Harmonic Filter Type Selection

Several types of harmonic filters were considered in this study. The two preferred types selected were the standard leaky-wall type and the "large-aperture" leaky wall type which were shown in Figure 3.8. Others considered but rejected for this program were:

Waffle Iron - a reflective type which is subject to multipacting (Ref. 4); absorption is preferred to reflection.

Helix Open-Periodic - data indicated poor $2f_o$ attentuation; would be excellent at $3f_o$ and higher (ref. 2).

Spiral Leaky-Wall - also had poor $2f_o$ performance but excellent higher harmonic performance (ref. 2).

Zig-Zag - physically small but high insertion loss; may be acceptable at low frequencies (ref. 7); see below.

The initial preference was for a leaky wall type which has proved to be effective, at least for the second and third harmonics (ref. 2 and 8). A typical response for this filter is shown in Fig. 5.6; this Figure also shows that the large-aperture type of leaky wall filter is more effective at the 4th and 5th harmonics.

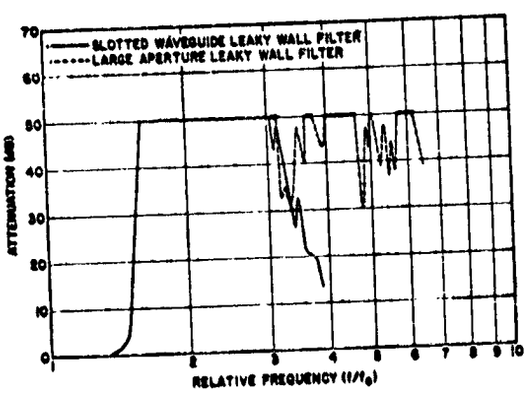

Figure 5.6 Filtering of Leaky-Wall and Large Aperture Filters

But the large-aperture type, essentially made up of open waveguide ends, would have about 0.5 dB loss at 12 GHz, compared to 0.2 dB for the slotted leaky wall type. Thus as a compromise, two short end sections of slotted leaky wall filter were separated by a short center section of the large-aperture type. The latter provides better high harmonic attentuation, and increases the overall loss by only a small amount. An all slotted type leaky wall filter might have a loss of 0.2 dB; the combination should have less than 0.3 dB. The improvement in harmonic attentuation at the 4th and 5th harmonics, and the probable higher coupling for other modes of lower harmonics, makes this approach optimum for the program.

The leaky wall filter for 8.36 GHz was about 45.7 cm (18 inches) in length. This translates to 31.8 cm (12.5 inches) at 12 GHz and to 1.45 meters (57 inches) at 2.64 GHz. Since the latter is rather unwieldy and is heavier and more voluminous than desired, the recommendation is to develop a zig-zag type for the 2.64 GHz frequency region. The general layout of this filter type is shown in Figure 5.7.

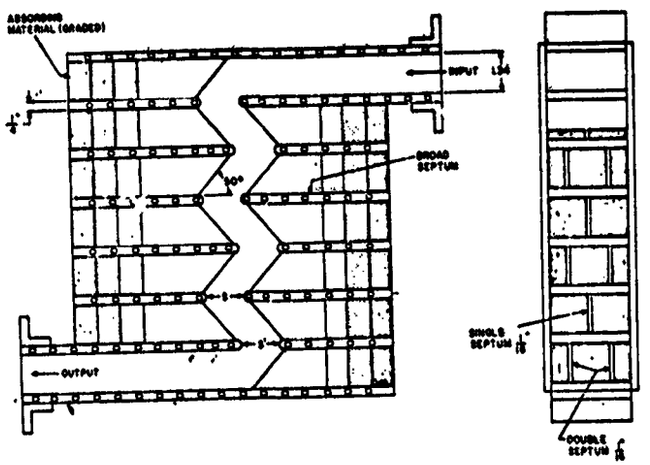

LOSSY AT HIGH FREQUENCIES
- GOOD AT S-BAND

Figure 5.7. Zig-Zag Harmonic Filter

Note it is very similar to a folded version of a large-aperture filter in that harmonics couple into attenuators through essentially open waveguide beyond fundamental frequency cutoff. The S-Band loss was estimated to be 0.25 dB; the unit would be about 35.5 cm (14 inches) square which is quite reasonable. The attenuation of this type at all harmonics of interest is 50 dB or better. It would have too much loss to be effective at 12 GHz, however, where loss is estimated at 0.55 dB or more.

For the slotted leaky-wall filter, the qualitative coupling for the broadwall and narrow-wall slots are as follows (ref. 9):

	TE_{10}	TE_{01}	TE_{11}	TM_{11}	TE_{20}	TM_{21}	TM_{31}
Broadwall	Medium	Low	High	Medium	High	Medium	Low
Narrow-Wall	Low	High	High	High	Low	High	High

These show good attenuation for all the modes noted. The large aperture center section of the filter would generally be higher in attenuation per slot. The filter length, in general, is paced by the TE_{10} mode attentuation requirement, and as long as this mode is satisfied, the other modes will be attenuated to a satisfactory level.

A technique considered but not evaluated was to use mode scramblers in a conventional leaky-wall filter to change energy content of the various harmonic modes in the filter to improve coupling to the side guides. The action is complex, however, and not easily analyzed. The above approach using large aperture coupling is preferred.

The types selected or recommended, therefore, are:

12 GHz - slotted tapered leaky wall types at ends, large-aperture leaky wall mid-section, 8.36 GHz component scaled to this type.

2.64 GHz - zig-zag type to reduce size and weight.

5.2.3 Slot Designs

The slot designs for the end sections of the filter follow a conventional design process, similar to that in reference 8. Each end of the filterhas six rows of 20 slots each, with two rows on each broadwall and one on each sidewall. The layout of the two end sections is shown in Figure 5.8, and slot dimensions are in the Table below.

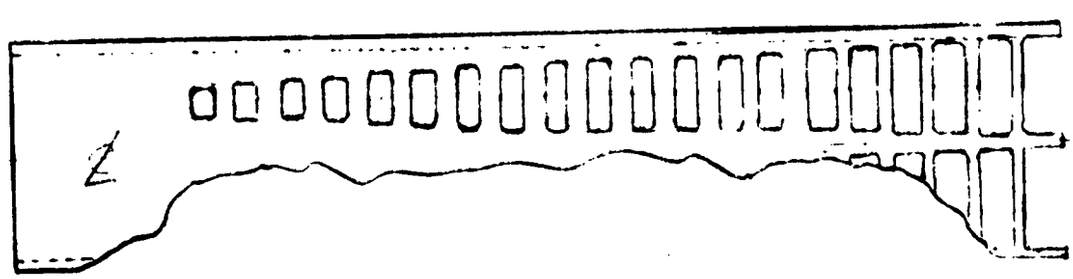

Figure 5.8. Slot Designs for Harmonic Filter

Station	Broadwall Length		Broadwall Width		Sidewall Length		Sidewall Width	
	cm	(in)	cm	(in)	cm	(in)	cm	(in)
1	.396	(.156)	.317	(.125)	.396	(.156)	.317	(.125)
2	.470	(.185)			.470	(.185)		
3	.546	(.215)			.546	(.215)		
4	.622	(.245)			.622	(.245)		
5	.698	(.275)			.698	(.275)		
6	.774	(.305)			.774	(.305)		
7	.850	(.335)			.850	(.335)		
8	.927	(.365)			.927	(.365)		
9	1.003	(.395)			1.003	(.395)		
10	1.003	(.395)			1.003	(.395)		
11	1.003	(.395)			1.003	(.395)		
12	1.003	(.395)			1.003	(.395)		
13	1.003	(.395)	.317	(.125)	1.003	(.395)	.317	(.125)
14	1.050	(.413)	.345	(.136)	1.036	(.408)	.345	(.136)
15	1.095	(.431)	.373	(.147)	1.070	(.421)	.373	(.147)
16	1.140	(.449)	.401	(.158)	1.103	(.434)	.401	(.158)
17	1.087	(.467)	.429	(.169)	1.136	(.447)	.429	(.169)
18	1.233	(.485)	.457	(.180)	1.169	(.460)	.457	(.180)
19	1.277	(.503)	.485	(.191)	1.201	(.473)	.485	(.191)
20	1.323	(.521)	.513	(.202)*	1.233	(.486)	.513	(.202)*

* Actually, these were .520 (.205) which resulted in an open end slot, per Fig. 5

The slots are spaced on 0.610 cm (0.240 inch) centers, and centered on the inside centerlines of the narrow wall and half-sidewall. The slot patterns in the first nine slots were tapered linearly to provide a gradual transition from the unslotted input waveguide to the several slots in the middle which were resonant at the second harmonic; the transistion resulted in a relatively small reflected signal from the early slots. The second tapering from slot #14 to #20 was to effect a transition to the center section which is made up of open waveguide ends. A sketch of the appearance of this taper is included in Figure 5.9. The height of the WR112 waveguide is less than half the width, so the narrow-wall slots above have a different dimension than the broadwall slots. In the case of WR75 or WR340 waveguide for 12 and 2.64 GHz, the narrow-wall slots would have the same taper as the broadwall slots.

The center section of the filter consists of 25 slots per row, and these are made up of .0762 cm (.030 inch) aluminum sheet. The waveguide wall looks like ends of waveguide cut for second harmonic operation at 16.72 GHz. The configuration is obtained in the assembly of the pieces, and does not involve a separate slotted piece of waveguide as do the two end sections.

Experimental evaluation of slot performance was performed at 3.3 GHz, which permitted measurements through the 5th harmonic with available test equipment. The tests used WR-284 waveguide with a one inch slot on one side of the broadwall. A test on the large-aperture type of coupling to an open waveguide was evaluated by using a section of WR-137 waveguide on the broadwall of the larger guide. The resulting attenuations per slot for the TE_{10} mode were:

Harmonic	2.54 x .794 cm Slot (1" x 5/16")	WR137 Slot
2	.20 dB	.14 dB
3	.08	.12
4	.035	.10
5	.022	.08

The effect of the open-waveguide type of slot is evident for the higher harmonics. The transition slots in the tapered regions would give varying amounts of attenuation and were not evaluated in detail. A check was made on a 2.54 cm (one inch) narrow wall slot with the TE_{10} mode, and coupling was low as expected, about .01 dB. However, the latter is effective for TE_{On} modes, and all TM modes.

5.2.4 Tab and Slot Assembly

The leaky wall harmonic filter involves a large number of small waveguide sections surrounding the main transmission guide. To build this component up by any way but dip brazing would be very expensive. The filter consisted of several types of parts which were precision cut, assembled by inserting tabs thru slots and twisting same to achieve a rugged egg-crate type package, and then dip brazed to electrically seal all the seams in the entire component. The initial attempt to dip braze the harmonic filter used external jigs rather than tab and slot construction, but the brazing did not fill all the seams. This was thought to be due to the extreme softening and sagging of the aluminum which reaches a temperature only about 5°K below the melting point of the aluminum, and the jig did not provide a complete support for the parts. A second filter of tab and slot construction worked very well. A couple of seams were still open, which was attributed to the minor inaccuracies in the cutting of the parts by a nibbler. This suggests that future filter parts be die cut to insure high accuracy and uniformity. Open seams in many cases lead to substantial reflected signals. Further, repairing open seams satisfactorily is very difficult because of the small openings and deep tunnels formed by the cell type of construction that results.

The filter, shown in Figure 5.9, is made up of 66 cross sections like the one shown in the figure, which hold 10 side pieces in place. In addition, two sections of WR112 waveguide are used for the tapered-slot section at each end of the filter. Dip brazing was then performed; this preceded the inclusion of the absorbing terminations used in each of the side waveguides. A cross section of the center section where the propagating waveguide is formed by the cross plate and side piece edges is shown in Figure 5.10. Included are the 20 tabs used on each of the 66 cross section members.

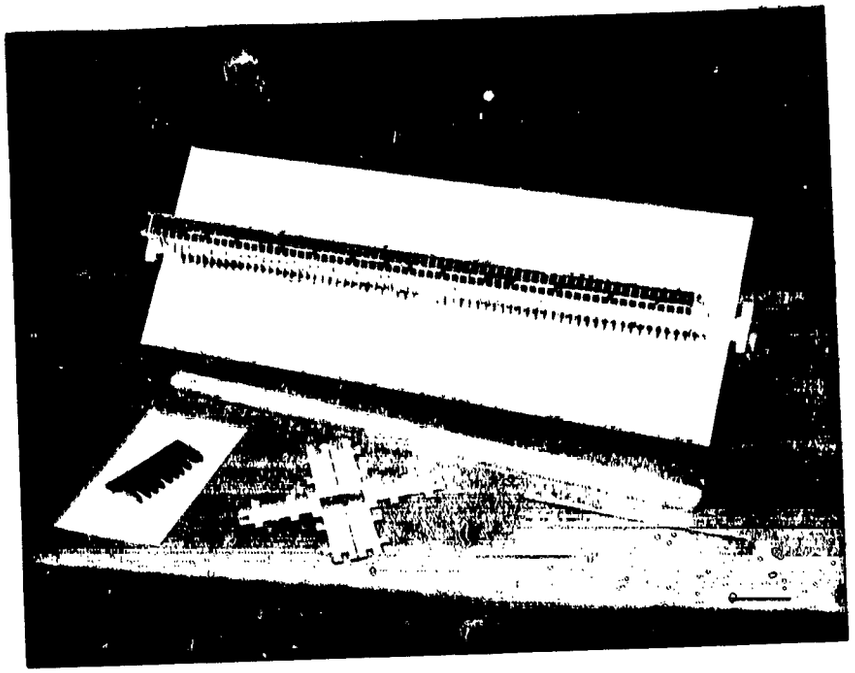

Figure 5.9 Harmonic Filter With Parts

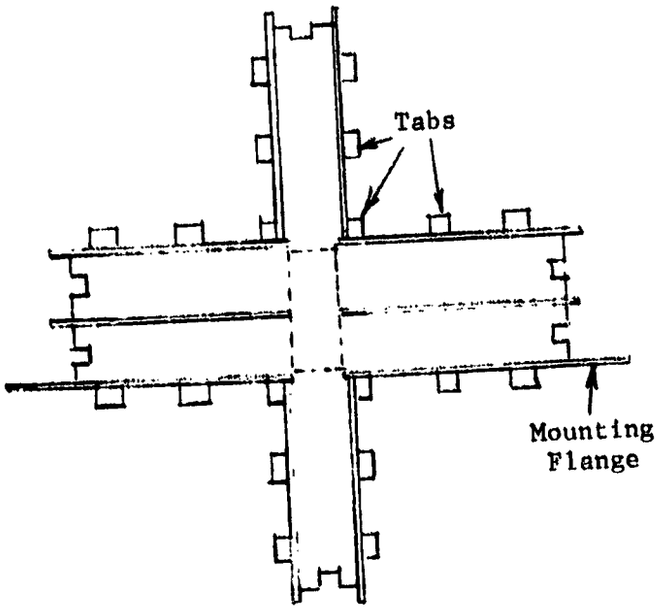

Figure 5.10 Center Cross-Section of Harmonic Filter

5.2.5 Termination Design

The harmonic filter required a total of 390 terminations for the ends of the side guides that absorb the harmonic power. Single terminations such as used elsewhere in the system used individual SiC spears, metalized and affixed with a bolt. This would be prohibitively expensive for the harmonic filter. Instead, the spears were cut in groups of 11 before firing, and thus each was able to provide the termination requirements for 11 compartments. Actually, the SiC distorted somewhat during curing, and some touchup with a diamond wheel was necessary. Some of the pieces separated, so pieces weren't all 11 units in length. However, the technique still permitted a mechanical arrangement whereby the SiC pieces were fitted into slots in the crosspieces; note the slots at the extremities of the cross section pieces of Figure 5.10.

A typical piece of the SiC termination material is included in Figure 5.10. These pieces are held in place in the egg-crate assembly by 0.8 cm (5/16 inch) thick cover plates, with an intermediate beryllium-copper strip spring. For a flight model, the latter would give better thermal transfer if it were brazed to the cover strips. The thermal absorption is relatively small in each anyway, so this is not a critical factor.

The material used was type SP silicon carbide which was found to be entirely adequate. No baking was performed, and a small amount of outgassing persisted during the tests in a vacuum. Usually, for high vacuum use, the material is baked for several hours or more at 873°K (600°C) which would be recommended. The material is used in vacuum tubes and so is suitable for a space waveguide component, particularly when vented. Venting, in this case, involved drilling .12 cm (3/64 inch) holes in the cap strip, one for each compartment in the egg-crate configuration.

Other materials considered for the terminations were:

Eccosorb ZN and NZ ferrite material

Silicon Carbide, Norton Co.

EMAiron

EMA-9030 and 9040

The materials used in formulating some of these weren't known, and there was little outgassing data. However, it appeared that they should all be applicable with a bakeout. The decision was largely on moulding capability for make a number of spears in a single piece to facilitate installation as well as to minimize cost.

5.2.6 Impedance Matching

The filter as constructed showed a remarkably good VSWR, about 1.02, but at a frequency near 8.2 GHz. At 8.36 GHz, it had increased to about 1.12 which is not within tolerance. The assembly did not lend itself to adding metal irises as required, but the main points of discontinuity were identified as being the transistion points between the slotted-leaky-guide sections on the ends and the open-waveguide large

aperture center section. The recommendation in this case was to revise the length of the center section and to build the tapered slotted sections in copper to determine a best size and arrangement of slots to minimize reflections. In addition, irises may be added in the initial fabrication, and reduced in size to an optimum value during component testing. For the current filter, two small boron nitride posts were added to achieve a reasonable impedance match. The final VSWR peaked at 1.03 at 8.45 GHz. The matching process was adjusted to show a 1.00 VSWR at center frequency on the display, which is subject only to measurement equipment variation which may be 1.02 or less.

5.2.7 Performance

The harmonic filter requires two sets of performance data: the ability to attenuate harmonics, and the ability to avoid attenuation of the fundamental. In all cases, the VSWR should be low since TWT amplifiers are quite sensitive to reflected signals at the output cavity, which can cause serious distortion in the tube.

Second harmonic attenuation was as follows:

TE_{10} mode: more than 60 db over the band

TE_{01} mode: 45 db at low end, 39 db at high end of band

The VSWR's for the second harmonic peaked at:

TE_{10} : less than 1.12

TE_{01}: less than 1.05

These are all well within the specifications of Section 2.1.3. Extrapolations to higher harmonics indicated that all harmonics will be heavily attenuated, based, for example, on the response of Figure 5.6.

Attenuation of the fundamental was also found to be low, varying from 0.16 dB at the low end, to 0.22 at center frequency, to a maximum of 0.25 at the upper frequency limit of the band. The VSWR, as mentioned above, was zeroed on the indicator of the measuring equipment at carrier, and measured 1.015 at the low end of the band and 1.03 at the peak near the upper end. A measurement of the complete waveguide assembly VSWR confirmed that an excellent match had been achieved.

5.3 POWER MONITORS

5.3.1 Reverse Power Monitor

5.3.1-1 Requirements

Reverse power is an important parameter in that TWT's and other microwave tubes are sensitive to reflected power at the output cavity. High reflected power levels lead to serious distortion of signal transfer characteristics, instability and possible damage to the tube (in extreme cases). For this program, the reflected power was to be less than .06% of the forward power (VSWR$\leq$1.05) at the carrier frequency, and more than eight times this permitted over the band. Accuracy was to be $\pm$1.5 dB which is quite difficult to accomplish with such a small signal. The directivity was determined as follows:

Reverse signal = -32.22 dB

Accuracy; allot 0.5 dB to level calibration error, 1 dB in directional coupler; then

Reverse Signal Apparent Range Limits: -31.22 to -33.22 dB

Γ range: .0218 to .02745, one half total difference = .00283

Directivity is then 20 log (.00283) = -51 dB

Directivity at VSWR = 1.15 can be computed similarly to be -41.8 dB

These directivities can be relaxed somewhat if the detector calibration error is made less than 0.5 dB; for instance, an error to 0.4 dB changes the directivities to -50.2 and -41.0 dB, respectively.

A sketch of the directional coupler used for the measurement is in Figure 5.11; the actual coupler was shown in Figure 3.10. The approach selected for

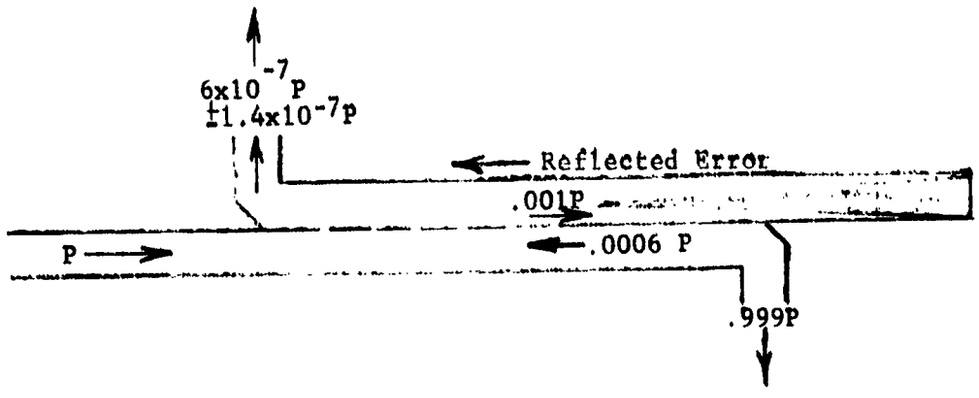

Figure 5.11. Reverse Power Monitor Relations, -30 dB Coupling

implementation of the high directivity waveguide coupler was to implement a multi-aperture array design with high directivity and good broadband coupling characteristics. In the reverse power coupler, the FORWARD wave signal is coupled into the fourth port termination at a level 32.22 dB higher than the REVERSE signal coupled into the detector port. The intrinsic directivity of the coupler can be altered adversely by the reflection of this forward signal sample from an imperfect termination. This problem was countered by controlling two factors. First, the VSWR of the termination was held to a low valve consistent with the directivity of the coupling array. In fact, it was selected so that the reflection from the termination was approximately equal to the component of the component of the FORWARD signal coupled to the detector port due to imperfect coupler directivity. Second, the termination position was determined experimentally where the approximately equal "reflection" and "directivity" components due to the forward wave are out of phase at the detector port at band center, thus, improving the overall midband directivity somewhat from that attained with the array alone. A long double tapered (pyramidal) silicon-carbide load with VSWR < 1.02 was used.

VSWR of the coupler at all three ports was minimized by inductive iris tuning at the signal input port and by optimum spacing of termination and detector port miter bend in the decoupled waveguide portion of the directional coupler.

The detector nominally measures 0.9 milliwatts under the optimum conditions. This power level would rise substantially if a large reflected signal is encountered, and with a VSWR of 1.30 as might be expected with a diplexer in the 12 GHz region, this power level becomes 25.4 milliwatts. However, with an arc or other breakdown at some point in the guide, the reflected power may approach the entire signal, which would produce a signal as high as 1.5 watts, for a 1.5 kW transmitter. To prevent this power level from damaging the diode detector, a limiter should be included. Representative solutions to this requirement are (1) a combination unit such as offered by Airtron which is rated at 1.5 watts, with limiting starting at 20 mW, or (2) the HPA 33800 detector which is rated at 0.1 watt (a little low for this application) combined with a limiter such as the Microwave Associates MA-8444-X75 which is rated for up to 2 watts average. This consideration also led to the selection of -30 dB for the coupling in the monitor since this results in convenient signal sample power levels under normal operational conditions, and implementation of detector protection is reasonable under fault conditions.

The bandwidth of the reverse power monitor is not a problem. Matching the unit to achieve the very high accuracy required is of concern but proved to be achievable with the design that evolved.

5.3.1-2 Design Approach

The design method used for the reverse power monitor followed the method of Levy (ref. 9) which showed the general design approaches and typical results for a WR90 unit. This was scaled to WR112; and the hole sizes were designed to provide the -30 dB coupling required. A sketch of the resulting hole pattern on the waveguide broadwall is shown in Figure 5.12. This coupling was placed between the two waveguides of Figure 5.11; flanges were affixed for the input, output, and detector terminals. The latter two ports required elbows to provide a means of achieving a compact two transmitter layout.

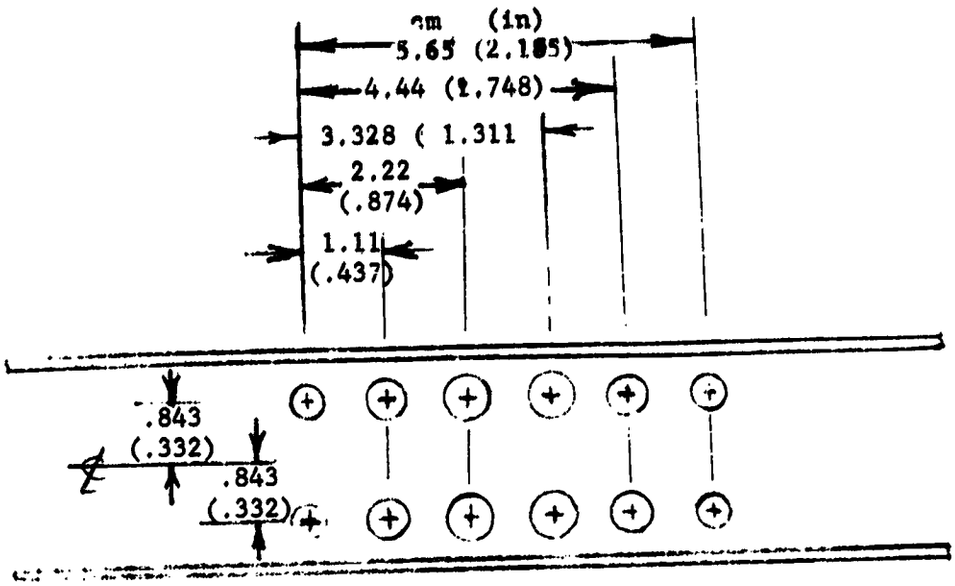

Figure 5.12. Hole Pattern for Multiaperture Coupler

The output is attached to the next component in the chain, the harmonic filter, and the detector port has a detector module attached. The fourth port is terminated as discussed previously. The predicted performance was 30.65 dB coupling and directivity varying from -48 to -61 dB over the band, using design and performance data similar to the WR90 coupler data of Figure 5.13. The measured performance was 29.6 dB coupling and variation of about $\pm$0.5 dB over than band; directivity was more than -50 dB. The unit was designed to have a total of 12 vent holes, 0.32 cm (1/8 inch) diameter, distributed along the exermal broadwalls of the waveguide used with a spacing of 1.724 cm (0.679 inches).

The termination was a 16½ cm (6½ inch) long silicon carbide spear tapered in both dimensions. A threaded insert was fastened to the large end so it could be bolted to a bracket which in turn was welded into the end of the waveguide. Before welding, the spear was positioned along the guide to give optimum directivity. It is a stock item and available from Electronautics.

5.3.1-3 Assembly

The two major sections, joined electrically by the 6-hole-pair coupling region, were of WR112 aluminum waveguide. The broadwall of the secondary section (detector and termination port) was cut so the coupling area would only be a single waveguide wall thick, .1625 cm (.064 inch) for the WR112. The flanges were the CMR112 types. The two elbows, at the output and detector ports, were MDL-112BE32 90° miter E types. These are the largest standard elbow of this particular group, and have a distance of 2.144 cms (0.844 inches) spacing between the centerline of the guide and the flange edge at the opposite end. In both cases, the waveguide wall was removed to adapt to the single-wall between the two main guides. Bolting

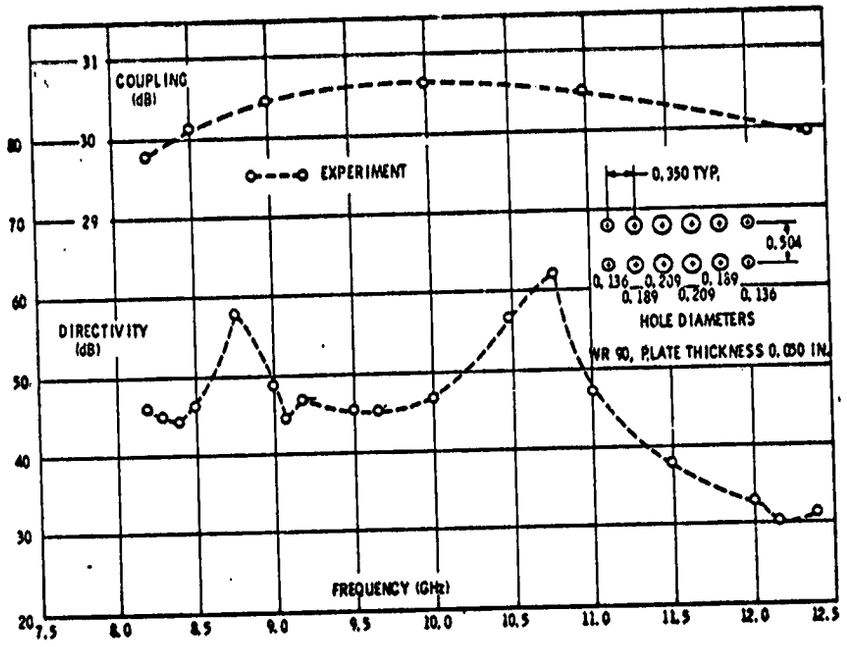

Figure 5.13. Typical Operation of Multiaperture Coupler

flanges to the thermal radiator used 8-32 bolts spaced 2.54 cm (one inch), and inverted-channel type vents were installed for outgassing control with 4 holes in the main guide and 8 in the secondary guide containing the SiC termination.

The entire unit was tack welded, jigged, and dip brazed. For dip brazed components, flanges used were the butt type, so the waveguide did not project all the way through the flange. Thus there were no breaks in the flange face. Aluminum was 6061. A small amount of warpage along the length of the component was noted; this was faced off to provide a flat, true surface to insure good contact for thermal purposes with the mounting plate.

5.3.1-4 Testing

The initial tests were to determine VSWR with a matched load. The unit required a small iris at the first elbow location, due largely to the reflections from the second elbow. The impedance matching was accomplished by a slight narrowing of the waveguide by small indentations in the narrow wall. Only a slight reduction of width was required, and this was more effective to implement than placing a metallic iris inside the guide and adjusting to size by filing. The VSWR resulting was under 1.01 and the insertion loss less than .02 dB.

Following this, the termination spear was located to provide a minimum reflected signal to the detector. By using an extremely well matched load on the output port, the effect of moving the termination was observable, and it was placed

where the reflection was a minimum at the detector, i.e. maximum directivity at midband. The termination mounting plate was then welded in place.

As noted previously, the coupling was slightly below the 30 dB objective, but coupling is not critical as long as it can be measured accurately. The directivity was also acceptable, with a level below -50 dB.

5.3.2 Forward Power Monitor

5.3.2-1 Requirements

The forward power monitor is required to measure transmitter power following the harmonic filter. An accuracy of 0.5 dB is required, which was found to be attainable with a Moreno cross-guide coupler. This is a relatively small component, and has no critical parameters. A forward coupling of -50 dB was selected to place the detector input signal at 15 mW level which is well within the linear range of the diode to be used. There is no danger of diode failure due to overload in this component because of the very light coupling set for coupling to the high power forward wave. Effect of reverse power coupling on the FORWARD power sample is negligible but a short termination of silicon carbide provided an adequate absorber for what little power was present.

5.3.2-2 Design Approach

The major design problem in the cross-guide coupler is the hole designs. These are shown in the form used in Figure 5.14 and were designed along the lines of those in standard literature (ref. 3, page 119, for example). From the guide wavelengths, the quarter-wave spacings in the direction of propagation for both the main and cross guides were:

8.36 GHz	1.153 cm	0.454 inches
12.0 GHz	0.739 cm	0.291 inches
2.64 GHz	3.88 cm	1.527 inches

The lengths of the slots and widths were computed from coupling equations developed by Bethe (ref. 10) which led to a determination of the lengths and widths of the crossed slots. Using two slots in the manner of Figure 5-14, the FORWARD coupled signal travels in the direction indicated where a detector is mounted to observe its magnitude.

The slots were designed to provide -50 dB coupling, and results were slots with lengths of .394 cm (.155 inches) and widths of .079 cm (.031 inches). These take into account the thickness factor in determining slot dimensions. The directivity of this type of coupler is theoretically -26 dB.

5.3.2-3 Assembly

The Moreno directional coupler shown earlier in Figure 3.11 was machined from two sections of waveguide, cutting a section of broad wall from one piece such that the coupling holes between the two sections were reduced thickness wall, .051 cm (0.20 inches). Flanges were placed on three ports, and the termination was placed at the fourth. Again, the termination was silicon carbide, but a piece the size

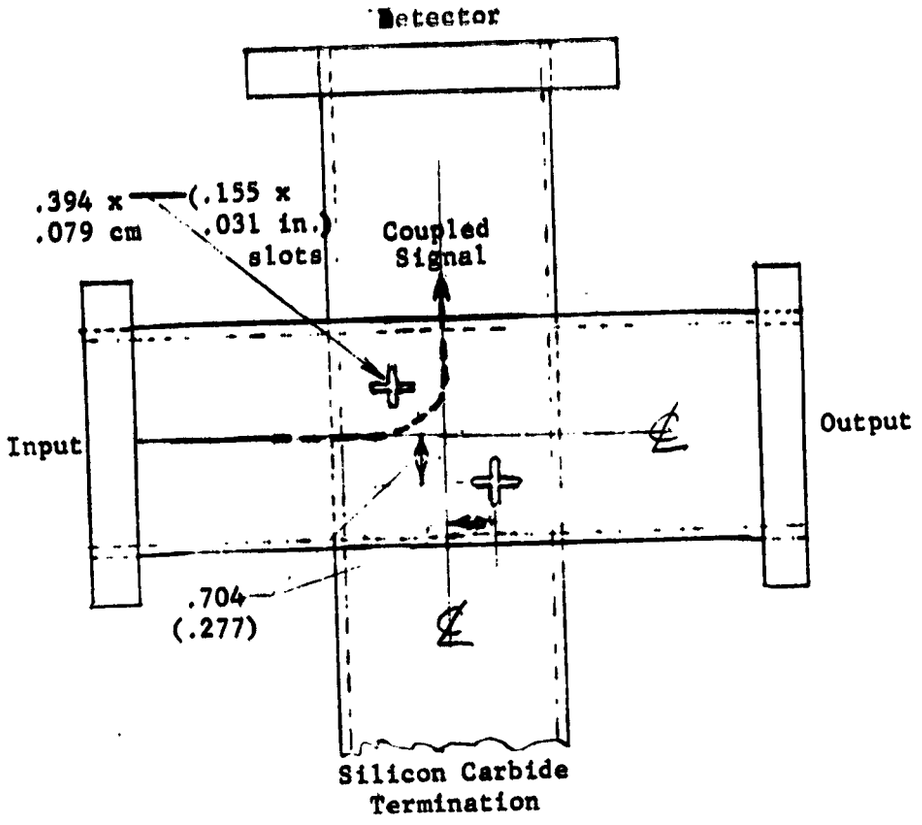

Figure 5.14. Hole Pattern for Moreno Cross-Guide Coupler

size of the waveguide interior was used with a quarter-wave input matching section formed into the material to minimize reflections. As noted, this termination does not have the severe VSWR requirements of the reverse power monitor.

The monitor was assembled by electron beam welding. Some distortion along transverse weld lines was noted (resulting in capacitive discontinuities). This distortion may have been aggrevated by the use of 6061-F aluminum alloy which does not lend itself to electron beam welding. A preferred material is an 1100 alloy. For future assemblies, dip brazing would be adequate, with electron beam welding being reserved for cases not covered by more conventional fabrication methods. The bottom of the coupler was faced to insure a good contact for thermal purposes with the mounting plate. A two-hole venting design was adopted for the secondary guide holding the silicon carbide termination; venting of the short main guide was through other components although a vent in each flange would be suggested as extra egress points in case of excessive outgassing in the system at any point.

The detector can be the same as for the reverse power monitor except no limiter is required. The termination was again adjusted to give a minimum reflection at the detector and was then welded in place via bolting to a flange which fit inside the waveguide.

5.3.2-4 Testing

Tests on the unit showed a coupling of -52 dB with a directivity of -26.5 dB. Thus the slots should be slightly larger for obtaining a -50 dB coupling, but this small difference is no particular consequence as long as its value is known accurately. A low VSWR, low loss, and 10% bandwidth were all adequate to produce no limitation on the overall subsystem operation.

5.3.3 Other Types of Couplers

The demanding specifications for the reverse power monitor led to a general evaluation of directional couplers. The type selected for the reverse monitor, the multiaperture coupler, was found to provide the best performance, but is quite large for lower frequency operation. The component at 8.36 GHz was 1161 cm (14 inches) in length, which would be about 1.117 m (44 inches) at 2.64 GHz. The cross-guide coupler could be used, but has a poor directivity. Five other forms of directional couplers were considered but generally not considered adequate for the reverse power monitor if the accuracy specified in this system is required. For the forward power coupler, the Moreno type had about the best combination of bandwidth and directivity. The several types are shown in Figure 5.15; the pertinent performance data is as follows:

Bethe-Hole:	Bandwidth 4%, Directivity 36.9 dB max. for basic design, small size and weight, bandwidth and directivity mediocre
Loop Coupler:	Bandwidth 7%, Directivity 36.9 dB max. for basic loop to waveguide design, small size and weight, considered suitable where size is important, and generally recommended for 2.64 GHz if requirements on reverse power coupler directivity can be relaxed.
Schwinger:	Bandwidth 10% but Directivity 25 dB, latter not good.
Riblet-Saad:	Performance same as Schwinger, Directivity considered poor for single hole-pair
Two-Hole Sidewall:	1% bandwidth inadequate

The loop coupler is the best type, following the multiaperture type and the Moreno cross-guide types. It is preferred where weight is critical since it requires no secondary waveguide but the signal comes off on a coaxial line which may be the detector/mount.

The loop type coupler has a disadvantage in some applications in that its sensitivity increases with frequency at 6 dB per octave. The 10% bandwidth of the 2.64 GHz band therefore would have about 0.6 dB difference in sensitivity, which would place a corresponding accuracy limit of $\pm$0.3 dB on the measurement. However, since this error is predictable, it can be biased out later in the data interpretation.

- BETHE-HOLE COUPLER

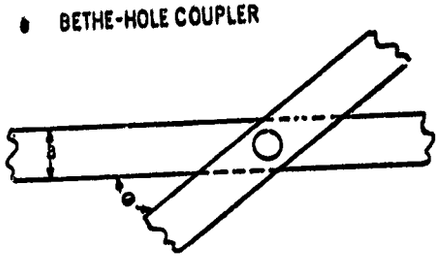

- LOOP COUPLER

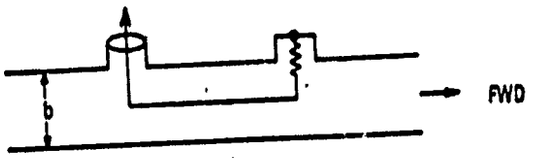

- SCHWINGER

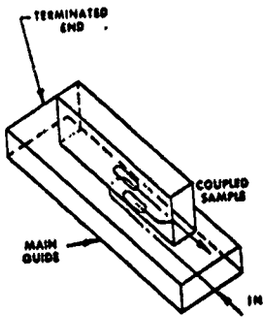

- RIBLET-SAAD

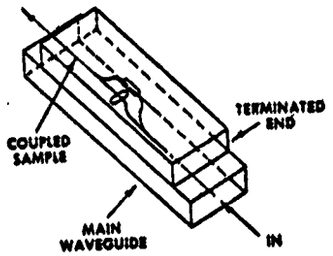

- TWO-HOLE, SIDEWALL

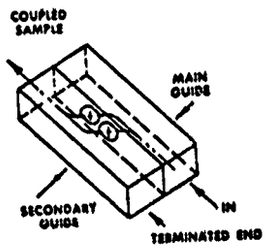

Figure 5.15. Alternate Forms of Directional Couplers Considered but Not Preferred.

5.4 DIPLEXER

5.4.1 Requirements

The diplexer is the component which permits two transmitters on different frequencies to function with a common antenna, and without mutual interference. This is accomplished by the use of a four port device incorporating a directional filter. The latter is so arranged that a signal at one end of the filter will go to only one of the two ports at its output and not the other. Also, a signal in the second port at the filter's output passes by the filter and goes out the same port, providing of course it is outside the bandpass of the filter. The sketch of Figure 3.12 showed the operation. A fourth port of the diplexer is terminated in a matched load to absorb leakage power, preventing reflection to the input ports.

The initial filter specifications of this program were for a 30 MHz bandwidth at 12.5 GHz at the -0.2 dB points; the 2.64 GHz requirement permitted a 25 MHz bandwidth. In the 12.5 GHz case. the bandpass skirt was to be 25 dB down at 50 MHz from the band edge; the 2.64 GHz case was to have the same dropoff in 25 MHz. Figure 5.16 shows the 12.5 GHz requirement, and also the theoretical performance of the three cavity filter originally proposed. A 36 MHz bandwidth is recommended (and shown) to permit some detuning from thermal and critical tuning considerations.

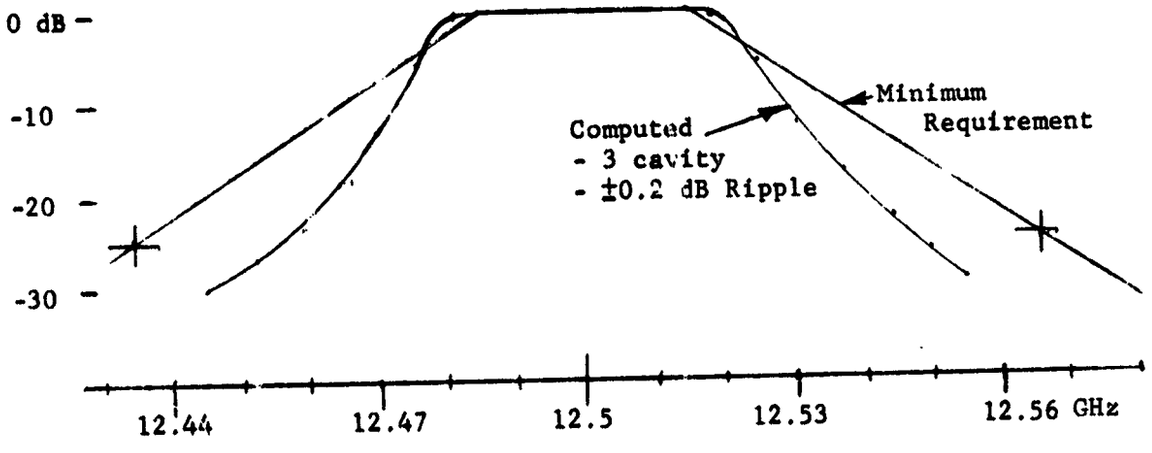

Figure 5.16. Diplexer Bandpass - Original 3-Cavity Filter

The bandpass requirements subsequently were changed substantially to have a 0.2 dB ripple bandwidth of 120 MHz at 12 GHz, a 150 MHz bandwidth at the -3 dB points, and a skirt slope dropping to -30 dB at 90 MHz from the -0.2 dB point. In both cases, the nominal insertion loss was to be less than 0.8 dB at 12 GHz and 0.4 dB at 2.64 GHz. Figure 5.17 shows the bandpass required and the theoretical bandpass as computed. The bandpass of the 8.36 GHz filter as fabricated was scaled to show an equivalent 12 GHz performance although an exact correspondence is not likely in practice. The latter would be improved with some additional trimming of irises and changing the dielectric loaded end irises to an open type. This will be discussed in more detail in Section 5.4.4.

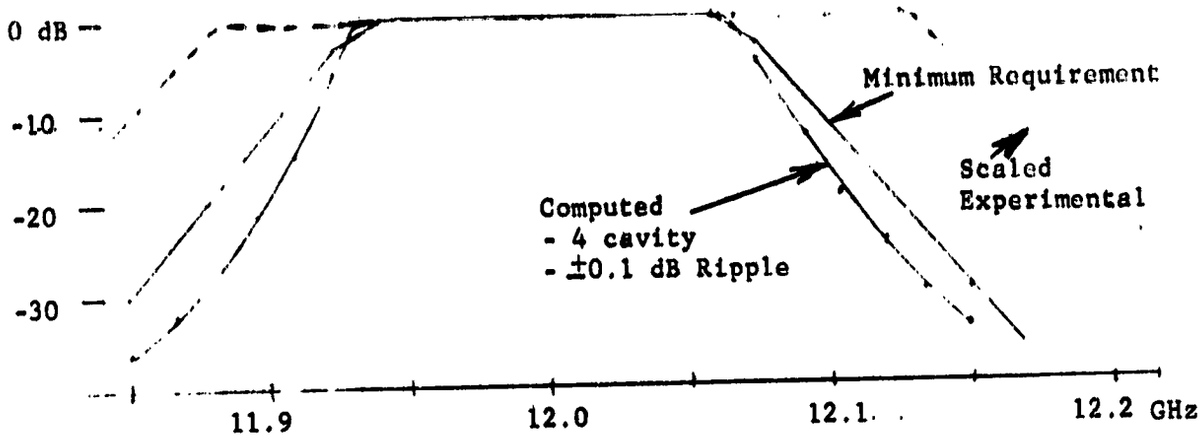

Figure 5.17. Diplexer Bandpass - 4-Cavity Filter

Other requirements for the diplexer include the ability to maintain tuning over a substantial temperature range, and survive repeated temperature swings to 193°K (-80°C) up to well over 373°K (100°C). Invar is required in the fabrication to insure accurate cavity dimensions over a reasonable range of temperatures, even though it will not have to operate at the low extreme of around 193°K (-80°C). The device, with an insertion loss of 0.8 dB, will absorb about 250 watts, which puts a considerable demand on the thermal mounting for the diplexer to get the heat to the thermal plate and distribute it as well as possible. The expected insertion loss is about half this amount, which will not present any difficulty. The invar must be silver plated to insure high Q cavities in the filter; invar by itself has extremely poor conductivity, about 1/40 of silver. The major problem in mounting is to devise a compressible member to take up the wide difference in invar and aluminum expansions. Initial calculations showed either the invar or the aluminum would fracture over a 453°K (180°C) temperature excursion if no specific relief element was included. Specific designs are postponed until Section 5.4.6 at the end of the diplexer discussion.

5.4.2 Design

Narrow-Band Design: The initial design for a three-cavity directional filter form of diplexer was developed over a period of time, and was reported some time ago in literature (ref. 11). The general design involved two rectangular waveguides having TE_{10} mode propagation coupled through three series cavities with TE_{111} modes. A circular iris couples the rectangular waveguide TE_{10} power to the circularly polarized cylindrical cavities through an iris so placed in the rectangular waveguide that the H_x and H_z components are equal. Ideally all of the energy transforms into the TE_{111} mode within the cavities, which are coupled by circular irises. Each cavity has four tuning screws to permit fine tuning to compensate for small variations in analysis approximations and dimension tolerances during fabrication. A sketch of the equivalent lumped circuit for this arrangement is included in Figure 5.18, showing the series-tuned

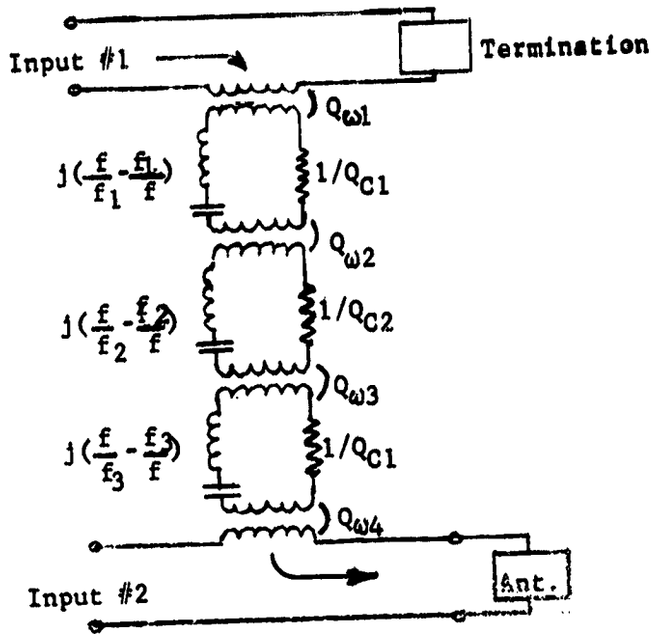

Figure 5.18. Equivalent Series Circuit of Directional Filter

version, which can also be arranged as a parallel tuned circuit. The constants are used in the equations of reference 11. The original development was incorporated into a computer program, but was modified since the diplexers equations were for a maximally flat (Butterworth) response which turns out to have poor skirt selectivity. The Tchebycheff response used had considerably steeper slopes at the band edges, and could operate well within the ±0.2 dB ripple limit for 12 GHz. These equations and computer program will not be detailed here since the requirements changed and a four-cavity filter then became necessary.

Typical design values from the computer program for f_o = 12,500 MHz were as follows:

Filter	Bandwidth	Ripple	Band Edge Attenuation*	Skirt Width at -25 dB from Band Edge
Objective	30 MHz	±0.2 dB	-0.4 dB	50 MHz (65 MHz from Center)
Butterworth	30	0	-0.4	42.3 (57.3 from Center)
3-Cavity Butterworth	36	0	-0.2	53 (71 from Center)
4-Cavity Tchebycheff	30	±0.1	-0.2	45 (60 from Center)
3-Cavity Same	36	±0.2	-0.4	26 (44 from Center)
Same	45	±0.2	-0.4	34 (56½ from Center)

(*Does not include insertion loss)

These typical combinations of parameters show that the Butterworth has broader slopes at the bandpass edges, and should be avoided. The Tchebycheff can easily provide the low ripple desired, ±0.2 dB, and provide very steep edge slopes while performing with a larger than minimum bandwidth. The 36 MHz bandwidth is considered a minimum desirable level to tolerate a small amount of thermal drift.

The computer program for this calculation can be derived from the more complex version used in the four-cavity version required for the wider bandwidth of Figure 5.17. The basic equations in all cases were extracted from Dishal's and Cohn's papers (ref. 12 and 13), combined with Williams' Butterworth filter analysis (ref. 11), with added equations relating to the coupling of the TE_{10} rectangular mode to the circular TE_{111} mode as extracted from papers by Nelson and Young (ref. 14 and 15).

Wide-Band Design: The design of a four cavity directional filter is quite complex relative to the three cavity type. The computer programs were developed for the designs of the cavities, the coupling irises, and for thick-iris corrections. The programs evolved directly from the equations of the several filter papers of literature, with an assumption of symmetry and very high Q cavities incorporated. The programs are included in Appendix III, and are in BASIC language. These specifically are:

III.A - Circular Waveguide Tchebyeheff Filter (CHEBFIL 2)
III.B - Directional Tchebycheff Filter Design (CHEBFIL 3)
III.C - Iris Hole Dia. Correction by Cohn's Corrected Eqs. (HOLCOR 2)

A typical result printout is included in each case; the designs were prepared for the 8.36 GHz operation (calculations at 8.35 GHz which was not a significant difference at this point). The first program describes the bandpass, ripple, and phase characteristics of the filter. The result was used to plot the curve of Figure 5.17 at 12 GHz. The second program led to the design of the filter in terms of the two different cavity lengths, the three iris dimensions, and the offset of the end irises in the rectangular waveguides. The third program was then used to determine corrections to the iris diameters required because of the thickness and large size of the irises. The data was derived in terms of selected initial diameters and interpolated to obtain a final design. The iris diameter correction was about a 17.6% increase over that determined from the design program.

The actual iris diameters used were slightly different from calculated; they were based on an earlier less accurate program. However, the result was a somewhat broader bandwidth than required, which is not a serious problem, and a little greater loss, about 0.4 dB worse than specification, in two small regions of the bandpass. The use of the newer design should eliminate this situation.

5.4.3 Fabrication

The entire diplexer was fabricated of invar, furnace brazed, and silver plated. The two rectangular waveguides were of invar to reduce the possibility of thermal stresses at the junction with the cylindrical filter sections. The flanges were also made of invar.

The rectangular waveguide was drawn from a piece of invar without plating, and silver plated after the unit was assembled. The cylindrical filters were cut from cylindrical bar stock and notched around the periphery. The five iris plates were from flat stock and fitted between each pair of parts of the components. Grooves .254 mm (.010 inches) square were placed at all junctions for the brazing material. The assembled unit was even brazed.

A removable bushing was placed in the outside wall of the rectangular guide that was on the input end of the diplexer, and an optical diode was mounted in the opposite rectangular guide. These were aligned with the axis of the cylindrical cavities such that when they were removed, a gold or rhodium rod could be placed through the entire unit after assembly for flashing the silver surface. The optical diode was used to observe electrical breakdowns within the diplexer if one should occur.

In addition, a multipactor probe was placed in the wall of each cavity to provide a detection means if a breakdown should occur. The probes were small coaxial by-pass capacitors trimmed such that the probe is flush with the inside wall of the cylinder. The probe was .127 cm (.050 inches) diameter in an opening of .178 cm (.070 inches) diameter. A typical by-pass capacitor is the Erie 2425-001-X5U-101AA; this particular one was 100 pfd. The capacitor was in an invar tube, and has a one inch section of RFI absorber surrounding the output lead. The probe has a +15 volt bias, and current is measured by voltage drop across a 100,000 ohm resistor in series with the probe.

The problem of RF leakage was considered to be minor. The probe opening will couple a small amount of power since the assembly acts as a coaxial probe, and will conduct all frequencies. The coupling should be less than -80 dB (ref. 3) and the RFI material was expected to add about 100 dB. However, the material was found to provide only about 40 dB, but no rf was detectable in leakage tests with a sensitivity of over 120 dBw. Future systems should use a little more RFI material, perhaps two inches, to add a margin of insurance. The RFI material used was manufactured by the Lundy company, and shows excellent performance at 8.36 GHz and all higher frequencies. Attenuation is less at 2.64 GHz, about half as many dB per inch (see Section 5.7) and multipactor probes should have perhaps 10 cm (4 inches) of material on the probe leads.

The optical diode was mounted to look through the cylindrical cavities. This was one of the three included in the assembly. Refer to Section 5.6.2 for details.

After completion of the initial design, operation was found to be different from expected, and a subtle typographical error was discovered in the literature. After correction, the input and output iris diameters were computed to be 1.726 cm (0.68 inches) while the space available within the rectangular waveguide was only 1.244 cm (0.49 inches). Thus some method for obtaining an electrical aperture larger than the physical aperture was required to obtain sufficient coupling at the two end irises. This is covered in a separate section which follows because of its relative significance to future diplexers.

5.4.4 End-Iris Problem

This program was the first in which a four-cavity directional filter was developed. After assembly and initial test, it was determined that a circular iris could not be large enough to provide the coupling required, at least with the specifications on bandwidth and ripple of this program. This circumstance required that one of three actions, or combinations thereof, be taken:

- the end irises could be loaded with a dielectric to increase coupling.
- the waveguide height could be reduced to about .127 cm (.050 inches), which could change impedance and coupling to a correct value.
- The coupling iris could be made up of three slots, each of which could be longer than the circular iris diameter, and dual slots could be used in the z direction to achieve additional coupling.

For this program, time and resources were limited, and the dielectric loading appeared to be suitable. This was finally accomplished with a .254 cm (.100 inch) thick disk of boron nitride in each of the end irises. Tests were conducted and good results achieved; these are described in Section 5.4.5. However, a problem appeared when high power operation was attempted.

This problem involved heating of the boron nitride dielectric as a consequence of a radial or circumferential resonance mode. The small air gap between the dielectric disk and the iris is just about one wavelength in circumference and is effectively two wavelengths in the dielectric. Without the dielectric, this resonance should not be significant except to heat the iris somewhat, an expected problem but of no detriment with a good silver plating on the iris edge.

The heating of the iris was such that the optical diode would trip off when the input power reached about 300 watts. The iris could be observed through the bushing in the rectangular waveguide which had a .16 cm (.063 inch) diameter hole for outgassing venting, and a definite red glow was seen to start at about the 200 watt level.

The recommendation therefore is to use a combination of the other two techniques. Three slots would be cut into the waveguide instead of the single circular iris for each end of the filter section. The requirement is only that the H_x and H_z components in the cylindrical filters be equal. The initial effort would be to determine the sizes required for the x-slot and z-slot(s) to provide sufficient coupling in each of the dimensions. With the independent slotting, the cylindrical cavities may be centered, which could ease the mechanical problems in construction and cooling. Practically, it is necessary to keep the coupling aperture smaller than the cavity internal dimensions. This may turn out to be a problem also, so a preferred approach is to design slots for more coupling than with the 1.219 cm (.480 inch) diameter circular iris, but smaller than the equivalent 1.726 cm (.680 inch) diameter required. Then the waveguide height about the iris could be reduced using the technique set forth for the special breakdown test section of waveguide, Section 5.7.

The waveguide height with no change in the present iris (in air) would require a height of about .127 cm (.050 inches), which is a function of $(R_{old}/R_{req'd})^6$. The old radius is 1.219 cm (0.480 inches) and the required is 1.719 (.705), the value from Appendix IIIB with some correction for thickness and size from Appendix IIIC. The impedance matching of a 1.219 cm (.050 inch) height waveguide would be quite difficult, so a recommended approach is to use a waveguide height of .508 cm (.200 inches) which would require an equivalent iris size of 1.422 cms (.560 inches). This should be easily accomplished with the three-slot arrangement. Such an arrangement may be as indicated in Figure 5.19. Fabrication and testing in brass will give the exact dimensions required.

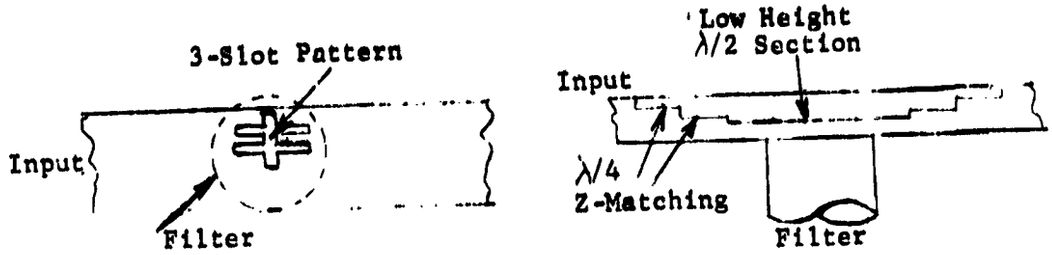

Figure 5.19. Iris Design Approaches Required

5.4.5 Testing

The diplexer was tested in terms of bandpass, insertion loss, VSWR, and skirt slope for inputs to both of the input terminals of the diplexer. The overall bandpass characteristic for the frequency within the bandpass was shown in Figure 3.14. This is wider than required, but indicated bandedge slopes to the -30 dB point of about those desired:

Specification	Upper Skirt	Lower Skirt
75 MHz from -3 dB point	85 MHz	61 MHz
90 MHz from -.4 dB point	99 MHz	73 MHz

No attempt was made to improve these. As can be noted, the tests should be performed with a larger test signal than available, but this was not considered of consequence for this program. The redesign of the end irises without the dielectric disks is expected to change the characteristics, and should provide slopes at least as good as indicated, and probably better since boron nitride has a small loss and would tend to reduce the Q's of the end cavities.

Additional test results with signal in the bandpass region are indicated in Figures 5.20 through 5.22. These indicate the signal levels in the three ports for a signal in No. 1 port. The three in order are the terminated port, trans-

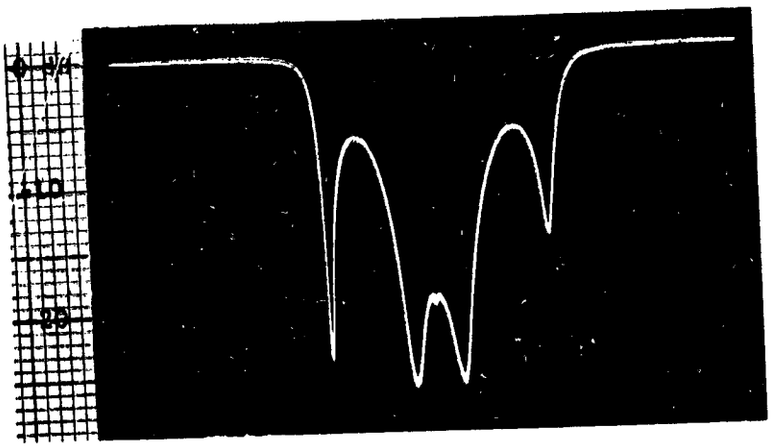

Figure 5.20. Output to Port 2 from Port 1 (Terminated)

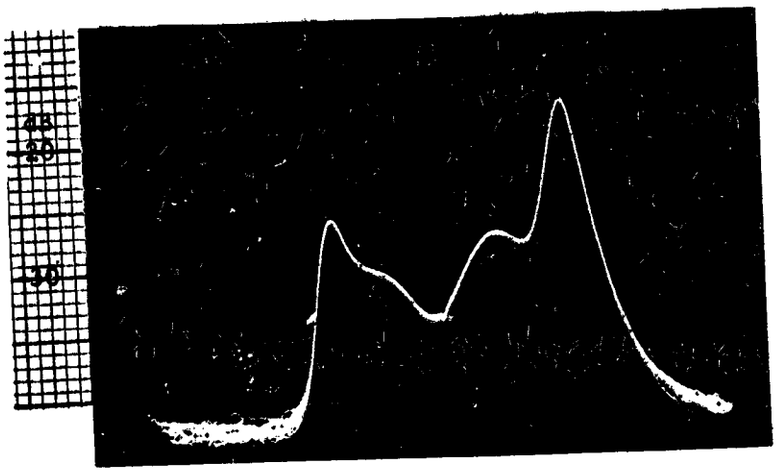

Figure 5.21. Output to Port 3 from Port 1 (Transmitter #2 Input)

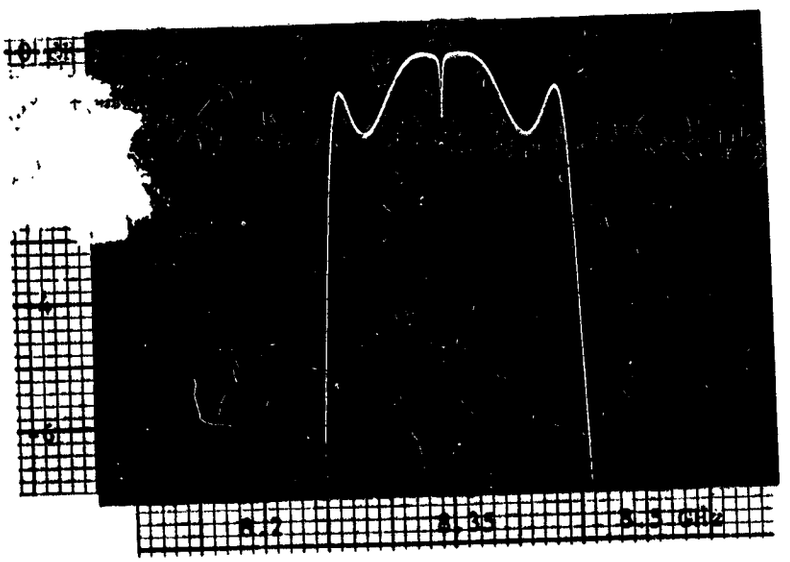

Figure 5.22. Output to Port 4 from Port 1 (to Antenna)

Diplexer Operation

mitter #2 port, and the output port. These demonstrate that in the center of the band, excellent performance is obtained. Figure 5.23 indicates the reflected signal to the input port, leading to VSWR calculation of 1.12 at 8.36 GHz and varying between 1.06 and 1.2. Insertion loss was determined to be about 0.22 dB, subtracting the losses or reflections noted at the first three ports from the loss shown at the fourth port. Reflection to port 3 would appear to result in a VSWR of about 1.04 at center frequency which is more than ultimately desirable but is not considered a critical factor.

A check was also made on the performance of the diplexer for a transmitter signal into Port 3, the second input port. In this case, the transmitter frequency is outside the bandpass of the filter, and performance is determined on that basis. From results, there is no essential difference between frequencies above and below the passband. The stray signal reflected back to port 1. The first transmitter input port, from the port 3 signal is shown in Figure 5.24. This is about -30 dB at center frequency, equivalent to a VSWR in Channel #1 of about 1.066. This is higher than the specification, but not seriously so. A further design effort to change the end irises of the diplexer would be expected to improve on this somewhat. The upper frequency limit VSWR approaches 1.29 which is quite large, and would be reduced by design refinement. Insertion loss here is very low since the signal does not go through the filter, but only through the section of waveguide. The losses in the channel are largely those of the extraneous signals coupling to ports 1 and 2 and the reflection within the channel.

For testing in the assembled waveguide subsystem, tests were run near the center of the bandpass spectrum. This still led to the high heating effect. In air, the two end irises exceeded 373°K (100°C) with water cooling while the other components were operating in the vicinity of 323°K (50°C). Normally, the center of the diplexer should have the highest temperature. There was little thermal contact between the dielectric disks and the metal iris, so the heat was removed largely by radiation and somewhat by convection. In the vacuum, the heating was observed visually. Iris temperatures at the ends of the filter also rose heavily in a vacuum, and was around 373°K (100°C) with water cooling and about 200 watts input.

The test equipment used in the component testing is shown in Figure 5.28. This setup permitted simultaneous readings at all four ports. In the assembled waveguide subsystem, similar measurements were made, as considered in the discussion of bench testing, Section 6.2.

An additional test was performed on performance of the diplexer as a harmonic filter. The test was performed with a TE_{10} second harmonic signal, and attenuation exceeded 60 dB, the limit of the measurement system as shown in Figure 5.28 with the appropriate 16.7 GHz equipment utilized. Thus the diplexer can be used without the leaky wall harmonic filter where the diplexer is required in the selected system configuration.

5.4.6 Thermal Control and Mounting

The major thermal/mechanical problem in the program is a consequence of the rf losses in the diplexer which are expected to be as large as all the other components combined, and which will be generated in a small concentrated space.

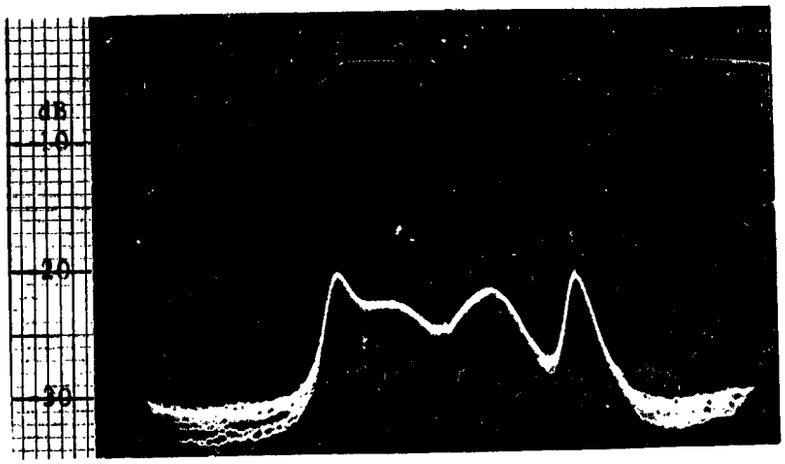

Figure 5.23. Reflected Power at Port 1 - VSWR at Center = 1.12

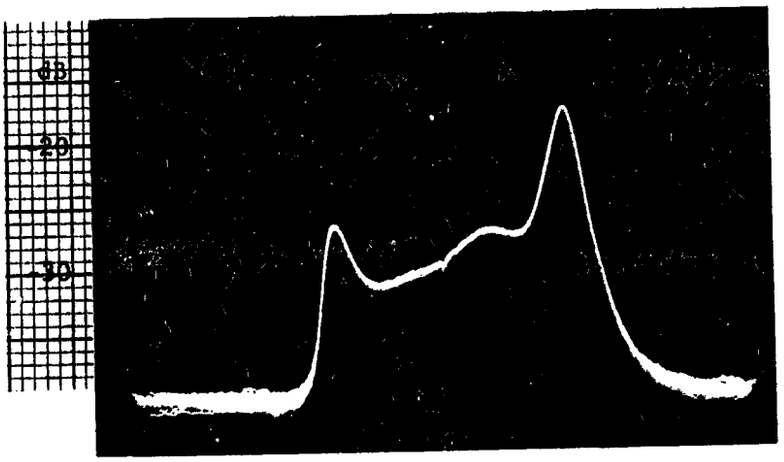

Figure 5.24. Output to Port 1 from Port 3 (Transmitter #1 Input)

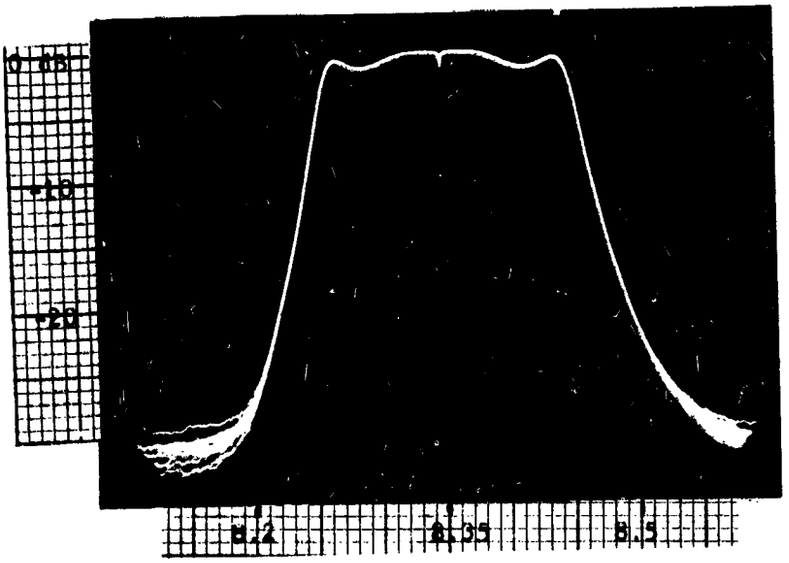

Figure 5.25. Output to Port 2 from Port 3 (Terminated)

Diplexer Operation

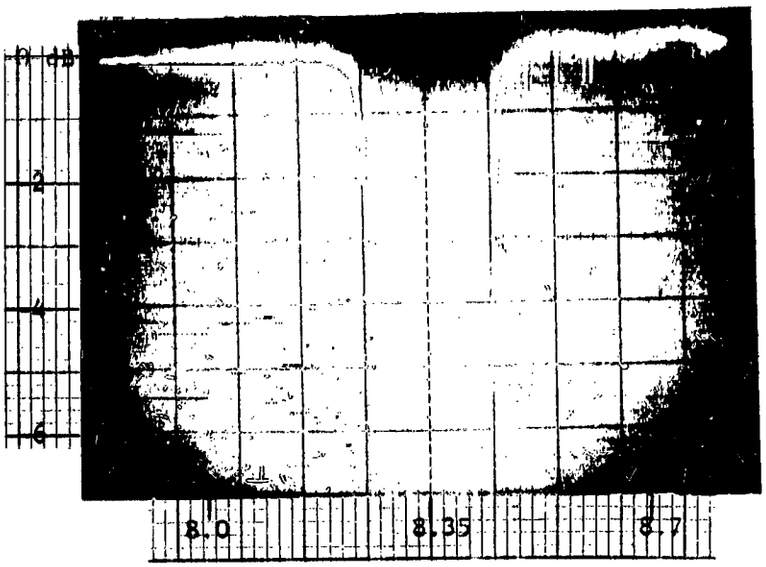

Figure 5.26. Output to Port 4 from Port 3 (to Antenna)

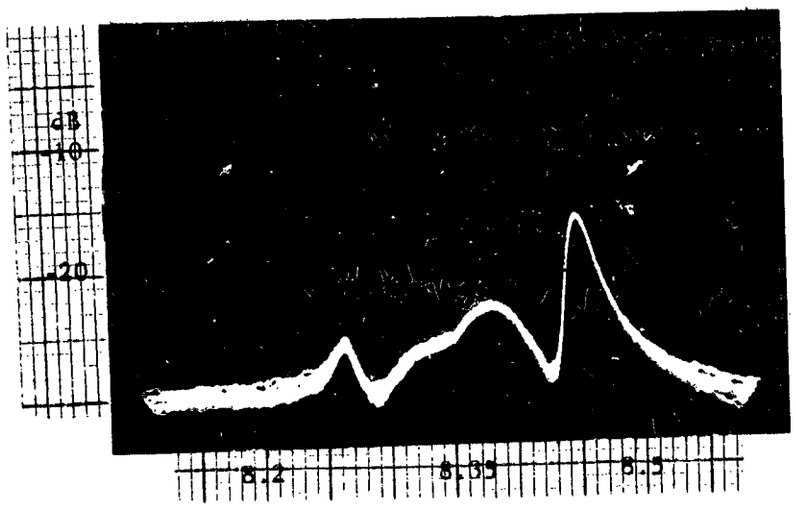

Figure 5.27. Reflected Power at Port 3 - VSWR at Center = 1.066

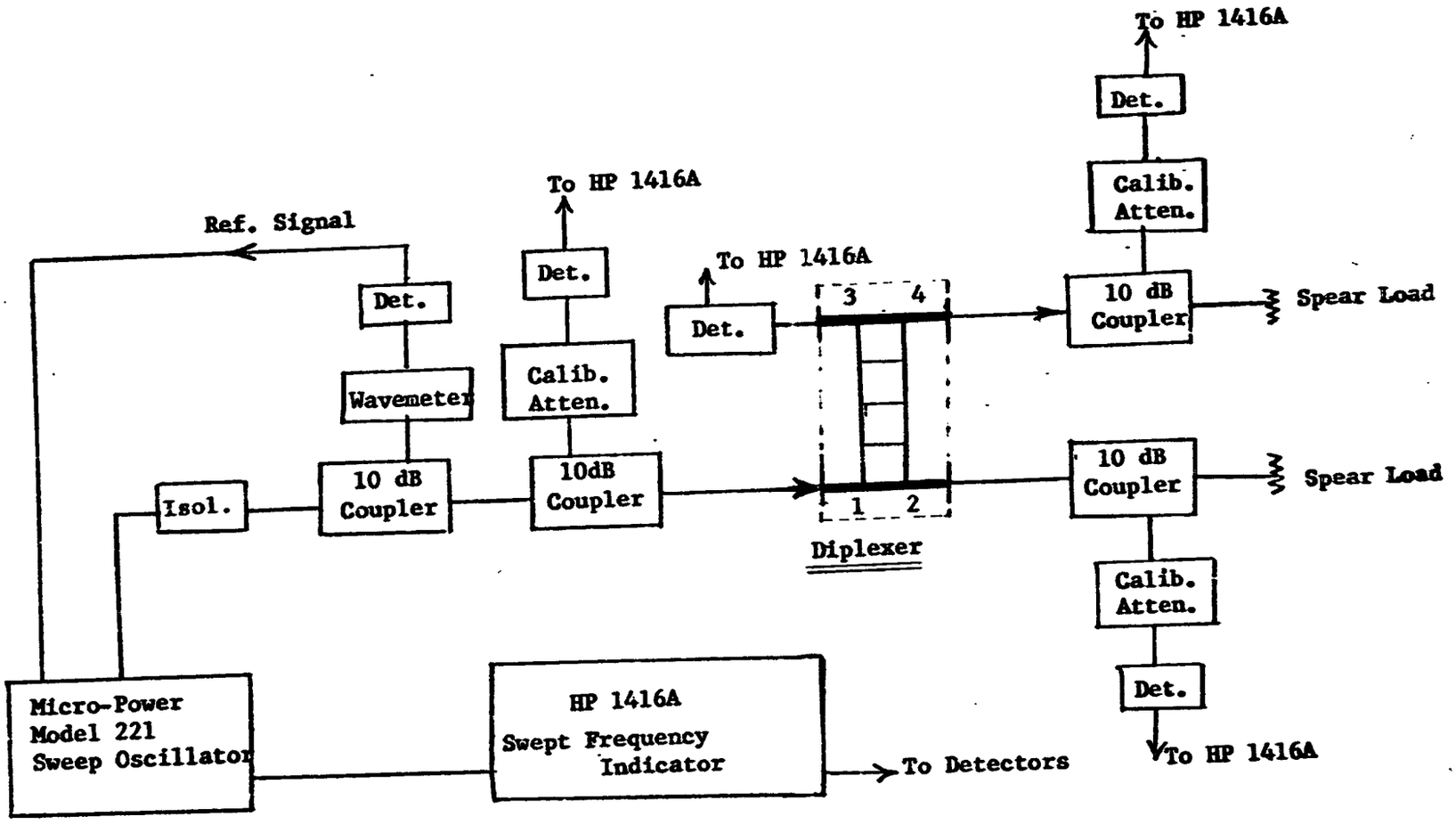

Figure 5.28. Test Equipment Arrangement for Diplexer Testing

Previous 3-cavity diplexers showed losses up to 0.5 dB (ref. 11) although 0.2 dB at 8.35 GHz and 0.3 dB at 12 GHz would be likely with carefully fabricated and adjusted units. The loss in the diplexer is assumed to be in the general range of 70 to 100 watts. A heat radiator surface then would require over 1161 cm^2 (180 square inches) of area to reject this amount of heat to the space sink at 373°K (100°C). The larger problem is to conduct this heat from the diplexer itself to the radiating plate used also to support the waveguide assembly. The effects of this heat source on overall thermal operation is in Section 5.5; here the concern will be on the construction of the diplexer and developing an efficient heat transfer technique.

Diplexer: The diplexer is of invar, which has a very low thermal conductivity, around 0.1152 Joule/sec/cm^2/°K/cm (80 BTU/hr/ft^2/°F/in) compared to a constant of 2.16 (1500) for aluminum and 4.176 (2900) for silver. Thus the iris disks and the barrels of the diplexer are marginal heat conductors, and as much surface must be contacted as possible by the high conductance material of the mounting to carry the heat to the radiating plate.

Silver or copper cladding is recommended for all parts of future diplexers to improve the thermal properties. A calculation of heating of the inner iris is enlightening on the poor conduction effect in invar by itself. The iris has inner and outer diameters of 0.881 and 3.326 cms (0.347 and 1.310 inches), respectively, and a thickness of .076 cm (.030 in^2). An estimate of the rf loss in the center iris is 1/5 the total diplexer loss, or about 20 watts. As a rough approximation, the cross section is assumed to have an average diameter of 1.700 cm (.670 inches), or an average cross section of 1.600 cm^2 (.063 in^2). These conditions result in a temperature drop of about 300°K between inner and outer edges of the iris. This assumes one-half the power is lost on the inner third of the plate diameter. The calculation may be refined to include how the current distribution tends to heat the iris, radiation losses which will contribute, and other factors, but such would not likely change the result by a significant amount. Adding the 300°K to a barrel temperature of the filter cylinders of at least 373°K (100°C) gives an iris temperature of 673°K (400°C). However, if more power is lost at the iris itself, the temperature will go up considerably; all the loss at the iris edge, unrealistic but indicative, would give a temperature drop through the iris plate of 520°K; expected temperature is somewhere between this and 300°K. Temperature drop goes up directly with power loss, and would be worse if insertion loss increased. There is a definite advantage in cladding the iris with silver to reduce the iris temperature.

The temperature drop between inner iris and outer diplexer barrel would be only 1/6 of the numbers noted above (50° to 87°K) if the iris were made up of .152 cm (.060 inch) invar with .0127 cm (.005 inches) of silver clad on each side. The thicker invar is desirable for mechanical purposes since silver tends to expand faster than invar by a factor of 25. The combination of lower temperature differential and heavier invar results in less distortion than the .076 cm (.030 inch) invar presently used. The possible conditions of separation of silver cladding from the invar was not evaluated.

Silver cladding is also recommended for the invar cylinders of the cavities. This is because the thermal clamps to transfer the heat to the radiating plate cannot cover the entire filter because of the 16 tuning screws, and also the multipactor probe cylinders. The diplexer would then have a more uniform and

somewhat lower thermal expansion.

Thermal-Clamp: A mechanical clamp is used to provide a tight mechanical connection, required for good thermal conductance, to the mounting block. A sketch of the clamp and mounting block are in Figure 5.29.

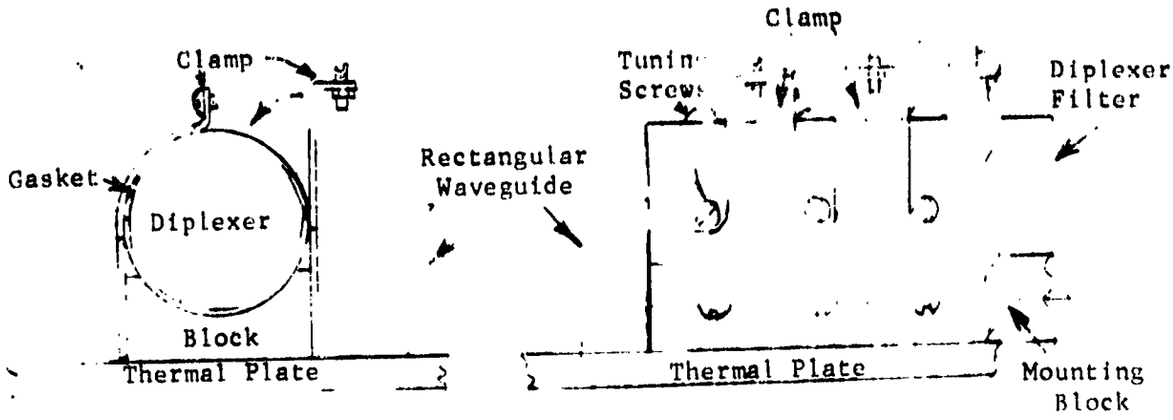

Figure 5.29. Diplexer Mounting Block and Clamp

For this program, this mounting was considered adequate at the scaled power for 1.5 kW at [illegible] GHz, which is about 2 kW at 8.36 GHz for comparing on conduction effect of heat. This is more than adequate for most other effects considered if the heat is generated equally around the cylinder periphery, and good thermal transfer is achieved. A calculation of temperature at the top of the clamp shows it will be 46°K greater than at the mounting block. This is a little higher than ultimately desired although it is not critical. The tie-down clamp may be of silver, soft copper, or heavier aluminum to reduce this temperature differential.

The major difficulty with the diplexer mounting is the large differential thermal expansion between the invar and the aluminum mounting plate; an interface is unavoidable, and it must have some flexibility or fracture will result either in the aluminum clamp or in the invar itself. The technique employed for this program is adequate, and is adaptable to space. A silicone material was used (Chomerics 1224) even though it will outgas to some extent. The significance of this outgassing will depend on the presence of other gas sources and sensitive circuits which may be susceptible to arcing. The Chomerics material was baked at 423°K
by the vacuum gauge attached to the waveguide during the tests. Measurements also indicated a relatively small outgassing would be observed, but well below a dangerous level (Appendix II). The material was cut to completely surround the diplexer barrel with cutouts for the tuning screws and the cylinders holding the [illegible]ltipactor probes. The material is a sandwich arrangement of copper screen and

ERRATA SHEET

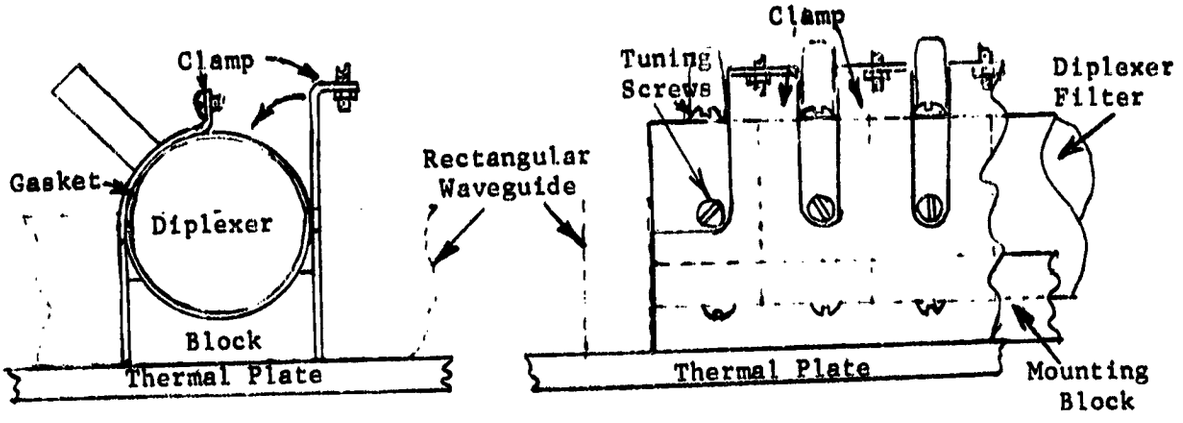

small silver spheres imbedded in the silicone. The thermal conductivity of the combination is about .0029 Joule/sec/cm^2/^{o}K/cm (2 BTU/hr/ft^2/^{o}F/in), which results in about a 6^{o}K drop through the material. The two sides of the material interfacing with the filter and clamp, respectively, would have temperature drops estimated to be about 7^{o}K at the bottom of the cylinder and about 17^{o}K at the top where more material had been cut away to accommodate the multipactor probe cylinders.

An alternate concept, evolving late in the current program, uses an aluminum bellows type of gasket which would be brazed in place rather than operating under mechanical clamping. This would eliminate both the silicone and the contact interfaces. A suggestion on implementing such an approach is sketched in Figure 5.30.

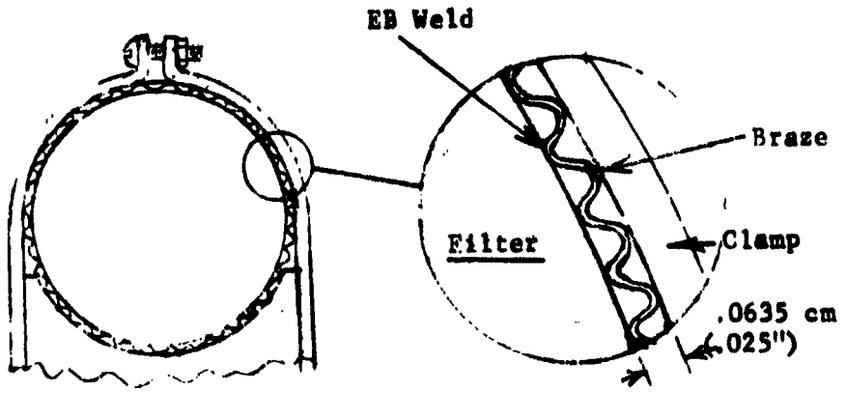

Figure 5.30. Compressible Thermal Aluminum Gasket

The corrugated bellows would be electron-beam welded to the invar cylindrical filter (or to the silver if cladding is used on the outside) since these are dissimilar metals. The resulting assembly would be placed on the mounting block and clamped. The block is bolted to the thermal plate and then brazed to obtain a good thermal path. Also, the bellows peaks can be brazed to the clamp at the same time. This approach will require additional thermal engineering to insure no fractures between the brazing temperature and 193^{o}K (-80^{o}C), but this does not appear to be a problem with the configuration used. The effect is to eliminate all contact interfaces and provide optimal heat transfer from the diplexer. The corrugated bellows typically might be of .013 to .018 cm (.005 to .007 inch) aluminum formed with a peak to peak spacing of .127 cms (.050 inches) and a height of .064 cms (.025 inches).

However, a stress/strain analysis is required to determine an optimum design. The compression of a perfectly elastic gasket with the invar cylinder and the aluminum clamp enclosing it show that it would be required to change thickness from .064 cm (.025 inches) at 373^{o}K (100^{o}C) (assumed) to .0305 cm (.012 inches) at 193^{o}K (-180^{o}C). The approach then must consider a moderately compressible gasket where the sine-waveform of Figure 5.30 is compressed such that the bulging tends toward a squarish pattern. The limit in how far the gasket can be compressed without exceeding the bending limit is to be determined. This will be a function of the thickness of the gasket material and of the specific allow used.

The stress/strain relations in the gasket can be integrated with the stress/strain relations and limits in the invar cylinder and the aluminum clamp. Ideally, the design will balance the stresses in three members so the burden will be proportioned according to compressive and tensile limits. The invar will be under compression from the gasket/clamp, and has half the linear displacement of aluminum. The gasket will be under compression for the most part, while the clamp will be under tension from the resistance of the other two members. A computer program should be generated to arrive at an optimum balance. Circumstances did not permit a detailed design.

Mounting Block: The mounting block was solid aluminum with openings to permit access to the tuning screws at the bottom part of the filter barrel. The thermal mounting plate is also required to have holes drilled for this access. The upper part of the block is cylindrical with a diameter of 3.81 cm (1.5 in). The filter cylinder has a diameter of 3.683 cm (1.450 inches). The .127 cm (0.050 inch) differential was taken up by compression of a .076 cm (.030 inch) thick gasket to .064 cm (.025 inches) on each side. The block was bolted to the thermal plate for the 8.36 GHz test component, but should be brazed in a flight configuration, particularly at 12 GHz where the thermal flux density is much higher.

5.4.7 Termination

The unused port of the diplexer, designated as #2 port, was terminated with a SiC load that could absorb the power that might bypass the diplexer and also have a low VSWR such that reflected power was negligible. Note that reflected power shows up directly at port #3 which connects the second transmitter. Thus to keep the second channel VSWR low, the termination must be well matched. The component developed is in Figure 5.31. Basically, it is a seven inch double-spear of SiC affixed to the end piece of the waveguide with two bolts. Four venting holes in the waveguide wall lead into an inverted channel type vent. The component is bolted to the thermal plate after facing has insured a firm physical contact. The termination could absorb as much as 38 watts at center frequency with a 3 kW input, but substantially more would be absorbed near the bandpass extremes. With the diplexer characteristics shown in Figure 5.20, the input to the termination then would be much higher than permissible, emphasizing the need for trimming the diplexer operation to eliminate the outer dips in the bandpass characteristic. No problems were encountered in the low power testing with the diplexer. The termination was not required for the testing with the diplexer out of the assembly.

Figure 5.31 Diplexer Termination

5.5 THERMAL CONTROL

The thermal control task was largely concerned with the radiating area, effectiveness, and temperature of the mounting plate, and the mounting techniques for the components. The calculations were directed at the 8.36 GHz experimental subsystem with extensions to the 12 GHz case. The larger 2.64 GHz components make this frequency region less of a thermal problem and more of a size problem.

5.5.1 Mounting Plate

5.5.1-1 Temperature

The losses in the waveguide subsystem are listed in Table 5.3. The 8.36 GHz values are about those measured except for a more optimum diplexer, and the 12 GHz data are predicted based on engineering estimates for the harmonic filter and diplexer. An average temperature on the 2 ft x 3 ft plate can be obtained by assuming all heat is radiated from a constant temperature mounting plate into space at near $0^{o}K$, and to the satellite interior at $323^{o}K$ ($50^{o}C$). For the 8.36 GHz case using an optimum surface aluminum plate:

$$358\ W = 0.8\ (.610m \times .915m)\ (57 \times 10^{-9})\ (2T^4 - 109 \times 10^8)$$

$$= 0.8\ (24'' \times 36'')\ (36.8 \times 10^{-12})\ (2T^4 - 109 \times 10^8)$$

or

$$T^{o} = 334^{o}K\ (61^{o}C)$$

The external side of the plate radiates at T^{o} to near 0^{o} of space, and the inside surface at T^{o} radiates to the vehicle interior at $323^{o}K$ ($50^{o}C$). This is the condition used in the estimating of the temperature contours on the plate.

Table 5.3. Losses in Waveguide Components

Component	8.36 GHz 3 kW Loss %	8.36 GHz 3 kW P Watts	12 GHz 1.5 kW Loss %	12 GHz 1.5 kW P Watts
Reverse Power Monitor & Elbow	1.0%	30	1.35%	20
Harmonic Filter	4.5%	135	9 %	133
Forward Power Monitor & Elbow	0.3%	10	0.4 %	5
Diplexer	4.8%	135	10.0 %	134
Diplexer Termination	1.1%	30	1.5%	18
Output Waveguide	0.7%	18	0.9%	11
Power Lost		358		321
RF Power Output		2642		1179

A more realistic indication of temperature across the plate was obtained by assuming line and pointheat sources, as in Figure 5.32, and sectioning the plate into 39 subsections, mostly 10 cm (4 in) squares.

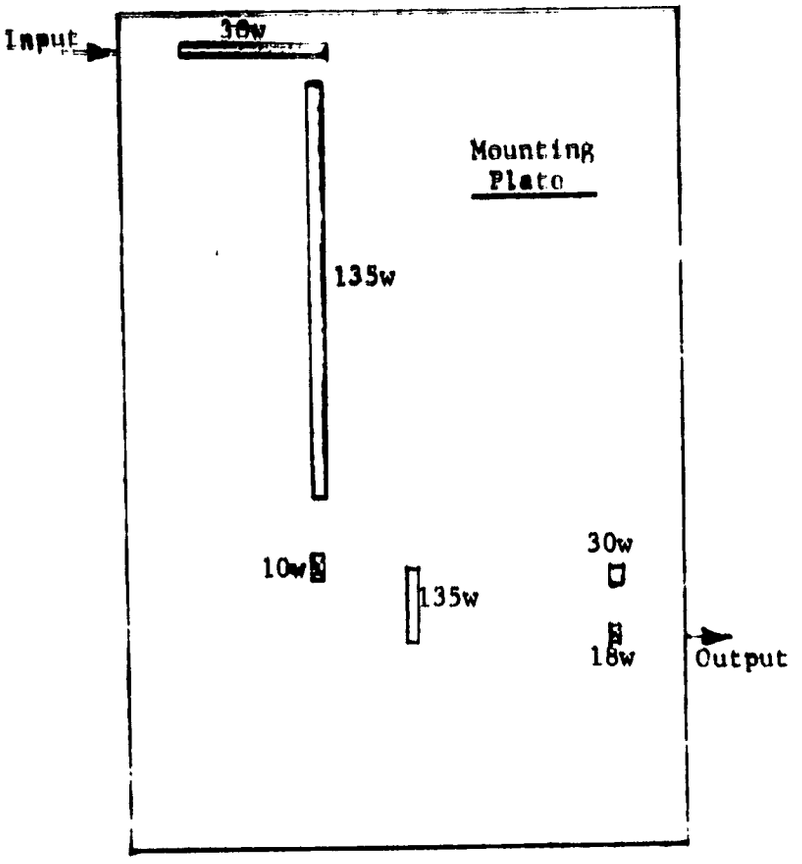

Figure 5.32. Thermal Sources On Mounting Plate

Each subsection is assumed to be at constant temperature. A computer program then determined temperature based on heat input at the edges and heat radiated at the computed temperature (one sided radiation). The unradiated heat constitutes the inputs to adjoining sections of the plate. The sectioning and resulting temperatures are shown in Figure 5.33.

These temperatures represent a lower bound since, in practice, the 0.8 emissivity constant is a little better than would be obtained consistently. Some typical values for the emissivity constant, ϵ , are found in literature and values tend to vary in the different sources, but the average are about as follows:

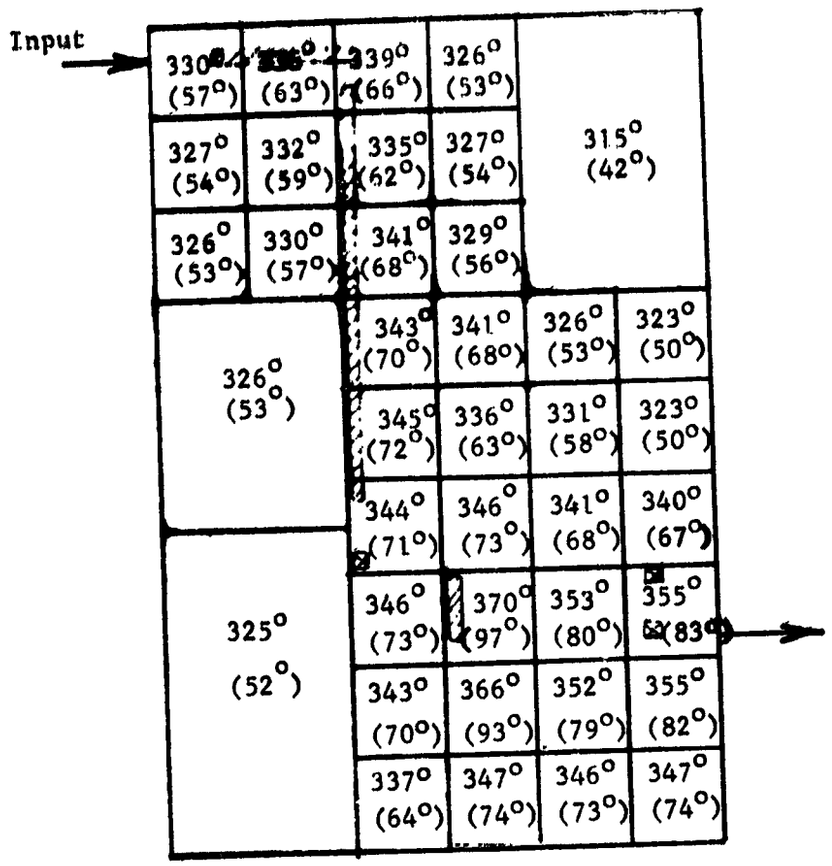

Figure 5.33. Temperature Distribution Estimate for Mounting Plate - ^{o}K (^{o}C)

Material	ϵ Pure Metal	ϵ Oxide
Aluminum	.07	.75*
Copper	.10	.70
Silver	.07	-
Nickel	.10	.37
Stainless	.08	.79

* For 7×10^{-4} cm (2.76×10^{-4} in) thickness

Specific values will vary with temperature and surface preparation but these are sufficient for estimating ranges of temperatures.

A near optimum plate would have an aluminum-oxide surface finish, more than 7 microns (2.76×10^{-4} in) in thickness (anodized). For the 12 GHz case, radiation will be quite important since the power dissipation is nearly as great as for 8.36 GHz, but the effective plate size is about 2/3 as large. With a .406 x .610 meter (16 x 24 inch) mounting plate, and an ϵ of 0.75, the average temperature is 378°K

(105°C). This is a high but tolerable level. The maximum temperature at the diplexer for the assumed conditions would approach 413°K (140°C), high but still not an unreasonable temperature. Special care would be required to keep the photodiodes sufficiently cool. Alternately, a larger mounting plate would be desirable and should be considered.

The plate used in the 8.36 GHz program was a 0.635 cm (1/4 inch) thick aluminum plate (a jig plate for flatness). The calculations leading to Figure 5.33 were based on this value. Temperatures on a 0.318 cm (1/8 inch) plate would be a little higher near the components and a little lower at the extremities. The average power radiated is the same, so the temperature variations will not be very significant. If the satellite structure calls for less than 0.318 (1/8 inch) plate, the temperature distribution should be recomputed to ascertain feasibility of obtaining adequate temperature control.

5.5.1-2 Water Cooling of Plate

Assume that a water temperature rise of 20°K is permitted, and the cooling pipe is arranged appropriately on the thermal plate to correspond to the contours for radiation cooling. The data of Figure 5.33 was used to roughly determine thermal contours of Figure 5.34 which are equivalent to those to be encountered

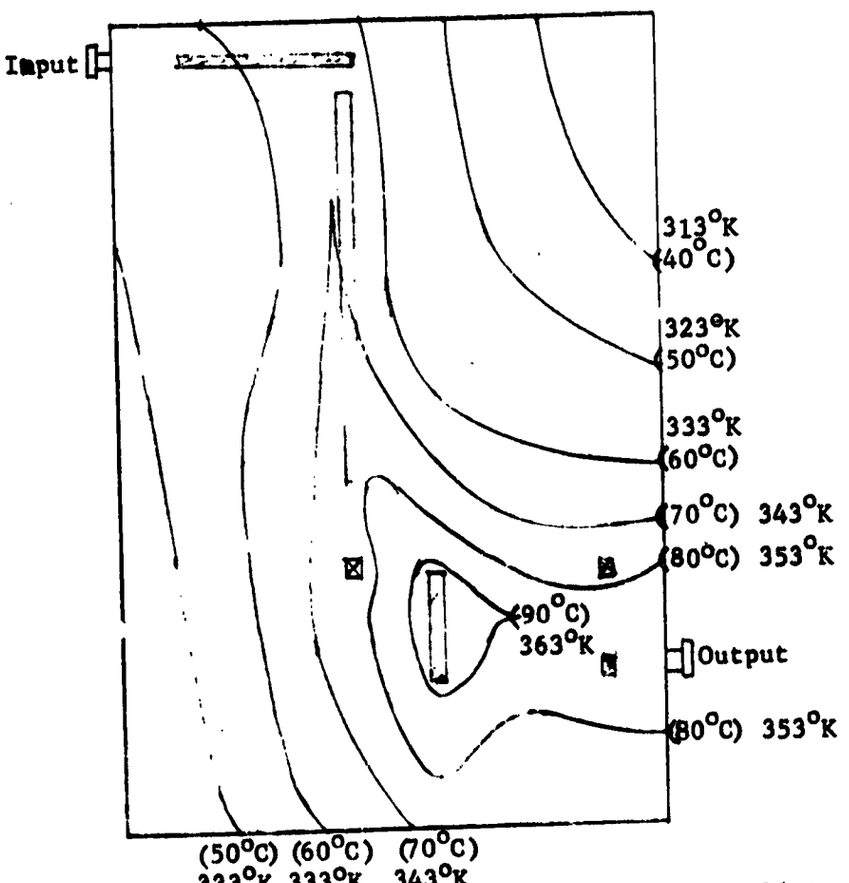

Figure 5.34: Approximate Temperature Contours on Plate

in space. Power consumption (12 GHz) is 321 watts (joules/sec.), per table 5.3 (18.25 BTU/min). Then a water flow of 3800 cc (one gallon) per 15 minutes is adequate. The flow rate would be twice this to hold the water temperature rise to $10^{o}K$. The cooling problem then becomes one of using a small enough orifice to give a steady reliable flow rate of 15.2×10^{3} cc to 30.4×10^{3} cc (4 to 8 Gallons) per hour.

The cooling pipe used in the 8.36 CHz equipment and shown in Figure 5.35 is a 0.635 cm (1/4 inch) copper tubing affixed to the underside of the mounting plate. Copper and aluminum is best joined by electron beam welding. The aluminum also can be silver plated, and soft solder used for a temporary setup or mockup. Conducting epoxy has also been used for mockups but tends to be brittle, and must be well cured before using in a vacuum. The latter was used here in the absence of any immediate mechanical requirements.

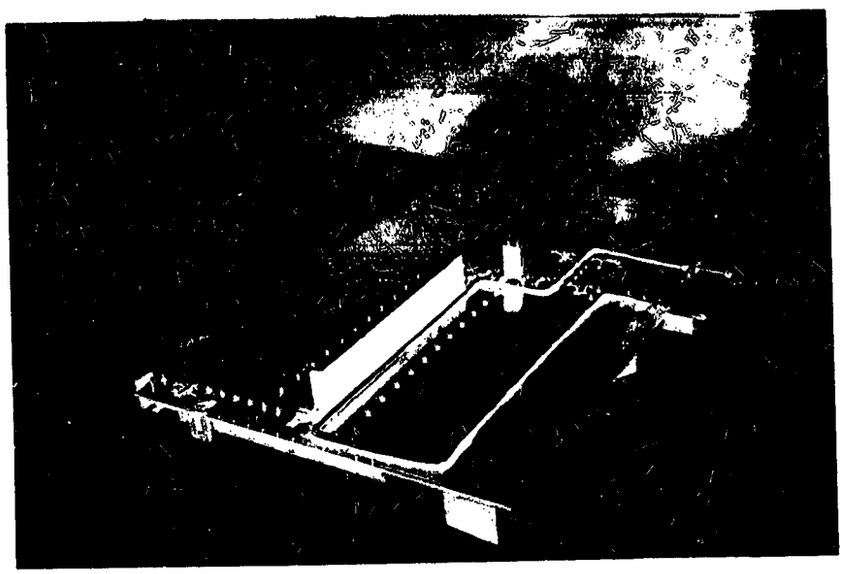

Figure 5.35. Mounting Plate With Cooling Pipe

The cooling pipe in Figure 5.35 was placed to cover the highest temperature region. A different pipe routing might better simulate the equivalent of space radiation by estimating water temperatures along the pipe and relating this to sources and contours. There will be some restrictions on the cooling pipe location because some components, particularly the harmonic filter and cross-guide coupler, project through the plate. Access to disconnect flanges must also be maintained. Temperature control can be improved if a more consistent valve for fine-stream water control were included as an external component to the testing system.

5.5.1-3 Air Cooling

Air cooling can also be effected quite easily and would only require an adjustable deflector to vary the air rate on the equipment. It is of no value in vacuum tests, so a water cooling capability is still required. (A liquid nitrogen wall could be used if available.) For atmospheric cooling, values may be:

321 joules/sec (18.25 BTU/min)
ΔT = 5°K (9°F)
Rate = $3m^3$/min (105 cfm.)

This can be accomplished with a 190 W (1/4 HP) fan motor if the back-pressure is less than 3400 N/m^2 (one-inch Hg) (ref. 13). Practically, the pressure drop should be only a fraction of this, and a much smaller motor should suffice. A disconnectable tube can carry the cooling air against the radiating side of the plate. Control of temperature contours would be a problem in simulating space operation.

5.5.2 Thermal Mounting of Components

5.3.2-1 Temperature Effect

Most of the components will be adequately cooled if just clamped tightly to the thermal plate. The temperature drop across a clamped junction varies, but with milled flat surfaces and using one to two bolts per effective 6.45 cm^2 (square inch), the temperature differential is about 0.56°K per watt per 6.45 cm^2 (square inch). Typical temperature drops for the several components are listed in Table 5.4.

Table 5.4 Temperature Control Effects for Clamped Components

	8.36 GHz			12 GHz		
Component	W/cm^2	W/in^2	°K	W/cm^2	W/in^2	°K
Power Monitor, etc., Reverse	0.51	(3.3)	1.84	1.63	(10.5)	5.9
Harmonic Filter	0.93	(6.0)	3.36	1.83	(11.8)	6.7
Power Monitor, Forward	0.71	(4.6)	2.57	0.67	(4.3)	2.4
Diplexer	4.29	(27.7)	15.5	8.53	(55.)	30.8
Diplexer Termination	0.81	(8.0)	4.5	1.47	(9.5)	5.3
Waveguide, Other	0.45	(2.9)	1.62	0.54	(3.5)	1.96

Obviously the diplexer is of greatest concern, particularly at 12GHz. The other components may be clamped with no concern over temperature differentials across the junction. Some components, the harmonic filter in particular, will lose some heat by direct radiation as well as conduction to the thermal mounting plate because of its large surface area.

5.5.2-2 Diplexer Mounting

The 8.36 GHz experimental diplexer had three mechanical contact interfaces, which indicated a likely operating temperature of 413°K (140°C). This could be reduced if two of the junctions were brazed resulting in about a 386°K (113°C)

final diplexer temperature. At 12 GHz, the temperatures would be higher, although the shorter thermal paths will compensate somewhat. For a single interface with the other two brazed, the temperature at 12 GHz is estimated to be about 400°K (127°C) based on one-half the transfer area of the mounting block.

The diplexer thermal design was covered in Section 5.4.6 in which an aluminum block provided the thermal path to the mounting plate as well as the mechanical support for the diplexer. The diplexer is best brazed or electron-beam welded to a compressible member such as a pleated aluminum gasket which is brazed to the block which in turn is brazed to the mounting plate. The problem that results is the differential thermal expansion between the invar and aluminum. The pleated aluminum gasket, adequately designed, will perform this function. However, the thermal problems should be reviewed on an overall basis, considering the practical aspects of fabrication.

5.5.3 Thermal Distortion

All parts of the waveguide assembly including mounting plate are aluminum, except for the invar diplexer. Consequently, there should be little mechanical stress as the temperature varies over a wide range if all parts expand and contract equally. The nominal range for the thermal plate is about 453°K (180°C), from 193°K (-80°C) during eclipse to perhaps 373°K (100°C) maximum during operation. The dimensions for the waveguide assembly and mounting plate for hot and cold conditions are shown in Figure 5.36.

The dimensional changes of 0.4% for the 180°K range would overstress conventional aluminum if it were dimensionally constrained. The tensile force would be 2815 kg/cm^2 (40,000 lbs. per in.^{2}) which is about the limit for tempered aluminum and over four times the limit for soft aluminum.

A waveguide assembly which has sufficient freedom requires that the connecting waveguide should be oriented to permit some lateral bending to replace the longitudinal contraction during the cold eclipse periods. Possibly, the antenna end would go to 193°K (-80°C), but the TWT end would not. The length and width of the assembly at the waveguide terminals change by .241 and .264 cm (0.095 and 0.104 inches), respectively; these contractions must not overstress the waveguide components nor must it overstress any connecting components including the TWT window. A conventional displacement/stress calculation shows that connecting waveguide should have a free length equivalent to a cantilever of 5 to 10 inches in length, depending on the strength of the aluminum used and whether stress relief is at both ends. The stress in a flexed piece of waveguide is

$$s = \frac{Mc}{I}$$

where

M = newtons of force x length,

c = distance to worst case point in cross section 0.794 cm (.3125 in) for WR 112

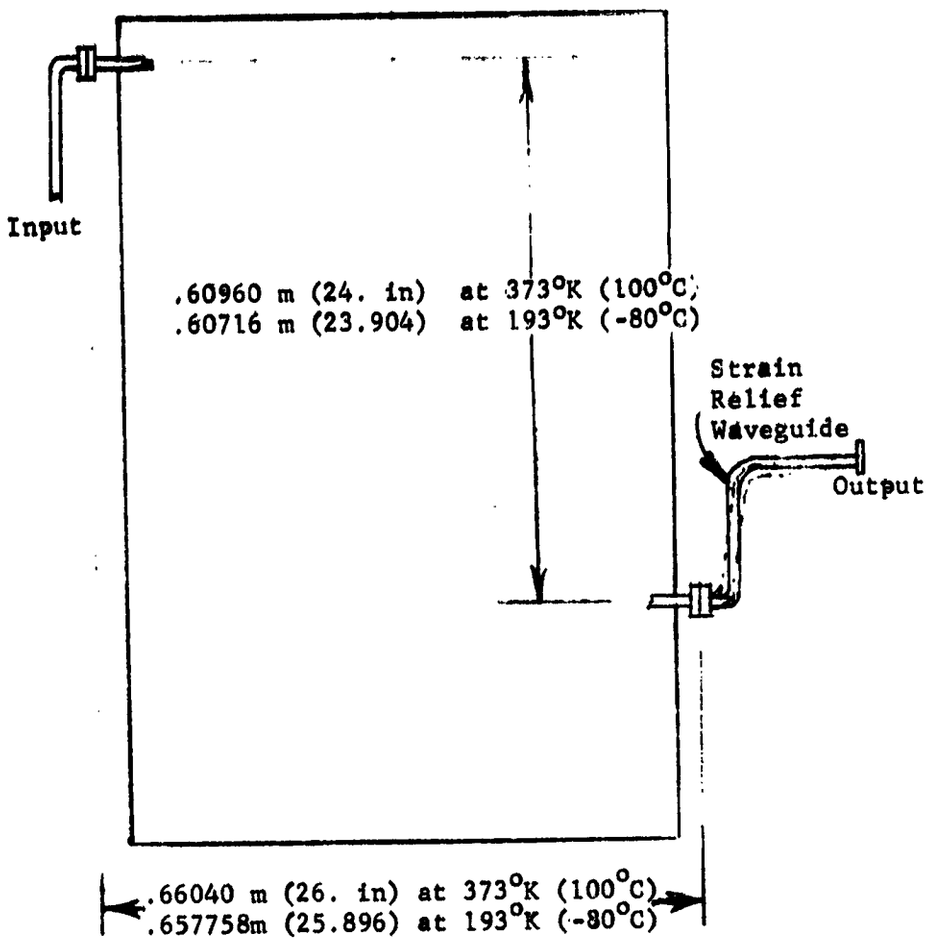

Figure 5.36. Thermal Distortion of Mounting Plate

I = moment of inertia .583 cm^4 (.014 in^4) for bending in the narrow wall direction.

s = 632.3 kg/cm^2 (9000 psi) for soft aluminum, 1264 kg/cm^2 (18,000 psi) for average aluminum, 3161 kg/cm^2 (45,000 psi) for annealed aluminum.

With this range of stress the Pl range is:

$$P \cdot l = M = 460 \text{ kg cm (400 lb in) minimum}$$
$$= 2300 \text{ kg cm (2000 lb in) maximum}$$

This is then used in the deflection equation for a cantilever:

$$y = \frac{Dl^3}{3EI}$$

where E is the modulus of elasticity, equal to 10^7 , this gives

$$P\,l^3 = 74{,}200$$

Then using the previous maximum and minimum values of P1,

l = 25.4 cm (10") maximum

l = 10 cm (4.5") minimum

An 18 cm (7") free length may be used at one or both ends of the assembly to provide a good margin.

Alternately, some form of temperature control may be considered, such as thermostatically controlled louvers to cover the plate during cold periods and retard the outflow of stored heat. This approach would be considered only after a thermal evaluation of the entire satellite shows problems would be encountered due to unequal strains in the waveguide assembly caused by some external component.

5.6 BREAKDOWN SENSORS

5.6.1 Requirements

The basic requirement of the sensors is to provide a means to positively detect an electrical fault in the waveguide which may be a multipactor breakdown or any of several types of arcing, and provide a suitable signal which can turn off the rf before the breakdown can cause permanent damage to the transmitter tube or some critical component. The sensors should be sensitive to a small breakdown, or preferably to the start of a breakdown which would avalanche into a major operation fault.

Three effects can appear from a breakdown: a large reflected signal appears which can be detected by the reverse power monitor, an arc with visible light output appears in some cases which can be detected with a photo diode, and an electron or ion cloud forms in some cases which can be detected by a Faraday Cup (a biased probe). The three approaches were evaluated first in a special breakdown test section, described in Section 5.7 which follows, and the results interpreted to determine how the sensors could be best integrated into the waveguide assembly.

5.6.2 Optical Sensor

The optical sensor is a photo diode, suitably biased, and with output to an amplifier/trigger circuit which can trip a gate in the rf drive circuit. The diode's physical integration into sections of waveguide can be seen in Figure 3.15, and in the sketch of Figure 5.37 which extracts the parts used. The diode support configuration must tolerate certain other system requirements, including no deterioration to the rf signal in the waveguide, low rf leakage paths, low outgassing, and rugged construction.

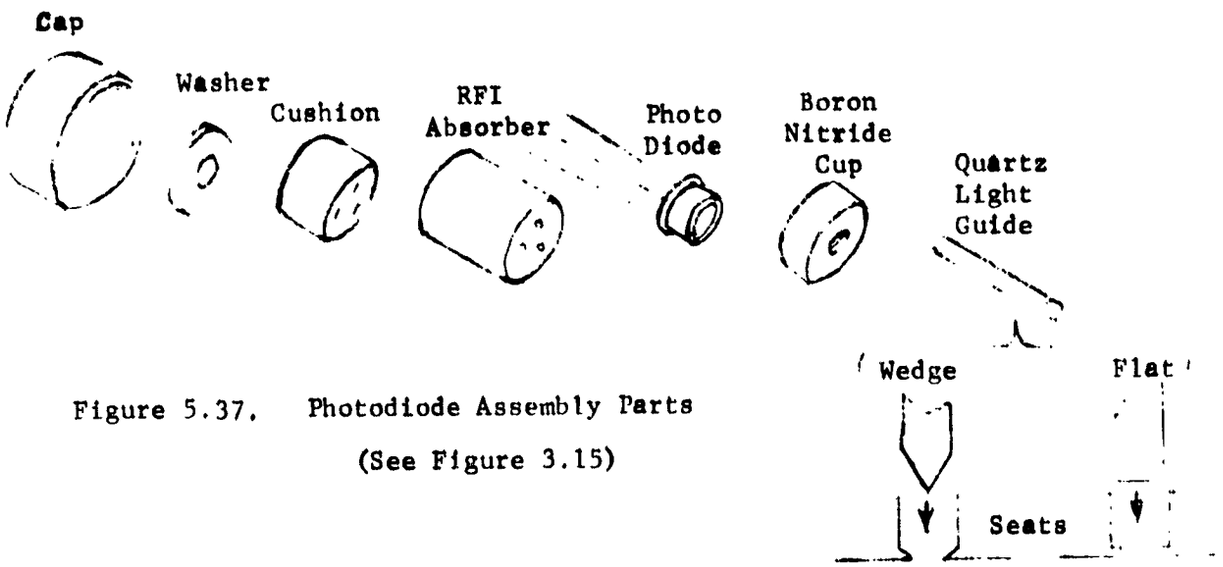

Figure 5.37. Photodiode Assembly Parts

(See Figure 3.15)

The diode used was an EG&G SGD-100A photodiode. The diode is mounted on a quartz rod light guide affixed to its window. The far end of the quartz rod is placed on or inside the inner waveguide surface, using an appropriate arrangement to observe the regions required. For looking both ways along a straight waveguide, the quartz rod has a wedge shape with angles of 38° between the wedge side and rod axis. Any light present would then be deflected into the quartz rod and to the diode. The rod was seated in a hole into the waveguide having shoulders to prevent it from dropping into the guide. In the 8.36 GHz test equipment, a .318 cm (.125") rod was used with a .254 (.100) opening to the guide. The shoulder is shown in Figure 5.37; the wedge point required a square hole which was milled, using a .08 cm (1/32 inch) mill for the corners, so that the flat sides of the wedge will have a full support. The length of the rod was determined by the seating dimensions, the thickness of the waveguide wall, .163 cm (.064 inches) here, the depth of the end of the cylindrical holder, and the boron nitride cup used at the upper end of the rod for firm mechanical physical positioning against motion from vibrations and accelerations. The boron nitride was required to insulate the diode which has a floating case as used here. The compartment is vented with a small hole through the wall of the tube holding the diode assembly, retaining the 5:1 length to diameter ratio.

Looking into the diplexer with a photodiode, which is seen in Figure 3.1, requires a flat face quartz rod since only one direction, coincidental with the rod and diode axis, is viewed. This rod is supported by a circular seat at the waveguide. This seat is .025 cm (.010 in.) and has a .254 cm (.100 in.) opening; thus the face of the rod is .025 cm (.010 in.) short of the waveguide inside wall.

A third photodiode was placed in an elbow, shown in Figure 3.15. This diode also used a flat face, even though the look angle was then 45° rather than the more optimum 38°. This arrangement permitted the diode to see light sources or arcing through either the harmonic filter or the rectangular waveguide of the diplexer, forward power monitor, and diplexer termination.

The other elements of the assembly in Figure 5.37 include a section of rf absorber material. This was a necessary item because the quartz rod used did not provide for 3rd and higher harmonic cutoff. The rf absorber would also insure a further reduction of any fundamental and second harmonic leakage. The small opening for the quartz rod would provide only a very small rf coupling. The rf absorber was to attenuate 100 dB per 2.54 cm (inch) above 10 GHz, but a measurement indicated about 1/3 of this was achieved for the .635 cm (.250 in.) diam. material used. This is still quite adequate, but an additional length may be desirable for further reduction in harmonic leakage from the diode holder preceeding the harmonic filter. The rf absorber was manufactured by Lundy Electronics and Systems, and used a base of Epon 828 epoxy. An earlier attempt to include the rf absorber granules (not identified by Lundy) in Steatite for machinability and an inorganic base was unsuccessful in that the materials tended to decompose or combine during curing of the Steatite and the absorbing properties became very poor. An attempt was then made to incorporate the rf absorber material in a cement type base but this combination did not have sufficient mechanical strength. Dow Corning 93-500 is the next preferred base; it is quite expensive and would provide somewhat better outgassing characteristics, but the requirement on performance for this application is nominal and the Epon 828 proved to be entirely adequate. For a case where high power is involved, a different material might be desirable. The material was cleaned thoroughly and baked for about 24 hours just before final assembly.

The additional items in the diode assembly in Figure 5.37 include a silicon cushion to provide a small amount of pressure to the diode, but this pressure must be light in order not to fracture the diode glass. A metal washer and cap completed the assembly.

The diode was used with an amplifier circuit to provide a trip signal in the event that the diode output current exceeded a threshold. The circuit of Figure 5.38 uses a type 3064/12C module (Burr-Brown) to drive a Schmitt trigger type 525 module (California Electronic Manufacturing Co., Inc.) which drove a final one-shot multivibrator using another 3064/12C module. The circuit had been developed previously and was adapted for this program. Note here that the three diode leads

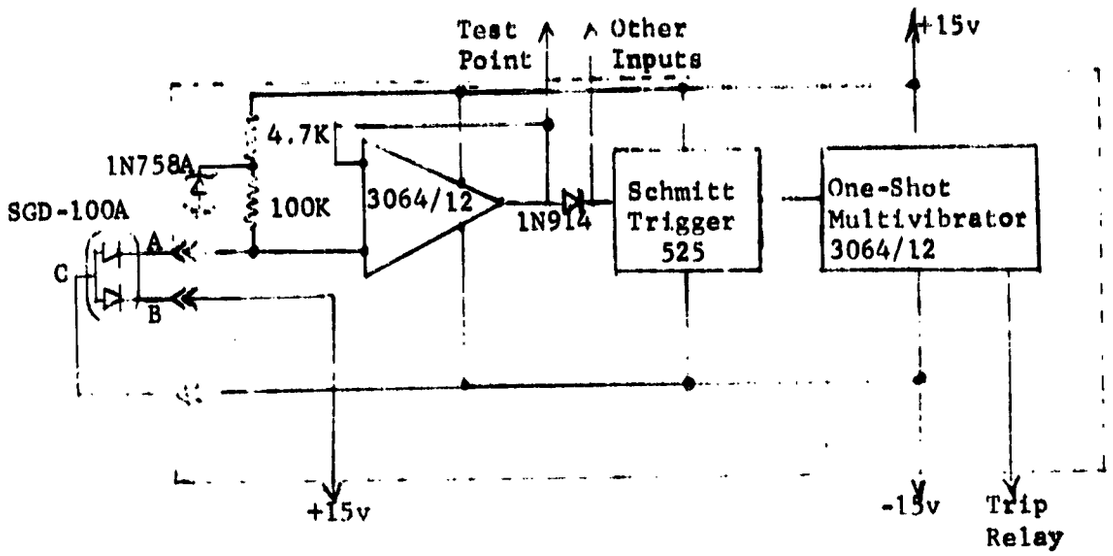

Figure 5.38. Photodiode Amplifier Block Diagram

are floating with none grounded, leading to the necessity for the boron nitride insulating cup for the diode as in Figure 5.37. For testing, the three photodiodes in the assembly were paralleled which reduced sensitivity only slightly since the diode's dark resistance, about 150K ohms, is high compared to the input resistor of 10K ohms and the resistance of a conducting diode, about 1000 ohms.

5.6.3 Multipactor Breakdown Sensor

The multipacting phenomenon is a consequence of an electron cloud oscillating between the broadwalls of a waveguide in synchronism with the applied rf electric field. The field voltage is such that an electron, emitted from one wall of the waveguide, arrives at the other wall while being accelerated by the rf electric vector. This electron, on the average, dislodges more than one secondary electron. The electric field polarity then is reversing and the new secondary electrons are in a strong electric field which accelerates then back to the first wall. The secondary electron cloud continues to build up, travelling back and

forth in synchronism with the electric field direction. There are certain conditions under which this type of action occurs; Figure 5.39 indicates experimental ranges of breakdown voltages for given values of product of frequency and electrode spacing. Material is also significant in that the secondary electron emission varies; tungsten carbide will not sustain a multipactor action while most p[illegible] metals, and many non-metals, will (ref. 4).

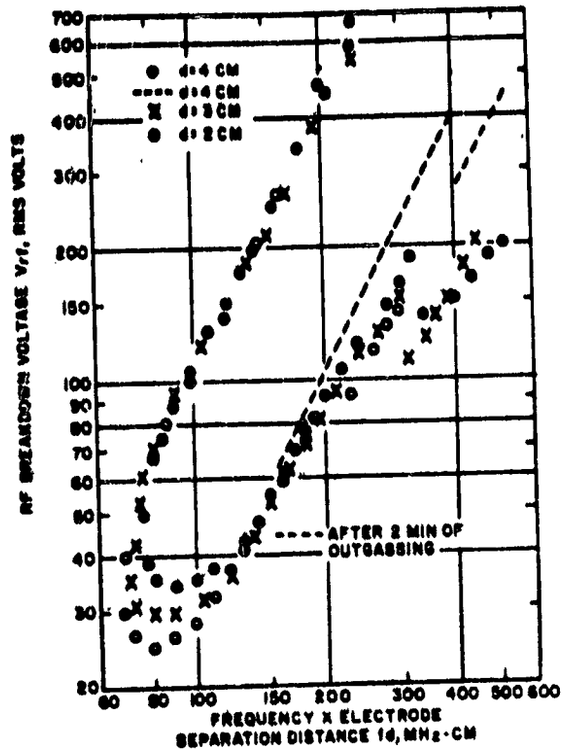

Figure 5.39. Conditions for Multipactor Breakdown

The sensors for multipactor breakdown are simply biased probes (Faraday cups) set at about 15 volts and connected through a 100,000 ohm resistor. The current will be of the order of a few microamperes under average conditions, so the voltages generated are of the order of tenths of a volt at best. This voltage is then fed into the same amplifier as used by the photodiodes at a suitable point, Fig. 5.38.

The probes used were small bypass capacitors as noted in Section 3.3.6; the specific type used here were Erie 2425-001-X5U-101AA, which had a coaxial configuration and a value of 100 pfd. These were mounted at one end of a cylinder with a part drilled and tapped for the 8-32 thread of the capacitor. The ends of the capacitors were cut to be flush with the inside of the waveguide surface, and they were carefully straightened since the probe end is of relatively soft metal and tends to bend easily. The probe is .127 cm (.050 in.) in diameter while the opening for the probe was .178 cm (.070 in.). Figure 5.40 is a sketch showing the cross section of the probe and the holding cylinder.

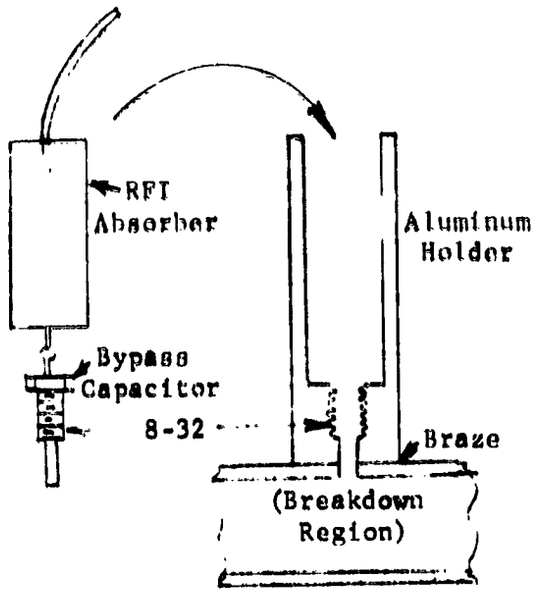

Figure 5.40. Multipactor Breakdown Probe and Holder Cross Sections

The cylinder above the probe is for rf absorbing material, again that manufactured by the Lundy company. The probe acts as a coaxial line, and is not cut off for any frequency. The probe's small size will couple relatively little of the rf power into the capacitor which tends to reduce the outflow by acting as a low impedance circuit. Transfer is estimated at less than -45 dB (ref. 3, page 121), so about another 90 dB is desirable to insure no rf leakage. A 2.54 cm (one inch) piece of rf absorber was added, but later measured to have 36 dB attenuation per 2.54 cm (one inch). A longer piece, perhaps 5 or 7.5 cm (2 or 3 inches), is suggested for future assemblies. In spite of this apparent reduced attenuation, no rf was detectable in tests (Section 6.3.4) so the coupling into the probe must be much less than estimated. Perhaps also the rf absorber, in the configuration used, was more effective than 36 dB.

This type of probe was evaluated in the special breakdown test section and found to be a very effective indicator of multipaction. In the final waveguide assembly, there were no components identified as having conditions close to a breakdown. The cavities of the diplexer have high electric fields, however, which might lead to a breakdown for larger "gaps." The diplexer was not checked at high power, but the possible effects at lower power in terms of rf leakage showed the technique was quite satisfactory.

Multipacting would be expected in the waffle-iron harmonic filter under some conditions, and the probes could be built into the filter to determine conditions under which a given design would break down; these conditions would limit the utilization of such a filter although not eliminate it as a contender for certain applications.

5.6.4 VSWR Sensor

The reverse power monitor described in detail in Section 5.3.1 is also a good indicator of a breakdown. Any arcing of electron flow between the walls of a waveguide represents a lowered impedance path, and a significant signal is usually reflected. It maybe much larger than the normal reflected signal, and can be used to generate a cutoff signal. The output tends to be a rapidly increasing signal which can give a reasonably good output voltage; in an initial CW test, the indication went off-scale with a maximum of 0.5 volts. This signal is also tied in with the trip signal amplifier used by the photodiode and the multipactor probe, with sensitivity such that the normal reverse power indication will not cause a trip.

5.6.5 Pressure Sensor

Pressure sensors of the vacuum ion gauge type were used in the waveguide (at the output end) and in the vacuum tank during the testing of both the special breakdown section and the complete waveguide assembly. The waveguide ion detector was a good indicator of a breakdown since breakdowns release gas and particles which can be detected. However, the gas buildup is relatively slow, and the indicator is considered inadequate in response time to provide good protection for the transmitter tube.

5.7 SPECIAL BREAKDOWN TEST SECTION

5.7.1 Requirements

The special test section, designed specifically to break down at relatively nominal power levels, was developed and tested to determine the performance capabilities of the breakdown sensors just discussed Section 5.6. Both multipactor breakdown and arcing are of interest, and effective use of the three sensors; photodiode, biased probe, and VSWR indicator; were to be evaluated. The test unit fabricated was in two parts, the low-height waveguide section shown in Figure 3.17, and an optical sensor as in Figure 3.15. The reverse power monitor associated with the test facility was used to detect a high reverse power level.

5.7.2 Low Height Waveguide Section

The data of Figure 5.39 was used to select a waveguide height that would result in a multipactor breakdown with a power level of one kilowatt or less. The product of frequency (8360 MHz), and spacing was selected to be near 170, making the spacing .018 cm (.007 in.) for a power level of 600 watts. Lower power would require a smaller spacing which would be more difficult to implement. The .018 cm (.007 in.) high waveguide has an impedance of 6.05 ohms, which must be matched to the waveguide, 430 ohms for WR112. The large difference in impedances can be matched with a 51 ohms quarter wave line, or a two-step arrangment of quarter wave lines with the step impedances of 148 ohms and 17.5 ohms. These are based on using the relations (ref. 13):

$$Z_1 = \sqrt[4]{Z_o^3 \cdot Z_3}$$

$$Z_2 = \sqrt[4]{Z_o \cdot Z_3^3}$$

The corresponding step heights are directly proportional to impedances:

Guide height - 1.260 cm (.497 inches) (standard waveguide)
First region height = .437 cm (.172 in.), step is .826 cm (.325 in.) high
Second region height = .508 cm (.020 in.), step is 386 cm (.152 in.) high
Third region height = .018 cm (.007 in.)(selected), step .033 cm (.013 in.)high

The impedances are subject to some variation depending on the overall spectral response: the two step match will have a wider bandwidth an a single step which has a very sharp response (ref.13). The response can be adjusted for a Butterworth, Tchebycheff, or elliptical response. For this application a wide bandwidth was not critical but the two-step matching Butterworth was desirable.

The quarter-wave lines also have to be foreshortened since the steps are capacitive, and the shortened line provides a compensating inductive effect. The capacity can be determined from literature (ref.14) which shows the equivalent capacitors to be approximately :

First step = .21 pfd
Second step = .17 pfd
Third step = .13 pfd

The corresponding shortening of the quarter wave sections to provide a matched interface can be determined from a Smith chart. In the cases of interest, the shortenings were determined to be as follows, where a quarter wave line is 1.153 cm (.454 in.):

.437 cm (.172 in.) section: shorten .117 cm (.046 in.) to 1.036 cm (.408 in.)
.051 cm (.020 in.) section: shorten .033 cm (.013 in.) to 1.120 cm (.441 in.)

Sensors in the .007 inch high waveguide section were biased probes (Faraday cups) for multipactor detection; a separate waveguide with a photo diode as described in Section 5.6.2 was used for detecting visible light. A cross section view of the low-height section is in Figure 5.41 which indicates the steps and biased probes.

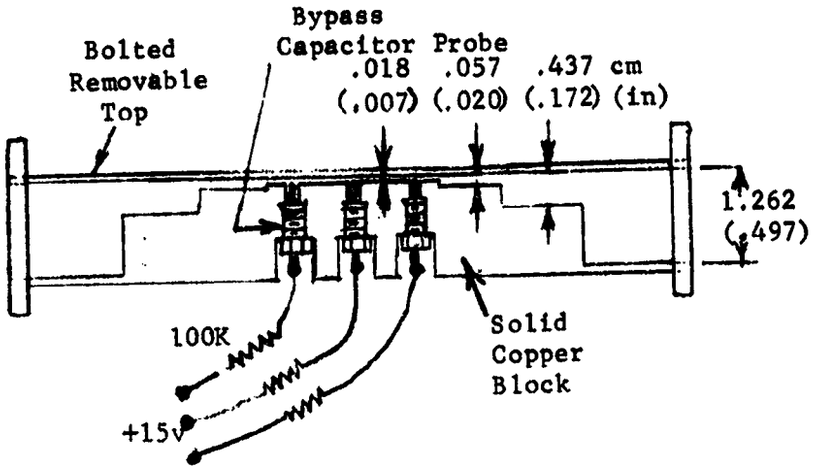

Figure 5.41. Cross Section of Low Height Waveguide Special Test Section

The latter were identical to the ones described in Section 5.6.1, except the RFI material was not required here. The probes were carefully cut to be flush with the .018 cm (.007 in.) surface and were centered in the .178 cm (.070 in.) openings as in Figure 5.40. Nine probes, three at the center and three at each end of the .018 cm (.007 in.) breakdown section, were used in the testing, with each group of three tied to a +15 volt supply through a 100,000 ohm resistor.

The breakdown block was cut from solid copper 1.424 x 3.175 x 8.128 cm (.561 x 1.25 x 3.02 inches). Corners were left with a 1/32 inch radius where an end mill could not be used. The block formed three sides of the waveguide; the fourth side, the top, was a flat sheet of hard copper bolted to the block. The waveguide narrow-wall edges on the copper block were bevelled slightly so the bolted top would have a firm seat against the narrow-wall edges inside the guide to minimize losses from the mechanical junction. Brass flanges were soft-soldered to the two ends of the unit. Note that some of these techniques would not be acceptable for

high reliability space equipment, but were tolerable in a test component which was to break down anyway. Zinc in the brass and tin in the soft solder both tend to "whisker" in a high vacuum and result in electrical arc breakdowns. Unfortunately, no such interesting breakdowns were observed in the tests, but strict avoidance of such metals should be observed for flight models.

The resulting breakdown section was shown in Figure 3.17. Note that the top was configured to fit inside the flanges so all discontinuities are at the flange. The top was bolted in place, and the flanges faced so the removable top would not cause a significant discontinuity at the flanges. The photodiode unit, essentially that of Figure 3.15, used a wedge tip quartz rod which was located on the top broadwall to view the .018 cm (.007 inch) section.

Bench testing was performed to check the VSWR, which was 1.29, indicating that if this were to be included in the system, some trimming would be desirable for a better match. The insertion loss was 0.65 dB due to the high I^2R of the low height section. This is close to a calculated value. Asuume the loss per foot in standard size copper waveguide to be about .050 dB or .006 dB in the length equal to the low height section 2.306 cm (.908 in) plus an equivalent of 1/3 of the length of the two adjacent matching steps = 3.053 cm (1.202 in), then the loss is approximately

$$.006 \left(\frac{1.263}{.018}\right) = 0.43 \text{ dB}$$

A more rigorous comparison would determine the losses in each of the steps of the matching sections as well as a more exact roughness factor for the unsmoothed surfaces of the machined copper block. These would increase the estimated loss closer to the measured value.

A water cooling pipe was added since the 0.65 dB is equivalent to 140 watts for a kilowatt input. This would heat the section excessively in a vacuum. But pulse operation was used with a 3% duty factor and no heating problem was present. Where CW tests were made the test durations were short.

5.7.3 Installation

The special breakdown test section and the optical sensor were installed in a vacuum chamber as in Figure 5.42. A waveguide window at the left provides the input for up to 5 kW. At the right, the signal is absorbed in a water cooled load external to the chamber.

Instrumentation included leads from the three groups of multipactor sensors as noted previously, three leads from the photodiode just to the left of the breakdown section, and temperature sensor. External instrumentation were two vacuum gauges, one each for the chamber and the waveguide end, the reverse power VSWR measurement at the input, and forward power at the waveguide output. No water cooling was required.

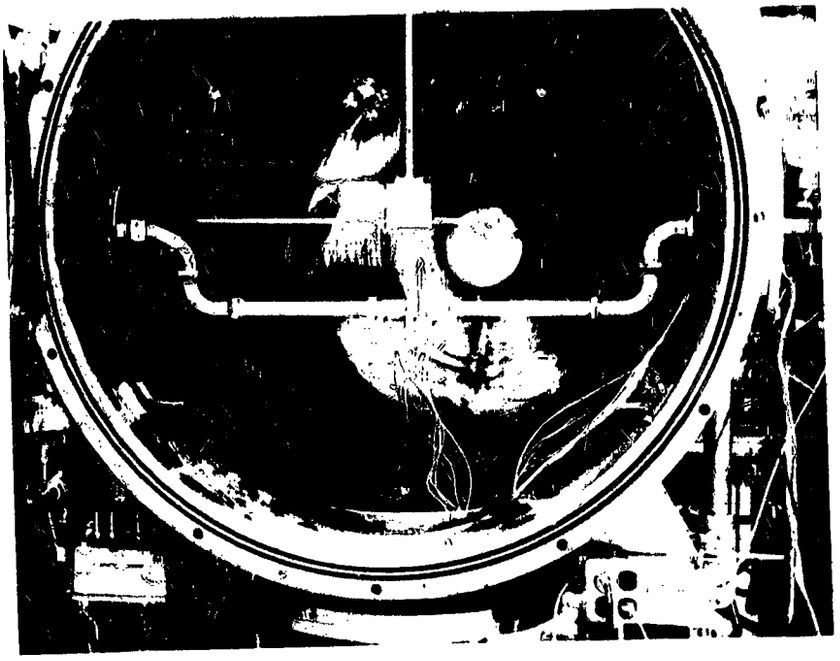

Figure 5.42. Special Breakdown Test Section in Vacuum Chamber

Test data was obtained with an eight channel recorder on which was recorded:

power output
tank vacuum
waveguide vacuum
reverse power (VSWR)
photodiode output
photodiode trip
multipactor probe (2)

In addition, all three multipactor probe groups were monitored visually with meters, and temperature was observed on a meter.

5.7.4 Test Results

5.7.4-1 General Summary

A series of breakdown tests were conducted to determine the merits of the three types of sensors used. The first test performed used CW in a high vacuum,

and at the instant of breakdown, all sensors except the photodiode went off scale. The pressure gauge returned to a normal reading in about 30 seconds. This breakdown provided a cleaning action but was too drastic to draw any suitable conclusions. Subsequently, all tests were made with a low duty cycle pulse transmission. Frequently a breakdown could be observed to start, but would not build up sufficiently during the 15 microsecond pulse to trigger the sensors, particularly after the earlier breakdowns had cleaned the surfaces. The test program included a total of 31 additional multipactor breakdown and 17 arcing tests, some of which included more than one breakdown per test. (The use of pulse power has no significance in terms of breakdown conditions).

Breakdown Power:	900 watts for multipacting a little above theoretical; 3000 watts used for arcing tests with no determination of the minimum (but estimated to be 260 watts)
Multipactor Breakdown Probes:	strong indication for multipacting; no response for arcing (at high pressure end of pressure range.)
Photodiode	Generally reliable indication for gas arcs; four failures may have been due to arcs at the remote end of the breakdown test section where most of arc wasn't visible; variable somewhat for multipacting.
VSWR:	Generally good for both types of tests; CW tests suggest a small time lag exists but not critical as for the ion gauges. Should be used in conjunction with other sensor for redundancy.
Ion Gauge:	Usually gave a definite reading from a fault, but rise time was too slow to be useful.

The biased probes, photodiodes, and reverse power sensor should all be included where appropriate such that a redundant protection situation exists.

The multipactor breakdown tests were peformed at a high vacuum, and the rf power was increased slowly until a breakdown was observed from the biased probes. The photodiode was usually used as the protective sensor for the test transmitter although an especially large reflected power level also would trip the transmitter's own VSWR threshold circuit.

The arcing tests were performed by approaching the arcover region from both the high pressure side and the low pressure side. From the high pressure side, the biased multipactor probes gave no output, indicating that the arc occurred in some other part of the breakdown test section. (From Figure 3.17 arcs are seen to have occurred near the sharp edges of the breakdown section, which is expected for low pressure arcing). The photodiodes worked well much of the time; the VSWR indication was not quite as good but still was valuable. The ion gauge provided a good indication also but with a slow response time.

Working from a high vacuum condition toward a higher pressure, the gas arcing conditions and multipact conditions did not vary appreciably, and both types occurred. In general, they could not be made exclusive, but the photodiode operated quite well on the combination. As the pressure was increased, the breakdown tended toward the ion arcing type. From Figure 3.17, the evidence of arcing appears at the larger gaps which clearly indicates ion arcs tend to occur over longer gaps rather than shorter gaps for a higher vacuum condition.

5.7.4-2 Summary of Multipactor Breakdown test Data

The recorded data is summarized in Table 5.5 for the 32 tests performed. The VSWR channel operated well for the first five tests; it was later found to be inoperative and corrected after test 26. Results were positive for tests 27 to 29. The final tests established the breakdown level as being about 900 watts. The equipment was operated at the threshold to result in a level that would not trip the protective circuit. Two signals were used for protective purposes here: the photo diode and the test facility VSWR circuit. The channel amplifier for the photo diode also was found to be faulty through much of the test, but the diode trip signal was generated quite reliably. The biased probes for multipactor breakdown detection worked very well and were most consistent. They were not tied in to the trip circuit in order to get a better indication of the nature of this breakdown. With the pulse operation, these signals were always widely variable, but always had a peak magnitude sufficient to trigger a control circuit if required.

The diode trip was considered less desirable since it usually permitted a multipacting situation to exist at low and moderate breakdown levels before a sufficient blip would occur to trigger the trip circuit. The VSWR measurement appeared to be good when the recorder channel operated properly.

An examination of pressure in the waveguide showed it usually increased with a substantial breakdown level, but the rise was slow and would not be acceptable for protective purposes. Early breakdowns were, in part, aggravated by surface contamination boiloff, but the final tests indicated quite clearly a relatively narrow power range between multipactor breakdown and no breakdown; an 867 watt level was firmly without breakdown while 933 watts was firmly in the breakdown region.

5.7.4-3 Summary of Gas Arc Test Data

The summary of the recorded data is in Table 5.6. Five tests were made at the high pressure side of the breakdown region, and 12 on the low pressure end. No previous data is available on arcing over small gaps, like the .018 cm (.007 in) used, in a waveguide. At the low pressure end, the arcing tends to occur in the larger gaps of the impedance matching quarterwave sections, but there was also multipactor breakdown at the pressures and powers used. Thus determining an arcing breakdown point is rather unreliable.

The first five tests indicate the pressure was about 5330 N/m^2 (40 mm Hg) for arcover in the .018 cm (.007 in) section ($p \cdot d$ = 93 N/m^2-cm (0.7 mmHg-cm)) for a power level of 3.3 kW (voltage was 140 volts across the gap). This

TABLE 5.5. MULTIPACTOR BREAKDOWN TEST DATA

TEST #	PRESSURE M/m²	PRESSURE (TORR)	PEAK POWER	PHOTO DIODE	TRIP	VSWR*	MULTIPACT
1-CW	9.3×10^{-3} to far off scale	(7×10^{-5}) to far off scale	810 W	Firm (no calibr.)	(diode)	off scale - over 10X normal	0.7 - 1.0 V (visual)
ALL OTHER TESTS PULSED.							
2	9×10^{-3}	(6.8×10^{-5})	730 W	Off Scale (10 V)	(diode)	X3.5	Visual - no record
3	CHECK FOR TRANSIENTS IN SENSORS - NONE NOTED ON CHART RECORD						
4.	9×10^{-3} burst to 13×10^{-3}	(6.8×10^{-5}) burst to 10^{-4}	2 kW	Good	(diode)	X2.5	Off scale at 1V F.S.
5.	9×10^{-3}	(6.8×10^{-5})				slight	
6.			630 W to 1.25 kW	slight	Chatter & Trip (diode)	Inoperative	1 to 3 V
7. (14 trips)			1.5 kW (9 trips)	Channel Faulty	Chatter & Trip (diode)		0.4 to 3 V (strong)
			1.25 kW (5 trips)				
8. (10 trips)	9×10^{-3}	(6.8×10^{-5})	1.1 kW				0.4 to 1.8 V (consistent)
9. (5 trips)			1.2 kW				0.2 to 0.5 V
10. (4 trips)			1.2 kW				0.1 V
ADD β SOURCE, THALIUM 204, 60 μCURIES							
11.	7×10^{-3} (burst)	(5.3×10^{-5}) (burst)	2.8 kW to 1.2 kW	1V	no. trip		1 volt
12.			3.1 kW	0.5 V	Chatter - no trip		.65 V
13.			3.1 kW	None (Faulty)	Chatter - trip		.4 V
14.	8.7×10^{-3}	(6.5×10^{-5})	1.6 kW		Chatter - trip		.85 V
15.			1.6 to 3.5 kW		Chatter - trip		.2 to .4 V
16.			3.5 kW				.5 V
17.							.6 V
18.							.4 V
19.				Noisy			.45 V
20.			3.9 kW		Trip (Diode)		.2 to .5 V
21.			3.9 kW to 3.5 kW				.25 to 1 V
22.			3.5 kW				.45 V
23. (over 8 minutes)			1.4 kW to 1.9 kW to 2.4 kW		Trip at end		Low to 0.4 V to 2.0 V (variable)

TABLE 5.5 (Continued)

24.	8.7×10^{-3}	(6.5×10^{-5})	1.2 kW	Noisy	Trip	Inoperative	1 V
25.			1 kW				.35 V
26.			2 kW			(repaired)	0.7 V
27.			2 kW			none	2 V
28.			2 kW	0.7 V		small	2.2 V
29.			1 kW	0.3 V		good	1.4 V
30.			2.2 kW	0.6 V	Chatter - Trip	small	2.1 V
31.			0.6 to 1 kW	0.2 to 0.5 V	none		0.2 to 0.6 V (none below 830 W)
32.			0.5 to 1 kW	0.1 to 0.5 V	none		0.3 to 0.4 above 900 W (only)

* VSWR NOTED RELATIVE TO NORMAL LEVEL OF ABOUT 1.3

TABLE 5.6. GAS ARC TESTS

TEST #	PRESSURE N/m^2	(TORR)	PEAK POWER	PHOTO DIODE	TRIP	VSWR*	MULTIPACT SENSOR
33.	2.67×10^{4} to 1.02×10^{4}	(200 to 77)	3.3 kW	0.4 V	Xmtr VSWR		None
34.	1.2×10^{4}	(90)		0.2 V	(Diode)	X2.5	
35.	1.46×10^{4}	(110)		none	no trip	(blip)	
36.	to 5.3×10^{3}	(to 40)		none		X.2	
37.	to 5.6×10^{3}	(to 42)		0.2 V		X2.4	
38.	133	(1)		none		X2.4	
39.	47	(.35)		none		X2.4	Slight
40.	13.3	(0.1)		0.5 V		X2.5	to .2 V
41.	1.6	(.012)	2.3 kW	1.4 V	(Diode)	X1.5	.2 to .3 V
42.			3 kW	low	no trip	slight	.9 V
43.				0.7 V		X2.5	0.8 V
44.	6.0 to 50	(0.045 to 0.370)		low to 1.0 V - erratic		X2.4	0.1 to 2.5 V erratic
45.	50	(.370)	1.2 kW CW	0.2 V	(Diode)	**	.35 V
46.			to 2.2 kW CW	0.2 V			to .8 V
47.			2.5 kW CW	0.2 V			to 1.5 V
48.			1.7 dw CW	0.3 V	Manual		0.5 V
49.			1.5 kW CW	0.2 V			0.4 V

* VSWR relative to normal power with VSWR = 1.3

** Fault in instrumentation

point can be used to determine the upper part of the arc breakdown curve for a very low height waveguide with height to width = .006. At the low end, the curve is not well defined since the arcing occurred at other points than in the low height section. Figure 5.43 shows the upper region of the arcing curve for the low height section (b/a = 160).

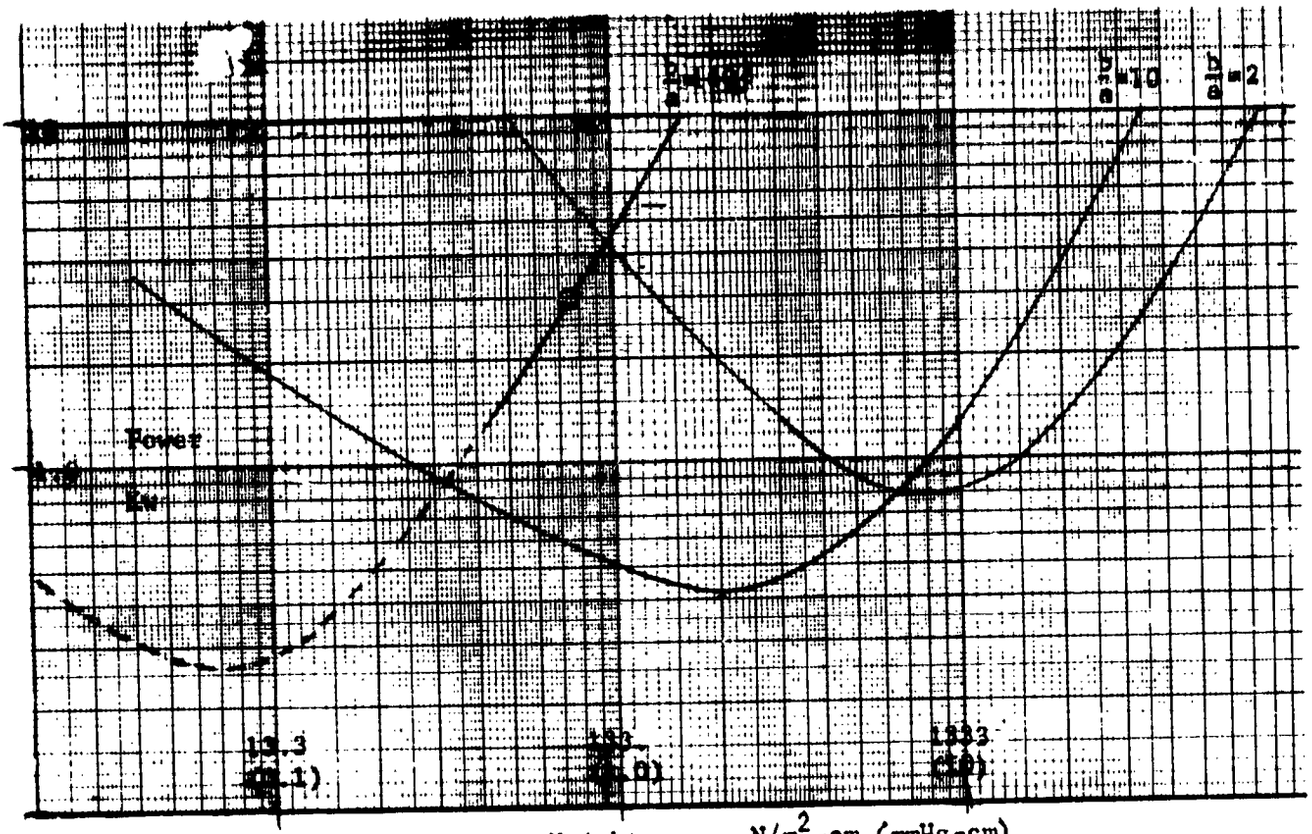

• Pressure x Height - N/m^2-cm (mmHg-cm)

Figure 5.43. Paschen's Data for Low Height Waveguide (DC Data)

The VSWR proved to be a reliable sensor here, and gave a strong indication in all but two cases. The photodiode was also quite reliable, particularly for the lower pressure operation. The results indicate the desirability of including both types of sensors. The biased probes, for detection of multipactor breakdown, were ineffective for detecting gas arcs at high pressures, and only operate when the breakdown is at the probe.

5.7.4-4 Magnetic Field Effects

A magnetic field of about 100 Gauss was applied next to the breakdown section. It was found that the field had no effect. When a breakdown was

occurring, the breakdown continued at the same level. When the power level was just below the breakdown threshold, the magnetic field would not induce any breakdown. The magnetic field and power were both varied over ranges up to a maximum (930 watts peak).

5.7.4-5 Breakdown Prevention

No effort was included specifically to determine techniques to prevent breakdowns should they occur. Gas arcs can only be prevented by operating at low power levels, probably under 200 watts as indicated in Figure 5.43, or by maintaining the high vacuum. Multipactor breakdowns are best eliminated by suitably dimensioning the components so the critical frequency x spacing factor is avoided, per Figure 5.39. On another program, the ability to prevent multipacting was evaluated for other types of surfaces, particularly perforated broadwalls backed by a biased electrode, and coated walls with low secondary electron emission coefficients. These are described in Appendix I. Essentially, the perforated approach is quite feasible and should be considered were all else fails. The coatings which will prevent breakdowns tend to be very lossy and should only be considered for points or lines, not surfaces. Neither completely eliminates the effect, but there is no buildup of any significance beyond perhaps a little electrical noise. The perforated section could have been more effective if more heavily perforated, and both surfaces had been so modified.

5.8 HIGH VOLTAGE DC BLOCKING FLANGE

5.8.1 Requirements

TWT's having a voltage-jump section to improve efficiency require that one of the ends of the device be at a substantial dc voltage, as high as 10,000 volts. An investigation was performed on the parameters and design of a waveguide choke section which could withstand this dc voltage with an rf power level of 1500 watts, but which would have a negligible effect on VSWR and loss. This flange would normally be placed at the TWT output flange to minimize the extent of the system having the very high voltage present.

A number of factors must be considered for a practical dc blocking flange. Materials should be inorganic in nature for low outgassing and sublimation, and should have a reasonable safety factor with long life continuous operation. RF leakage through the flange is required to be low enough so that the entire waveguide assembly meets the leakage specification of -111.75 dB. The harmonic leakage specification was implied by the overall assembly leakage specification. In addition, the rf loss in the flange will have to be distributed to a heat sink to control temperature.

This task was carried to the conceptual design stage, but the problems identified led to the deferment of additional effort. The fabrication of such a flange would be quite complex to achieve the performance objectives, and operation appeared to be marginal. Harmonic leakage would be a very difficult problem in that the second harmonic would have to rely completely on absorption by a lossy material in the flange. Adding filters for the harmonics as well as the fundamental would result in an impractically large, complex, and costly flange. In addition, it would only be effective if all other rf leakage points in the system, including the TWT input circuit, the voltage-jump interface, and the collector also were heavily shielded. Some practical factors are considered in Section 5.8.4.

5.8.2 Flange Filter Design Analysis

At the time of the design, a specification was applied which indicated that total rf leakage from the dc blocking flange should not exceed a level about 130 dB below the rf level propagating through the waveguide. The basic configuration of the dc blocking flange structure is illustrated in Figure 5.44a. The illustrated structure is depicted schematically in Figure 5.44b, which is a "one-line" representation of the waveguide circuit. The waveguide wall, represented by the vertical line is cut to provide a gap with dc isolation between input and output terminals. This gap alone through the waveguide would introduce an intolerably high VSWR into the system, which can be reduced to an acceptable value over a narrow frequency range by adding an open-circuited radial line section at the cut. If the radial line is nominally a quarter-wavelength from the waveguide wall to the open-circuited perimeter of the line, the open-circuit at the perimeter is transformed to an electrical short circuit at the waveguide wall. This results in minimization of the disruption to rf current in the waveguide walls and a moderately low VSWR over a narrow bandwidth. However, it will not meet the requirements of this application since rf radiation is high at the radial line open end and the low-VSWR bandwidth is not likely to be acceptable with dielectric gaps (i.e. radial line spacings) large enough to safely withstand 10 kV.

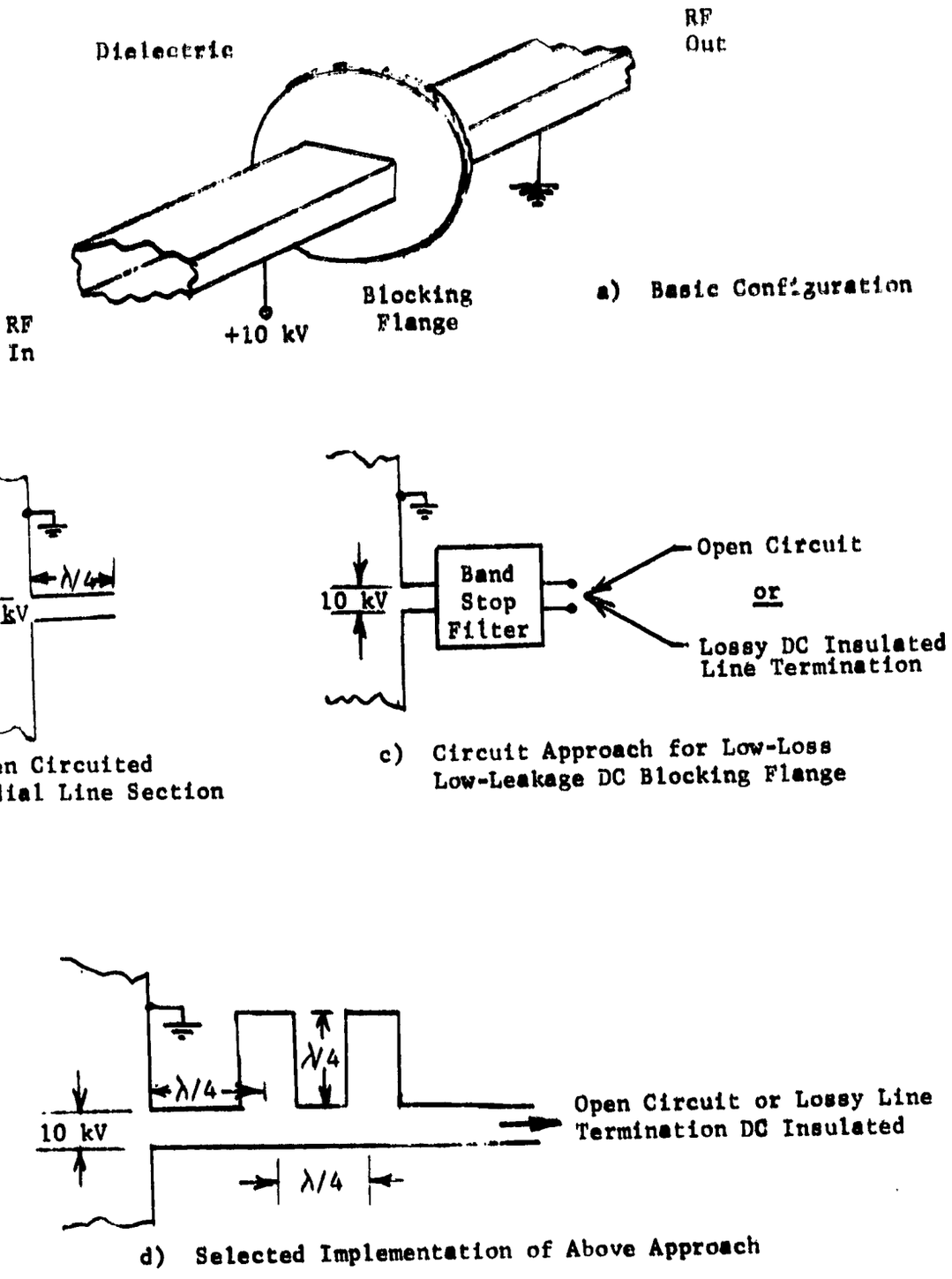

Figure 5.44. Design Approach to DC Blocking Flange

RF requirements can be met with the use of a more sophisticated band stop filter than the radial line section. This approach is indicated in Figure 5.44e. A satisfactory band stop filter structure, of course, must include dc isolation across the gap. The filter section could be designed for an open circuit termination, in which case it must provide the total required isolation to rf leakage (130 dB), or it could be designed for lower isolation (say 30 dB) and terminated with a dc isolated, lossy transmission line section to provide the balance (100 dB) of required isolation.

Consideration of possible band stop filter rf structures which would provide the necessary dc isolation across the waveguide gap and which would lend themselves to being applied around the circumference of the waveguide led to the selection of the approach illustrated in Figure 5.44d. This band stop structure consists of a series of one-quarter-wavelength short-circuited resonators connected in series with one conductor of a transmission line connected across the gap in the waveguide. These resonators are each spaced one-quarter-wavelength apart along this transmission line. The filter can be designed to operate open-circuited or with a lossy line termination as mentioned above. Matching sections, such as the $\lambda/4$ section between the waveguide and first stub in Figure 5.44d, may be required for impedance matching purposes and to permit maximum flexibility in dimensioning the band stop filter components.

Before designing the filter structure, it is necessary to consider the prototype design. The general band stop filter selectivity characteristics are shown in Figure 5.45. For a required minimum attentuation in the ω_{1A} to ω_{2A} stop band, a given prototype will have a certain lower pass band extending from dc to a pass band upper frequency ω_1 and a "minor-image" upper pass band beginning at ω_2.

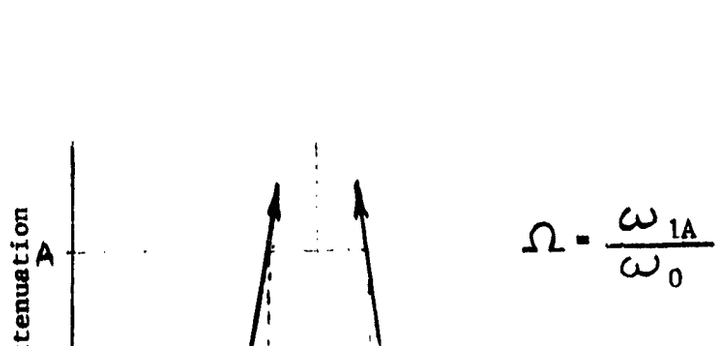

Figure 5.45. Band-Stop Filter Rejection Characteristics

Insight into the filter requirement can be obtained by evaluating several filter prototypes for a variety of conditions. The results for representative cases of multi-resonator filters are tabulated in Table 5.7. The cases of

TABLE 5.7
A Comparison of Stop-Band to Pass-Band Ratios for a Number of Prototype DC Blocking Flange Bandstop Filter Designs

Tchebychev - Prototype

3.0 dB Ripple - Lossless element case

Number of Resonators	Ω for 130 dB Isolation	Ω for 30 dB Isolation
3	33	2.15
5	9	1.38
7	4	1.18

Butterworth Prototype

Number of Resonators	Ω for 130 dB Isolation	Ω for 30 dB Isolation
2	--	6.3
3	40	3.2
5	20	2.0
7	7.0	1.65
9	4.7	1.47

where $\Omega = \frac{\omega_{1A}}{\omega_1}$

attentuation A = 130 dB represent the open circuit terminated filter. Actually this termination is a non-infinite impedance since the radiation resistance at the "open-circuit" at the end of the filter may be a fairly good impedance match. Thus, both open circuit and terminated cases were considered. Here, all of the required rf leakage suppression is supplied by the filter alone and the end leakage should be at least -130 dB. A second series of cases was determined for 30 dB attenuation, which requires a lossy-line termination of 100 dB insertion loss. The stop-band to pass-band frequency factor Ω, defined by:

$$\Omega = \frac{\omega_{1A}}{\omega_1} .$$

Large values of Ω are indicative of severe filter parameter requirements where difficult-to-realize resonator and transmission line values are required. This will be seen later for computed cases.

The element dimensions for the band-stop filter were determined (ref. 16) for a three-resonator filter circuit, shown with expression for element values in Figure 5.46. Terminating admittances Y_A and Y_B and the transmission lines

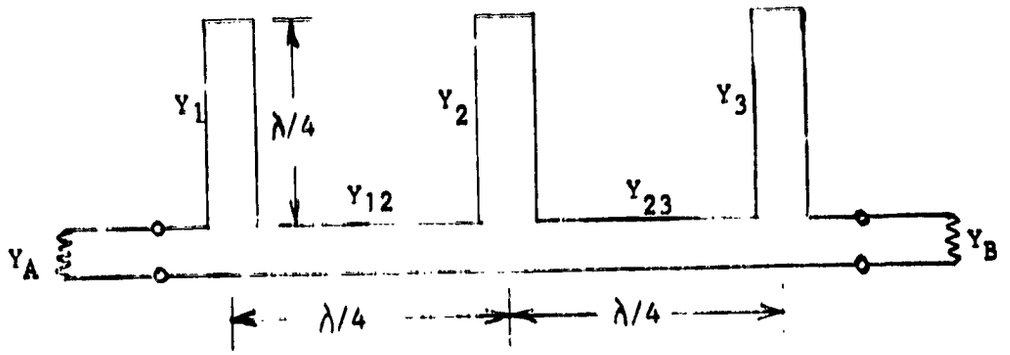

$$Y_A = 1/793 \text{ mho} \qquad Y_3 = \frac{Y_A g_0}{g_4}\left(1 + \frac{1}{\Lambda g_3 g_4}\right)$$

$$Y_1 = \frac{Y_A}{\Lambda g_0 g_1} \qquad Y_{12} = Y_A\left(1 + \Lambda g_0 g_1\right)$$

$$Y_2 = \frac{Y_A g_0}{\Lambda g_2} \qquad Y_{23} = Y_A \frac{g_0}{g_4}\left(1 + \Lambda g_3 g_4\right)$$

$$\Lambda = \cot\left(\frac{\pi}{2}\frac{\omega_1}{\omega_0}\right) = \cot\left(\frac{\pi}{2}\left(\frac{\omega_0 - \frac{BW}{2}}{\Omega\ \omega_0}\right)\right)$$

Figure 5.46. Expressions For Element Values for a Three Resonator Band-Stop Filter

admittances Y_{12} and Y_{23} were selected to be equal to the source impedance at the waveguide gap. At this point, the characteristic impedances of the two waveguides are in series and equal to a total of 792 ohms. The normalized low pass filter prototype element values, g_k, are obtained from published tables (ref. 17) and are listed in Table 5.7. Simple Fortran routines were written for one, two, and three resonator cases (see Appendix IV). Calculated results are given in Table 5.8. Cases for more than three resonators were judged to be too unwieldy for practical fabrication and were not considered further.

TABLE 5.8

Calculated Bandstop Filter Designs for DC Block Flange

Case No.	Number of Resonators	(dB) Isolation	(dB) Prototype Ripple*	Termination (ohms)	Resonator Z_o $Z_1=Z_3$	Resonator Z_o Z_2	Transmission Line Z_o $Z_{12} = Z_{23}$
1	1	30	-	792	30,785	-	-
2	2	30	3	792	701	601	91
3	2	30	0*	792	661	158	132
4	2	20	3		635	1140	157
5	3	30	0*	792	521	207	272
6	3	130	0	792	763	15.2	29.4
7	3	130	0	∞	(Z_1 = 736) (Z_3 = 7.9 x10^{12})	22.9	(Z_{12} = 55.7) Z_{23} = 20.3)

* Butterworth

Impedance values calculated and listed in Table 5.8 were too high for practical application in most cases. It is desirable to use the aforementioned $\lambda/4$ transformer between the waveguide gap and the first resonator to permit optimization of impedance levels in the bandpass filter choke section. As will be discussed later, it will be advantageous to build the choke assembly folded onto the surface of the waveguide rather than using the radial configuration shown in Figure 5.44a. For this configuration, transmission line impedances can be calculated on a parallel plate model with little error using the relation:

$$Z_o = \frac{377 \cdot a}{\sqrt{\epsilon_r}\ b}$$

where a is the dielectric thickness and b is the nominal perimeter of the transmission line or resonator section. For the purpose of this calculation, the material selected for a dielectric in the choke region is pyrolytic (chemical vapor deposited) boron nitride which has relative dielectric constant (ϵ_r) of about 3 to 5 depending on the process used. A nominal value of $\epsilon_r = 4$ is used for illustration. Pyrolytic boron nitride has good insulating qualities; ideally a thin section of .0127 cm (.005 in) will withstand 10 kV. For the perimeter of WR75 waveguide, which is 6.371 cm (2.65 in), the characteristic impedance of the

lowest impedance line could be transformed to

$$Z_o = \frac{377 \cdot 0.005}{2 \cdot 2.65} = 0.355 \text{ ohm for}$$

Case 7 of Table 5.8. The impedances normalized to Z_{23} for these three resonators, open circuited, 130 dB isolation case would then be

$Z_1 = 12.8$ ohms
$Z_2 = 0.4$ ohms
$Z_3 = 4.9 \times 10^{14}$
$Z_{12} = 0.99$ ohms
$Z_{23} = 0.355$ ohms

and the $\lambda/4$ matching transformer would be

$$Z_o = \frac{792}{\sqrt{20.34/0.355}} = 104.6 \text{ ohms}$$

In practice Z_{12} would be terminated with an open circuit and Z_3 and Z_{23} omitted. Two difficulties in this design are the still too-high impedance required for the matching transformer, and producing a very high impedance at Z_3 since the radiation resistance of the open circuited Z_{12} line is of the order of only 50 Z_{12} or 50 ohms. Thus, the expected attenuation of 130 dB would not be achieved.

Similar problems exist in the other 130 dB isolation designs, with values of transmission lines or resonator impedances being obtained which are impractical to implement. The 30 dB bandstop filter plus 100 dB dissipative transmission line attenuator gives more reasonable transmission line impedances for implementation. Normalizing Case 2 of Table 5.8 to $Z_{12} = 0.355$ ohms gives element values as follows:

$Z_1 = 2.74$
$Z_2 = 2.35$
$Z_{12} = 0.355$

which require boron nitride dielectric thicknesses in the range of .013 to .102 cm (0.005 to 0.04 inch). In this case the input matching transformer could be any convenient impedance since it is merely necessary to transform the high stopband impedance at the input of Z_1 to a very low impedance in series with the waveguide gap. The conceptual approach to physcially implementing this bandstop filter choke plus lossy dielectric termination is illustrated in Figure 5.47.

5.8.3 Blocking Flange Fabrication Approach

The method of fabricating the high voltage blocking flange was examined to determine a reasonable size and rugged construction. The first approach considered was a disk arrangement with the quarter wave filter sections radiating out from the waveguide, as shown in Figure 5.44; it was rejected on general grounds in favor of a folded arrangement like in Figure 5.47 which would be lighter, more rugged, and be less susceptible to undesirable resonances in the filter structure.

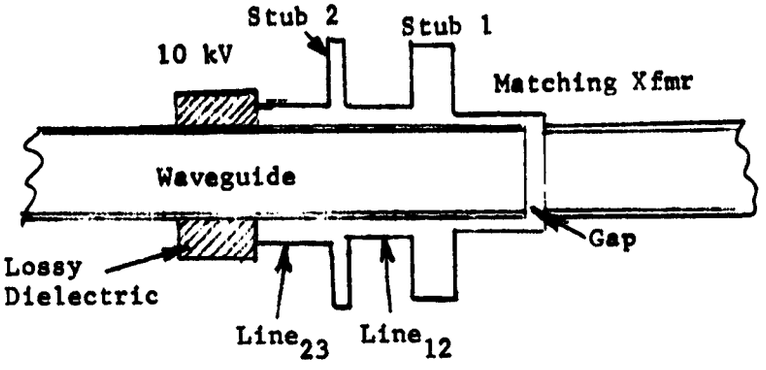

Figure 5.47. Schematic of an Approach to Implementing a Two-Resonator Filter

The folded filter would be fabricated by a series of depositions and machining of boron nitride and metal. This approach eliminates much of the concern for air pockets in the assembly which otherwise could result in possible outgassing and electric field distortion. The progression and final configuration are shown in Figure 5.48. The boron nitride insulation must be effective both in the air and in vacuum, so the path length inside the guide is required to insure no arcing from the 10,000 volts. The design must be checked carefully to minimize reflections as the reverse power monitor will not include this point in its measurement. The BN may be set into the waveguide surface somewhat, with a pathlength determined from Paschen's Law, with dimensions to minimize reflections. Mechanical rigidity during this stage of the fabrication will have to be carefully observed. The deposition of the lossy dielectric has not been pursued, but the material would be the same as the Lundy rfi material used for attenuating rf in the optical and biased-probe sensors as considered in Section 5.6. This material has a high dc resistance but a further evaluation would be required.

The resulting fabricated choke flange approach is similar to that of Figure 5.47 except more folding is used. The first sketch in Figure 5.48 shows the first application of boron nitride which covers both the inside and outside of the waveguide. This is then machined to provide a notch for the quarter-wave lines that will be added. The third sketch shows metalizing; this provides $line_{12}$ of the previous figure. This metal is filled with boron nitride, and the surface planed with a notch again over the quarter-wave section. The next metalizing operation of the fifth sketch forms the side of stub 1, and covers some of the other parts of the boron nitride which must be removed. The third and final deposition of boron nitride in the sixth sketch provides the dielectric for the second stub of Figure 5.47. The surface is planed with an appropriate notch above Stub 2 as required. The lossy dielectric can now be added, followed by the final metalizing of the last sketch in the figure.

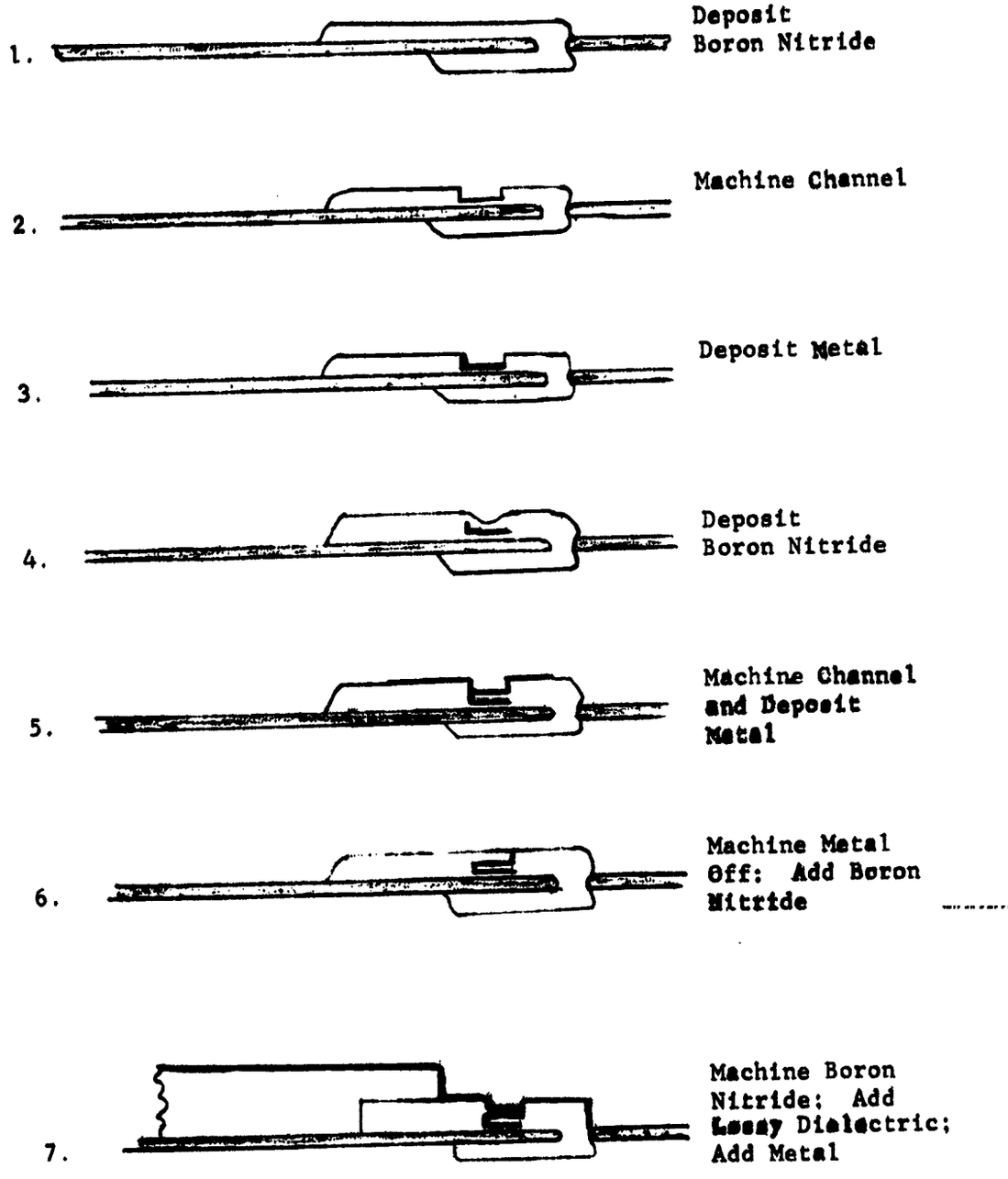

Figure 5.48. Fabrication Sequence for Two-Resonator Filter

The final package has the quarter-wave matching transformer at the gap. The rf goes past Stub 1, which is the middle section of the three stacked quarter wave lines, then through $line_{12}$ which is at the surface of the waveguide. Stub 2 is the top of the three stacked quarter-waves. The wave then goes to the left through a matching section of boron nitride, as required, and into the lossy dielectric which has whatever length is required for 100 dB of attenuation.

The most critical breakdown region is in $line_{12}$ which may be from 0.13 to .102 cm (.005 to .040 inches), depending on final design. Pyrolytic boron nitride will normally handle this voltage, but this region is the one of greatest concern in achieving a good final design.

5.8.4 Practical Application Problems

A general objective throughout this program was to hold rf leakage to a very low level. The design shown in the previous discussions can hold the fundamental leakage to a level of -130 dB. The harmonics will rely on the rf absorber which might be adequate. But the overall transmitter system is subject to rf leakage from the voltage-jump section of the TWT, the input circuitry, and the collector. The latter is of particular concern since it also is a new element considered for the overall transmitter system.

The dc blocking flange may be placed in three different places:

1. Input waveguide which would shift all biases and permit the output flange of the TWT to be at ground potential. This has a strong advantage in that the signal will be 30 dB to 40 dB below the output, and there will be much less concern over rf leakage. In addition, harmonics can be removed more easily from the driver stage output.

2. At the TWT output flange, which is the approach discussed in the previous sections. RF leakage is the greatest concern because of the large signal with moderately high harmonic content.

3. After the harmonic filter, which would remove the concern for harmonic leakage and the design shown would be completely adequate. However, the large harmonic filter would have to be insulated for the 10,000 volts, and thermal control would be more difficult.

The possibility of leakage and its control from sources other than the blocking flange should be examined in considerable detail, and the trade-offs of developing this flange in the presence of possibly worse sources of rf leakage should be examined thoroughly. The three sources of particular concern are the voltage-jump region, the collector if the multi-ring depressed collector is used, and the antenna backlobes. Upon determining that the dc blocking flange is definitely required, the preceding design should be reviewed and a program directed toward developing a breadboard model to ascertain that all problems in design and fabrication have been identified, and all are adequately solved.

5.9 SCALING TO OTHER FREQUENCIES

A basic requirement for performing experimental work at 8.36 GHz is that the effects can be interpreted in terms of performance at 12 GHz and 2.64 GHz. This was done by considering the phenomena of interest, and developing a function to relate each one in terms of frequency and waveguide dimensions. The specific factors are discussed briefly here. Results were shown previously in Table 3.2.

Terminology used here is arbitrarily defined as follows, which corresponds to that of Table 3.2:

$$f = \frac{f_{ref}}{f_{new}}$$

or $$f_{12} = \frac{12}{8.36} = 1.435$$

or $$f_{2.64} = \frac{2.64}{8.36} = 0.316$$

and $$\gamma = \frac{(b/a)_{8.36}}{(b/a)_{other}} = 0.886$$

The latter comes about because the WR112 waveguide used in the experimental work has a height to width ratio, b/a, different (by .886) from the ratio either WR75 (12 GHz) or WR340 (2.64 GHz).

5.9.1 Ionization Breakdown

Paschen's Law indicates that arcing due to ions is a function of voltage and electrode spacing. In the case of waveguide at a given pressure, the height is the spacing factor, and voltage is determined from the required power level and guide impedance. The power in a waveguide can be expressed as:

$$P = \frac{V^2}{Z} = \frac{V^2}{k \cdot b/a}$$

where k is a constant relating waveguide dimensions to wave impedance. To determine the power at one frequency that will simulate the ionization breakdown at another frequency, the voltage gradients in the guide should be the same:

$$\left(\frac{V}{b}\right)_{new} = \left(\frac{V}{b}\right)_{ref.}$$

Using this in the above equation:

$$\frac{P_{new}}{P_{ref.}} = \frac{(a.b)_{new}}{(a.b)_{ref.}}$$

The value of f can be expressed in terms of waveguide widths (assuming operation at a proportionate part of the band):

$$f = \frac{a_{new}}{a_{ref.}}$$

Then

$$\frac{P_{new}}{P_{ref.}} = \gamma f^2$$

From the requirement for 1.5 kW at 12 GHz, the equivalent 8.36 GHz power is 2.74 kW. This equation can be extended to the 2.64 GHz case, substituting values at that frequency for the 12 GHz ones. In this case, a 1.5 kW signal is simulated at 8.36 GHz by a level of 133 watts, indicating a low problem likelihood at the lower frequency of interest. In all cases the 2.64 GHz simulations require power less than or equal to that for 12 GHz.

5.9.2 Multipactor Breakdown

This type of breakdown is concerned with the time for an electron to traverse the distance between the waveguide broadwalls relative to the frequency. For a comparison, the effects of the sine wave is assumed to be the same for both frequencies, so a static calculation illustrates the result. The time to accelerate the distance b with a voltage V is derived from $b = \frac{1}{2}(\text{accel.})t^2$, or:

$$t = \left[2\, b/k \cdot (V/b) \right]^{\frac{1}{2}}$$

where k is a constant relating acceleration to voltage gradient, V/b. The condition for multipactor breakdown is that this time be a half-cycle interval, or the values of $k_2 \cdot t/f$ be used in determining voltage for the two sets of conditions. Carrying this analysis through and placing the voltage ratio in the power ratio equation, the conclusion is that the phenomenon is independent of frequency, and is only altered by the γ factor:

$$\frac{P_{8.36}}{P_{12}} = \gamma^3 = 0.6955$$

The same expression holds for relating 8.36 GHz and 2.64 GHz since the value of γ is the same in both cases. Thus for a 1.5 kW signal, the simulation can be achieved with a power level of 1.05 kW. However, from Figure 5.39, there is a considerable range in breakdown power (voltage) levels and in some cases, there is a change with spacing. The above gives a reasonable direction of power change, however.

5.9.3 Paschen's Minimum Breakdown

The minimum breakdown voltage for a gas arc is constant, and depends on the product of electrode spacing and gas pressure. If the electrode spacing changes, such as going from WR75 to WR112 waveguide, the minimum breakdown voltage stays the same except it will occur at a slightly different pressure. The only contributing factor, where the minimum point is of interest, is that the power involved will vary with waveguide height, since the same voltage is necessary to effect the same minimum. Referring to the first equation of this section and noting that the two voltages must be equal, then the equivalent power is only a function of b/a which is found to be:

$$\frac{P_{8.36}}{P_{12}} = \frac{1}{\gamma}$$

The resulting simulation power is then 1.7 kW for a 1.5 kW input at 12 GHz.

5.9.4 Paschen's Pressure Minimum

The pressure minimum varies with spacing, but the product of pressure and spacing should remain a constant. Denoting pressure by p:

$$(p \times b)_{8.36} = (p \times b)_{12}$$

from which

$$P_{8.36} = P_{12} \cdot \frac{1}{\gamma f}$$

This indicates the test pressure to operate at the minimum breakdown point is about:

$$P_{8.36} = P_{12} \cdot 1.27$$

relative to 12 GHz. There is no power involved in this expression, only pressure.

5.9.5 I^2R Loss Per Unit Length

The power lost in a waveguide wall is directly dependent on current flow and on resistance which varies with waveguide dimensions and frequency. Power lost is proportional to power input, surface resistivity, and skin effect loss. Thus for a unit length (ref. 15):

$$P_{I^2R} \propto \frac{P_{in}}{b}\left(1 + \frac{b}{a}\right) \quad (\text{freq.})^{\frac{1}{2}}$$

where the last term is the skin effect. The ratio of I^2R losses for two frequencies is:

$$\left(\frac{P_{new}}{P_{ref}}\right)_{I^2R} = \frac{P_{new}}{P_{ref}} \cdot \frac{b_{ref}}{b_{new}} \frac{\left(1 + \frac{b}{a}\right)_{new}}{\left(1 + \frac{b}{a}\right)_{ref}} \frac{1}{f^{\frac{1}{2}}}$$

The $(1 + \frac{b}{a})$ terms are nearly equal and were cancelled. Then for equal I^2R losses:

$$\frac{P_{new}}{P_{ref}} = \gamma f^{3/2}$$

Thus

$$P_{8.36} = 2.29 \text{ watts}$$

to simulate 1.5 kW at 12 GHz.

5.9.6 I^2R Loss Per Guide Wavelength

The lengths of waveguide components are frequently scaled to wavelength, so the losses at 8.36 GHz should include this factor in many of the components that might be used. Scaling to wavelength merely reduces the above function by 1/f, assumed to be at proportionate points relative to cutoff. Then the simulation (new) power relates to reference power by:

$$P_{new}/P_{ref} = \gamma f^{\frac{1}{2}}$$

A 1.5 kW requirement at 12 GHz is simulated by slightly less than 1.6 kW at 8.36 GHz.

5.9.7 Thermal Conduction

The change in thermal conduction as a function of frequency band includes the effect of path length, power absorbed per unit area, and cross section area of the conductor. The objective is to find the power relations to give equivalent maximum temperatures; the power absorbed, all of which is conducted to the heat sink, was given in the relation in Section 5.9.5.

The temperature between the hot spot and the sink is (ref. 4):

$$\Delta T = \frac{L^2 Q}{2 K A t}$$

where L is the path length (a + b/2), Q is total power absorbed in a length z, K is the conductivity, A is surface area absorbing the heat and equals $2(a+b) \cdot z$, and t is metal thickness. The latter is assumed to vary in accord with the thickness of the waveguide walls; then γ is used as the ratio of t_{new}/t_{ref}:

$$\gamma_{12} = t_{8.36}/t_{12} = .064/.050 = 1.28$$

$$\gamma_{2.64} = t_{8.36}/t_{2.64} = .064/.080 = 0.8$$

The Q/z is power lost for a given P_{in}, and from 5.9.5 is:

$$\frac{P_{new}}{P_{ref}} = \gamma f^{3/2}$$

If the process is to conduct all the heat away regardless of temperature, the function from Section 5.9.5 applies since all I^2R losses are conducted away. The ΔT's, relating to input powers via Section 5.9.5, may be equated to determine what input powers will give the same ΔT's:

$$\frac{\Delta T_{new}}{\Delta T_{ref}} = \frac{(Q/z)_{new}}{(Q/z)_{ref}} \cdot \frac{L_{new}^2 (a+b)_{ref}\, t_{ref}}{L_{ref}^2 (a+b)_{new}\, t_{new}}$$

$$= 1$$

The concern must be of trends rather than absolute value since this expression is not as convenient as previous ones. For simulating at 8.36 GHz (ref.) operation:

$$\frac{L^2_{new}}{L^2_{ref}} = \frac{\left(a + \frac{b}{a}\right)^2_{new}}{\left(a + \frac{b}{a}\right)^2_{ref}} = .957\, f^2$$

and $$\frac{(a + b)_{new}}{(a + b)_{ref}} = 0.962\, f$$

This ratio is nearly f. Thus

$$\frac{\Delta T_{new}}{\Delta T_{ref}} = \frac{\left(\frac{I^2R}{z}\right)_{new}}{\left(\frac{I^2R}{z}\right)_{ref}} \frac{f}{\gamma}$$

From Section 5.9.5:

$$\frac{\left(\frac{I^2R}{z}\right)_{new}}{\left(\frac{I^2R}{z}\right)_{ref}} = \left(\frac{1}{f}\right)^{\frac{1}{2}} \frac{P_{new}}{P_{ref}} \frac{1}{\gamma f}$$

and this equals γ/f from above.

Then $$\frac{P_{new}}{P_{ref}} = \gamma \gamma f^{\frac{1}{2}}$$

This is for the same temperature drops in the two cases; for 1.5 kW at 12 GHz,

$$P_{8.36} = 2.04 \text{ kW.}$$

5.9.8 Thermal Radiation

Thermal radiation leads to a temperature determined by area and power, and depends on the sink temperature. The basic radiation equation is:

$$P = Q = k \cdot (a + b) \cdot \sigma \cdot (T^4 - T_o^4)$$

where k includes the emission coefficient. For the same radiating temperature of the reference and simulation (new) frequencies, the power levels are:

$$\frac{P_{new}}{P_{ref}} = (\gamma f^{3/2}) \cdot f = \gamma f^{5/2}$$

which uses the expression from Section 5.9.5 for the heat, Q, involved. This function indicates a relatively high power level is required for simulating thermal radiation from a waveguide:

$$P_{8.36} = 3.27 \text{ kW}$$

for simulating 1.5 kW at 12 GHz.

SECTION VI. TESTING

6.1 TEST PLAN

A comprehensive test plan was prepared to define tests required and test procedures. Included are:

Bench Test:
- VSWR and tuning
- Insertion Loss
- Bandwidth
- Harmonic Performance
- Power Monitor Performance

These tests were performed separately with and without the diplexer. (Component test results were discussed for each component separately and won't be repeated).

High Power Vacuum Chamber Test:
- Arcing
- Multipacting
- Outgassing
- Magnetic Field Effect
- Thermal Effects

RF Leakage Test:
- Fundamental
- 2nd Harmonic

For each test, the requirements provided the basis for the type, conditions, and quality of measurement. All bench tests were performed with matched terminations. The elements of the test plan are integrated into the discussions of the tests which follow.

6.2 BENCH TESTS

6.2.1 VSWR and Tuning

6.2.1-1 Requirements

The assembly was required to have a VSWR of less than 1.05 at center frequency and 1.15 over a 10% bandwidth at 2.64 GHz or 4% at 12 GHz; these scale to about a 4.8% bandwidth, or 400 MHz at 8.36 GHz. With the diplexer, the VSWR is based largely on the diplexer's effect, and should be less than 1.8 which corresponds to a reflected power of 8.2%.

6.2.1-2 Measuring Method

The test arrangement used for this test is shown in Figure 6.1. The equipment used were:
- HP8690B Sweep Generator
- HP423A Crystal Detector
- HP8734A PIN Modulator

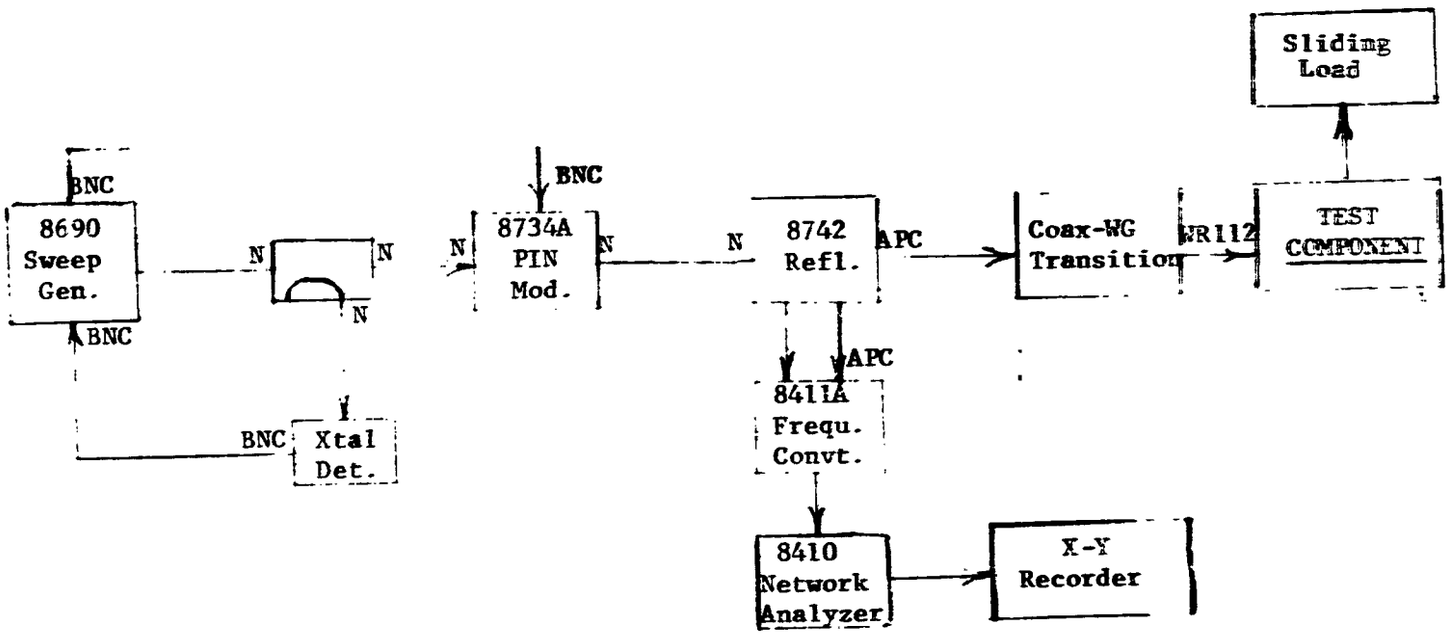

Figure 6.1. Test Arrangement - VSWR Bench Test

20dB Directional Coupler
HP8742 or 3 Reflection Test Unit
8410 Network Analyzer
HP135 X-Y Plotter
MRC H80 Load
MRC H40 Transition APC7/WR112
8411A Frequency Converter

The VSWR accuracy is expected to be ±.02 without diplexer and ±.05 with diplexer.

The measurement system was first checked without the waveguide assembly in place for calibration. An expanded Smith chart was used to adjust sliding terminations for best results over the 10% band used for the test.

6.2.1-3 Tuning

Obtaining a low VSWR required tuning to compensate for reflections from various points in the system. This task was minimized by tuning the individual components to minimize each one's reflections. Matched terminations were used throughout the bench testing.

The waveguide assembly required one additional capacitive iris at the elbow following the harmonic filter to achieve a low VSWR. The elbow had not been checked for a match previously. The tuning was performed with no diplexer. The iris was made oversize and trimmed in two steps; the three check points permitted an accurate extrapolation to the best match condition and the final trimming resulted in a VSWR as close to ideal as possible.

6.2.1-4 Results

The results, as noted in Section 3.2.1, showed the VSWR to be less than 1.02 at center frequency and 1.03 ± .02 over the bandwidth with no diplexer.

The diplexer brought the VSWR up to about 1.15 at center frequency, but no additional tuning effort was performed because the mismatch is largely inherent in the diplexer. The peak VSWR was 1.28 which could be improved by further work on the diplexer.

6.2.2 Insertion Loss and Bandpass

6.2.2-1 Requirements

The insertion loss was required to be less than 0.5 dB without the diplexer and 1.5 dB with the diplexer. In addition, the performance of the two power monitors could be determined at the same time, and the isolation objective of 25 dB between transmitter input guides checked with the diplexer in place.

The bandwidth characteristics measurement with the diplexer would confirm its performance relative to requirements as in Section 2.1.3 and Figure 2.2.

6.2.2-2 Measuring Method

The test circuit used for the loss and bandpass measurements is in Figure 6.2. The components are essentially the same as for the VSWR tests of Section 6.2.1 except an 8740 transmission test unit and two coax-to-waveguide transitions are required. An additional waveguide detector is also required for checking power monitor operation.

Accuracy in measurement was expected to be $\pm$ .1 dB per 10 dB difference between reference and test channels, $\pm$ 0.2 dB for differences from 10 to 40 dB, and up to $\pm$ .5 dB for 52 dB difference.

A loss calibration for the measuring system was taken with three pieces of waveguide having lengths differing by 60°, and results averaged. The waveguide assembly was then placed in the circuit and loss measurements obtained.

6.2.2-3 Results

The basic results of the tests were indicated in Section 3.2.2-1.

Summarizing:

Insertion Loss, no diplexer

- at center frequency: 0.3 dB
- range over band: 0.3 $\pm$ 0.2 dB

Insertion Loss, with diplexer

- at center frequency: 1 dB
- out of band: > 40 dB

Isolation: 22 dB at center frequency

Bandwidth at -3 dB points: 145 MHz (this is greater than required).

Additional detailed tests on the power monitors were not warranted on the basis of previous tests. A check was performed which confirmed previous measurements; the forward coupler showed the small reduction in output due to the loss in the harmonic filter and other components preceding it.

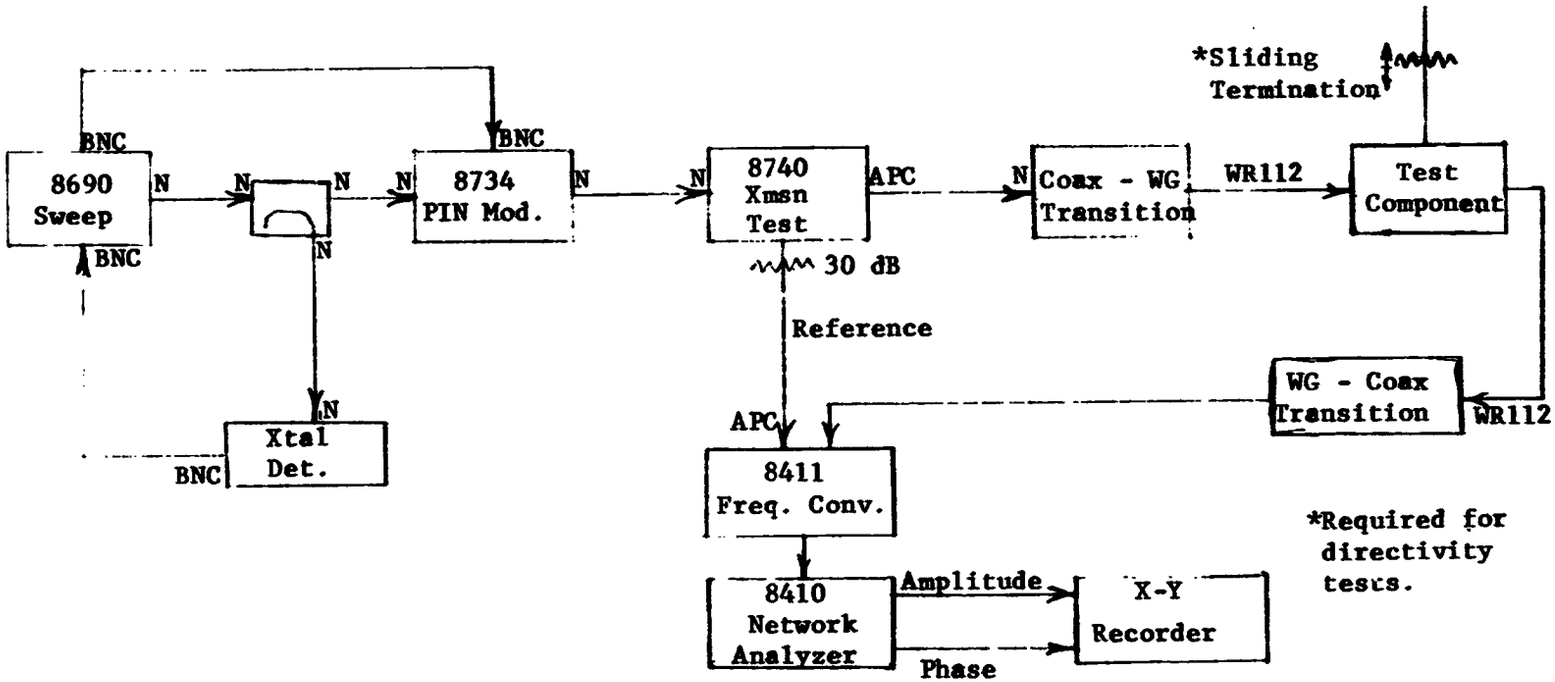

Figure 6.2. Test Arrangement - Insertion Loss Bench Test

6.2.3 Harmonic Performance

6.2.3-1 Requirements

The second harmonic performance was measured for the TE_{10} and TE_{01} modes at the time the rf leakage tests were being performed. The harmonics were to be attenuated at least 30 dB to keep total antenna emission below 50 dB, assuming the TWT harmonic output is 20 dB below the fundamental. In addition, the harmonic VSWR was to be under 1.5.

6.2.3-2 Measuring Method

The harmonic performance test was made in conjunction with the rf leakage tests; refer to Section 6.4 and Figure 6.8 for the test circuit.

The harmonic VSWR of the harmonic filter was measured during bench tests (see Section 5.2), and the results were good enough that additional detailed tests weren't warranted.

6.2.3-3 Results

From the tests on the harmonic filter and diplexer, a very high second harmonic attenuation was expected. With a sensitivity of about -95 dB, no signal was observed from the waveguide assembly output. A signal would have been observed with the diplexer removed, but the harmonic filter component tests indicated the specification was significantly bettered, the worst case being 9 dB better than required. The VSWR had been measured at 1.15 for the harmonic filter so the requirement of 1.5 appeared to be easily met. Only an added elbow and -30 dB coupler (at the fundamental frequency) would contribute some reflection but this would not be great.

6.3 HIGH POWER VACUUM CHAMBER TESTS

6.3.1 General Requirements

The waveguide assembly was to be placed in a vacuum chamber, and operated for 60 hours at a power level scaled from 1.5 kW at 12 GHz to observe possible component or operational problems. Fault sensors were incorporated into the assembly, following evaluations of the special breakdown test section of Section 5.8. The scaled power was determined to be 2.04 kW for the long range effects, largely thermal, and additional tests could be performed to determine possible breakdowns at lower and higher power levels. In addition, the effect of a strong magnetic field was to be evaluated using a scaled field as noted in Figure 2.1.

6.3.2 Test Facility

The two principal elements of the test facility were a vacuum chamber four foot in diameter by six foot long with a vacuum capability better than 1.33×10^{-9} N/m^2 (10^{-7} Torr), and a 5 kW CW klystron at 8.36 GHz. The vacuum chamber is shown in Figure 6.3 which also shows the output waveguide elements used in testing, including the ion gauge, vacuum window, output

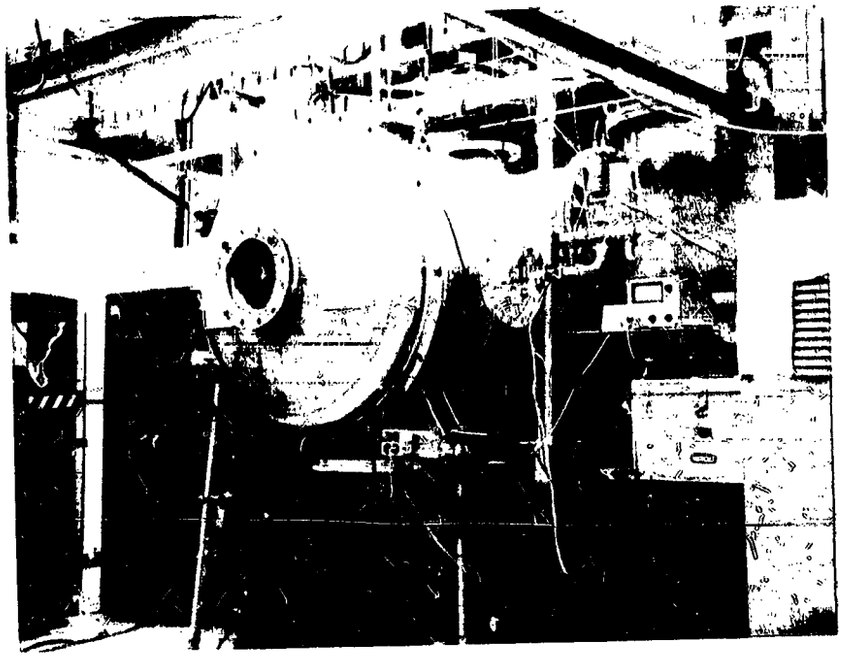

Figure 6.3. Vacuum Test Chamber

power measuring coupler, and 7 kW load. The tank ion gauge for measuring pressure is on the top of the chamber. At the left side of the chamber are two windows (later one defaulted) with a reverse power monitor. A plug arrangement carried 52 lines for instrumentation. Water lines are located on the top of the chamber for any water cooling required. All three waveguide vacuum windows were water cooled.

The test arrangement is shown in the diagram of Figure 6.4. This includes the klystron and its auxiliary equipment, and also the instrumentation used. The thermal measurements were recorded separately with a single channel recorder and a stepping switch to record nine points at two minute intervals. Locations and typical temperature record are shown in Figure 6.5. The multichannel recorder covered the waveguide pressure, power output, photodiode output, photodiode trip, and VSWR. Tank pressure was recorded manually.

In the initial tests, the waveguide pressure was much higher than anticipated. This was traced to a cracked window in the input channel. The transmitter was then shifted to the second window on the input side of the chamber, and the faulty window replaced with a cover.

The vacuum gauges on the waveguide and on the chamber differed somewhat, indicating a possible small leak in the output waveguide window. For instance, turning on the cooling water for the window reduced the ambient reading in the waveguide ion gauge, suggesting that possibly the contraction tended to reduce the leakage slightly. In addition, the pressure readings were made with the output waveguide open to the chamber and with nothing attached. In this case, the pressure differences tended to diverge as the pressure was reduced:

Tank Pressure		Waveguide Pressure	
4.9×10^{-2} N/m^2	(3.4×10^{-4} Torr)	6.0×10^{-2} N/m^2	(4.5×10^{-4} Torr)
3.1×10^{-3} "	(2.3×10^{-5} ")	3.6×10^{-3} "	(2.7×10^{-5} ")
3.2×10^{-4} "	(2.4×10^{-6} ")	3.6×10^{-4} "	(3.6×10^{-6} ")
0.7×10^{-4} "	(0.5×10^{-6} ")	1.7×10^{-4} "	(1.3×10^{-6} ")

Thus in the tests, a higher reading of the waveguide ion gauge is expected than that shown by the tank gauge. With the waveguide attached, the cold ambient pressure was 6.7×10^{-4} N/m^2 (5×10^{-6} Torr) while the tank was 6.7×10^{-5} N/m^2 (0.5×10^{-6} Torr).

6.3.3 Test Procedures and Results - Initial Tests

A series of preliminary tests were performed with the equipment in the vacuum chamber. It was here that the diplexer iris heating was first encountered. The tests prior to the 60 hour continuous run were used to remove initial outgassing and to determine the suitability of the instrumentation. One waveguide window was found to be cracked which caused a high reading of waveguide pressure, higher than reasonable and close to a potential arcing level. When the diplexer was removed, the third (faulty) window was no longer required in the test system. All tests used CW power. The tests and key results were as follows:

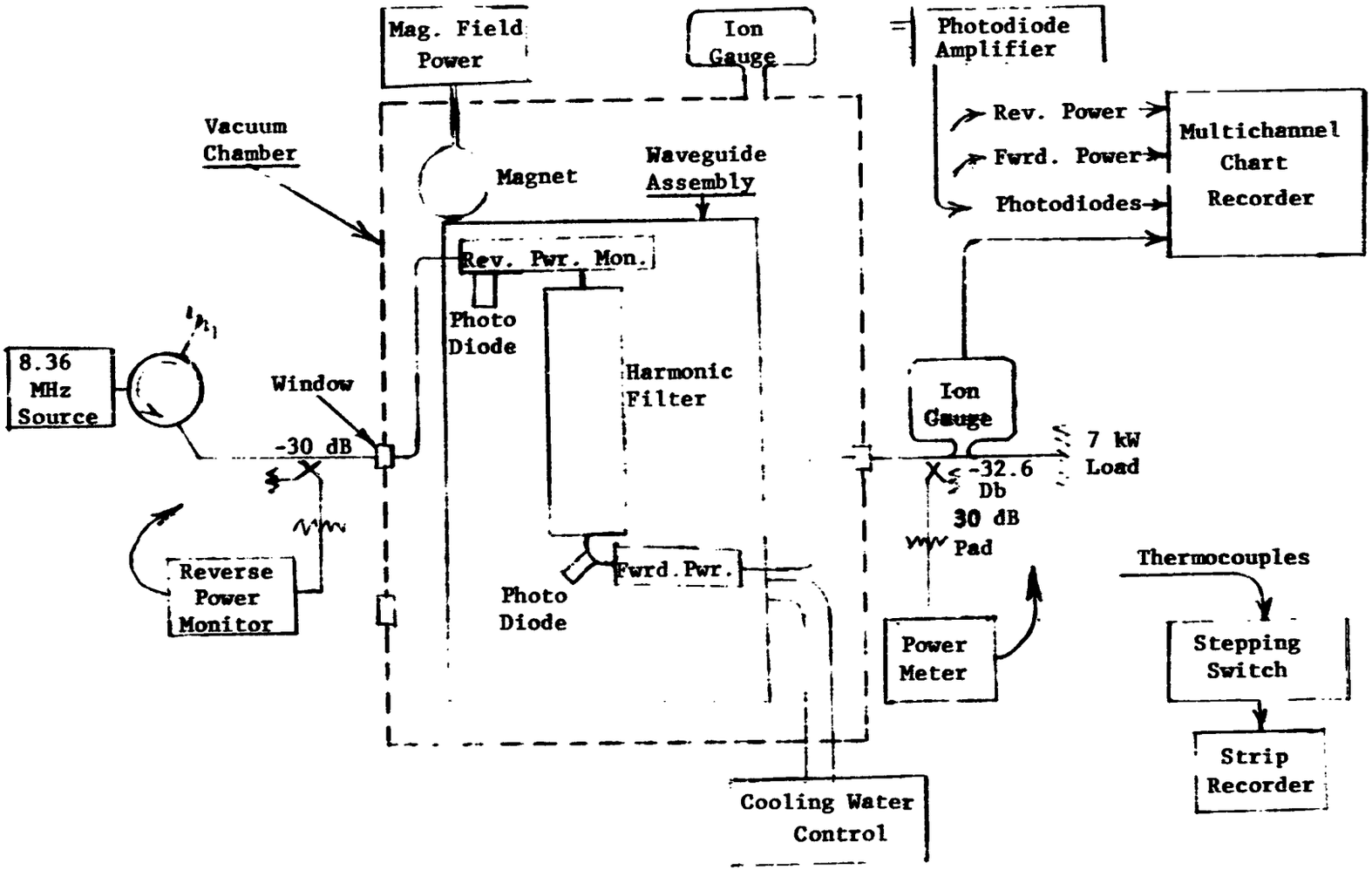

Figur 6.4. Test Arrangement - High Power Vacuum Tests

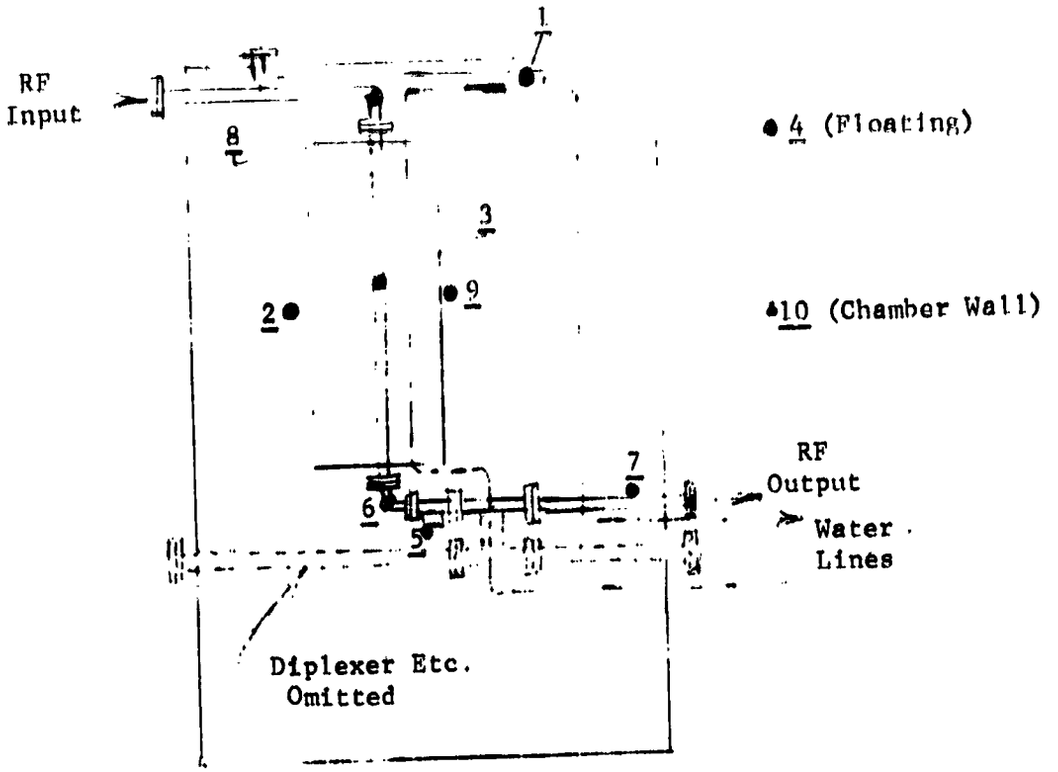

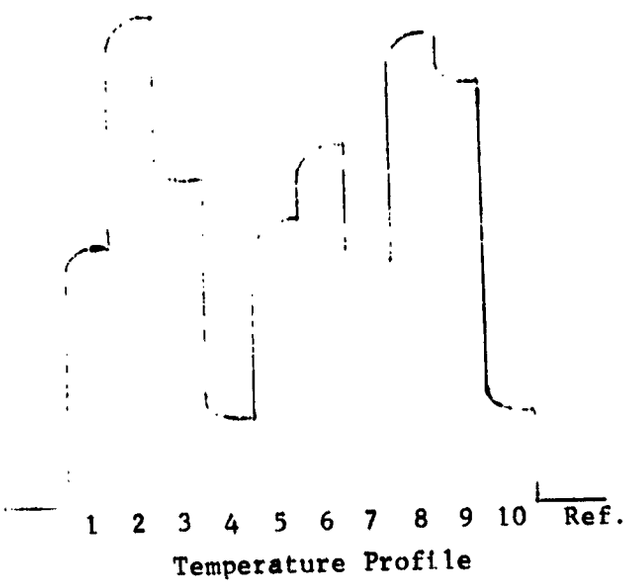

Typical Temp.

	°K	(°C)
1.	373°	(50°)
2.	363°	(90°)
3.	335°	(62°)
4.	291°	(18°)
5.	332°	(59°)
6.	345°	(72°)
7.	320°	(47°)
8.	360°	(87°)
9.	354°	(81°)
10.	291°	(18°)
Ref.	273°	(0°)

Figure 6.5. Thermal Measurement Points

DAY	TEST TYPE	TEST RESULTS (CW POWER)
1.	1. Full System - Vacuum - High Power	1. Automatic trip at 480 watts via photodiode. 2. With 270 watts, thermal runaway after 4 minutes from diplexer photodiode.
	2. Thermal Stability - Vacuum - High Power	1. 180 watts limit to keep photodiode below trip threshold 2. Flashlight check on photodiode; operates well
2.	Thermal at Atmospheric Pressure	1. Checked at 800 watts; end of diplexer at 381°K (108°C) while all other parts at 333°K (60°C). 2. No photodiode signal.
3.	1. Repeated thermal at Atmospheric Pressure	1. To 1350 watts; diplexer to 343°K (170°C) at end, 350°K (77°C) center, 311°K (38°C) at thermal plate over 2 hour period.
	2. Same in vacuum	1. Added visual facility to observe diplexer iris; strong red glow at 270 watts.
4.	Replaced Faulty waveguide window	
	1. Recheck system in vacuum	1. Waveguide pressure down to about 1.3 x 10^{-4} N/m^2 (10^{-6} Torr) with no power 2. Visual glow at 270 W.
	2. Removed diplexer - Atmospheric Pressure	1. Power to 4 kW; no problems
	3. Diplexer out - Vacuum	1. To 1600 watts, pressure to 1.067 x 10^{-3} N/m^2 (8x10^{-6} Torr) over 70 minute build-up. 2. Tank pressure up 20% to 1.3 x 10^{-4} N/m^2 (10^{-6} Torr). 3. Rectifier failed; shutdown for replacement.
5.	Vacuum sustained from here to end of test program	
	1. Power raised, vacuum operation.	1. No cooling, pressure to 2 x 10^{-2} N/m^2 (1.5x10^{-4} Torr) with 1.8 kW. 2. Add water cooling, pressure down to 1.33 x 10^{-2} N/m^2 (10^{-4} Torr) and power to 2.7 kW. 3. Short run at 4.0 kW, pressure near 0.8 x 10^{-2} N/m^2 (6x10^{-5} Torr) with water cooling

		4. Applied hot water for 3 hours, 338°K (55°C), no rf power.
6.	Power Run in Vacuum	1. Initial pressure = 1.07×10^{-3} N/m^2 (8×10^{-5} Torr) 2. Raised to 3.6 kW in 30 minutes, pressure to 26.7×10^{-3} N/m^2 (20×10^{-5} Torr) after one hour, light water cooling. 3. Raised to 4.2 kW, pressure off to 1.33×10^{-3} N/m^2 (10^{-5} Torr) after total run of 2 hours 10 minutes.
7.	Power Run in Vacuum	1. Raised to 4.2 kW in 5 minutes; pressure peak to 0.8×10^{-2} N/m^2 (6×10^{-5} Torr) after one hour. Run 100 minutes. 2. Hot spot on thermal plate at 350°K (77°C) with 200 watts removed by cooling water. Estimate radiation cooling is 63 watts max.

This completed the preliminary runs to effect outgassing and to confirm the instrumentation. The 60-hour run followed these tests; vacuum was sustained from day 5 until the end, in day 9.

6.3.4 Sixty-Hour Test

The sixty hour test may be best characterized as uneventful. There were no indications of a possible fault at any time. The cooling water and radiated heat reasonably matched the expected rf loss. The power was set at 3.75 kW for the 60 hours to provide an extra margin over the minimum requirements.

The test was run from 0000 on Tuesday, 8 February to 1200 on the following Thursday. The following describes the tests. At the end, a short period of higher power was enacted.

Time	Parameter	Comments
Day 1		
0000	Power	Raised to 3.6 kW CW in 4 steps over 4.5 minutes. Waveguide pressure at 0.67×10^{-3} N/m^2 (0.5×10^{-5} Torr.)
0200		Then to 3.75 kW after 20 minutes.
	VSWR	1.17
0110	Cooling	Water turned on; plate hot spot at 363°K (90°C). See Figure 6.5 for nominal temperatures held through tests.
0120	Waveguide pressure	5.86×10^{-3} N/m^2 (4.4×10^{-5} Torr) peak.
0320	Pressure	Dropped to 2.67×10^{-3} N/m^2 (2×10^{-5} Torr); tank at 1.07×10^{-4} N/m^2 (0.8×10^{-6} Torr). Tended to vary with small changes in cooling water rate.
0720	Pressure	1.73×10^{-3} N/m^2 (1.3×10^{-5} Torr), hot spot at 363°K(90°C)

1500	Pressure	1.33×10^{-3} N/m^2 (1×10^{-5} Torr), Tank at 6.7×10^{-5} N/m^2 (0.5×10^{-6} Torr).
2400	No changes	Hot Spot to 368°K (95°C).
Day 2 1200	Pressure	1.33×10^{-3} N/m^2 (1.0×10^{-5} Torr), Tank at 8×10^{-5} N/m^2 (0.6×10^{-6} Torr).
	Temperature	363°K (90°C) at hot spot.
2400	Pressure	9.3×10^{-4} N/m^2 (0.7×10^{-5} Torr), Tank at 6.7×10^{-5} N/m^2 (0.5×10^{-6} Torr).
Day 3 0600	Temperature	Held at 368°K (95°C)
	Pressure	1.33×10^{-3} N/m^2 (1×10^{-5} Torr).
1200	Complete 60 hours Pressure	1.33×10^{-3} N/m2 (1×10^{-5} Torr), Tank 6.7×10^{-5} N/m^2 (0.5×10^{-6} Torr)
	Temperature	Hot spot at 368°K (95°C)
1230	Magnetic Field	100 Gauss applied for 8 minutes. No effect
1240	Power	Raised to 6.5 kW
	Temperature	To 380°K (107°C) at hot spot
	Pressure	Rising
1250	Pressure	To 1.6×10^{-2} N/m^2 (12×10^{-5} Torr), temperature is 380°K (107°C) at hot spot.
1304	Power	To 7.2 kW
1305	Power	To 9.0 kW for 10 seconds
	Pressure	To 1.33×10^{-2} N/m^2 (10×10^{-5} Torr)
1306	Power	Back to 3.6 kW
	Pressure	To 2.67×10^{-2} N/m^2 (2×10^{-5} Torr) in 5 minutes
1310	Power	Off

Calculations were performed on the reverse power, VSWR, cooling, and magnetic field.

Reverse Power: Meter reading of 0.60 mw with a -30 dB coupler and a 16 dB pad; reverse power is 24 watts. Forward power was 3750 watts.

VSWR: 1.17

Radiation Cooling: Assume ϵ = 0.1, temperature average about 343°K (70°C) with 293°K (20°C) ambient

$$W = 0.1\ (2 \times .610m \times .915m)\ (57 \times 10^{-9})\ (343^4 - 293^4)$$
$$= 0.1\ (2 \times 24'' \times 36'')\ (36.8 \times 10^{-12})\ (343^4 - 293^4)$$
$$= 82 \text{ watts.}$$

Water Cooling:

$$W = 1.16 \times 10^3 \text{cc (liters) per hour} \times \Delta^\circ K$$
$$= 1.16 \times 10 \times 17^\circ K$$
$$= 200 \text{ watts}$$

Power Dissipated for 3 dB loss:

$$W = .068 \times 3750$$
$$= 225 \text{ watts.}$$

The difference can be ignored for a calculation of this nature where ϵ was not measured and the average plate temperature may change considerably with changes in cooling water rate.

Magnetic Field: The magnetic field scaling from the 12 GHz requirement to the 8.36 GHz test frequency was based on determining the initial velocity of an electron which will just graze the far broadwall in the 12 GHz case, assume the same initial velocity for the 8.36 GHz case, and determine the corresponding field which would again make the electron just graze the far wall. Figure 6.6 shows the 8.36 GHz scaled magnetic field requirement, and compares it with the measured field actually used. The test field is slightly larger down to about the one Gauss level; beyond this, it should have a negligible effect.

6.4 RF LEAKAGE TESTS

6.4.1 Requirement

The leakage from the waveguide assembly was to be less than -80 dBW relative to a 1.5 kW signal at 12 GHz (an original specification of -90 dBW was relaxed to -80). The same figure was assumed for the second harmonic except that signal would be no more than 15 watts, and considerably less for a good TWT. Thus the total radiation integrated over a sphere surrounding the waveguide assembly should show a total leakage of less than:

fundamental	-111.76 dB
second harmonic	-91.76 dB

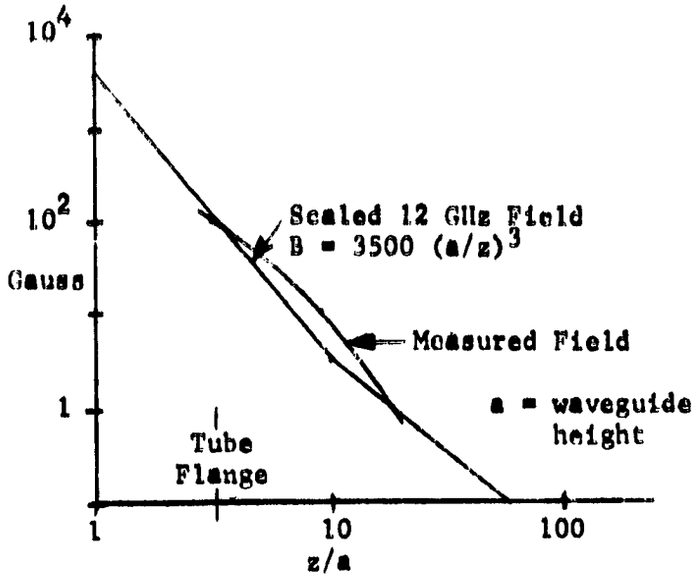

Figure 6.6. Test Magnetic Field

This can be measured at points on the far-field sphere and integrated. However, the leakage was not detectable at that distance with the test setup used. The test horn was placed at the component, which increased sensitivity by about 10 dB in this case, and the power detected could then be assumed to be a point source. All point sources would then be added for a worst case.

6.4.2 Facilities

The tests were first performed in a shielded room. The effect of no rf absorbing material on the room's walls was to make the location of the leakage points uncertain. This turned out to be only a minor problem here because all points of leakage turned out to be at flanges except for the termination holding bolt on the reverse power coupler; tightening eliminated this problem. Thus tests in an anechoic chamber were not required and the screen room tests were adequate.

The test equipment assembled is shown in Figure 6.7 for the fundamental frequency tests and Figure 6.8 for the second harmonic tests. The rf source was fed through a waveguide window which was soldered in place to provide an rf-tight connection.

The second harmonic signal of 50 mw was fed into the waveguide assembly through WR62 to WR112 tapers; one gave a TE_{10} mode and the second provided a coupling of t e TE_{01} mode.

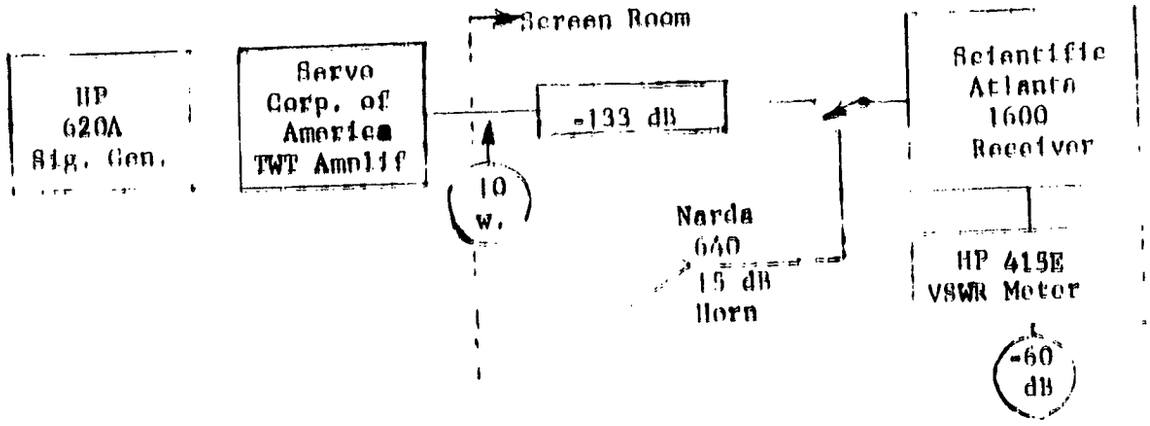

Figure 6.7. Test Arrangement - RF Leakage at 8.36 GHz

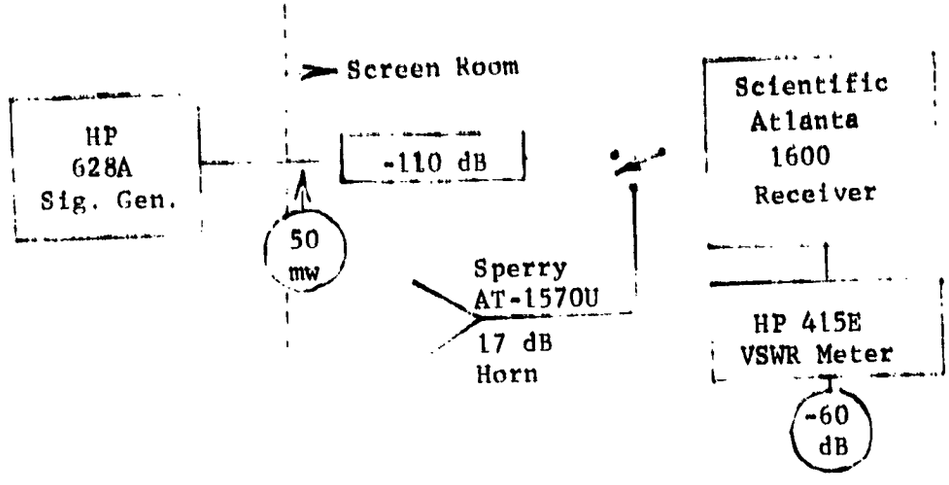

Figure 6.8. Test Arrangement - Harmonic RF Leakage

6.4.3 Sensitivities

6.4.3-1 Fundamental

The test equipment of Figure 6.8 had a noise level of 1.6×10^{-13} watts. The calibration is shown on the Figure. A 10 watt signal gave a meter reading of -60 dB when attenuated 133 dB, and a -65 dB reading was noted with no input.

An estimate of the effective attenuation or leakage of the waveguide assembly can be performed by using the one-way transmission formula:

$$P_{(rcv)} = \frac{P\ (xmt)\ G_1\ .\ G_2\ .\ \lambda^2}{(4\pi R)^2}$$

where R is the far field distance for the Narda horn used. This horn had a maximum dimension of 7.5 cm (3 inches) so

$$R = \frac{2D^2}{\lambda} = \frac{2x58}{3.6} = 32.3 \text{ cm } (12.7 \text{ in.})$$

The leakage G_1, if uniform over the spheroid surrounding the waveguide assemble, would be obtained from:

$$1.6 \times 10^{-13} = \frac{(10W)\ G_1\ (31.6)\ (12.96)}{1.67 \times 10^5}$$

or $G_1 = -111.9$ dB

This is about the maximum level of leakage permitted but there is no leeway to show any margin existing. The decision was to move the horn of the detector into the near field and assume the power variation is 1/R. Thus placing the receiving horn at about 3.18 cm (1-1/4 inch) from a possible leakage point would increase the sensitivity by about 10 dB. For a worst case then, the sources would be added for the most intense level. The total radiation leakage would be assumed to be the sum of the individual point sources observed. Thus the basic sensitivity was considered to be about -122 dB.

6.4.3-2 Second Harmonic

The second harmonic was checked similarly. A different receiver head was used which had a noise level of about 2×10^{-13} watts, and the horn gain was 17 dB. Far field from $2D^2$ resulted in an 27.9 cm (11 inch) distance for d=5 cm (2 in.) and = 1.8 cm (.707 inches). Then

$$2 \times 10^{-13} = \frac{(50 \times 10^{-3})\ G_1\ (50)\ (3.24)}{1.256 \times 10^5}$$

and

$$G_1 = 3.1 \times 10^{-9}$$

$$= -85 \text{ dB}$$

This is less than the desired sensitivity of -91.76 dB, so the horn again was moved into the near field. At 2.8 cm (1.1 in), the estimated sensitivity was

$$G_1 = -95 \text{ dB}$$

which is adequate for the current program.

Note that the harmonics are heavily attenuated in the harmonic filter, 40 to 60 dB, so no significant leakage source is expected beyond this component.

6.4.4 Measurements

6.4.4-1 Fundamental RF Leakage

The process of determining rf leakage was one of successively refining the measurement method and the corrective measures. The initial tests showed leakage from the rf source window into the screen room; it was eliminated by using a soldered flange to remove the stray leakage.

Following this, several sources of leakage seemed to be present. These were traced to the two power monitor detector flanges which had been shorted and to the second transmitter terminal at the diplexer. The shorting flanges were thought to be adequate without additional facing since a gasket was used and the flange on the waveguide assembly had been faced. This was not the case and some 56C conducting epoxy was applied to two of the junctions, and a soft copper shorting plate put on the third. These are not of concern since the final system should have both halves of a flange junctions faced carefully. Other flanges, in general, had no detectable leakage.

The exception was the flange between the optical sensor input section and the reverse power monitor input flange. There appeared to be some leakage from the flange and also from the back of the flange which had been heliarc welded. Dip brazing would have avoided the latter problem. A final system would also have required refacing of the flange, Some 56C conducting epoxy was used for expediency here at both the junction and the back of one flange.

Following this, no rf leakage could be detected in the assembly, using the test horn at a distance of about one inch from all susceptible points. None of the components had any indication of leakage through the vents; optical and multipactor sensors also did not radiate a detectable signal. The flanges not showing leakage had to be tightened to about the limit of hand tightening with an Allen wrench to achieve the no-leakage condition.

6.4.4-2 Second Harmonic RF Leakage

The second harmonic signal was attenuated sufficiently by the combination harmonic filter and diplexer that no signal was detectable at the open output waveguide. The only significant source was the mounting bolt on the reverse power monitor termination. This was tightened and all signal disappeared. Both the TE_{10} and TE_{01} modes were checked.

6.4.5 General Conclusions

The waveguide components as developed have no significant sources of rf leakage. The recommendations are:

1. All flanges should be carefully faced, and lapping may be considered. Gaskets are suitable, but only if the flanges are

flat to a fraction of a mil and the flanges are heavily tightened.

2. The photodiode mounting at the input to the waveguide assembly is not beyond cutoff to third and higher harmonics. This diode should have appreciably more rf attenuation material around the diode leads to insure no higher harmonic leakage.

APPENDIX I. ELECTRICAL BREAKDOWN PREVENTION

A special breakdown test section was fabricated and tested for multipacting characteristics, as described in Section 5.7. The question arises: What can be done to eliminate multipactor breakdown in a component when it occurs?

The preferred approach is always to change dimensions to operate remotely from the breakdown conditions. That is, the gap of the breakdown should be increased so the breakdown operating conditions of Figure 5.39 are avoided. In some cases, like for a waffle-iron harmonic filter, this is not always feasible.

Two other approaches have been considered elsewhere in the past, and will be mentioned here for record purposes. The first approach was a coating of low secondary emission material. With such a material on the broadwall of the waveguide, an electron accelerating to the opposite wall would remove an average of less than one secondary electron, and the multipactor effect would never build up. At least four materials are known which can accomplish this (ref. 18): tungsten carbide, titanium carbide, vanadium boride, and titanium boride. In a separate program, this approach was evaluated. The principal problem was the rf losses in the coated waveguide section. For a half wave long section of waveguide with tungsten carbide on one wall, the loss was measured to be over four times that of a standard waveguide. This becomes serious when the multipacting region is a small gap device. For a low height waveguide with a .018 cm (.007 in) between the broadwalls, as used in this program, the insertion loss was about 0.65 dB, or 14%. With the tungsten carbide on one surface, the loss from previous data would be about 57%. Thus this is not considered suitable for a high power system where surface multipacting might occur. The technique would be applicable to points and lines that are subject to breakdown and where the currents are limited in extent.

A second approach, considered in a previous program (ref. 19), involved perforating one wall with holes to reduce the area by 50% or more. The perforated area is then backed by a biased electrode so only half the electrons accelerated to this broadwall of the waveguide will hit metal and generate secondary electrons. The effect is to reduce the secondary emission ratio to less than unity.

A check on this type of operation was performed in two other programs, one at 200 MHz (ref. 19) and the second at 8.36 GHz, following somewhat the test procedures of Section 5.7. At 200 MHz, the onset of multipaction was changed from 5.7 watts with no perforations to 10.8 watts with one surface partly perforated (less than 50%). In the case of the 8.36 GHz, the problem was more difficult in that a small gap, like the .018 cm (.007 in) in the present program, required holes of a similar size or smaller. Otherwise multipactor breakdown would occur in spots and the perforation would be ineffective. In addition, the holes should not be too thick or the electric field of the biased back-up electrode would be ineffective. A perforated surface was prepared by photo-etching to create holes of .025 cm (.010 in.) diameter in a .025 cm (.010 in.)thick section of copper plate as used for a broadwall of the waveguide. The process tended to mechanically distort the

initially flat surface, but it was stabilized for testing purposes by a small piece of dielectric inside the waveguide and knife-edge brace above the section. The perforated section tended to be lossy, as would be expected, but was only about twice that of plain copper, also about what would be expected. Thus in a .018 cm (.007 in.) high waveguide section, the loss with the perforated section would be 1.5 dB (30%) versus 0.65 dB (14%) for plain copper.

An interesting aspect of both approaches was that the multipactor breakdown was still evident, but the magnitude was low and never to the point to result in tripping of the protective circuitry. In the case of the tungsten carbide, there is a possibility that some gas was trapped in the flame-spray process used in depositing the material, which was about .0025 cm (.001 in) thick. Also, it had only a 90% purity which could have contributed to its lower effectiveness. The loss would still be significant, however. Initial tests showed a substantial outgassing, but tests were run up to a 2 kW level where the reflected signal turned the transmitter off. Signals were present on the multipactor probes from about the 700 to 800 watt level, but never of high intensity. With higher purity of tungsten carbide, this effect should decrease.

The perforated wall testing included a measurement of current through the backup biased electrode behind the perforated area. Initial tests showed about 2.5 microamperes with a +40 volt bias, and a detectable light signal by the photodiode. The multipactor probes showed a small output at about the 1 kW level but it was quite small up through 2.5 kW. The +40 volt bias was changed to zero volts, then to -70 volts, and finally to as much as -300 volts. These would reflect the electrons back where they would tend to be picked up by the grounded perforated plate rather than go through and return into the waveguide. Any that did go through would not be in synchronism to increase the multipactor effect. Finally, the negative field may have been strong enough to act as a biased broadwall which can also eliminate multipactor breakdown by not letting the electrons traverse the waveguide height. The final test at zero volts bias went to over 7 kW with no catastrophic breakdown, although some electron flow was observed. The general conclusion was that this technique is effective, but further effort would be desirable to assess the effect of the little breakdown bursts on the signal, either in terms of noise or increased VSWR. The perforated wall approach would be ideal for the waffle-iron type harmonic filter where the top broadwall could be perforated just in the small area over each post while leaving the rest of the surface unchanged.

Surface contamination during the course of the experiment from vacuum pump oil or other surfaces may have been responsible for the failure of the test fixture to clean up completely and cease multipacting, as expected, after the initial cleanup period. Further investigation into this area with a cleaner system might further resolve the degree of effectiveness of the perforated surface technique for multipactor suppression.

APPENDIX II. OUTGASSING OF CHOMERICS 1224 MATERIAL

The problem of leak-proof seals for flanges in a waveguide assembly has been considered elsewhere in terms of off-the-shelf gaskets. The two types considered most suitable were the Chomerics, using Choseal 1224 material, and the aluminum type used in this program and described in Section 3.3.1-3. The aluminum type is patterned after a Parker Seal with some modifications.

The possibility of Chomerics 1224 gaskets has been explored in terms of determining the outgassing resulting after suitable baking in a vacuum. The seals were later used in the test facility with no serious problems. The outgassing measured was relatively low in the overall system, and appeared to be from some part of the system, probably the harmonic filter terminations, which were very sensitive to power level. On the basis of this situation, the use of Chomerics gaskets appears feasible as long as they are suitably processed before high power is turned on.

Three samples were tested at 32.3°K, 373°K, and 423°K (50°C, 100°C, and 150°C) respectively. The weight loss rate was checked after about 200 hours and was about 40 parts per million per hour at that time for operation at 423°K (150°C), and 14 and 2 parts per million per hour for temperatures of 373°K 100°C and 323°K 50°C respectively. These might be significant for a large piece of material but in the waveguide assembly, the exposed material is the inside perimeter of the waveguide 8.22 cm (3.238 inches) at 8.36 GHz and 5.71 cm (2.250 inches) at 12 GHz, multiplied by the compressed thickness, about .064 cm (.025 inches).

A rough calculation was performed to estimate the equivalent pressure of the outgassing and sublimation from the material at the 40 parts per million per hour rate. The sample used in the outgassing/sublimation tests weighed 9.72 grams, which translates to 0.81×10^{23} molecules if the density of the material is about four times that of water, or 12×10^{-23} grams. This is considered satisfactory for the purpose of this calculation. With a deterioration rate of .00004 per hour, then the number of molecules per hour is 3.24×10^{18}, or 0.9×10^{15} per second. The sample area was 24.1 cm^2, so particles per cm^2 were 3.73×10^{13} per second.

This emission of particles can be related to gas density if the emission velocity of the particles is known. This can be estimated from the energy relations:

$$\tfrac{1}{2} m v^2 = 3/2 \, k T$$

where $k = 1.4 \times 10^{-16}$ erg/°K and T° will be assumed to be 350°K (77°C). Then the molecule velocity is:

$$v = 35{,}000 \text{ cm/sec.}$$

Thus the molecular density in a cubic centimeter at the material surface is:

$$\text{density} = 1.07 \times 10^{9}$$

Referring to charts, this is equivalent to a gas pressure of about

$$p = 4 \times 10^{-6} \text{ N/m}^2 \quad (3 \times 10^{-8} \text{ Torr}).$$

In the case of the 12 GHz waveguide flange gasket, the exposed area is only 0.4 cm^2, and the material emerges into a relatively large volume. The molecules per second are thus about 1.5×10^{13}. The pressure from a single vent, per Figure 5.4, is estimated roughly to be about 1.3×10^{-4} N/m^2 (10^{-6} Torr) for a single 0.254 cm (0.1 inch) diameter vent, and less for more vents.

This calculation shows that a low outgassing material like in the Chomerics 1224 gasket would be acceptable for space if an initial baking is performed and a reasonable number of vents are included in the waveguide components.

APPENDIX III. DIPLEXER DESIGN COMPUTER PROGRAMS

A. Circular Waveguide Tschebycheff Filter (CHEBFIL2)

Program (BASIC)

```
$OLD CHEBFIL2

READY

$LIST

03/01/72   16:47


00010 DIM F(60), L(60), G(60), M(60), A(60)
00020 READ F0, B, D
00025 READ N1, A1
00030 READ N, B1
00035 READ T5, S5
00040 PRINT "CIRCULAR WAVEGUIDE TSCHEBYCHEFF FILTER"
00050 PRINT
00060 PRINT "CENTER FREQUENCY ="; F0; "MHZ";";  BANDWIDTH =";
                                                        B; "MHZ"
00070 PRINT
00080 PRINT "WAVEGUIDE DIAMETER ="; D; "INCHES"
00090 PRINT
00100 PRINT "NUMBER OF CAVITIES ="; N1; ";  RIPPLE LEVEL =";
                                                        A1; "DB"
00105 IF T5 = 3 THEN 150
00106 IF T5 <> 5 THEN 110
00107 PRINT
00108 PRINT
00109 GO TO 330
00110 PRINT
00120 PRINT "FREQUENCY", "OMEGA P", "ATTENUATION"
00130 PRINT "   MHZ",    "RADIANS", "    DB"
00140 PRINT
00150 LET C = 2.99793E4
00160 LET P1 = 3.14159265
00170 LET P2 = 1.8412
00180 LET L1 = (2*P1/P2)*D/2
00190 FOR J = -N TO N
00200 LET I = J + N + 1
00210 LET F(I) = F0 + J*B1
00220 LET L(I) = C/F(I)/2.54
00230 LET G(I) = L(I)/SQR(1 - (L(I)/L1)↑2)
00235 NEXT J
00240 LET J1 = B/2/B1
00242 IF (J1 - INT(J1)) <> 0 THEN 260
00250 LET G1 = G(-J1 + N + 1)
00252 LET G2 = G(J1 + N + 1)
00254 LET G0 = G(N + 1)
00256 GO TO 280
```

(III.A cont.)

```
00260 LET F1 = F0 - B/2
00262 LET F2 = F0 + B/2
00264 LET W1 = C/F1/2.54
00266 LET W2 = C/F2/2.54
00270 LET G1 = W1/SQR(1 - (W1/L1)↑2)
00272 LET G2 = W2/SQR(1 - (W2/L1)↑2)
00274 LET G0 = G(N + 1)
00280 LET M1 = 1.0
00282 LET K2 = EXP(A1/4.343) - 1
00285 FOR I = 1 TO (2*N +1)
00290 LET M(I) = 2*M1*(G0 -G(I))/(G1 - G2)
00292 LET M2 = ABS( M(I) )
00293 IF M2 > 1.0 THEN 305
00294 IF M2 = 0   THEN 298
00295 LET T1 = ATN( SQR(1 - M2↑2)/M2 )
00296 GO TO 300
00298 LET T1 = P1/2
00300 LET A(I) = 4.343*LOG(1 + K2*COS(N1*T1)↑2)
00302 GO TO 310
00305 LET T2 = LOG( M2 + SQR(M2↑2 -1) )
00307 LET A(I) = 4.343*LOG(1 + K2*( (EXP(N1*T2) + EXP(-N1*T2))/2)↑2 )
00310 LET A(I) = INT(1000*A(I) + 0.5)/1000
00312 LET M(I) = INT(1000*M(I) + 0.5)/1000
00315 IF T5 = 3 THEN 320
00318 PRINT F(I), M(I), A(I)
00320 NEXT I
00321 PRINT
00322 PRINT
00323 IF T5 = 1 THEN 450
00324 IF T5 = 2 THEN 330
00325 IF T5 = 3 THEN 330
00326 PRINT
00327 PRINT
00328 LET T5 = 5
00329 GO TO 40
00330 PRINT "FREQUENCY                    ATTENUATION IN DB"
00332 PRINT "   MHZ"
00335 IF S5 = 5 THEN 342
00336 IF S5 = 1 THEN 344
00340 PRINT"        50      40      30      20      10      0"
00341 GO TO 350
00342 PRINT"        5       4       3       2       1       0"
00343 GO TO 350
00344 PRINT"        1.0     0.8     0.6.    0.4     0.2     0"
00345 GO TO 350
00350 PRINT"        +-------+-------+-------+-------+-------+"
00360 DIM P(60)
00362 READ S$, L$
00370 FOR I = 1 TO (2*N + 1)
00372 LET P$ = L$
```

(III.A Cont.)

```
00380 LET P5 = INT(50*A(I)/S5 + 0.5)
00382 IF P5 > 50 THEN 398
00384 LET J5 = 51 -P5
00386 CHANGE P$ TO P
00388 LET P(J5) = 42
00390 CHANGE P TO P$
00398 PRINT F(I); S$; P$
00400 NEXT I
00410 PRINT
00412 PRINT
00420 DATA 12500, 30, 0.833
00425 DATA 3, 0.021
00430 DATA 13, 5
00435 DATA 4, 50
00440 DATA " "
00442 DATA "+                .                .                .                .                .                ."
00450 END

READY
```

Printout

```
$OLD CHEBFIL2

READY

00420 DATA 12500, 120, 0.833
00425 DATA 4, 0.2
00430 DATA 11, 15
00435 DATA 4, 50

$SAVE CHEBFIL2

READY

$BASIC
03/01/72    17:12



CIRCULAR WAVEGUIDE TSCHEBYCHEFF FILTER

CENTER FREQUENCY = 12500 MHZ;  BANDWIDTH = 120 MHZ
```

(III.A Cont.)

WAVEGUIDE DIAMETER = 0.833 INCHES

NUMBER 3F CAVITIES = 4 ; RIPPLE LEVEL = 0.2 DB

FREQUENCY MHZ	ØMEGA P RADIANS	ATTENUATIØN DB
12335	-2.832	39.32
12350	-2.567	36.153
12365	-2.304	32.035
12380	-2.043	27.321
12395	-1.783	21.781
12410	-1.524	15.023
12425	-1.266	6.635
12440	-1.01	0.273
12455	-0.756	0.184
12470	-0.503	0.053
12485	-0.251	0.057
12500	0	0.2
12515	0.249	0.058
12530	0.497	0.049
12545	0.744	0.191
12560	0.99	0.141
12575	1.234	5.503
12590	1.477	13.612
12605	1.718	20.239
12620	1.959	25.642
12635	2.198	30.205
12650	2.436	34.165
12665	2.673	37.668

CIRCULAR WAVEGUIDE TSCHEBYCHEFF FILTER

CENTER FREQUENCY = 12500 MHZ; BANDWIDTH = 120 MHZ

WAVEGUIDE DIAMETER = 0.833 INCHES

NUMBER 3F CAVITIES = 4 ; RIPPLE LEVEL = 0.2 DB

(III.A Cont.)

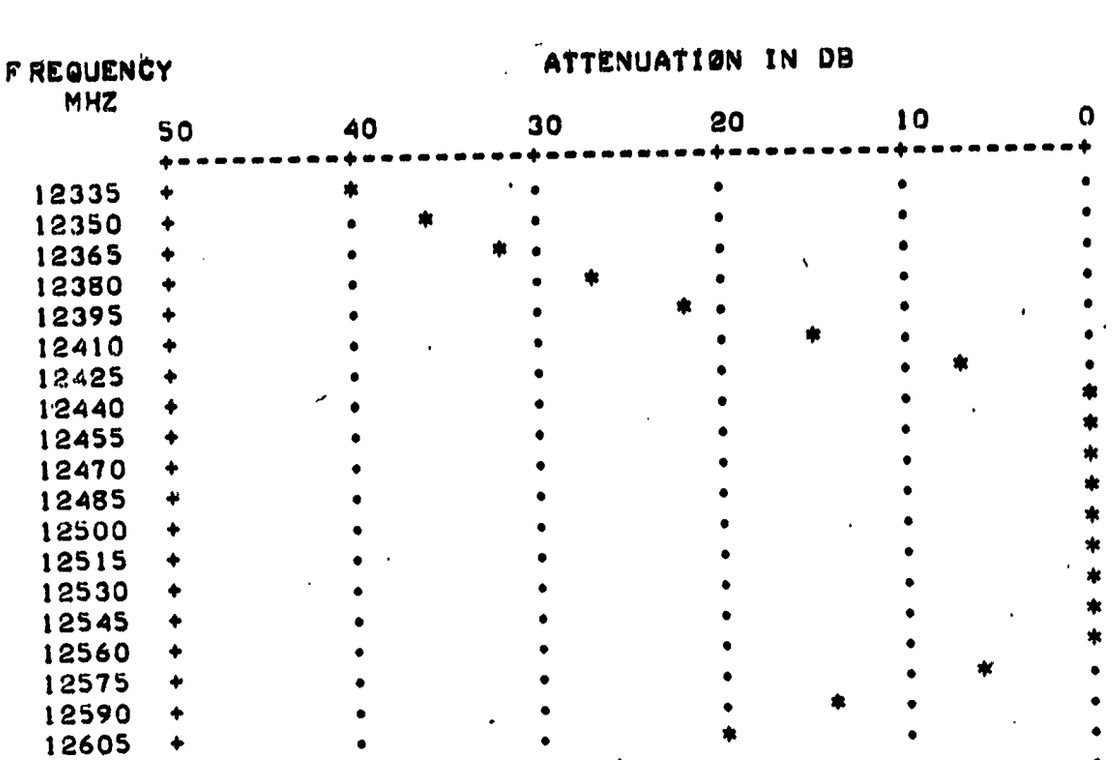

TIME 0.78 SEC.

READY

B. Directional Tschebychoff Filter Design (CHEBFIL3)

Program (BASIC)

```
!LIST CHEBFIL3
02/28/72    17:03


00010 READ F0, B
00020 READ D, A0, B0
00030 READ N1, A1
00040 READ Q0
00050 PRINT "DIRECTIONAL TSCHEBYCHEFF FILTER DESIGN"
00060 PRINT
00070 PRINT "CENTER FREQUENCY ="; F0; "MHZ";";  BANDWIDTH ="; B;
                                                          "MHZ"
00080 PRINT
00090 PRINT "WAVEGUIDE DIAMETER ="; D; "INCHES"
00100 PRINT
00110 PRINT "RECT WAVEGUIDE DIM:  A ="; A0; ",  B ="; B0; "INCHES"
00120 PRINT
00130 PRINT "NUMBER OF CAVITIES ="; N1; ";  RIPPLE LEVEL ="; A1;
                                                          "DB"
00140 PRINT
00150 PRINT "UNLOADED CAVITY Q ="; Q0
00160 LET C = 2.99793E4
00170 LET P1 = 3.14159265
00180 LET P2 = 1.8412
00190 LET L1 = (2*P1/P2)*D/2
00200 LET F1 = F0 - B/2
00210 LET F2 = F0 + B/2
00220 LET W1 = C/F1/2.54
00230 LET W2 = C/F2/2.54
00240 LET G1 = W1/SQR(1 - (W1/L1)↑2)
00250 LET G2 = W2/SQR(1 - (W2/L1)↑2)
00260 LET W0 = C/F0/2.54
00270 LET G0 = W0/SQR(1 - (W0/L1)↑2)
00280 LET R1 = W1/SQR(1 - (W1/(2*A0))↑2)
00290 LET R2 = W2/SQR(1 - (W2/(2*A0))↑2)
00300 LET R0 = W0/SQR(1 - (W0/(2*A0))↑2)
00310 LET G5 = SQR(G1*G2)
00320 LET W5 = G5/SQR(1 + (G5/L1)↑2)
00330 LET R5 = W5/SQR(1 - (W5/(2*A0))↑2)
00340 LET D2 = 1/Q0
00350 LET M2 = 1/SQR(EXP(A1/4.343) - 1)
00360 LET M4 = (LOG(M2 + SQR(M2↑2 + 1)))/4
00370 LET S4 = (EXP(M4) - EXP(-M4))/2
00380 LET F8 = (G1 - G2)/G5
00390 LET C1 = 2.61*S4*F8
00400 LET C2 = (1 + 3.41*S4↑2)*F8↑2
00410 LET C3 = S4*(1.69 + 2.61*S4↑2)*F8↑3
00420 LET C4 = (0.125 + S4↑2 + S4↑4)*F8↑4
00430 LET D1 = C1/2 - D2
```

(III.B Cont.)

```
00440 LET D4 = D1↑3 + 3*D1↑2*D2 + 3*D1*D2↑2 + D2↑3
00450 LET K4 = (C3 - C2*(D1 + D2) + D4)/(D1 - D2)
00460 LET K3 = SQR(C4 - K4*D1↑2) - D1*D2
00470 LET K1 = SQR(K3)
00480 LET K2 = SQR(K4)
00490 LET M5 = 2*(W5/G5)↑2/P1
00500 LET B1 = M5/K1
00510 LET B2 = M5/K2
00520 LET N3 = 3*D↑3/4.2
00530 LET N5 = 2*D/G5
00540 LET H3 = N3/(B1*N5 + 2.344)
00550 LET H4 = N3/(B2*N5 + 2.344)
00560 LET H1 = EXP(LOG(H3)/3)
00570 LET H2 = EXP(LOG(H4)/3)
00580 LET S5 = G5/(4*P1)
00590 LET S1 = S5*ATN(2/B1)
00600 LET S2 = S5*ATN(2/B2)
00610 LET L2 = G5/2 - S2 - S1
00620 LET X1 = ATN(2*A0/R5)
00630 LET X0 = X1*A0/P1
00640 LET Q1 = 1/D1
00650 LET B6 = (2*P1/Q1)↑2*(G5/W5)↑4
00660 LET C6 = SQR(B6 + (B6/2)↑2) - B6/2
00670 LET N6 = 27*A0↑3*B0*D↑2*G5
00680 LET D6 = 8*P1↑2*R5*(SIN(X1))↑2
00690 LET H6 = (N6/D6)*C6
00700 LET H0 = EXP(LOG(H6)/6)
00710 LET B3 = (N3/H0↑3 - 2.344)/N5
00720 LET S0 = S5*ATN(2/B3)
00730 LET L1 = G5/2 - S1 - S0
00740 LET K5 = (C2 - K4 - D1↑2 - 4*D1*D2 - D2↑2)/2
00742 LET K7 = (C3 - 2*K4*D1 - 2*D1*D2↑2 - 2*D1↑2*D2)/(2*(D1 + D2))
00744 LET K6 = SQR(K5)
00746 LET K8 = SQR(K7)
00750 PRINT
00752 PRINT
00754 PRINT "WAVELENGTH IN AIR ="; W0; "INCHES"
00756 PRINT
00760 PRINT "CIRC GUIDE WAVELENGTHS IN INCHES"
00770 PRINT
00780 PRINT "    G1 ="; G1
00790 PRINT "    G0 ="; G0; "    MEAN G0 = G5 ="; G5
00800 PRINT "    G2 ="; G2
00810 PRINT
00820 PRINT "RECT GUIDE WAVELENGTHS IN INCHES"
00830 PRINT
00840 PRINT "    R1 ="; R1
00850 PRINT "    R0 ="; R0; "    MEAN R0 = R5 ="; R5
00860 PRINT "    R2 ="; R2
00870 PRINT
```

(III.B Cont.)

```
00860 PRINT "DESIGN CONSTANTS"
00890 PRINT
00900 PRINT "    D2 ="; D2; ",   S4 ="; S4; ",   FR ="; FR
00910 PRINT
00920 PRINT "    C1 ="; C1; ",   C2 ="; C2
00930 PRINT "    C3 ="; C3; ",   C4 ="; C4
00940 PRINT
00950 PRINT "    D1 ="; D1; ",   LOADED Q1 ="; Q1
00960 PRINT
00970 PRINT "    K1 ="; K1; ",   K2 ="; K2
00972 PRINT
00974 PRINT "    ALT K1 FROM EQ 2 ="; K6
00976 PRINT "    ALT K1 FROM EQ 3 ="; K8
00980 PRINT
00990 PRINT "IRIS SUSCEPTANCES AND HOLE SIZES"
01000 PRINT
01010 PRINT "    EQUIV B0 ="; B3; ",   B1 ="; B1; ",   B2 ="; B2
01020 PRINT
01030 PRINT "    H0 ="; H0; ",   H1 ="; H1; ",   H2 ="; H2; "INCHES"
01040 PRINT
01050 PRINT " CAVITY LENGTHS"
01060 PRINT
01070 PRINT "    S0 ="; S0; ",   S1 ="; S1; ",   S2 ="; S2
01080 PRINT
01090 PRINT "    L1 ="; L1; ",   L2 ="; L2; "INCHES"
01100 PRINT
01110 PRINT "WAVEGUIDE CTR LINE OFFSET"
01120 PRINT
01130 PRINT "    X0 ="; X0; "INCHES"
01140 PRINT
01150 DATA 8350, 92
01160 DATA 1.250, 1.122, 0.497
01170 DATA 4, 0.2
01180 DATA 10000
01190 END

READY
```

Printout

```
DIRECTIONAL TSCHEBYCHEFF FILTER DESIGN

CENTER FREQUENCY = 8350 MHZ;  BANDWIDTH = 92 MHZ

WAVEGUIDE DIAMETER = 1.25 INCHES

RECT WAVEGUIDE DIM:  A = 1.122 ,  B = 0.497 INCHES
```

(III.B Cont.)

NUMBER OF CAVITIES = 4 ; RIPPLE LEVEL = 0.2 DB

UNLOADED CAVITY Q = 10000

WAVELENGTH IN AIR = 1.41352 INCHES

CIRC GUIDE WAVELENGTHS IN INCHES

G1 = 1.90635
G0 = 1.88758 ; MEAN G0 = G5 = 1.88771
G2 = 1.86926

RECT GUIDE WAVELENGTHS IN INCHES

R1 = 1.83678
R0 = 1.81998 ; MEAN R0 = R5 = 1.82009
R2 = 1.80353

DESIGN CONSTANTS

D2 = 0.0001 , S4 = 0.587461 , FB = 1.96495 E-2

C1 = 0.030128 , C2 = 8.40475 E-4
C3 = 1.15466 E-5 , C4 = 8.78361 E-8

D1 = 0.014964 , LOADED Q1 = 66.8271

K1 = 1.51326 E-2 , K2 = 1.24503 E-2

ALT K1 FROM EQ 2 = 1.50922 E-2
ALT K1 FROM EQ 3 = 1.50922 E-2

IRIS SUSCEPTANCES AND HOLE SIZES

EQUIV B0 = 1.57041 , B1 = 23.5902 , B2 = 28.6724

H0 = 0.68067 , H1 = 0.346324 , H2 = 0.325867 INCHES

CAVITY LENGTHS

S0 = 0.13597 , S1 = 1.27054 E-2 , S2 = 1.04614 E-2

L1 = 0.795181 , L2 = 0.92069 INCHES

WAVEGUIDE CTR LINE OFFSET

X0 = 0.317618 INCHES

TIME 0.51 SEC.

C. Iris Hole Diameter Correction by Cohn's Corrected Equations (HOLCOR2)

Program (BASIC)

```
00130 DATA 0.300, 0.010, 6

!SAVE HOLCOR2

READY

!LIST
03/01/72    15:15


00010 DIM M(11), D(11)
00012 DIM P(11), S(11)
00014 DIM R(11), T(11)
00016 DIM N(11), H(11)
00020 DIM C(11), E(11)
00030 PRINT "IRIS HOLE DIA CORRECTION BY COHN'S CORRECTED EOS"
00031 PRINT "        FOR SEVERAL INITIAL DIAMETERS"
00032 PRINT
00034 PRINT "   J",  " MAG POL", " D INCHES", " CORRECTION"
00036 PRINT
00040 LET T = 0.030
00050 LET W0 = 1.41352
00058 READ D1, D2, N1
00060 FOR J = 1 TO N1
00062 LET D(J) = D1 + (J - 1)*D2
00065 LET M(J) = (D(J))↑3/6
00070 LET C(J) = (1 - (1.7*D(J)/W0)↑2)
00080 LET E(J) = EXP( (1.6*T/D(J))*SQR( C(J) )/0.4343 )
00090 LET P(J) = M(J)/C(J)
00092 LET R(J) = M(J)*E(J)
00094 LET N(J) = P(J)*E(J)
00100 LET S(J) = EXP(LOG(6*P(J))/3)
00102 LET T(J) = EXP(LOG(6*R(J))/3)
00104 LET H(J) = EXP(LOG(6*N(J))/3)
00110 PRINT J, M(J), D(J), "  NONE"
00112 PRINT "  ", P(J), S(J), "  SIZE ALONE"
00114 PRINT "  ", R(J), T(J), "  T ALONE"
00116 PRINT "  ", N(J), H(J), "  SIZE AND T"
00118 PRINT
00120 NEXT J
00130 DATA 0.300, 0.010, 6
00150 END
```

(III.C Cont.)

Printout

IRIS HOLE DIA CORRECTION BY COMM'S CORRECTED EQS
FOR SEVERAL INITIAL DIAMETERS

J	MAG POL	D INCHES	CORRECTION
1	0.0045	0.3	NONE
	5.17347 E-3	0.314276	SIZE ALONE
	6.34503 E-3	0.336404	T ALONE
	7.29462 E-3	0.352413	SIZE AND T
2	4.96517 E-3	0.31	NONE
	5.76675 E-3	0.325857	SIZE ALONE
	6.91205 E-3	0.346141	T ALONE
	8.02794 E-3	0.363847	SIZE AND T
3	5.46133 E-3	0.32	NONE
	6.41087 E-3	0.337564	SIZE ALONE
	7.51179 E-3	0.355876	T ALONE
	8.81783 E-3	0.375409	SIZE AND T
4	5.9895 E-3	0.33	NONE
	7.10932 E-3	0.349403	SIZE ALONE
	8.14511 E-3	0.365608	T ALONE
	9.66796 E-3	0.387105	SIZE AND T
5	6.55067 E-3	0.34	NONE
	7.86589 E-3	0.361382	SIZE ALONE
	8.81288 E-3	0.375338	T ALONE
	1.05823 E-2	0.398943	SIZE AND T
6	7.14583 E-3	0.35	NONE
	8.68463 E-3	0.373509	SIZE ALONE
	9.51599 E-3	0.385065	T ALONE
	1.15651 E-2	0.41093	SIZE AND T

TIME 0.32 SEC.

APPENDIX IV. DC HIGH VOLTAGE BLOCKING FLANGE FILTER DESIGN PROGRAMS

The following Fortran programs were used for computing the element values of the bandstop filter sections of the DC high voltage blocking flange, Section 5.8.

A. One Resonator Case

```
READY
$LIST WGCH1

09/24/70  15.350

00010 *CALCULATE LINE IMPEDANCES OFA A 1-SECTION CHOKE DESIGN
00020 *BASED ON PAGES 32 - 35 OF NOTEBOOK #967 (MTI-12, #1, P.6)
00030 DIMENSION ZSTUB(3),Z(2,3)
00040 READ:YA,F0,DELF,F1RAT,G0,G1,G2,G3,G4
00045 F1=(F0-DELF)/F1RAT
00050 PI =3.14159265
00060 SCALE=COTAN((PI/2.0)*(F1/F0))
00070 ZSTUB(1)=1.0/(YA/(SCALE*G0*G1))
00075 ZA=1./YA
00111 ZB=1./YA*G0*G3
00120 PRINT:"ZSTUB=",ZSTUB(1),"ZLINE=",Z(1,2)
00130 PRINT:"ZSTUB=",ZSTUB(2),"ZLINE=",Z(2,3)
00140 PRINT:"ZSTUB=",ZSTUB(3),"ZLLOAD=",ZB
00150 PRINT:"SCALE=", SCALE, "ZSOURCE=",ZA
00160 STOP
00170 END
```

B. Two Resonator Case

```
READY
$LIST WGCH2

09/24/70  15.079

00010 *CALCULATE LINE IMPEDANCES OF A TWO SECTION CHOKE DESIGN
00020 *BASED ON PAGES 32 - 35 OF NOTEBOOK #967 (MTI-12, #1, P.6)
00030 DIMENSION ZSTUB(3),Z(2,3)
00040 READ:YA,F0,DELF,F1RAT,G0,G1,G2,G3,G4
00045 F1=(F0-DELF)/F1RAT
00050 PI =3.14159265
00060 SCALE=COTAN((PI/2.0)*(F1/F0))
00070 ZSTUB(1)=1./(YA*(1.+1./(SCALE*G0*G1)))
00075 ZA=1./YA
00090 Z(1,2)=1.0/(YA*(1.0+SCALE*G0*G1))
00091 ZSTUB(2)=1.0/(YA*G0)/(SCALE*G2)
00111 ZB=1./YA*G0*G3
00120 PRINT:"ZSTUB=",ZSTUB(1),"ZLINE=",Z(1,2)
00130 PRINT:"ZSTUB=",ZSTUB(2),"ZLINE=",Z(2,3)
00140 PRINT:"ZSTUB=",ZSTUB(3),"ZLLOAD=",ZB
00150 PRINT:"SCALE=", SCALE, "ZSOURCE=",ZA
00160 STOP
00170 END
```

(IV Cont.)

C. Three Resonator Case

```
 $LIST WGCM3

 09/24/70  16.784

 00010 *CALCULATE LINE IMPEDANCES OF A THREE SECTION CHOKEDESIGN
 00020 *BASED ON PAGES 32 - 35 OF NOTEBOOK #967 (MTT-12, #1, P.6)
 00030 DIMENSION ZSTUB(3),Z(2,3)
 00040 READ:YA,F0,DELF,F1RAT,G0,G1,G2,G3,G4
 00045 F1=(F0-DELF)/F1RAT
 00050 PI =3.14159265
 00060 SCALE=COTAN((PI/2.0)*(F1/F0))
 00070 ZSTUB(1)=1./(YA*(1.+1./(SCALE*G0*G1)))
 00075 ZA=1./YA
 00090 Z(1,2)=1.0/(YA*(1.0+SCALE*G0*G1))
 00091 ZSTUB(2)=1.0/(YA*G0)/(SCALE*G2)
 00100 Z(2,3)=1./((YA*G0)*(1.+SCALE*G3*G4)/G4)
 00110 ZSTUB(3)=1.0/((YA*G0)*(1.0+1.0/(SCALE*G3*G4))/G4)
 00111 ZB=G4/(YA*G0)
 00120 PRINT:"ZSTUB=",ZSTUB(1),"ZLINE=",Z(1,2)
 00130 PRINT:"ZSTUB=",ZSTUB(2),"ZLINE=",Z(2,3)
 00140 PRINT:"ZSTUB=",ZSTUB(3),"ZLLOAD=",ZB
 00150 PRINT:"SCALE=", SCALE, "ZSOURCE=",ZA
 00160 STOP
 00170 END
```

SECTION VII
REFERENCES

1. Haviland, R.P., Foster, D.E., and Dysinger, J.H., An Investigation of Network Television Distribution Satellite Systems - Volume II, Technical Report, Prepared by General Electric Co., Space Systems Operation, Philadelphia, for the Public Broadcast Service, Washington, D.C., February 1971.

2. Johnson, F.O., "Interference Emission Filtering in High Power Microwave Transmitters", Microwave Journal, January 1970, pages 67-72.

3. Microwave Engineers Technical and Buyers Guide, 1 February 1968, published by Microwave Journal.

4. Multikilowatt Transmitter Study for Space Communications Satellites, Volume II, Technical Report, Phase II, General Electric Company, Philadelphia, Pa., for NASA/MSFC, Huntsville, Ala., Contract NAS8-21886, 30 July 1969.

5. Dushman, S., and Lafferty, J.M., Scientific Foundations of Vacuum Technique, John Wiley and Sons, Inc., New York, 1962.

6. Scannapieco, J. F., Eagles, A. E., and Amore, L. J., MKTS Materials Evaluation Final Report, Task B-2 Report, Contract NAS8-21886, General Electric Company, Space Division, Philadelphia, Pa., for NASA/Marshall Space Flight Center, 15 January 1969.

7. Schiffman, B. M., and Matthaei, G. L., "A new Type of Low Pass Filter that Attenuates by Dissipation", IEEE transactions on Microwave Theory and Techniques, September 1965, pages 699-700.

8. Price, V. G., Stone, R. H., and Met, V., "Harmonic Suppression by Leaky-Wall Waveguide Filter", IRE Wescon Convention Record, Part 1, 1959, pages 112-118.

9. Levy, R., "Analysis and Synthesis of Waveguide Multiaperture Directional Couplers", IEEE Transactions on Microwave Theory and Techniques, Vol. 16, No. 12, December 1968, page 995.

10. Matthaei, G. L., Young, L., and Jones, E. M. T., Microwave Filters, Impedance Matching Networks, and Coupling Structures, McGraw Hill, New York, 1964, Section 5.10, pages 229 through 242.

11. Williams, R. L., "A Three-Cavity Circularly Polarized Waveguide Directional Filter Yielding a Maximally Flat Response", IRE transactions on Microwave Theory and Technique, September 1962, pages 321 to 328.

12. Strock and Koral, Handbook of Air Conditioning, Heating, and Ventilation, Industrial Press, New York, 1965, page 5-79

13. Reference Data For Radio Engineers, International Telephone and Telegraph Corp., New York. Fourth Edition, 19 , page 583.

14. Ramo, S., and Whinnery, J. R., Fields and Waves in Modern Radio, John Wiley & Sons, Inc., New York, 1944, Page 376.

15. Southworth, Principles and Applications of Waveguide Transmission, D. Van Nostrand Co., Inc., New York, 1950, page 104-106.

16. Schiffman, B. M., and Matthaei, G. L., "Exact Design of Band Stop Filters", IEEE Transactions on Microwave Theory and Techniques, Vol. 12, January 1964.

17. See Ref. 11, Chapter 4.

18. Viestra, A., and Butman, R. C., Secordary Emission Characteristics of High Power Microwave Tube Surfaces, Lincoln Laboratory, MIT Technical Report No. 257, February 1962.

19. Development of Circuitry for a Multikilowatt Transmitter for Space Communications Satellites, Technical Report, General Electric Company, Philadelphia, Pa., for NASA/MSFC, Huntsville, Alabama, Contract NAS8-24771, 20 February 1971, pages 168 to 173.